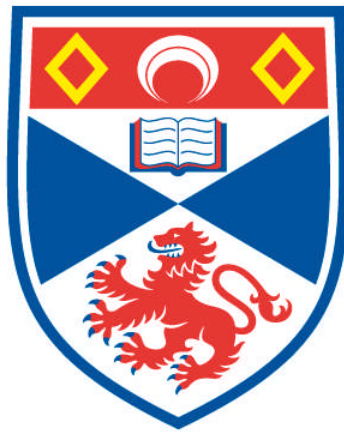


THE USE OF ACTIVE SONAR TO STUDY CETACEANS

Matteo Bernasconi

**A Thesis Submitted for the Degree of PhD
at the
University of St Andrews**



2012

**Full metadata for this item is available in
Research@StAndrews:FullText
at:**

<http://research-repository.st-andrews.ac.uk/>

Please use this identifier to cite or link to this item:

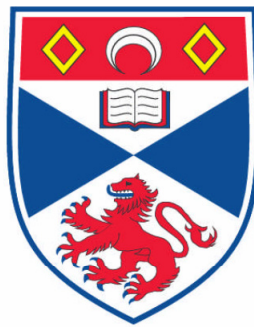
<http://hdl.handle.net/10023/2580>

This item is protected by original copyright

**This item is licensed under a
Creative Commons Licence**

The use of active sonar to study cetaceans

Matteo Bernasconi



Submitted in partial fulfilment of the requirements
for the degree of Doctor of Philosophy

University of St Andrews

July 2011

The use of active sonar to study cetaceans

Matteo Bernasconi

TABLE OF CONTENTS

DECLARATIONS	V
ACKNOWLEDGMENTS	VII
ABSTRACT	IX
1. INTRODUCTION	1
2. UNDERWATER ACTIVE ACOUSTIC	13
2.1 Historical notes	15
2.2 Sound: basic concepts	17
2.2.1 Sound propagation	18
2.2.2 Sound pressure and intensity	20
2.2.3 The decibel	21
2.2.4 Transmission Loss	22
2.2.5 Sound Speed	25
2.3 Transducers and beams	26
2.3.1 The beam pattern	28
2.3.2 The equivalent beam angle	29
2.3.3 Pulse and Ranging	30
2.4 Acoustic scattering	31
2.4.1 Target Strength	32
2.4.2 Target shape and orientation	33
2.4.3 Volume/area scattering coefficient	34
2.5 The sonar equation	35
3. CALIBRATION	39
3.1 The on-axis sensitivity	41
3.2 Nearfield and Farfield	42
3.3 The TVG function	43
3.4 Standard experimental procedure	44
3.5 Calibration spheres	46
3.6 Calibration test of omnidirectional Sonar	47
3.6.1 Introduction	48
3.6.2 Method	49
3.6.3 Results & Discussion	51
3.6.4 Conclusion	57
4. METHODS FOR MEASURING CETACEAN TARGET STRENGTH	59
4.1 Overview of Past studies	61
4.2 Coordinated ecosystem survey of the Norwegian Sea	64
4.3 Instruments	67
4.3.1 Scientific echosounder: Simrad EK500 and EK60	67
4.3.2 Omnidirectional Sonars: SIMRAD SH80 and SX90	68
4.3.3 CTD samples and the Lybin ray tracing model	70
4.4 Omnidirectional sonar signal processing: basic MATLAB codes	72

5. ACOUSTIC OBSERVATIONS OF DUSKY DOLPHINS (<i>LAGENORHYNCHUS OBSCURUS</i>) HUNTING CAPE HORSE MACKEREL (<i>TRACHURUS CAPENSIS</i>) OFF NAMIBIA.	77
5.1 Introduction	79
5.2 Methods	82
5.2.1 Dolphin behavior	82
5.2.2 Predator response reactions	83
5.3 Results	85
5.4 Discussion	87
6. FIN WHALE (<i>BALAENOPTERA PHYSALUS</i>) TARGET STRENGTH MEASUREMENTS	95
6.1 Introduction	97
6.2 Methods	99
6.2.1 Data collection	99
A. Acoustic data	99
B. Whale position data	100
C. Vertical CTD cast	100
6.2.2 Data analysis	101
6.3 Results and discussion	103
6.3.1 TS measurements	103
6.3.2 TS variation with breathing	105
6.3.3 TS variation with swimming motion and depth	106
6.3.4 Behavioral patterns observed in sonar screen video sequences and raw data	109
6.4 Conclusions	110
7. THE EFFECTS OF FREQUENCY AND DEPTH ON TARGET STRENGTH OF THE HUMPBACK WHALE (<i>MEGAPTERA NOVAEANGLIAE</i>)	111
7.1 Introduction	113
7.2 Methods	114
7.3 Results and Discussion	116
7.3.1 Omnidirectional sonar TS measurements	116
7.3.2 TS variation with depth	118
7.3.3 Cetaceans TS frequency response	119
7.4 Conclusions	120
8. GENERAL DISCUSSION	123
REFERENCES	135
LIST OF SYMBOLS	149
APPENDIX A	153

DECLARATIONS

I, Matteo Bernasconi hereby certify that this thesis, which is approximately 43000 words in length, has been written by me, that it is the record of work carried out by me and that it has not been submitted in any previous application for a higher degree.

I was admitted as a research student in [September, 2007] and as a candidate for the degree of PhD in [September, 2008]; the higher study for which this is a record was carried out in the University of St Andrews between [2007] and [2011].

Date Signature of candidate

I hereby certify that the candidate has fulfilled the conditions of the Resolution and Regulations appropriate for the degree of PhD in the University of St Andrews and that the candidate is qualified to submit this thesis in application for that degree.

Date Signature of supervisor

In submitting this thesis to the University of St Andrews I understand that I am giving permission for it to be made available for use in accordance with the regulations of the University Library for the time being in force, subject to any copyright vested in the work not being affected thereby. I also understand that the title and the abstract will be published, and that a copy of the work may be made and supplied to any bona fide library or research worker, that my thesis will be electronically accessible for personal or research use unless exempt by award of an embargo as requested below, and that the library has the right to migrate my thesis into new electronic forms as required to ensure continued access to the thesis. I have obtained any third-party copyright permissions that may be required in order to allow such access and migration, or have requested the appropriate embargo below.

The following is an agreed request by candidate and supervisor regarding the electronic publication of this thesis. Embargo on both [for the all thesis] of printed copy and electronic copy for a period of 2 years on the following grounds:

- publication would be commercially damaging to the researcher, or to the supervisor, or the University;
- publication would preclude future publication;

Date Signature of candidate

Date Signature of supervisor

ACKNOWLEDGEMENTS

First of all I thank my family: my wife Salome', my father Francesco, my mother Liviana, my brother Federico, without forgetting my pets Comi, Maui and Tobi, for their constant patience and love in good and bad times since I started to work with science and conservation issues.

To be fair I have to make a long list of colleagues who helped me through the past five years to evolve my research interests into a PhD and grow as a scientist, but more important as a honest man. I thanks and express all my deep respect to my present and former colleagues at the Institute of Marine Research (Havforskningsinstituttet) in Bergen, Norway: Ruben Patel, Terje Torkelsen, Lucio Calise, Geir Pedersen, Reidun Heggø Sørensen, Hector Peña, Egil Ona, Olav Rune Godø, Jens-Otto Krakstad, Bjørn Erik Axelsen, Marianne Holm, Øyvind Tangen, Valantine Anthonypillai and Rolf Korneliussen.

I also thank my colleagues at the University of St Andrews Martin Cox, Clint Blight and Carl Donovan and Prof. Riccardo Groppali (Universita' degli studi di Pavia) for their support.

A special mention goes to both the crew onboard M/V "Eros" and "Libas" who always gave me high professional assistance during the field work but more important they gave me a true friendship that makes everything presented in this work actually real.

I also thank for their cooperation and technical advises: Matt Wilson and Toby Jarvis (MYRIAX), Ole Bernt Gammelsæter, Frank Reier Knudsen and Lars Nonboe Andersen (Simrad AS) for sharing information and for the technical support that made me cross the finish line of this PhD.

Special thanks go to my supervisors Dr. Leif Nøttestad (Institute of Marine Research / Havforskningsinstituttet) and Prof. Andrew S Brierley (University of St Andrews) that trusted and supported me even when failure could be a hypothetical conclusion of my PhD pilot project.

This thesis work is dedicated to my beloved grandparents and in memory of my great friend and mentor Professor Sergio Frugis (Universita' degli studi di Pavia) who would all be so proud of this important step of my life and are the reasons why I never quit something in which I strongly believe in.

Ciò che seminai nell'ira
crebbe in una notte
rigogliosamente
ma la pioggia lo distrusse.

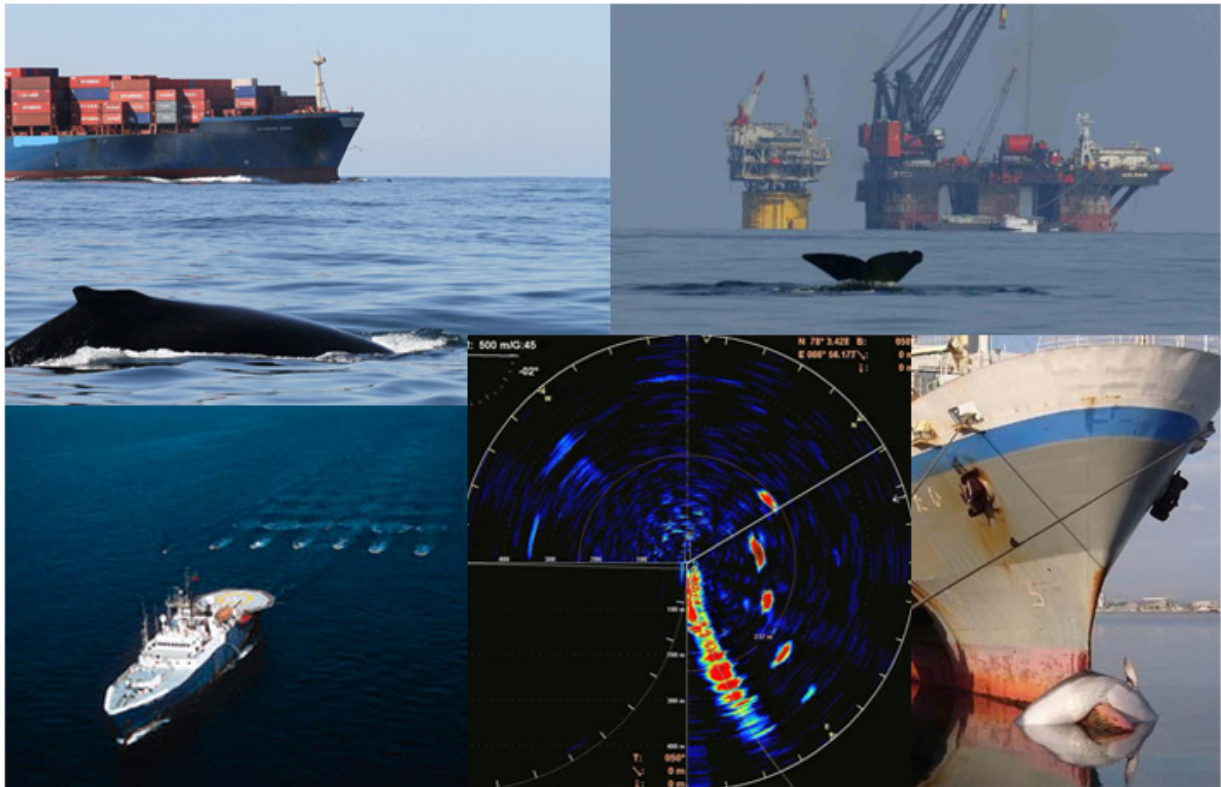
Ciò che seminai con amore
germinò lentamente
maturò tardi
ma in benedetta abbondanza.

PETER ROSEGGER

ABSTRACT

Cetacean species face serious challenges worldwide due to the increasing noise pollution brought to their environment by human activities such as seismic exploration. Regulation of these activities is vaguely defined and uncoordinated. Visual observations and passive listening devices, aimed at preventing conflicts between human wealth and cetaceans' health have some fundamental limitations and may consequently fail their mitigation purposes. Active sonar technology could be the optimal solution to implement mitigation of such human activities. In my thesis, the proper sonar unit was used to test the feasibility to detect cetaceans *in situ*. Omnidirectional sonars could be the optimal solution to monitor the presence of cetaceans in the proximity of potential danger areas. To use this class of sonar in a quantitative manner, the first step was to develop a calibration method. This thesis links *in situ* measurements of target strength (TS) with variation trends linked to the behavior, morphology and physiology of cetacean. The butterfly effect of a cetacean's body was described for a fin whale insonified from different angles. A relationship between whale respiration and TS energy peaks was tested through a simple prediction model which seems very promising for further implementation. The effect of lung compression on cetacean TS due to increasing depth was tested through a basic mathematical model. The model fit the *in situ* TS measurements. TS measurements at depth of a humpback whale, when post-processed, correspond to TS measurements recorded at the surface. Sonar technology is clearly capable of detecting whale foot prints around an operating vessel. Sonar frequency response shows that frequencies between 18 and 38 kHz should be employed. This work has established a baseline and raised new questions so that active sonar can be developed and employed in the best interest for the whales involved in potentially harmful conflicts with man.

CHAPTER 1



INTRODUCTION

1. INTRODUCTION

Overexploitation by the whaling industry is recognized as the main factor that led to serious decline for the majority of the world's populations of large whales i.e., the 14 recognized baleen whale species and the sperm whale (IWC 2001). For example, only about 300–350 North Atlantic right whales (*Eubalaena glacialis*) remain, concentrated along the east coast of the USA (Katona and Kraus 1999; IWC 2001). The situation is unclear in the Sea of Okhotsk for the North Pacific right whales (*Eubalaena japonica*), as they have disappeared from most of its range and are thus considered in grave danger of extinction (IWC 2001). Some populations of other species, such as the gray whale (*Eschrichtius robustus*) in the North Atlantic (Mead and Mitchell 1984) and possibly the blue whale (*Balaenoptera musculus*) in the western North Pacific (Reeves et al. 1998) have been exterminated. Other populations remain at extremely low levels after having been reduced by intensive commercial whaling in earlier times. For example, the gray whale population in the western North Pacific (Brownell et al. 1997; Weller et al. 2002) and bowhead whale (*Balaena mysticetus*) populations in the Sea of Okhotsk and in Arctic waters adjacent to the North Atlantic Ocean (IWC 1992; Zeh et al. 1993; Clapham et al. 1999) are severely depleted, and their prospects for recovery are highly uncertain.

The status and recovery of some populations of great whales is showing how the measures adopted to reduce the impact of whaling could provide good results. Some populations of southern right whales (*Eubalaena australis*) (IWC 2001), humpback whales in many areas (e.g., Bannister 1994; Smith et al. 1999), gray whales in the eastern North Pacific (Jones and Swartz 2002), and blue whale populations in the eastern North Pacific (Carretta et al. 2001) and central North Atlantic (Sigurjónsson and Gunnlaugsson 1990) have shown signs of recovery under protection. In contrast, the continued small numbers of North Atlantic and North Pacific right whales, southern right whales in some areas of former abundance (e.g., around New Zealand, off Peru and Chile) (IWC 2001), bowhead whales in some areas (see above), and blue whales and fin whales (*Balaenoptera physalus*) in the Southern Hemisphere, mean that there is no reason to be overconfident about their future (Clapham et al. 1999). Measures to conserve cetacean species need to be evaluated and updated constantly for them to be effective due to the increasing threats that wildlife in general is facing worldwide (e.g. ship traffic, seismic shooting, oil and gas exploration, military activities and commercial fishing).

In the 1980s and 1990s, direct exploitation was less of an immediate threat to most endangered whale populations compared to accidental mortality from ship-strikes and entanglement in fishing gear. Threats to cetaceans can be identified in two distinct, but broad categories. The first one represents the threats which short-term results involve direct death (e.g. hunting) or accidental mortality (e.g. bycatches in fishing gear and ship strikes). The other category of threats is more difficult to identify

and quantify and these have become additional major concerns in recent decades. This long-term category of factors could affect the overall population fitness with respect to reduction in prey availability as a result of overfishing (Bearzi et al. 1999) and possibly climate change (Würsig et al. 2001), the direct effects of pollution on health and reproduction (O'Shea et al. 1999; Reijnders et al. 1999), and the disturbance caused by noise from ship traffic and industrial activity (Gordon and Moscrop 1996; Würsig and Richardson 2002).

Recently, Nowacek et al. (2007) reviewed the knowledge about the impact of anthropogenic noise on cetaceans updating Richardson et al. (1995). There has been little change in the source of noise, with the notable addition of noise from acoustic deterrent and harassment devices (ADDs/AHDs) which are audible alarm devices to warn small cetaceans and pinnipeds away from commercial fishing gear and aquaculture operations by emitting sound pulses. Their use has received mixed success and the issue of habituation is significant (Bordino et al. 2002; Cox et al. 2001; 2004). Little evidence exists that large whales would, in fact, respond to such a sound signal (Nowacek et al. 2004). Furthermore, such approaches have the potential to create stress in animals if they are alarmed repeatedly or periodically (Wright et al. 2007). In addition, exposure to alarms or alerting stimuli may result in whales abandoning a desired feeding or mating area, which could result in significant adverse effects on the population (Johnston and Woodley 1998; Morton and Symonds 2002).

Overall, the noise sources of primary concern for whales remain ships, seismic exploration and sonar of all types (Nowacek et al. 2007). These sources are the reasons for the scientific investigations conducted here and aimed at mitigating these significant threats to the whales. New knowledge and possible mitigation measures are presented in my PhD thesis.

Ship traffic and seismic explorations are well established and fundamental activities for the life styles of our modern society. Seismic surveying is widely used in the marine environment, mainly by the oil and gas exploration and production industry, in order to identify and analyze subsurface geological structures and is one possible cause of serious injury to various cetacean species (Madsen et al. 2006; Miller et al. 2009). Shipping traffic can also disturb marine mammals (Laist et al. 2001; Jensen et al. 2004), and direct collisions by ships on whales have had major impacts on some whale populations (Kraus 1990; Knowlton et al. 2001). As the effects of seismic surveying and ship traffic on whales are not fully understood, precautionary mitigation measures aimed at preventing possible injury and minimizing the risk of biologically significant behavioral changes are imposed or suggested through laws and guidelines by different countries: shipping routes have been altered to reduce conflict (CFR 2008), and in many regions (e.g. The MMPA 1972; IBAMA 2008; EPBC Act 2008; JNCC guidelines

2009) seismic survey vessels are required to deploy marine mammal observers and to cease seismic shooting if whales are seen in the vicinity of the vessel.

There is limited evidence for the impact of seismic activities on marine mammals, either on hearing (Lucke et al. 2009) or behavior (Miller et al. 2009). Although sightings of marine mammals close to vessels might be interpreted as zero or minimal impact on their populations (Harris *et al.* 2001), some researchers have associated cetacean stranding with seismic surveys (*e.g.* Malakoff 2002; Engel *et al.* 2004) and others have documented alterations in behavior due to noise from air-guns (*e.g.* Richardson et al. 1995; Goold 1996). If we exclude the work of Madsen *et al.* (2002), many other studies reported negative effects of loud anthropogenic noises on cetaceans (*e.g.* Evans *et al.* 1993; Mate et al. 1994; Goold 1996; McCauley *et al.* 2000; Malakoff 2002; Gordon *et al.* 2004). Goold and Coates (2006) showed how the airgun acoustical output covers, at substantial energy levels, the entire frequency span known to be used by cetaceans. This study is in agreement with the findings of Madsen et al. (2006), that reported substantive energy between 0.3 and 3 kHz received by sperm whales (*Physeter macrocephalus*) exposed to airgun pulses. Seismic airguns produce low frequency impulsive sounds at intervals of 10–15 s, with broadband source levels of 220–255 dB re 1 μ Pa at 1m. The dominant frequencies of airgun pulses lie within the 0–120 kHz range, reaching frequencies well beyond the interest of seismic exploration (Goold and Fish 1998). The dominant frequencies overlap with those used by baleen whales (10 Hz–1 kHz), with the high frequency component also overlapping with the frequency range used by many odontocetes in the range 10–150 kHz (Richardson et al. 1995).

Many countries have currently adopted regulations which emphasize mitigation of exposure to intense anthropogenic sound sources (Southall et al. 2008). The US Marine Mammal Protection Act (1972), for instance, calls for shutting down seismic surveys and other activities when marine mammals are detected within an exclusion zone close to a vessel, typically several hundred meters (Harwood 2002; Hildebrand 2005; Madsen et al. 2006). The JNCC guidance (2009) became statutory in 2001 with the introduction of the European Union (EU) Habitats and Species Directive (92/43/EEC) into national law. Despite being referred to as guidelines, the JNCC measures are thus now a legislative requirement in most EU countries. However, relatively few aspects of current guidelines or seismic survey mitigation methods have a firm scientific basis or proven efficacy (Weir and Dolman, 2007). Current mitigation of seismic surveys is largely based on common sense measures and it is difficult to establish whether they work and/or could be made more effective (Department of Trade and Industry 2002). The main weakness is inadequate planning, which includes a lack of sufficient data upon which to base decisions. Furthermore, inadequate account is currently being taken of science available to determine the range of impacts. Mitigation measures currently in place may, in some cases, reduce some of the

acute impacts of marine noise pollution. But they do not mitigate against the chronic degradation of habitat caused by repeated use of this far-travelling and high-intensity noise (Parson et al. 2009). Concerning the JNCC guidelines, although varying considerably in the details, many countries based their guidelines on this model (see Weir and Dolman, 2007). Such guidelines have become a widely accepted approach to resolve the problem of the various effects of noise pollution during seismic surveys. This reliance on the JNCC guidelines by other countries is arguably premature (Parson et al. 2009; Leite-Parente and Araújo 2011).

Furthermore, hearing may only constitute one part of the combination of factors that determine an individual's response to an exposure to noise (see Beale 2007; Wright et al. 2007a). Physical damage includes damage to body tissues resembling decompression sickness ('the bends') and auditory damage. Symptoms resembling decompression sickness may result from the initiation of bubble growth caused by sound, or from hypothesized behavioral changes to normal dive profiles such as a faster ascent rate (Crum and Mao 1996; Jepson et al. 2005).

Auditory damage in terms of reduction in hearing sensitivity due to exposure to high intensity sound can be either temporary (TTS: temporary threshold shift), or permanent (PTS: permanent threshold shift) depending on the exposure level and duration (Richardson et al. 1995). Other than physical damage, the key auditory effect is the increase in background noise levels, such that the ability of an animal to detect a relevant sound signal is diminished, which is known as auditory masking (Richardson et al. 1995; Wartzok et al. 2003). Masking marine mammal vocalizations used for finding prey, navigation and social cohesion may compromise the ecological fitness of populations (Parson et al. 2004).

The recognition that temporary or permanent hearing impairment in marine mammals is greatly increased within a few hundred meters of the sound source (Richardson et al. 1995) brought to the definition, (within any given set of guidelines), of exclusion or safety zones around the sound source to reduce the chance of causing physical damage to cetaceans (very long sentence). Generally, exclusion zones are defined as the radius where received sound levels are believed to have the potential for at least temporary hearing impairment (HESS 1999). The safety radius common to the UK, USA and Canadian guidelines and regulations is 500 m, which is deemed to be the distance at which cetaceans may be reliably observed (JNCC 2009). While this distance may be sufficient to prevent physical injury, the potential for TTS, behavioral disturbance and auditory masking is likely to extend beyond this zone (Harwood 2002). It seems clear that with significant responses occurring beyond the fairly arbitrary mitigation zone of 500 m, guidelines that include this zone are failing to minimize disturbance. DeRuiter et al. (2006) illustrated that, in many cases, airgun received levels will not

decrease monotonically with increasing range, so that a simple spreading law will not accurately predict the observed pattern of received levels at increasing distances from the sound source. Studies off the west coast of the British Isles have shown that dolphins react to air-gun noise at distances greater than 1 km from the source (Goold & Fish, 1998). A precautionary procedure that is widely adopted is the airguns soft start (ramp up), but there is little information on its efficiency in evoking an appropriate response from marine mammals. Stone and Tasker (2006) noted no difference in the distance of cetaceans from seismic arrays when systems were ramping up (compared to periods when airguns were off or in full operation), although Wier (2008) notes that this finding is based on simple sketches (often by inexperienced observers) of animal movement relative to a ship and uses combined datasets from many different airgun configurations, species, and water depths. The soft-start procedure is based upon the assumption that animals will move away from the seismic source as the sound builds and becomes potentially more aversive, thus limiting the chance of auditory or other physiological damage. The effectiveness of the soft-start method is likely to vary between species and circumstances (Pierson et al. 1998), and there is concern that this procedure may lead to habituation, as has been reported with regards to the use of acoustic harassment devices (AHDs) to keep marine mammals away from fishing gears (Hildebrand 2004; Nowacek et al. 2007). A further potential problem with the ramp-up method is the possibility of attracting animals by initially weak sounds (Pierson et al. 1998). Sperm whales, exposed to a received sound level below 160 dB re 1 μ Pa at 1m, showed an unexpected reaction orienting towards the sound source rather than moving away from it (Shapiro 2006). Alternatively, animals may ignore or tolerate the increasing noise, perhaps to remain in a food-rich area. Studies in other (non-cetacean) species have found that hungry animals may remain in an area despite disturbance (Beale and Monaghan, 2004).

Currently, marine mammal observers are the most common method used to fulfill regulatory obligations proposed by different guidelines, but the probability of detecting marine mammals at sea is often relatively low (e.g. Barlow 1999). If we add that in many countries observers do not need any experience or expertise (indeed they may need not ever have seen a cetacean at sea before) and that the number of observers onboard seismic vessels doesn't allow to schedule rotation with the consequence that the monitoring is not constant, we may then question the effectiveness of these programs for mitigating risk to the animals. This is especially true when operations persist in times of reduced visibility such as in fog and at night. The importance of using experienced MMOs is shown by the British government's own research (Stone, 2003). When marine mammals were detected within the 500 m zone of impact by dedicated, experienced MMOs, the guidelines were followed and the survey was delayed 70% of the time. This figure fell to 0% when Fisheries Liaison Officers or ship's crew was used.

Passive acoustic monitoring can additionally provide some detection capability in such conditions (e.g. Barlow and Taylor 2005), but this relies on animals actually vocalizing, which they certainly do not do all of the time (Gordon and Tyack, 2002). One study on common dolphins in the UK showed that although vocalization rates were relatively high at night, they decreased for portions of the day (Wakefield, 2001). Fin whales ceased all vocalization during seismic surveys and did not resume vocalizing for hours or days afterward (Clark and Gagnon, 2006). Sperm whales have also decreased vocalizations or become completely silent in response to seismic surveys (IWC, 2007), as well as in the presence of pinger sounds (Watkins and Schevill, 1975), mid-frequency military sonar signals (Watkins et al., 1985), and low-frequency anthropogenic sounds (Bowles et al., 1994). Nevertheless, real-time PAM should be used in conjunction with visual observation, to maximize the probability of detection.

Neither visual sightings nor passive detection fully resolve the problem of reliable detection of animals at risk of coming within designated exclusion zones. There is a strong need for a standard reliable protocol and a tool capable of detecting whales in proximity of seismic surveys with a higher probability of detection also during more adverse observational conditions.

The capability of active acoustic systems for probing oceanic life has been demonstrated clearly by the advances that such technologies have brought to fishery science (Simmonds and MacLennan 2005). However, few investigations have been made on large bioacoustics targets such as whales (Bernasconi et al. 2009; Lucifredi and Stein 2007; Miller 1999; Levenson 1974; Love 1973; Dunn 1969) and more information about their target strength (TS) is needed to generate a basic model of detection. TS is a stochastic variable that describes the backscatter echo energy generated by an insonified target. It is a logarithmic measure of the proportion of the incident acoustic energy which is backscattered by a submerged body. TS can be defined as the echo-signature or the acoustic footprint of a given species. It is mainly dependent on the transducer carrying frequency, the animal size, its physiology and its swimming behavior.

Although the use of active acoustics in the form of SONAR has received much attention (Miller et al. 1999; Lucifredi and Stein 2007; Bernasconi et al. 2009), as it could offer an alternative approach to prevent damage and mitigate the possible effects of noisy human activities on marine mammals providing real-time detection capabilities, significant concern exists as to its potential adverse effect on marine species by introducing additional noise into an already noisy environment (Rendell and Gordon 1999; Richardson et al. 1995; Watkins et al. 1985).

Active acoustic techniques could overcome the limitations of the methods actually employed to detect whales. One of the most promising applications for active acoustic detection may be in determining the locations of whales that are not vocalizing, but the use of such techniques presents at first glance something of a paradox. The commonly held view is that active sonars are, at the least, a source of nuisance to cetaceans (Rendell and Gordon 1999; Richardson et al. 1995; Watkins et al. 1985) and, at worst, are sometimes (military applications) a direct cause of death (Parsons et al. 2000; Frantzis 1998; Simmonds and Lopez-Jurado 1991). For most 'environmental activists' all around the world an excessive attitude to anthropomorphize cetaceans, has led to a clear misunderstanding and a wrong use of the word Sonar (Bernasconi et al. 2009; Chapman and Ellis 1998). I will particularly underline a widespread lack of knowledge about such technology and its multiple uses (Chapman and Ellis 1998; Economist 1998; Potter 1994). The world sonar brings to the public just negative thoughts; a sensational example is from 1994 with the Acoustic Thermometry of Ocean Climate (ATOC) experiment (Economist 1998). The acoustic technique used for this experiment can measure with a precision of 0.01 °C and detect subtle variations and trends of the ocean basin. The use of underwater sound did move the attention of the public leading to wrong conclusions that brought the delay of the project start (Potter 1994). It was evident that the delay was triggered by the lack of knowledge and the superficial approach of the media in presenting to the general public a delicate topic such as whale and noise (Potter 2011; Chapman and Ellis 1998; Au et al. 1997). However, I believe based on the experience and knowledge achieved through my PhD "journey" that at appropriate frequencies and source levels, active acoustic techniques could be used to protect whales in a very effective and non-invasive manner.

With this in mind, with the assistance of my supervisors, I embarked on a project with the long-term goal of exploring the possibility of using fishery omnidirectional sonars to detect cetaceans during seismic operations and to use such detections as triggers to stop potentially harmful seismic shooting. Ultimately, an automatic detector could help control operational periods for seismic surveys, and could perhaps be applied also to reduce the incidence of whale strikes by commercial freighters around the world. For instance, the actual management regulations (CFR 2008) could implement whale safety using active acoustic techniques and achieve maximum protection effectiveness with respect to North Pacific and North Atlantic Northern Right whales in particular.

Acoustic detection is a scientific discipline in itself within signal processing. Traditional methods based on the principle of Constant False Alarm Rate (CFAR) are well described in radar and sonar literature (Urick 1983; Levanon 2004). Detection methods usually rely on some kind of threshold setting. In the case of cetaceans, detections may be affected by different factors other than just the received signal

intensity. The side aspect dependency (Au 1996), the variability due to the cetaceans' dorso-ventral swimming behaviour (Bernasconi et al. 2007) and the depth dependency depending on collapse of the lungs (Ridgway and Harrison 1986; see also Chapter 7) are all relevant factors that could affect the TS (Ona 2003). Other components investigated and presented in this thesis could all be reliable signals to be able to accept or reject an acoustic detection in an operational setting.

My thesis is structured in an unconventional way; I want indeed to guide the reader not familiar with active acoustic techniques, to a more complete understanding of this technology. Instead of focusing immediately on what is the subject of the research itself, an overview of the acoustic theories behind the conservation issue is given at first as useful background, for a more comprehensive reading of the scientific achievements presented in chapters 5, 6 and 7.

If applied in the correct way, sonars could provide us with a new tool to study marine mammal behavior and ecology with high resolution, and create a base for a more concrete regulatory approach to whale conservation.

I want to provide the operator in charge of detecting whales with an instrument (modern fisheries sonar) over which he/she has control over concerning all parameters of the sonar equation (see paragraph 2.5) except TS, which is quite dynamic for whales depending on aspect angle and depth. I aim to put the basis for the development of a real time reliable detection instrument to mitigate the impact generated by different human activities on marine mammal behaviour with particular emphasis on seismic survey regulations. It is not my objective to define whether such activities are in conflict with whales or not (Bernasconi et al. 2011). My objective is to prevent, if possible, disturbances demonstrated by dedicated experiments (see Miller et al. 2009), and start developing a reliable tool which is operative in offshore situations.

Notwithstanding the final ambitious goal of converting fishery sonars into whale detectors; the short term goals presented and described in my thesis were to:

- Verify if commercial (ready and available on the market) omnidirectional sonar could be used to detect whales and if such techniques has the potential to be implemented.
- Define which frequency (in the sonar range of frequency) give the better response and should be used to develop a proper whale detector.
- Collect new information about the target strength of different cetacean species during fishery survey.

- Identify physiological features that could influence cetacean target strength and be used as classifiers during real time operations, as previously done for fish.

To develop a protocol to calibrate omnidirectional sonars is a first important step towards the ultimate goal (Paragraph 3.6). This dedicated work will be edited in a report by the ICES SGCAL (Study Group on Calibration of Acoustic Instruments in Fisheries Science). Two methods will be used; one to accurately measure *in situ* TS of selected marine mammal species displaying their natural behavior while swimming freely, and the second method to observe and quantify ecologically important situations, such as feeding aggregations, and predator-prey interactions (See chapter 5; Bernasconi et al. 2011; Nøttestad et al. 1999, 2002; Axelsen et al. 2001).

The sparse nature of the literature regarding cetacean TS also has led to the review of whale target strength which is presented in Chapter 4. The review includes the scenario and the description of different hardware and software needed to develop and study the concrete possibility of reaching in the near future the proposed objective of an automatic active acoustic whale detector.

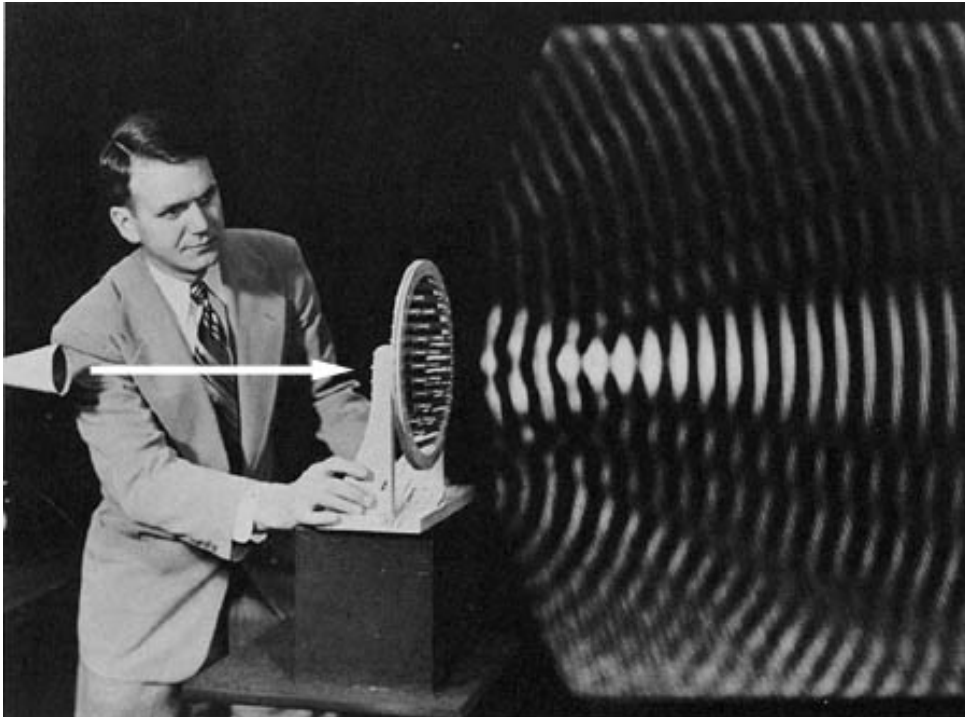
Chapter 5 (Bernasconi et al. 2011) describes and quantifies a valuable dataset on predator-prey interactions recorded off Namibia. A large group of dusky dolphins actively feeding on a large school of Cape horse mackerel was observed hydroacoustically with a vertically orientated scientific echosounder. The dolphins' behavior greatly affected the fish school dynamics and vertical distribution. The effects were quantified using available fisheries analysis methods. The dataset also provided important new information about the dolphin TS that was in general agreement with the few other available scientific studies on this subject (Au 1996; Benoit Bird et al. 2004, 2009).

In Chapter 6 (Bernasconi et al. *submitted*) I move on to apply active acoustic methodology to a more delicate and controversial topic: the mitigation of seismic activities to protect whales. The first approach to the subject was about the coverage of the water around the vessel. For this reason an omnidirectional sonar was chosen. This type of sonar has 360° radar like coverage. We could verify the effect of insonification angle over large targets such fin whales and obtain the TS range for this species. The most interesting results came by looking at the TS variation of selected animals. This could be linked to the respiration rhythms and patterns of an individual whale over time. The air contained in the lungs had a measurable effect on the recorded TS. A depth dependent model was tested on acoustic data coming from the whale swimming underneath the surface (between 5 and 15 m depth). Characteristic prints left by the whales on the sonar screen have been observed consistently during all performed surveys investigating this behavior. This observed behavioral aspect was suggested as important for further development for active acoustic detections of cetaceans (Nøttestad et al. 2010).

Chapter 7 links all the observations, from the first recordings of hunting dolphins to the developed depth dependency model of whales. In summer 2009 the TS of a Humpback whale was recorded acoustically with omnidirectional sonar, while the whale was diving between 190 and 230 m underneath the ship that was equipped with a multi-frequency scientific echosounder (18, 38, 70, 120 and 200 kHz). The acoustic data showed the potential usefulness of the model explored and presented in Chapter 6. This chapter opens a new door to explore further TS relationships with whales.

Sonar technology is constantly bringing new and valuable knowledge and a better understanding of marine ecosystems through non-invasive methods. As done for many years in fisheries biology, it will be possible to observe cetacean behavior with high resolution and prevent conflicts between whales and human activities. I believe it is now timely to test new ways for a concrete approach to conservation and management of whales and dolphins. We should not forget at the end of the day, that most species of whales and dolphins in the world's oceans are totally dependent on their "biological" sonar for hunting, navigation, communication and ultimately their own survival. No wonder, perhaps, that sonar technology may be a future blessing for marine science in general and whale and dolphin conservation purposes in particular.

CHAPTER 2



BASIC UNDERWATER ACTIVE ACOUSTICS

2. BASIC UNDERWATER ACTIVE ACOUSTICS

2.1 Historical notes

The origins of Sonar (SOund Navigation And Ranging), the use of actively transmitted pulses of sound to detect distant objects, date back to the start of World War I. However, the conceptual ideas that form the base of modern underwater acoustics have their roots deep in the past. The earliest reference to sound propagation beneath the sea surface was by Leonardo da Vinci. In 1490, two years before Christopher Colombo discovered America, he wrote “If you cause your ship to stop, and place the head of a long tube in the water and the outer extremity to your ear, you will hear ships at a great distance from you”. This earliest example of passive sonar was extremely simple and didn’t give any information about direction or intensity of the detected target. The simple idea of listening underwater was kept and applied in World War I with the adoption of a second tube. That enabled direction to be obtained and the bearing of the target to be determined. The first quantitative measurements of underwater sounds were probably made by a Swiss physicist, Daniel Colladon, and a French Mathematician, Charles Sturm with an experiment performed in Lake Geneva in Switzerland (1827). By timing the interval between a flash of light and the striking of a bell underwater, they determined the speed of sound underwater to a surprising degree of accuracy (Figure 2.1).

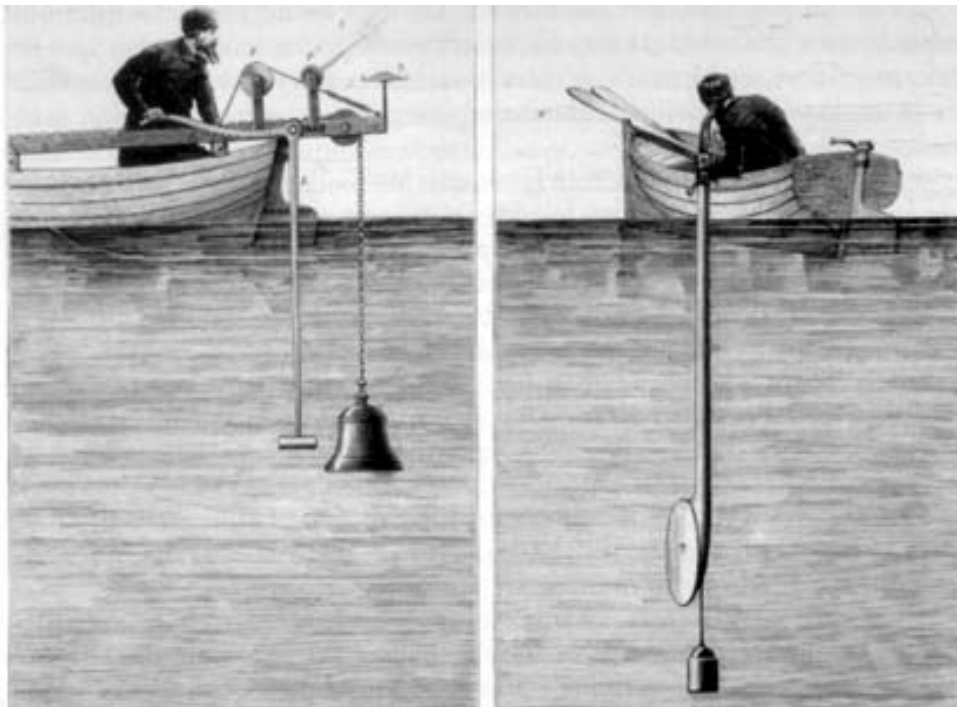


Figure 2.1 With their system, Daniel Colladon and Charles Sturm, could determine the speed of sound underwater to a surprising degree of accuracy.

Later on in the nineteenth century, a number of famous physicists of the time associated themselves indirectly with underwater acoustics through their interest in the phenomenon of transduction – the conversion of electricity into sound and vice versa. Fundamental to this was the 1880 definition of piezoelectricity - the ability of certain crystals, when physically stressed, to develop an electrical charge across certain pairs of crystal faces - a discovery commonly attributed to Jacques and Pierre Curie. It wasn't the clear aid to navigation and sea exploration that drove the development of active acoustic technology. It was the outbreak of World War I (WWI) that generated great interest for a tool that could prevent what Sir Winston Churchill described as the most dangerous of all man's occupations: the development of submarines. Due to technical problems related to the generation of high voltages required for the acoustic projector, during the First World War extensive use had been made of Leonardo's air tube for passive listening. The system was improved by the use of two tubes to take advantage of the binaural directional sense of a human observer. The so called MV device consisted of a pair of line arrays of 12 air tubes each, mounted along the bottom of a ship on the port and starboard sides and steered with a special compensator. It is remarkable the achieved precision that was able to be obtained of the bearing of a noisy target; untrained observers could easily accomplish the task with a precision of 5° (Weaver 1964).

It was soon after the end of WWI that the Germans published the first scientific paper about underwater acoustics (Lichte 1919). This paper described theoretically the bending of sound rays produced by slight temperature and salinity gradients in the sea, underlining their importance in determining target range. Longer ranges were predicted in winter than in summer, and the prediction was verified by measurements of transmission ranges in all seasons in six different areas. With the imminence of World War II (WWII), a large number of American vessels were made ready and equipped with both listening and echo ranging devices. By 1935, several fairly adequate sonar systems had been developed, including the recording echosounder which produced echograms on paper (Wood et al 1935). Once this instrument became commercially available at a reasonable cost, its potential as fishing aid was immediately clear. In 1933 the British skipper Ronnie Balls tested an echosounder on his herring drifter "Violet and Rose", reporting the work later in 1948. At the same time a Norwegian skipper Reinert Bonk was conducting similar investigations from his seiner "Signal". Bonk is credited with the first example of a fish echogram to be published. Other Norwegian investigators made notable contributions, publishing cod echograms (Figure 2.2a) generated using a magneto-strictive transducer onboard the research vessel "Johan Hjort" (Sund 1935). This research revealed many unsuspected features of fish distribution and, as a prelude to modern fisheries applications; in 1937 the Norwegians conducted acoustic surveys to map the distribution of Herring schools (Runnström 1937).

From a scientific standpoint, knowledge development in the years between WWI and WWII focused on understanding sound propagation in the sea. A period of rapid development occurred after WWII, when fishermen discovered the civilian application of acoustic techniques (Hodgson 1950; Hodgson and Fridriksson 1955).

The power and resolution of sonars continued to improve as new instruments were designed specifically for fish detection. In 1951 Simrad developed and presented the first ever fishing echosounder based on a military design. After a complete re-design in 1957 Simrad introduced the first commercial echosounder to the fishing world (Figure 2.2b) changing the ways and means of fishing and evolving it to become technology based. Since then, following a deal between Simrad and the Institute of Marine Research in Bergen, Norway, sonars have been used for many other purposes than military applications.

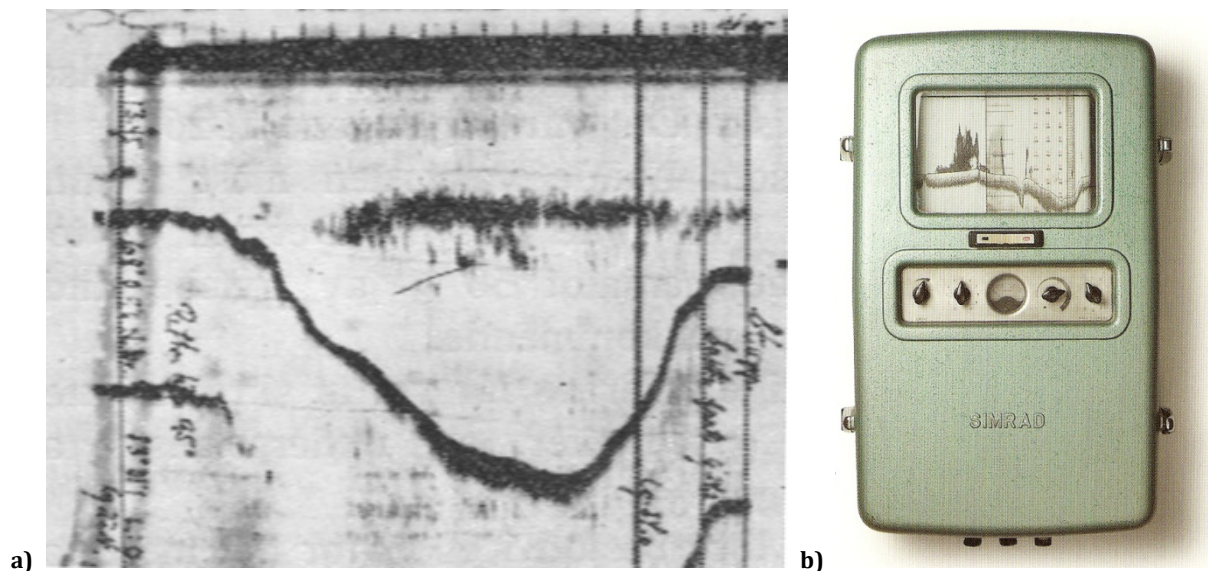


Figure 2.2: a) one of the first echograms presented by Sund (1935) and b) the first echosounder from Simrad, the Skipper Sounder, launched in 1957 it was small enough to be mounted in the wheelhouse.

2.2 Sound: basic concepts

The theory of sound propagation is similar in many aspects to that of light transmission. Both concern waves which propagate through a medium. Both are subject to scattering, reflection and absorption, which complicate the simple idea of waves transmitting energy in a homogeneous, lossless medium as is explained in elementary physic textbooks. In water, sound can be transmitted over much longer ranges than light, but water is nevertheless an imperfect acoustic medium. Energy is removed (scattered and absorbed) from the sound wave by suspended solids, biota or entrained gas, or simply converted to heat by physical absorption. All these effects need to be considered in fisheries

applications, where the usual intention is to deduce quantitative features of remote targets from the acoustic signal detected by sonar.

2.2.1 Sound propagation

Sound waves are used for detection of underwater objects because they travel relatively long distances without being attenuated too severely as are electromagnetic waves (radio, radar and light). Sound is transmitted through waves by the periodic compression and expansion which is permitted by the elasticity of water. The sonar transducer face vibrates and creates alternating zones of high and low pressure that propagate outwards from it through the water. This results in a travelling pressure wave as illustrated in Figure 2.3 for the case of sinusoidal variations at one frequency.

To simplify and describe a sound wave we start with three fundamental parameters:

- λ the wavelength: distance between two maxima on the sound wave (cm).
- f the frequency: the number of maxima which pass per second (kHz).
- c the sound velocity: the distance one maximum travels in one second (m/s)

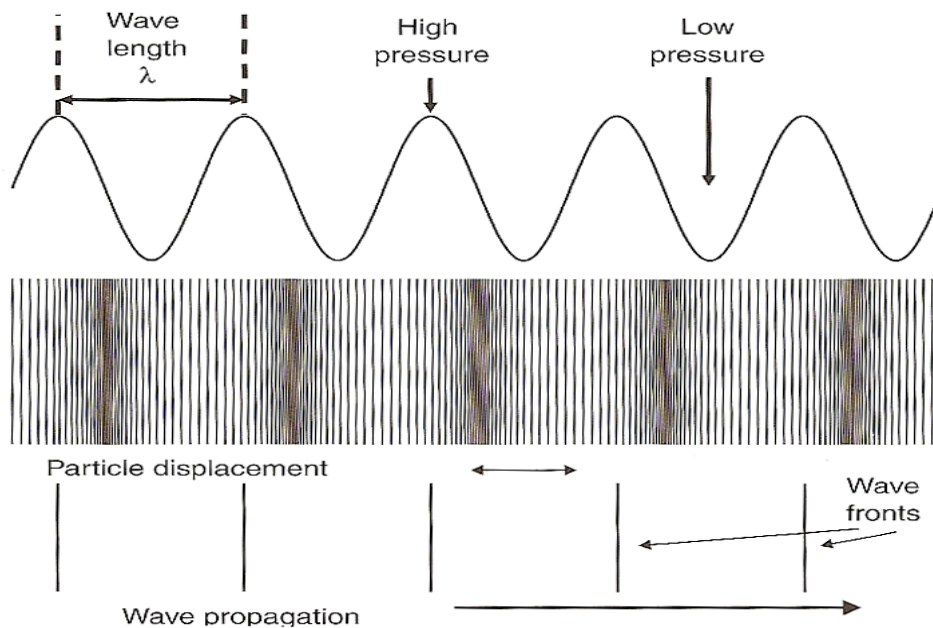


Figure 2.3: Illustration of a propagating sound wave. Top: the pressure varies cyclically as a sine wave; λ is the wavelength. Middle: the particle displacement is out of phase with the pressure. Bottom: the wave-fronts are lines which follow the maximum pressure (from Simmonds and MacLennan 2005).

Between the 3 parameters λ , f and c exists the relationship, valid for all kind of waves, described by the equation:

$$c = \lambda \times f \quad (2.1)$$

The speed of sound (c) in water (1500 m/s) is approximately five times greater than in air (300 m/s). This makes sound waves the best ocean scanning option guaranteeing long range coverage.

<i>Sound waves in water of $c= 1500$ m/s</i>	
Frequency (kHz)	wavelength λ (cm)
38	3.9
70	2.1
120	2.5

For the sound wave we define T , the period: time between two maxima in the wave. Since the frequency f is the number of maxima passing in one second we have

$$T = \frac{1}{f} \quad (2.2)$$

A sonar transducer transmits the sound waves in short pulses comprising a number of periods

$$\tau = n \times T \quad (2.3)$$

where τ is the pulse duration and n the number of periods in one pulse. For example a 0.6 ms pulse at 38000 Hz will have a period T of 0.026 ms and 23 periods in one pulse.

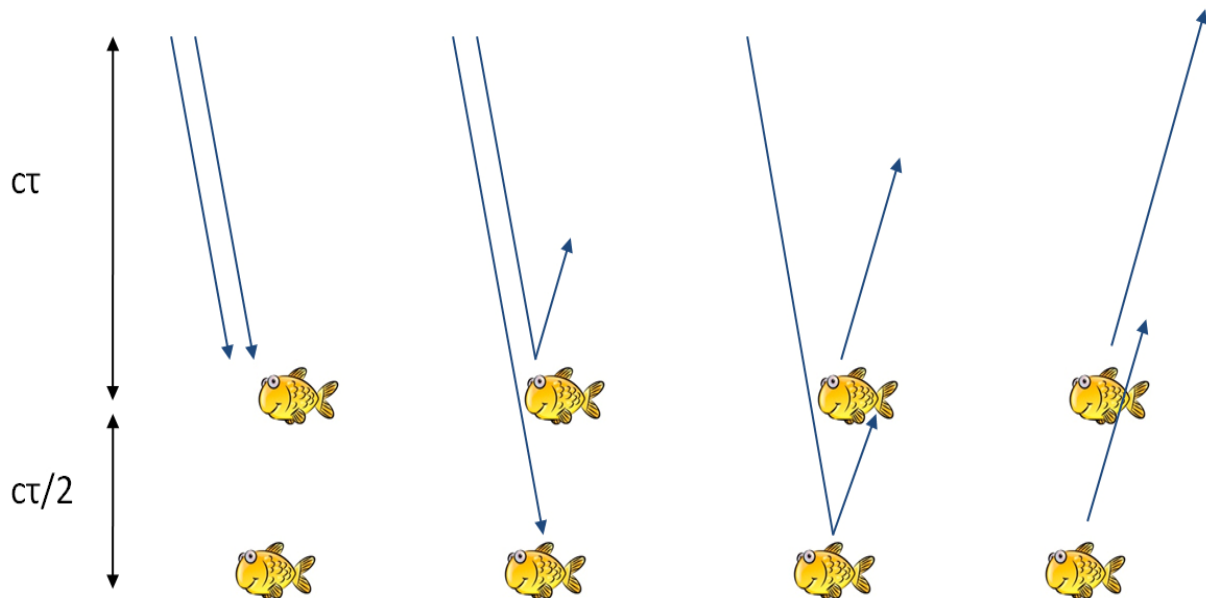


Figure 2.4: physical limitation connected to pulse duration, but not related to the transmitted signal, can interfere while trying to obtain clear single target detections.

As the pulse travels through the water it occupies a length $c\tau$. Figure 2.4 illustrates how the echoes from two point targets can be distinguished from each other if the targets are separated with a distance greater than $c\tau/2$. We refer to $c\tau/2$ as the resolution of an acoustic pulse. The factor $1/2$ enters because the sound pulse travels both directions, down and up.

The $c\tau/2$ relation is used to resolve the echoes from biomass volumes, where it represents the depth interval which at a given instant of time contributes to the echoes.

2.2.2 Sound pressure and intensity

An important feature of the travelling sound pressure wave is that it transports energy from one place to another with intensity I that represents the energy flux per unit time. In the International System of Units (SI) pressure is expressed in

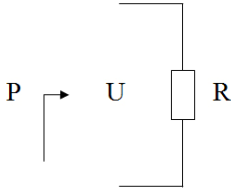
$$1 \text{ Pascal (Pa)} = 1 \text{ Newton/m}^2$$

and it is therefore convenient to use the Pascal unit in mathematical calculations. However, for convenience, measurements of sound pressure levels in the sea are expressed in decibels (dB) relative to 1 micro Pascal (dB/ μ Pa). The use of the dB unit in acoustics is convenient because of the necessity to work with very small quantities of energy and is treated in detail in the next paragraph (2.2.3).

The sound intensity is defined as the energy passing through a unit area per second. For a continuous sound wave, intensity is related to pressure by:

$$I = \frac{p^2}{c\rho} \quad (2.4)$$

where I is the intensity (W/m^2), p is the pressure (Pa), ρ is the water density (kg/m^3) and c is the speed of sound (m/s). To understand this equation it can be useful to look at the theory of electrical circuits, which has a corresponding equation for the power dissipated in a resistor:

$$P = \frac{U^2}{R} \quad (2.5)$$


The diagram shows a simple electrical circuit. On the left, there is a vertical line representing a wire. From this line, a horizontal line extends to the right, ending in an arrow pointing towards a rectangular box labeled 'R', which represents a resistor. Above the resistor, there is a horizontal line that connects to a vertical line on the right. This vertical line then extends downwards and connects back to the original vertical line on the left, completing the circuit. The voltage across the resistor is labeled 'U' between the top and bottom horizontal segments. The power entering the resistor is labeled 'P' at the start of the horizontal segment.

where R is the resistor value (ohm), U is the voltage across the resistor (V rms) and P is the power dissipated in the resistor (W). As a consequence of this correspondence between acoustic and electrical theory, the product $c\rho$ is named acoustic impedance (Z).

2.2.3 The decibel

Acoustic measurements are often quoted in dB rather than the more correct SI units for pressure, intensity etc. This is because the numbers involved can be very large or very small, covering many orders of magnitude. It is important, for sonar applications, that the relationship between electrical voltages and acoustic sound pressure is understood. This will give a reading key to follow the sonar raw data conversion process described in paragraph 4.6 and applied in chapters 6 and 7.

The dB is a dimensionless unit for representing the ratio of two values. In the case of power, the number n of dB is 10 times the logarithm of the power ratio:

$$n = 10 \log_{10} \left(\frac{P_2}{P_1} \right) \quad (2.6)$$

where P_1 and P_2 are two power values and n is the number of dB. It is convenient to let P_1 be a reference power level of 1 Watt. Then all power values P_2 can be represented by a number n of dB relative to 1 Watt. The dB notation is also used to express the ratio between two electrical voltages. Since the voltage U across a resistor is related to the dissipated power P by (2.5) we can use the previous dB definition (2.6) and obtain

$$n = 10 \log_{10} \left(\frac{P_2}{P_1} \right) = 10 \log_{10} \left(\frac{\frac{U_2^2}{R}}{\frac{U_1^2}{R}} \right) = 20 \log_{10} \left(\frac{U_2}{U_1} \right) \quad (2.7)$$

If U_1 is taken as a reference voltage of 1 V, then all voltages U_2 can be represented by n dB//1V. The following Table shows some examples.

U (V)	n (dB // 1V)
0.1	-20
1	0
2	6
10	20
100	40
1000	60

At this point the mentioned relationship between electrical and acoustic values can be summarized with a table showing their proportionality:

<i>Electrical</i>	<i>Acoustic</i>
power (W)	sound intensity
voltage (V)	sound pressure (Pa)

Recapping, looking at the sound intensities: the ratio of two sounds intensities I_1 and I_2 can be represented in dB by:

$$n = 10 \log_{10} \left(\frac{I_2}{I_1} \right) \quad (2.8)$$

the dB notation of sound pressure is subsequently derived by (2.8) and (2.4) as follows:

$$n = 10 \log_{10} \left(\frac{I_2}{I_1} \right) = 10 \log_{10} \left(\frac{\frac{p_2^2}{\rho}}{\frac{p_1^2}{\rho}} \right) = 20 \log_{10} \left(\frac{p_2}{p_1} \right) \quad (2.9)$$

When specifying a sound pressure value in the sea it is a widely used practice to let p_1 be a reference pressure of 1 μPa . Then all the pressure p_2 can be represented by a number n of dB//1 μPa (see table below).

$p \text{ (}\mu\text{Pa)}$	$n \text{ (dB // 1 } \mu\text{Pa)}$
0.1	-20
1	0
2	6
10	20
100	40
1000	60

2.2.4 Transmission Loss

The sea with all its boundaries is a complex medium for the propagation of sound, with its internal structure and upper and lower surfaces that generate many diverse effects upon the sound transmitted in the water by a transducer. While traveling underwater, a sound signal becomes delayed (slowed down), distorted, and weaker. The sonar transmission loss parameter describes quantitatively the weakening of sound between a point 1 meter from the source and a point at a distance in the sea. The transmission loss is due to two distinct factors: the geometrical spreading and the absorption loss.

Geometrical spreading

Consider a small source of sound travelling in a homogeneous, unbounded, lossless medium. In this simple propagation condition, the power generated by a transducer is radiated equally in all directions so as to be equally distributed over the surface of a sphere surrounding the source. Since there is no loss in the medium, the power P crossing all such spheres must be the same. Power equals intensity times area:

$$P = 4\pi r_1^2 I_1 = 4\pi r_2^2 I_2 \quad (2.10)$$

where r_1 and r_2 are the radii of two spheres and I_1 and I_2 are the sound intensities at these radii. From this it follows that the ratio between the two sound intensities is

$$\frac{I_2}{I_1} = \frac{r_1^2}{r_2^2} \quad (2.11)$$

This way of propagating of a wave away from the acoustic source point is called spherical spreading. The intensity decreases with the square of the range. Sound waves radiated from a transducer can be then described as follows:

In the transducer near field (see paragraph 3.2) the wave structure is complicated, and there is no need of a discussion about it in this work. In the transducer farfield, the zone of interest for biological applications of active acoustics, the sound waves take the form of expanding spheres. If we look at the sound intensity on a straight line from the transducer it follows the same law as described above (equation 2.11). Expressed in dB the geometrical spreading loss is:

$$TL_s = 10 \log_{10} \left(\frac{I_2}{I_1} \right) = 20 \log_{10} \left(\frac{r_2}{r_1} \right) \quad (2.12)$$

and with r_1 set to a reference distance of 1 meter the spreading loss is then:

$$TL_s = 20 \log_{10} (r) \quad (2.13)$$

Absorption

When a sound wave propagates through water, part of the wave energy is absorbed by the water and converted to heat. For each meter a certain fraction, A , of the sound intensity is lost. This phenomenon can be described by the formula:

$$dI = -AI \, dr \quad (2.14)$$

where dI is the change in intensity during dr which is a small range increment, I is the sound intensity at range r and A is the loss factor. The solution of this differential equation is:

$$I(r) = \frac{I_1}{e^{-Ar}} e^{-Ar} = I_1 e^{-A(r-r_1)} \quad (2.15)$$

that, expressed in dB, represents the absorption loss TL_a as:

$$TL_a = 10 \log_{10} \left(\frac{I_1}{I} \right) = \alpha(r - r_1) \quad (2.16)$$

where

$$\alpha = 10 A \log_{10}(e) \quad (2.17)$$

The absorption loss TL_a is proportional to the distance travelled $(r-r_1)$. For each traveled meter a certain number of dB are lost. If r_1 is taken as a reference distance of 1 m, and if the range r is much larger than 1 m, the absorption loss will be

$$TL_a = \alpha r \quad (2.18)$$

α is named the absorption coefficient. This value is generally calculated with reference to knowledge of the environmental conditions in the water. One formula used to calculate it was developed by Francois and Garrison (1982) and illustrated in Figure 2.5. α is obtained as the three frequency-dependent components representing the absorption due to boric acid, magnesium sulphate and water viscosity.

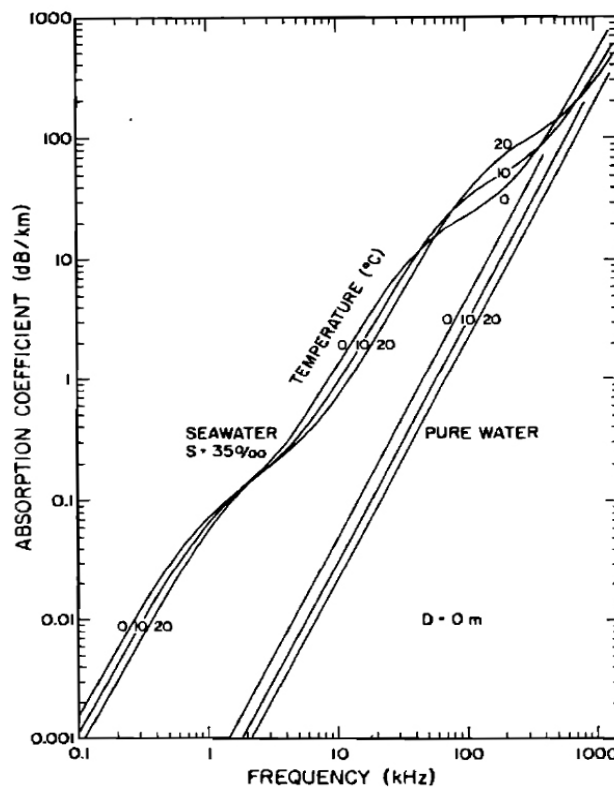


Figure 2.5: Seawater absorption at three temperatures (°C) for frequencies between 100 Hz and 1 MHz as presented by Francois and Garrison (1982) for Salinity of 35‰ and pH 8. The pure water lines were added.

The absorption coefficient increases strongly with frequency and it also depends on salinity, temperature and pressure. The very strong dependence on frequency has an important consequence: for detection at long range a low frequency must be used.

Total transmission loss:

In conclusion, when a sound wave travels from range r_1 to range r_2 it suffers both geometrical spreading and absorption. The ratio of sound intensity is then found as

$$\frac{I_2}{I_1} = \frac{r_1^2}{r_2^2} e^{-A(r_2-r_1)} \quad (2.19)$$

in terms of dB the resulting total one way transmission loss will be

$$TL = TL_s + TL_a = 20 \log_{10}(r) + \alpha r \quad (2.20)$$

2.2.5 Sound speed

As with the absorption coefficient, the sound speed c depends on the water temperature, salinity and depth and can be predicted by empirical equations. The algorithms used for estimating sound speed from hydrographic measurements in the ocean were developed by Del Grosso (1974) and by Chen and Millero (1977), and are still considered international standards. Mackenzie (1981) re-examined those equations later concluding that the work of Del Grosso provides the best agreement with measurements of long-range propagation. It was indeed clear that c could be estimated from physical parameters to better than 1%.

In the case of sonars that transmit horizontally, refraction is important because sound speed changes with depth. The temperature is normally highest at the surface, so the sound speed decreases with depth and the rate of change is most rapid at the thermocline. As a result, waves propagating near the surface bend downwards because the lower part of the wave-front is in cooler water and travels slower. When considering this effect, it is easier to understand what happens to the sound if we think of the acoustic wave's signals as travelling rays. A ray is a line which is everywhere perpendicular to the wave-front. The downwards bending caused by refraction limits the horizontal range at which a target can be detected. We can see this by simulating the ray tracing in various directions from the sonar transducer (see paragraph 4.5). When a ray meets the surface or the bottom, it continues as a reflection. The angles from the surface to the incident and reflected ray are the same. Some energy will be scattered in other directions, especially at the seabed if it is rough, but the simple reflection law is good enough for the ray diagram to show any hidden zone where targets will not be detected. Ray bending is particular severe when the gradient of the sound speed is uniform (Figure 2.6a). As a consequence of the thermocline position during the year, ray bending has a strong effect on the performance of sonars.

An interesting note relates to the Sound Fixing And Ranging channel (SOFAR) or deep sound channel (DSC) discovered and described by Ewing and Worzel in the 40s (Munk et al. 1995). The SOFAR channel is a horizontal layer of water in the ocean at the depth at which the speed of sound is minimal; it acts as a waveguide for sound, and low frequency sound waves within this channel may travel thousands of miles before dissipating. Near the surface, the rapidly falling temperature causes a decrease in sound speed, or a negative sound speed gradient. With increasing depth, the increasing

pressure causes an increase in sound speed, or a positive sound speed gradient. The refraction within these gradients has the strange effect of bending shallow waves downwards and deep waves upwards, confining the acoustic energy. Low frequency sounds propagate in the SOFAR channel with little change over hundreds of kilometers, and it is said that the great whales use it to communicate over long distances (Schevill et al. 1964).

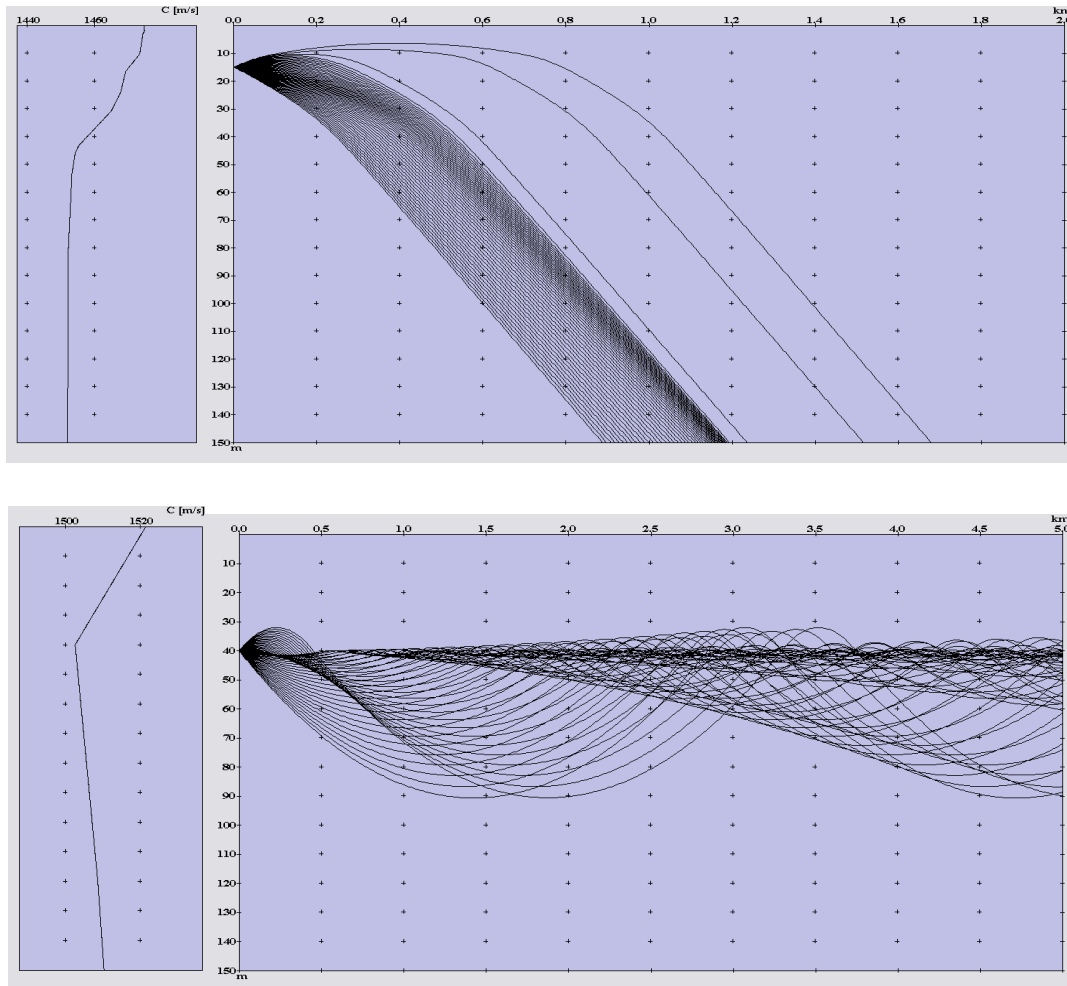


Figure 2.6 a) Severe ray bending due to uniform decrease of sound speed with depth b) Thermocline effect over a transmitted pulse generated at 40 m, the sound is channeled.

2.3 Transducers and beams

Transducers convert electrical energy to acoustic energy and vice versa, and are a vital component of a sonar system. Generally mounted on the vessel hull, the transducer radiates sound waves into the water and receives echoes back from submerged objects. The same transducer is usually used to send and receive signals (monostatic system), but in very specialized equipment it is possible to find two separated transducers (bistatic systems). The transducer can have many forms, but in all cases has a face which is the active area. This face vibrates with the working frequency of the sonar. The

movements are very small, for example a transmitter pulse of a high performance 50 kHz echosounder for fish detection generates vibrations of 1 μm (0.001 mm).

Various materials have the ability to convert electric energy into acoustic energy and vice versa. Today, piezoelectric ceramics are the most widely used materials. An alternating voltage, applied to electrodes on two opposite sides of a piezoelectric disc, causes the disc to vibrate and thus radiate a sound signal. Vice versa, if the piezoelectric disc is placed in a sound field and set into vibration, it generates an electric voltage across the disc. Manufacturers produce piezoelectric ceramics of different shapes (discs, rings, tubes, spheres) for application in various transducer types.

A sonar system radiates sound in a beam pointing in a fixed direction (e.g. echosounder are usually orientated downwards). Depending on the application, different transducers have different beam characteristics. Generalizing, we can describe them as narrow or wide.

A narrow beam is the best choice for:

- I. Long range detection. Concentrating the transmitted energy, a narrow beam is less sensitive to noise during the reception of the signal.
- II. High performance transducers with high transmission power; this characteristic is connected with the large dimensions of the transducer.
- III. Accurate bottom mapping.
- IV. Single fish resolution. Some scientific applications, such as target strength measurements require distinguishing between very close single targets so that each single echo can be studied.

A wide beam is the best choice for:

- I. Detection of widely scattered objects in the upper water layers. A wide beam covers a large volume of water and consequently detects more fish.
- II. Operation during severe vessel roll and pitch.
- III. Low costs. Wide beam transducers are smaller and consequently cheaper.

The beamwidth of a transducer is determined by the transducer size and the sound wavelength, it can be roughly estimated by:

$$\beta = \frac{\lambda}{L} \quad (2.21)$$

where L is the effective diameter of the active area on the transducer face (side for a rectangular area), β the beamwidth in radians and λ the wavelength. This equation is not valid for very small transducer, i.e. $L < \lambda$.

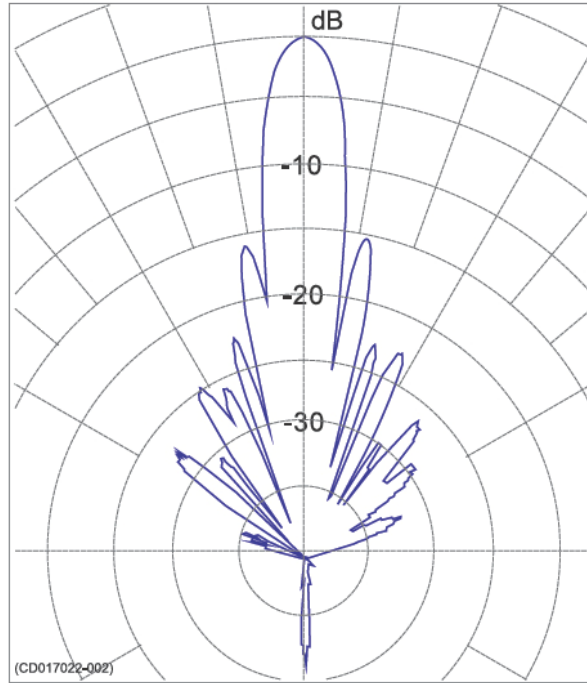


Figure 2.7: Typical graphical visualization of a transducer beam pattern. Usually the beam pattern is shown as a polar plot of the sensitivity against direction.

2.3.1 The beam pattern

The beam pattern of a transducer, in the active mode, describes how the sound energy is radiated in different directions. Most often the beam pattern is represented by a polar plot as shown in Figure 2.7. Important features in the beam pattern are the main lobe, the side lobes and the back radiation.

The transducer beamwidth is defined as the angle between the two points where the radiation is - 3 dB from the maximum level (Figure 2.8). As a rough rule of thumb the beamwidth is related to the size of the transducer by (equation 2.21). Piezoceramic transducers have equal beam patterns in the active and passive mode. When the transducer is used just to receive signals it acts as a hydrophone and its beam pattern represent the sensitivity. In most applications the side lobes are unwanted. Transducer tapering or shading is a technique used to reduce side lobe effects on the received signal. In a multi element transducer this is achieved by giving more power to the central elements than to the peripheral ones. The tapering is performed by utilizing a transformer with a number of taps, connected to the different elements. This technique prevents the unwanted effect of ghost echoes that would bias biomass estimation or target strength measurements (Figure 2.9).

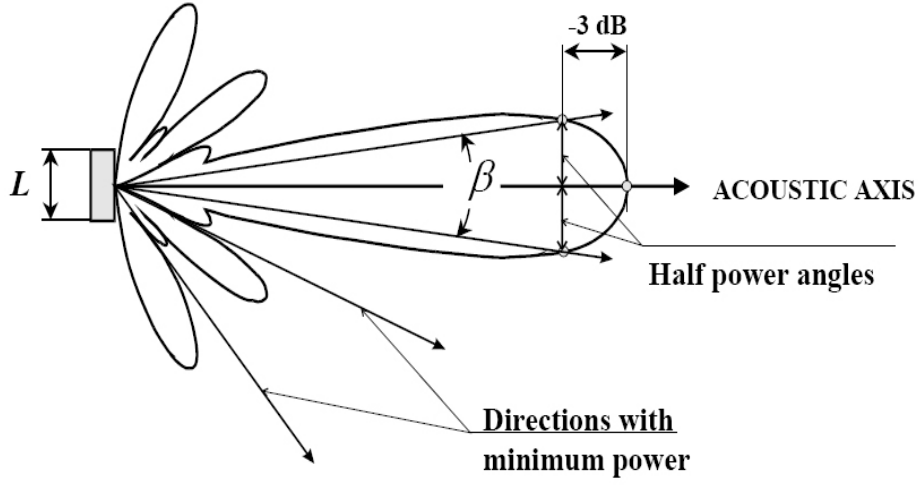


Figure 2. 8: Schematic representation of the transducer beamwidth (β) and the -3dB maximum sensitivity point.

2.3.2 The equivalent beam angle

Another measurement of the beam pattern is the equivalent beam angle, ψ , which sometimes is called the transducer reverberation angle. ψ is the solid angle at the apex of the ideal conical beam which would produce the same echo-integral as the real transducer when the targets are randomly distributed in the space. This conical beam would be like an ideal search light with $b=1$ for any direction inside the cone, and $b=0$ elsewhere (Simmonds 1984). ψ is a usual quantity to evaluate, but is not physically realizable in practice.

To describe the beam pattern in space, we use spherical polar coordinates which require two angles, θ and φ (measured in steradians), to determine the direction of any point P relative to the transducer origin O. θ is the angle of OP from the acoustic axis, and φ is the azimuthal angle of OP projected onto the plane of the transducer face. A simplified mathematical expression of ψ can be defined as:

$$\psi = \int_{4\pi} b^2(\theta, \varphi) \quad (2.22)$$

The integral is taken over the entire beam pattern, which is normally supposed to be the hemisphere in front of the transducer ($0 < \theta < \pi/2$; $0 < \varphi < 2\pi$) and b is defined in terms of pressure. Therefore, the equivalent beam angle is a measure of the width volume insonified by the transducer. It takes account of the signals from all targets, including those in the side lobes. However, for most sonar systems less than 1% of the transmitted energy is projected outside the main lobe.

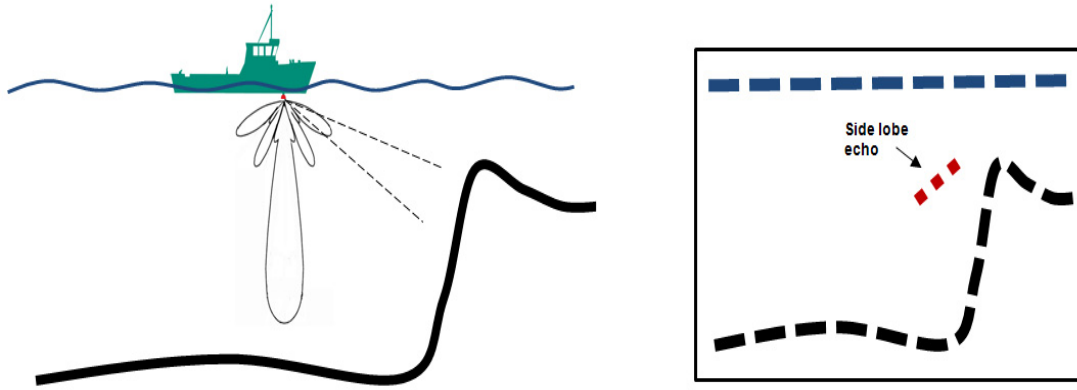


Figure 2.9: schematic example of the unwanted effect that could be generated by side lobes. Ghost echoes which do not originate from targets within the main lobe usually show up near to the rising slope of the bottom hit by a side lobe.

2.3.3 Pulse and ranging

When sonars transmit into the water they produce a short burst of sound called a pulse or ping, consisting of several cycles at the sonar operating frequency. In Figure 2.10 are illustrated 19 cycles generated by a 38 kHz transducer. The pulse duration (time from start to finish) is $\tau = (19/38000) = 0.5$ ms. If the sound speed is 1500 m/s, the pulse length in the water at any time is $L_p = c\tau = 75$ cm. The envelope of the pulse is the curve which shows the amplitude of the oscillations. The envelope in figure 2.8 is a rectangle because the amplitude is constant during the transmission.

When a transmitted sound pulse encounters a target, some energy is reflected as an echo. The echo is reflected back to the transducer and is received after a time t_e . The range R between target and transducer is obtained by measuring t_e . The two way path length is $2R$, so:

$$t_e = \frac{2R}{c} \quad (2.23)$$

$$R = \frac{c \times t_e}{2} \quad (2.24)$$

Suppose that there are two targets at range R_1 and R_2 . In order to resolve the targets and measure them individually, the range difference ($R_2 - R_1$) must be large enough for the two echoes not to overlap (as described in paragraph 2.2.1).

In practice the pulse duration should be selected according to the application:

Short pulses for fine vertical resolution

- I. Single target detection in a congregation of targets.
- II. Detection of target close to the bottom.

- III. Recording of detailed structure of a biomass layer.
- IV. Detection of single fish in plankton layers.

Long pulse for long range

- I. A long pulse allows a narrow receiver band pass filter, which means less noise.
- II. A long pulse gives a large bottom echo.
- III. A long pulse gives a large echo from biomass layers.

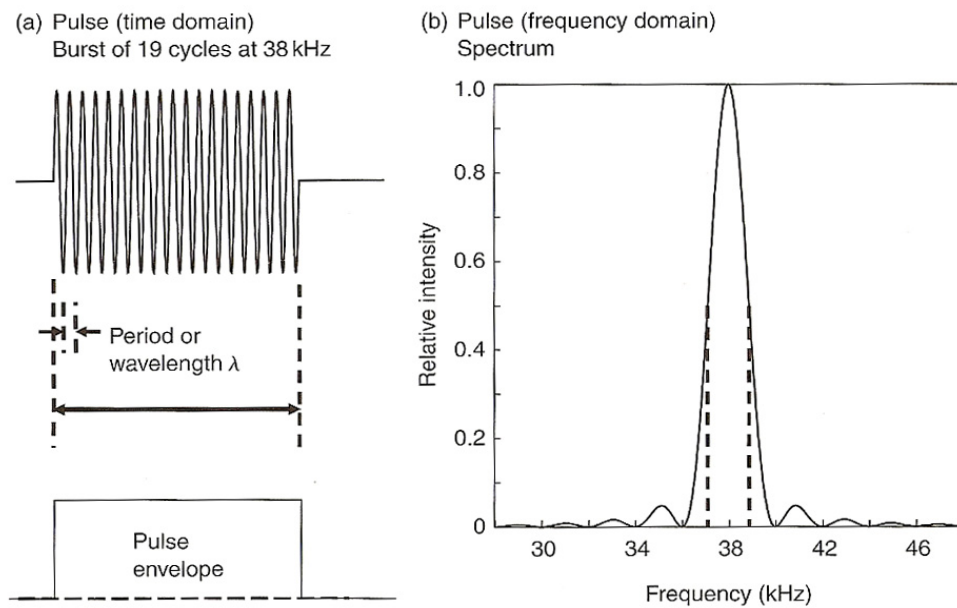


Figure 2.10: Illustration of a transmitted sonar pulse. As observed at the transmitter output, (a) the pulse is 19 cycles at 38 kHz (duration is 0.5 ms) in the time domain. In water the pulse length is 0.75 m when c is 1500 m/s. The envelope is the curve joining the maximum amplitudes. (b) In the frequency domain, the spectrum shows the frequency composition as the intensity or power relative to the peak value. The broken lines indicate the bandwidth between half power points, 1.8 kHz in this case (from Simmonds and MacLennan 2005).

2.4 Acoustic scattering

When a sonar ping hits a target, some of its energy is scattered, generating a secondary sound wave which propagates in all directions away from it. Reflection that occurs at a large smooth surface instead is particular, the secondary (reflected) wave is in this case confined to a single direction. More generally, acoustic scattering occurs wherever there is a spatial change of the acoustic impedance $Z = \rho c$ (see paragraph 2.2.2). The proportion of the incident energy in the reflected wave is determined by r_b ,

the coefficient of reflection at a boundary (Tucker and Gazey 1966). If Z_w and Z_r are respectively the acoustic impedances of the water and of the reflector, then:

$$r_b = \frac{(Z_r - Z_w)}{(Z_r + Z_w)} \quad (2.25)$$

The greater the change of Z across a boundary, the stronger is the scattered wave. The remaining energy passes through the boundary as the transmitted wave.

The energy reflected back towards the sound source is said to be backscattered. This component of the total scattering provides the sonar echo in the monostatic case. Small targets reflect energy in all directions, while large targets reflect most strongly in one direction. This applies to almost all active echosounders and sonars.

2.4.1 Target strength

The target strength is a logarithmic measure of the proportion of the incident energy which is backscattered by a target. The target may be a fish, a sonar reflector, a submarine etc. A target hit by a sound wave reflects the sound more or less uniformly in many directions. In our case only the acoustic energy travelling back to the transducer is of interest.

To understand better the nature of target strength we should start to understand its linear related quantity, the backscattering cross section (σ_{bs}) which is a more meaningful parameter in physical terms. σ_{bs} is measured in units of area (m^2) and it is defined in terms of intensities of the incident and the backscattered waves. Suppose I_i is the intensity of the incident wave at the target, and I_{bs} is the intensity at the midpoint of the backscattered pulse. I_{bs} will depend on the distance R from the target at which the intensity is measured. Assuming the target is outside the nearfield of the transducer the backscattering cross section is defined by the relationship:

$$\sigma_{bs} = \frac{R^2 I_{bs}}{I_i} \quad (2.26)$$

The inverse-square law of energy spreading means that ($R^2 I_{bs}$) is the same at any range, thus equation (σ_{bs}) gives a constant for a given target. Target strength is then expressed by converting the linear σ_{bs} to dB according to the formula:

$$TS = 10 \log_{10}(\sigma_{bs}) \quad (2.27)$$

The logarithmic TS is convenient to describe the great difference of size between aquatic organisms, which cover many orders of magnitude, from microscopic plankton to great whales. A modest span of dB is indeed sufficient to describe the target strength of all these creatures. For almost all fish, TS is

within the range -60 dB to -20 dB. The equivalent back scattering cross sections span four orders of magnitude, from 0.000001 to 0.01 m². To calculate σ_{bs} from TS:

$$\sigma_{bs} = 10^{\left(\frac{TS}{10}\right)} \quad (2.28)$$

The concept of logarithm units may seem rather strange to those not familiar with fields such as electrical engineering where their use is common. For this reason it is easier to think about the use of σ_{bs} which can be conceived as a physical area and related with the size of the target. Furthermore TS is more often used in practical work which involves calculation with real data, to provide numerical values within a convenient range. It is important anyway to remember that TS is a measure of a ratio. To say that one target is 3 dB more than another means that the stronger scatter backscatters twice the energy as the other; if the difference was 6 dB, the scattered energy ratio would be four times the other and so on. A -20 dB target, a large tuna perhaps, produces and echoes 10000 times as strong as one of -60 dB, such as a small sprat of about 4 cm in length.

2.4.2 Target shape and orientation

With the exception of a perfectly spherical target, or one that is very small compared to the wavelength, the scattered sound field depends on the shape of the target and how it is positioned relative to the incident wave direction. The target strength is still defined in the same way, but in general it is a function of shape and orientation as well as the material properties of the target. In this thesis we are particularly interested in cigar shaped objects, namely objects that are long compared to their width and height. This description is relevant to the swimbladder (the dominant reflecting organ in fish) and to fish bodies. With appropriate considerations, this concept will be applied and be the basis of a study regarding cetacean body reflectivity where the main reflective organ seems to be the lungs (Love 1973; Au 1996; Nøttestad et al. 2010). It is known that the target strength of such objects is strongly influenced by the tilt angle. This angle is defined as the angle between the long axis of the object and the incident wave front. In the case of asymmetrical targets like fish, it is necessary to distinguish head-up and head-down orientations for which the tilt angle are, respectively, positive and negative. As it will be shown in Chapters 5 and 6, a cetacean's body responds in the same way to insonification, but the different morphology and swimming dynamics generate a more complex acoustic response.

Figure 2.11 suggests an explanation as to why the tilt angle should have such a pronounced effect on acoustic scattering. When the transmitted pulse interacts with a long and thin target such as a swimbladder or a mammal lung, the energy in the reflected wave changes as the target tilts.

Firstly the apparent size of the target (its cross section), as seen from the transmitting transducer, decreases as the tilt angle increases. Secondly, while the apparent size varies as the cosine of the tilt angle, the echo energy may change even more rapidly because of interference between wavelets reflected from different parts of the target.

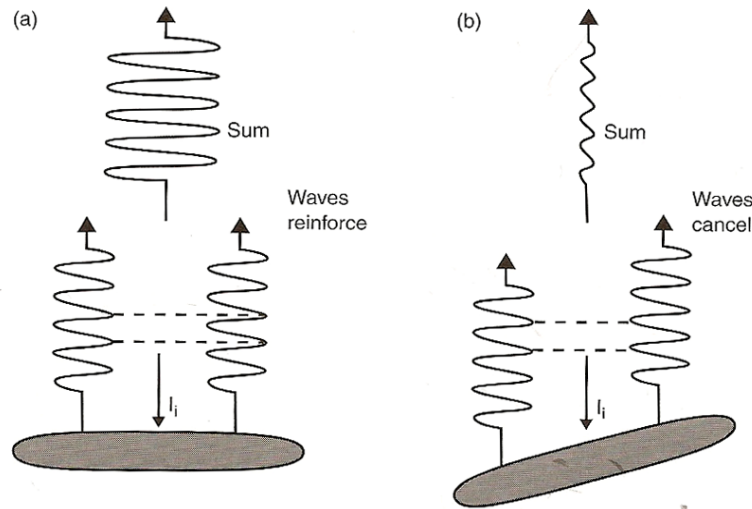


Figure 2.11: Effect of tilt angle on the echo from an oblong target, e.g. a fish swimbladder. Destructive interference reduces the echo amplitude when the path difference between opposite ends of the target is a substantial fraction of a wavelength (from Simmonds and MacLennan 2005).

When the target is parallel to the incident wavefront, as in fig 2.11a, all the reflected wavelets are in phase and they reinforce each other. When the target tilts, the wavelets originating at opposite ends of the target become progressively out of phase and the summed amplitude is reduced eventually to zero in the case of the wavelets that are exactly out of phase.

2.4.3 Volume/area scattering coefficient

When targets are very small and there are many of them in the sampled volume, their echoes combine to form a received signal which is continuous with varying amplitude. It is not possible to resolve single targets in this situation, but the echo intensity still provides a measure of the biomass in the water column. Its basic acoustic measurement is called the volume backscattering coefficient (s_v) and is defined by:

$$S_v = \sum \frac{\sigma_{bs}}{V_0} \quad (2.29)$$

where the sum is taken over all the discrete targets contributing to echoes from V_0 , the sampled volume. Its logarithmic equivalent is the volume backscattering strength $S_v = 10 \log_{10} (s_v)$ the unit of

which is $\text{dB}/1\text{m}^{-1}$. When we average s_v over a larger volume than V_0 , its logarithm equivalent is called the mean volume backscattering coefficient (MVBS), a measure commonly used for plankton aggregation studies. In figure 2.12 the echo integration concept over an insonified volume is simplified.

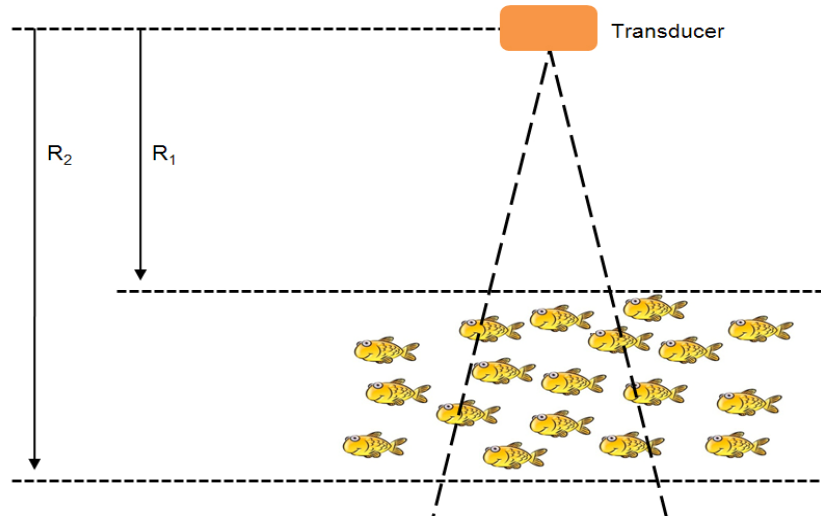


Figure 2.12: Principles of echo integration are based on the identification of the backscattering layer that defines the volume that will be sampled and measured in post processing (in this case in the range between R1 and R2).

Another way to describe the effect of acoustic layers on the response is the so called area backscattering coefficient (s_a). It is defined as the integral of s_v with respect to depth through the layers. This parameter is commonly used in fishery acoustics, where echo-integrators (sonars for which output is connected to a device which accumulates the energy of the received signals) provide data in terms of one layer over another. The basic SI unit for s_a , as defined above is m^2/m^2 , meaning the integrated σ_{bs} per square meter over the surface. There are various scales used to represent s_a . The standard in fisheries is the Nautical Area Scattering Coefficient (NASC) for which we use the symbol s_A and which can be defined by the conversion formula:

$$s_A = 4\pi(1852)^2 s_a \quad (2.30)$$

All the conversion factors between one parameter and another can be defined clearly by using definitive symbols as recommended by MacLennan et al. (2002).

2.5 The sonar equation

All the phenomena related to underwater sound propagation, described in the previous paragraphs, can be conveniently grouped together and resolved in a single form: the so called sonar equation. This equation considers the relationship between the various parameters and ties together the effect of the

medium, the target and the equipment. The essential and simple sonar equation has two practical applications:

- I. The prediction of performance of sonar equipments of known design.
- II. The design of new sonar.

The sonar equation is based on a basic equality between the desired and undesired portion of the received signal, when the function of the sonar is performed. These involve the reception of acoustic energy occurring in a natural acoustic background. Of the total energy received at the transducer, a portion may be said to be desired and is called the signal. The rest of the energy is undesired and is named the background noise. The engineers' objective is to find the means for increasing the overall response of the sonar system to the signal and to decrease its response to the background noise, and consequently increase what is called the signal-to-noise ratio.

For the goal of analyzing and describing the backscattering response from marine organisms, in this thesis I will use a simplified sonar equation, avoiding the use of Greek letters and subscripted symbols - However, a more detailed sonar equation will be used in paragraph 3.6.2 for calibration purposes. All the parameters are levels in dB relative to the standard reference intensity of 1 μ Pa. It should be noted that there are some differences in the application of the equation if the aim of using it is for single target detection or volume backscattering estimation (this aspect is discussed further in paragraph 3.3).

A transducer transmits into the water a signal of certain intensity that we call Source level (SL) and that is expressed in dB at a unit distance (1 m) on its axis. When the radiated sound reaches the target (if the axis of the sonar points toward the target), its level will be reduced by the transmission loss (TL), and becomes SL-TL. On reflection or scattering of a target of target strength TS, the reflected or backscattered level will be SL-TL+TS at a distance of 1 m from the acoustic center of the target in the direction back toward the sonar. In traveling back to the transducer, this level is again attenuated by the transmission loss and become SL-2TL+TS. This is the dB level (EL) received at the sonar transducer. All the passages described are then summarized by the formula:

$$EL = SL - 2TL + TS \quad (2.31)$$

In this explanation we have disregarded the 1 meter which both the SL and TS definition refer to. In normal use of sonars the distance between the transducer and the target is so long that one meter more or less does not matter. The sonar equation is however valid even if the distance is close to one meter or less than one meter, provided the target is in the farfield of the transducer beam pattern and vice versa (see paragraph 3.2). If the target is large, larger than one meter, such as a whale, the reference point 1m from the apparent sound center is somewhat fictional. It may be inside the target,

and it may be not possible to measure as a sound level at that point. To measure the target strength of a target like that, we need to put the transducer several meters away from it and then use the sonar equation.

TS > 0dB: not a paradox:

The target strength of a large target does in some cases exhibit positive values, and may mislead the observer to raise the question: how can the reflected intensity be larger than the incident? The answer is in the definition of target strength as the reflected intensity referred to a point 1 m from the acoustic center of the target. For large targets this point is inside their bodies and the real intensity at the surface of the target is lower, due to the law for spreading loss. The real reflected intensity at the target surface must be of course lower than the incident one.

CHAPTER 3



CALIBRATION

3. CALIBRATION

A principal requirement in scientific measurement is calibration of the measuring tool. In fishery acoustic surveys for stock abundance estimation, instrument calibration is essential for survey accuracy. Standard protocols have evolved over the last 3 decades in an ongoing effort to reduce instrument-related errors and minimize bias in acoustic stock estimates. The potential bias from calibrations performed with microphones in the 1970s could be as large as ± 3 dB or a factor of 2 (Blue 1984). Calibrations using elastic targets, or metal spheres, reduced this error drastically (Foote et al. 1987). Errors due to equipment performance are now minor (-1.2 dB in accuracy and 0.3 dB of precision - e.g. refer to Demer 1994) if calibration of a downward looking scientific echosounder is performed in accordance with international practice (Simmonds et al. 1984; Foote et al. 1987). The advent of more sophisticated instruments (e.g. multibeam sonars) has led to the requirement for new calibration methods, (Ona and Svellingen 1998; Foote et al. 2005; Knudsen 2009), although the principles described by Foote et al. (1987) are still valid and can be adapted as starting point.

Three main parameters are important to determine during calibration. (i) The on axis sensitivity, determined by reference to the echo from a target in a particular direction. Usually this direction is the transducer acoustic axis, along which sensitivity is maximum. (ii) The Time Varied Gain (TVG), parameter described by a function, which is intended to ensure that the same fish density will produce the same signal at any range. (iii) The beam pattern (see paragraph 2.3). In this chapter I present a brief introduction to calibration procedures of fishery active acoustic tools. In paragraph 3.6 I go on describing my first attempt to calibrate an omnidirectional sonar *in situ*, and show how the standard target calibration method presented by Foote et al. (2005) for multibeam sonars has been adapted to be used in an operational situation onboard a fishing vessel, rather than in a controlled environment.

3.1 The on-axis sensitivity

The acoustic axis of the transducer is the direction in which the transmitted energy is greatest, and from which the strongest echo is returned for a given target at a constant range. Calibration is performed to determine the combined transmit and receive sensitivity in this direction, from which the value C_a (Calibration factor for the on axis sensitivity) is calculated.

For field application with fishery instrumentation, the standard target method as described by Foote et al. (1987) is preferred for its accuracy. This method of calibration is based on the use of a standard target of known acoustic scattering properties. Usually the target is an homogenous solid sphere of copper (Cu) or tungsten carbide (WC) that is suspended below the transducer (in the case of a

vertically orientated scientific echosounder). During calibration the sonar is operated in the normal manner with the same pulse duration, TVG and power level as used during data collection. Measurements enable estimation both of the range of the target and the combined transmit-receive sensitivity of the sonar in the direction of the target. By moving the sphere across the beam, the position at which the echo is strongest for a given range can be found and the beam mapped. When the target is on the acoustic axis, C_a can be determined from the corresponding echo intensity measurements. The standard target technique is both accurate and simple to apply in practice (Simmonds et al. 1984). Aspects of the standard target approach are discussed in paragraph 3.5.

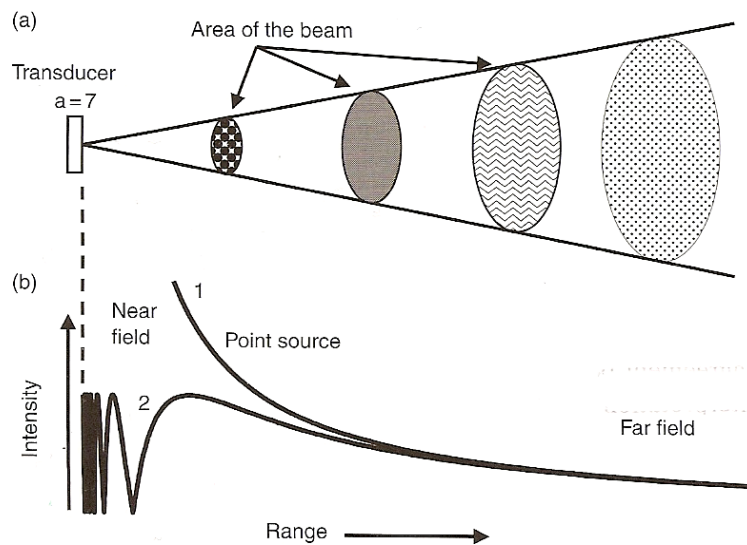


Figure 3. 1 Illustration of how acoustic energy propagates away from a transducer. (a) As described in paragraph 2.2.4 spherical spreading reduces the intensity at long range. (b) The intensity of a point source follows the inverse-square law at any range (curve 1). The near field effect limits the intensity near the face of a finite transducer (curve 2) in this case one of size 7λ (from Simmonds and MacLennan 2005).

3.2 Nearfield and farfield

There are difficulties interpreting quantitatively signals arising in the so-called near field or Fresnel zone. This is a region immediately in front of the transducer where the range dependency of the transmitted and received intensity is complicated because the wavelets produced by separate elements have not aligned coherently. At short range the traveling wave fronts produced by the transducer elements are not parallel; this factor alters the phase relationship if compare to the farfield or Fraunhofer zone. In the nearfield, the intensity varies rapidly with the range in an oscillatory manner (Figure 3.1). It is only in the farfield, with the wave fronts nearly parallel that the sonar beam is properly formed and the inverse square law applies (Paragraph 2.2.4, equation 2.14). If a in the

equation is the linear distance across the transducer face, the boundary between the near and far fields is approximately at the range:

$$R_b = \frac{a^2}{\lambda} \quad (3.1)$$

For example, the wavelength in seawater is about 1.36 cm at 110 kHz. If a in the equation is 7λ , the near field extends to $R_b=1.89$ m. Generally, lower frequency transducers with the same beamwidth would have a more extensive nearfield. The transition from near to far field conditions occurs gradually around R_b .

During the calibration procedure the reference target (sphere or reflector) must be outside the nearfield. The optimum position for the target is just outside the nearfield, at a distance from the transducer which may be estimated from the formula:

$$R_{opt} = \frac{2d^2 f_0}{c} \quad (3.2)$$

where d is the greatest width of the transducer face, f_0 is the echosounder frequency and c is the speed of sound in water. E.g. suppose that the sonar to be calibrated has a rectangular face of size 45x30 cm. The larger dimension is then 0.45 m. At 38 kHz with a sound speed of 1500 m/s, R_{opt} is $2 \times (0.45)^2 \times 38000/1500$, or 10.26 m. If the calibration target is placed at R_{opt} or further, the bias in the measured on-axis sensitivity resulting from near field effect will be negligible, and probably less than 1 %.

3.3 The TVG function

The purpose of the time-varied-gain (TVG) function is to compensate the range dependence of the received echo. For echo integration of dispersed targets (see paragraph 2.4) the appropriate TVG function is nominally $20\log_{10} R$, while for detection of single targets (and echo counting), as during calibration, the function used is $40\log_{10} R$. As most scientific echosounders now implement the TVG by digital signal processing, TVG-related errors should be negligible. Unfortunately, this is not always the case, and instruments like the one used for the purpose of this project are still in a test phase with the raw data processing that has to acknowledge all the transmission losses mentioned in Chapter 2 to arrive at the final quantitative result. The programmed TVG function should provide adequate range compensation for the distances to be sampled.

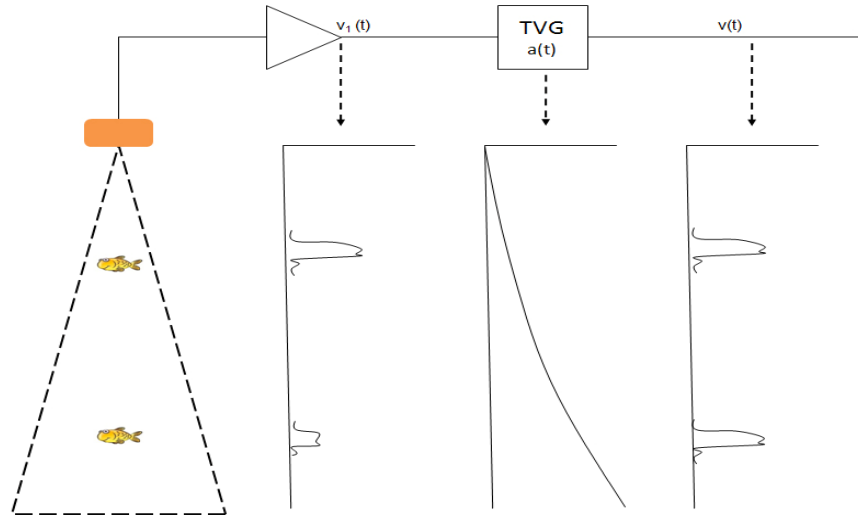


Figure 3.2: Range compensation by TVG for a single target. The term $v_1(t)$ is the uncompensated signal proportional to the echo amplitude, and $a(t)$ the receiver gain that increases with time. This generates the compensation that makes the output $v(t) = a(t)v_1(t)$ range independent. This is the so called '40 log R' TVG.

Theoretically the TVG function can be summarized supposing that a voltage gain of the receiver is proportional to $A(t)$ where t is the time after the start of the transmitted pulse. $A(t)$ is the actual TVG function of the sonar, but in general will not compensate the range correctly and the purpose of calibration is to estimate the associated error. To do this, measurements of $A(t)$ are compared with the ideal TVG function, $a_o(t)$, which does compensate the range dependence exactly. In the case of one isolated target at a range much greater than the pulse length, the appropriate TVG function is:

$$a_o(t) = (ct) \exp\left(\frac{\beta ct}{2}\right) \quad (3.3)$$

where c is the sound speed and β is the absorption coefficient. This function is commonly known as the "40 log₁₀ R" TVG. The range dependence is obtained by substituting the range $R=ct/2$ as an approximation, and calculating $20 \log_{10} [a_o(t)]$, which is the TVG expressed in decibels. The spreading losses increase with the range, as does the time delay until the echo is received. The echo amplitude is then multiplied by the TVG function with the result that output signals are not range dependent. In figure 3.2 this concept is summarized schematically.

3.4 Standard experimental procedure

Scientific acoustic transducers are calibrated by the manufacturer in a calibration tank using a reference-standard transducer. In the field, however, many variables affect the performance of an acoustic system. For this reason a standard procedure has been developed to take into account the

different conditions that will be encountered in performing acoustic measurements *in situ*. For scientific application in fisheries and ecosystem research, the use of downward looking transducers is common. The standard procedure for calibrating these instruments (Foote et al. 1987) has been taken here as a basis for the development of a calibration method for omnidirectional sonars.

During the calibration process a standard target, usually a sphere (see paragraph 3.5), is suspended below the transducer. This is normally done by attaching the sphere in a web of acoustically-transparent fishing line. The standard encapsulated target is then attached to three suspension lines, and moved through the sonar beam by adjusting their lengths. A practical precaution before calibration is to soak the sphere into a solution of water and soap, wetting its surface thoroughly so that air bubbles on the web are eliminated (bubbles are strong targets). To change the length of the lines and move the target under the sonar, booms supplied with reels are fitted to the ship's rails with the purpose to lead them clear of the ship hull. The common need is to place the calibration sphere at R_{opt} (see equation 3.2) to work in the farfield of the transducer. The sphere is moved across the beam so as to measure the signal strength from different points in the transducer acoustic beam and to find the position where the echo strength is greatest, i.e. the acoustic axis. For standard scientific applications (e.g. fishery surveys) the use, for split beam echosounder, of the methods proposed by MacLennan and Svellingen (1989) are appropriate, and for single beam echosounders the method described by Craig and Forbes (1969) is used. These two methods have been described and standardized in a practical guide edited by Foote et al. (1987). The work of Foote (1987) is actually under revision by a dedicated study group of the ICES, the SGCAL Group which is producing a new report considering the new technologies developed and routinely used up to date (ICES 2010). In the first method, the cross section of the beam is divided into seven regions of equal area, a circle in the center and six segments in the periphery. For a split beam transducer, the target direction is determined by the instrument itself. For a single beam transducer the echo energy varies due to changes in sensitivity across the beam (as well as the stochastic TS this effects split-beam too). It is assumed that the TS and the position of the target are uncorrelated. In both methods the target is moved so that the number of measurements is about the same in all regions of the transducer's main lobe with all its parts receiving similar attention.

Calibration has to be performed with care because mistakes are easy to make and can be costly because they may bring a bias in the estimation of fish abundance or target strength measurements. Use of routine protocol minimizes the potential for error. Simmonds (1990) investigated the accuracy that could be expected by a good calibration procedure and concluded that it should be possible to achieve echo-integration performance within 7%. Acoustic data present many opportunities for

problems to arise from their interpretation; there is definitely no need to list calibration error as one those.

3.5 Calibration spheres

The standard target calibration method requires use of a target for which acoustic scattering properties are known. Many different standard targets have been proposed, including table tennis balls (Welsby et al. 1972) and solid spheres made of different materials such as steel or brass (MacLennan 1982). However tungsten carbide (MacLennan and Armstrong 1984; MacLennan and Dunn 1984) and copper spheres (Foote 1982; Foote and MacLennan 1984) are now widely used and provide reliable results.

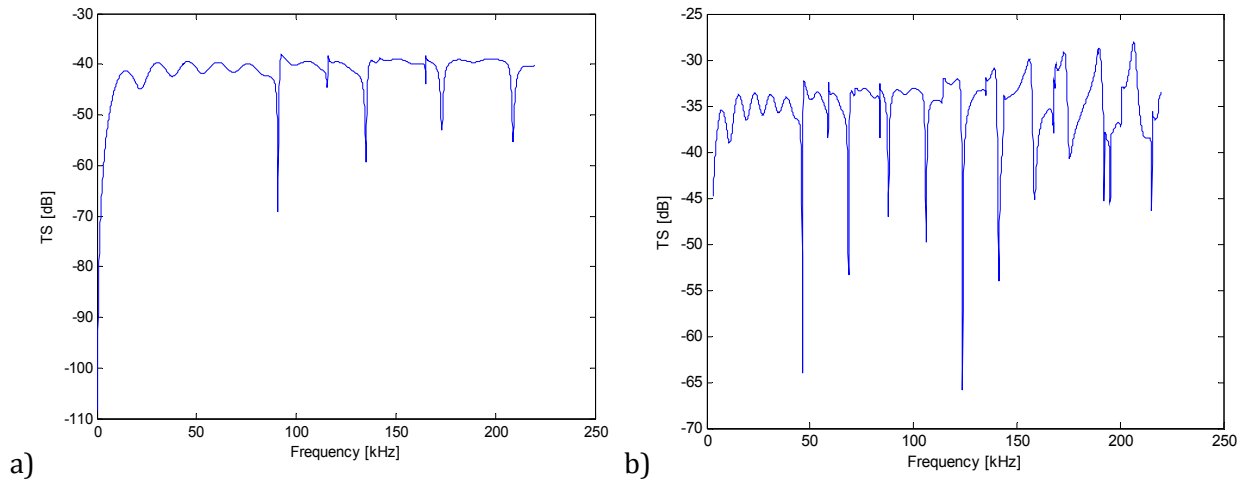


Figure 3.3 Frequency responses for two different tungsten carbide (WC) calibration spheres. a) a common WC38.1 used for high frequency, b) a customized 75 mm diameter calibration sphere used to calibrate multibeam system (Ona et al. 2009). While choosing a calibration sphere it is important to evaluate a flat response (plateau in the graph) at the frequency and in the bandwidth of interest to generate a set of data not influenced by the target itself.

The choice of a spherical shape gives the immediate advantage of homogeneity as the target rotates during measurements. Thus, the orientation of the sphere becomes irrelevant and the echo received at the transducer depends exclusively on its position relative to the main axis of the transducer. The theoretical calculation of the backscattering cross section related to material properties of a sphere is expressed as a proportion of those in water and is well established (Hickling 1962; Dragonette et al. 1974; MacLennan 1981). The functional dependence is:

$$\sigma_{bs} = (a^2/4)F(\omega a/c, \rho_1/\rho, c_1/c, c_2/c) \quad (3.4)$$

There are two sound speeds within a sphere, c_1 and c_2 , the longitudinal and transverse respectively. ρ_1 is the sphere density and a is its radius. ρ and c are the water density and the sound speed. Thus, change in the medium (sea water) density influences the scattering properties. F is the so-called form function, the ratio of the spherical scattering and geometric cross section. The TS variation with frequency for two tungsten carbide calibration spheres is shown in Figure 3.3.

Resonance, the tendency of a target to absorb more energy when it is forced or driven at a frequency that matches one of its own natural frequencies of vibration, depends on the sound speed ratios, with the material density playing a minor role. This frequency dependence is a function of the number of wavelengths in the sphere diameter. This means that for the same material and sound speed, the resonance frequencies are inversely proportional to the sphere radius. The larger the sphere, the lower the frequency will be that marks the beginning of the resonance. The choice of the standard target to use during calibration takes into consideration a consistent echo response well above the background noise, a flat TS response at the frequency of interest, and no resonance in the transmitting bandwidth of the sonar system (see Foote 2007).

The optimum sphere size is one for which target strength is less sensitive to changes in parameters. Assuming $F=1$, a first approximation of the sphere radius a is the size that gives the required TS at the sonar's center frequency f_0 . The TS value at this point is less important than the desire to avoid resonance. The calculations to choose optimal spheres for different transducer are performed around an approximate value to evaluate how TS changes with the expected variability of sound speed in water, pulse duration and other parameters. It is however not always necessary to perform these complex calculations, indeed sonar manufacturers normally recommend the optimal sphere for the calibration of their instruments. The approach to calibration has to be different when the instrument is in its development phase, as described in the following paragraphs.

3.6 Calibration test of omnidirectional sonar

Sonar technology advanced and achieved great goals due to highly precise estimations of fish stocks worldwide using vertical orientated echosounders. Major results of accurate stock estimation include management regimes that prevent fish stock collapse and sometimes remediation of unbalanced ecological situations (Dragesund et al. 1980; Hamre 1990; Toresen et al. 2001). Despite providing an unquestionable reliability and precision, vertical echosounders insonify only a very limited volume of the water column along the ship's track, and do not e.g. detect fish schools and other marine life close to the surface. This is called the acoustic blind zone (Patel et al. 2009; Scalabrin et al. 2009; Totland et

al. 2009; Axenrot et al. 2004). The increased areal coverage provided by multibeam and omnidirectional sonars without compromise of spatial resolution makes them well suited for studies of fish behavior and vessel avoidance covering in particular the above mentioned acoustic blind zone. In 2007 I started to test the possibility of quantifying sonar data of the Simrad SH80 fishery omnidirectional sonars taking advantage of its provision of the water-column signal, which is otherwise the exception in most commercial multibeam sonar systems. The potential of this instrument class for biological research drove me to test it quantitatively. Calibrations were conducted during piggy-back activities on survey in the Norwegian Sea (see paragraph 4.2). Fishery surveys are currently the means used by the Norwegian government to obtain quantitative data and knowledge on various commercially important fish stocks, and could be augmented using omnidirectional sonar. It was clear from the beginning that a fast *in situ* sonar calibration method was needed!

3.6.1 Introduction

A number of pioneering studies have tested the potential and performances of multibeam and omnidirectional sonars. Migration of schools of herring (*Clupea harengus*) in the North Sea has been observed, with concomitant measurements of swimming speed (Hafsteinsson and Misund 1993). Predator-prey interactions were studied by means of multibeam sonar. The movements of schools of herring induced by killer whales (*Orcinus orca*) and Fin whales (*Balaenoptera physalus*) have been measured (Nøttestad and Axelsen 1999, and Nøttestad et al. 2002a) as have the interactions between juvenile herring and the Atlantic puffin (*Fratercula arctica*)(Axelsen et al. 2001).

The several fisheries applications mentioned here have succeeded because of the qualitative imaging capability of multibeam and omnidirectional sonar in a high-signal, low-noise environment, supplemented by recording of the echo magnitude. In other desired applications beyond those of visualization (Mayer et al. 2002) a quantitative capability, hence calibration, is essential.

To date, omnidirectional sonar has rarely been used as quantitative tool (Bernasconi et al. 2009; Nishimori et al. 2009; Ona et al. 2009; Ona and Andersen 2008). This class of sonar is capable of being operated from a moving ship, with multi-frequency options, 360 degrees radar-like coverage, and gives the possibility of scanning dedicated sectors around the ship with an easy hardware interface capable of operational software implementation.

Recently fishery scientists have increased their effort in the quantification of multibeam sonar data (Cochrane et al. 2003; Foote et al. 2005; Ona et al. 2009), nonetheless, calibration of omnidirectional sonars has not been reported yet in literature. Scientific omnidirectional sonars are relatively new instruments and the potential for multi-frequency (110-122 kHz with 1 kHz step) and the large

number of beams (the Simrad SH Series has 64) imply a very long calibration procedure (to calibrate a single beam echosounder can take up to 3 hours; the potential exists that omnidirectional sonar calibration would be 64 single beams x 3 hours that is a lot of 'expensive' ship time). Since the advent of digital processors, fisheries sonars have been used both qualitatively and quantitatively for many years (e.g. Misund et al. 1995; Gerlotto et al. 1999), but these sonars often suffered from low resolution, no data output facilities, and poorly defined calibration procedures. Brehmer et al. (2006) described an application of this class of sonar for observational fisheries science, but quantified application was limited by the absence of acoustic data output. More recently Nishimori et al. (2008) developed a quantitative echo-integration method for estimating fish school abundance from omnidirectional sonars, which showed the clear potential of this class of sonar for covering wider areas than vertical sounders while surveying for fish stocks. To achieve the goal of quantifying the received signals from different acoustic targets *in situ* I started to develop a method to calibrate the Simrad SH80 unit (see paragraph 4.2 for a detailed description of the system) and generate correction values to apply to the received backscatter energies from fish schools and large whales.

Rather than a 65 mm tungsten carbide sphere, that would be an optimal choice for a frequency of 110 kHz, for reason of convenience three suboptimal spheres, all of which were readily available, were used:

- Cu 60 mm, a standard copper sphere optimal for 38 kHz transducers
- WC 38.1 mm, a standard tungsten carbide sphere optimal for 120 kHz transducers
- WC 75 mm, a custom tungsten carbide sphere built for multibeam sonar calibration

This *in situ* calibration method, which is still in a development phase, was implemented over several years considering the needs to reduce the ship time needed and the requirement for a deeper understanding of the single beam patterns influencing target detection. This report describes my first complete field calibration attempt of the Simrad SH80 using a WC75 mm sphere (ICES 2011).

3.6.2 Method

The Simrad SH80 was calibrated on the fishery vessel Eros M-60 HØ, anchored in calm weather conditions (Beaufort 0) at Lysefjorden the 9th of August 2008. Before and after calibration, a preparatory measure is that of measuring the hydrographic state of the environment. Sea temperature (T) and salinity vs. depth were measured using a SAIV SD202 CTD probe. The sound speed (c) was computed via the software MiniSoft SD200W and the absorption coefficient (α) by the accepted standard formula developed by Francois and Garrison (1982). Subsequently, a large calibration sphere

(75 mm diameter and 3.3 kg), made of tungsten carbide (WC) with a 6% cobalt binder, was used and the backscatter response of 8 beams was analyzed for the chosen frequency of 110 kHz at pulse durations ranging from 0.8 ms to 3.8 ms. This heavy calibration sphere, which was physically very stable when suspended underwater, provided intense echoes (-34.4 dB at 110 kHz), that were easily recognizable from the background noise and from any individual fish that occasionally passed through the beam being calibrated. The transducer was installed under the ship bow exactly at the center of the hull's main axis. The sonar's 360° area of coverage is divided in 64 sectors of 5.62°; the sectors' centers coincide with the single beam's main axis (8° opening angle), and the positions of beam centers were marked with tape on the ship's bow rail after reference to engineering plans of the ship. A standard target can be placed at an essentially arbitrary position in the sonar beam by purely geometrical considerations. Using these marks as reference, I lowered the calibration sphere to depths coinciding with the beam axis which, with the sonar tilt angle set at 0° (horizontally), was equivalent to the transducer depth (Figure 3.4).

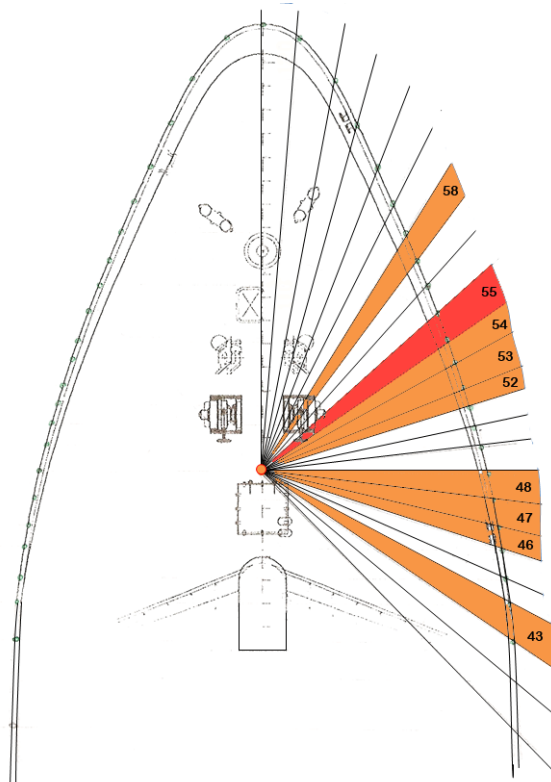


Figure 3.4 Schematic representation of the bow of the vessel M-60 Eros HØ, a 72 m combined purse seiner and pelagic trawler adapted and equipped to operate as a scientific platform. Measurements of a hanging wc75 calibration sphere were made for 24 beams (clockwise from 64 to 40). The beams directly and correctly calibrated; these data were used to define gain compensation to quantify the Simrad SH80 TS measurements presented in chapter 6 and 7, are marked in orange. In red is the beam tested to define the SH80 vertical beam pattern.

For the eight selected beams, I analyzed an average of 476 pings ($n_{\text{total}} = 3804$) to describe the signal response and stability of each beam at any chosen pulse duration considering all settings that were used during the surveys while measuring whales target strength (Bernasconi et al. 2009; see also Chapters 6 and 7). In addition I performed a detailed scan of the calibration sphere using the “electronic tilt angle control” of the sonar to describe the pattern of a single beam in the vertical plane. It was not possible to describe the echo response in the horizontal plane as did by Foote et al. (2005) for the impossibility to move precisely the sphere laterally.

I converted the resulting backscattered energies (mV) from their binary raw data format using the software ‘Sonar Data Converter 9.04’ (provided by the sonar manufacturer) and then processed all signals using dedicated Matlab scripts that I wrote. Calibration correction values were calculated using the sonar equation (3.5), to normalize the received dB level (EL) comparing it with the theoretical values at different distances by:

$$EL = SL + TS - 40\log_{10}(R) - 2\alpha R \quad (3.5)$$

I present a detailed review of the data processing in paragraph 4.4, where I described, along with some practical examples, the basic SH80 signal processing and how voltages (mV) were converted into acoustic units (dB// μPa) for subsequent data analysis.

For all the beams not directly calibrated I looked, using weighted background noise values, to see if any significant variability among them had to be considered or if the sonar beams’ sensitivities were all essentially equivalent. The null hypothesis (no difference between beams) was tested using a one way ANOVA applied to the received signals (from a finite number of pings, $n=35$) of a defined range (between 20 and 30 m) chosen considering the absence of targets at that range (See figure 3.7).

3.6.3 Results and Discussion

There is little reason to suspect instabilities in performance of omnidirectional sonars designed for scientific use, although their possible occurrence at high pulse repetition frequencies might be entertained. Measurement of the signal stability is straightforward. With the target held at a fixed position in the transducer beam, I measured the echo strength of the wc75 sphere over a relatively long period of time (a minimum of 200 s for every chosen pulse duration). An example of a measurement of signal stability is presented in Fig. 3.5. More complicated was the issue of determining the stability and equivalence of the received signals among beams. I initially planned to check 24 sonar beams and logged data from beam 64 to beam 40 (from the ship’s bow clockwise) in an attempt to cover the all starboard sonar sector used during the whale TS experiments (see Chapters 6 and 7).

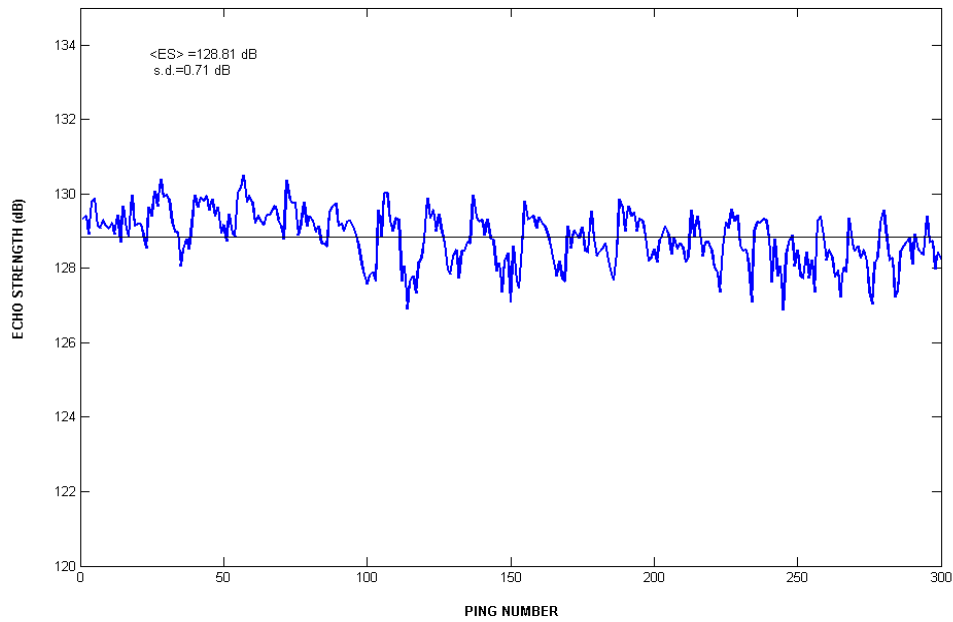


Figure 3.5 Received Echo Level (EL) from an on-axis standard target, wc75, as measured at 7.2 m range at Lysefjorden by the Simrad SH80 omnidirectional sonar over a time period of 160 s .

Considering the pilot nature of this project, I was pleased to get through different instrument tests (not described in this thesis) and overcome various technical issues. Indeed some applications of multibeam sonar reviewed by Reid (2000) showed limitations and so did omnidirectional sonar applications, especially the impossibility of choosing a pulse duration independently from the visualized range (indeed the sonar itself is configured internally with certain constraints that cannot be exceeded). However, it was not possible to be sure that the sphere was always exactly at the center of each of the beam axis when it was moved from one beam to another as it was done *ex situ* by Foote et al. (2005). The sphere was positioned in a qualitative way, by visually considering where the signal appeared stronger on the screen. For that reason, I carefully pre-scrutinized the raw data and this scrutinization revealed that for just eight beams the target was on axis. These beams were chosen for subsequent analysis (43, 46, 47, 48, 52, 53, 54 and 58). Over an average of 375 pings for each beam the fluctuations of the received EL were of the order of 8.5 dB over a range of distances between 7.2 and 5.5 m. Similar high variability was also observed by Ona et al. (2009) during calibration of high frequency multibeam systems. Figure 3.6 shows, for each beam considered in the analysis, the overall backscatter response of a 75 mm tungsten carbide sphere (WC 75). At the transducer depth of 6.2 m below the surface, observations from the CTD probe showed that T and c were stable at 15.6 °C and 1502.8 m/s, giving an absorption coefficient (α) of 0.035 dB/km. The theoretical EL received at 110 kHz for each considered beam (represented with a black diamond in figure 3.5 and described in detail for wider spectra in figure 3.3 b) were generated using the measured physical parameters and by

purely geometrical considerations of the calibration sphere distance from the transducer (calculated using the ship's technical drawing).

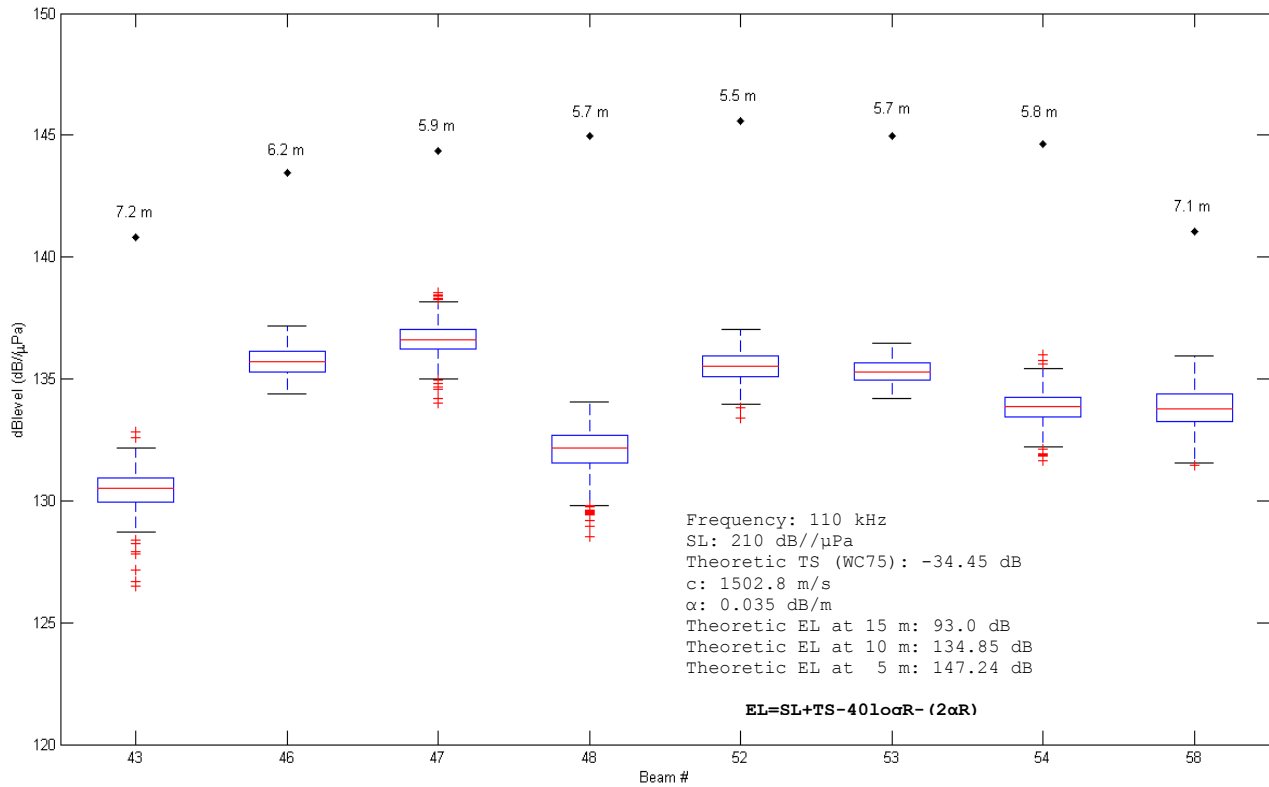


Figure 3.6 Received Echo Level (EL) for the eight beams considered during the data analysis. The black diamonds represent the theoretical EL calculated using equation 3.5 considering the exact geometrical distance of the sphere. Boxes represent the 25 % quartiles, red lines the median value, whiskers minimum and maximum values while red crosses plot the outliers (values more than 2 times the upper quartiles).

A first look at the uncalibrated TS values showed, as expected, lower TS values with shorter pulse durations. This observation agrees with the TS vs. pulse duration described by Urick (1983): short pulse durations yielded lower TS. In this case pulse duration of 0.8 ms gave mean uncompensated TS of -41.5 dB, i.e. 5.2 dB less than that using a pulse of 3.8 ms. The samples, as just mentioned, were not always taken for all the beams with the sphere exactly on the acoustic axis. The variability, in the order of 5 dB/μPa, cannot be explained just by the stochastic nature of TS, but I believe can be due to some degree of off-axis effects in positioning the sphere (e.g. I would only have to be mm out to get the observed effects). Furthermore, if we consider the single beam calibration method review described by Simmonds and MacLennan (2005), it is possible to consider all measures coming from different regions of a single beam transducer and extract the average correction needed for further whale TS measurements (Nøttestad et al. 2010; Bernasconi et al. 2009; Chapter 6 and 7). To do so, I had to be

confident about the sonar beams' receiving homogeneity. I examined homogeneity as follows: a ring of background noise (Fig 3.7) was selected and the resulting variability among beams' received signal noise compared using an ANOVA test. I assumed that the background noise was equal in all directions, for this reason the choice of the calibration site was made considering the almost total absence of ship traffic. The results were then analyzed by the mean of each beam. That was followed by the ANOVA test with resulting no difference among beams received signals ($p=0.125$), and the provision of confidence that adaptation of the standard target calibration method could achieve acceptable results if applied to a finite number of single SH80 beams (e.g. 6) and through the use of weighted background noises. To proceed and obtain final calibration corrections I mapped a single beam's sensitivity area through a vertical electronic scan of the calibration sphere, taking advantage of the tilt angle control command of the sonar. In that way I could describe the receiving sensitivity, in the vertical plane, of a single SH80 beam from the central axis to the periphery of the main acoustic lobe (-3 dB maximum sensitivity point; see paragraph 2.3.1) directing its acoustic axis away from the calibration sphere. I must underline that the *in situ* nature of this calibration test allowed us only to describe the beam pattern in the vertical plane. Further effort will need to solve this issue to maximize calibration results. My experiment referred in its design to the work done for multibeam sonar by Foote et al. (2005) and adapts it to the different *in situ* scenario. It has to be acknowledged that procedures executed *ex situ* are sometimes impossible to repeat from a vessel (e.g. the mechanical rotation of the transducer).

Figure 3.8 (a, b, c) shows sonar screen captures of three different moments of the scan. With the sphere lowered down to a set depth, the sonar beam was tilted between -29° and -16° . The sphere was on axis at approximately -24° coinciding with the center of the 8° opening angle (φ) of the SH80 beams. The backscatter energy received when the sphere was in the center of the beam gave detections in two adjacent beams (Figure 3.8b). This is explained by the overlap of the SH80 beams that start at approximately 12 cm from the transducer face, such that adjacent beams detect echoes coming from their peripheral beam areas (Figure 3.9); this phenomenon has been analyzed in detail by Nishimori et al. (2009) with regard to quantification of herring school data arising from an omnidirectional sonar.

The overall uncalibrated TS average ($n=3804$) was -37.9 dB [95% CI: -37.8 - 38.0]. Figure 3.10 a and b show how uncalibrated TS values distribution of all measurements could be all link with detection on-axis from a single SH80 beam. Even with the sphere not exactly at the beam center we can consider the measurements coming from different beam areas dividing them in three sensitivity categories: good, not in axis and bad (Figure 3.10b). After I was confident about beam shape and sensitivity I analyzed all received signals coming from the sphere, as if they were collected from a single beam, to generate the calibration correction gain used in post processing to measure whale TS. The basic statistics of the

calibration corrections are summarized for all the different pulse durations used during the survey in Figure 3.11 and Table 3.1.

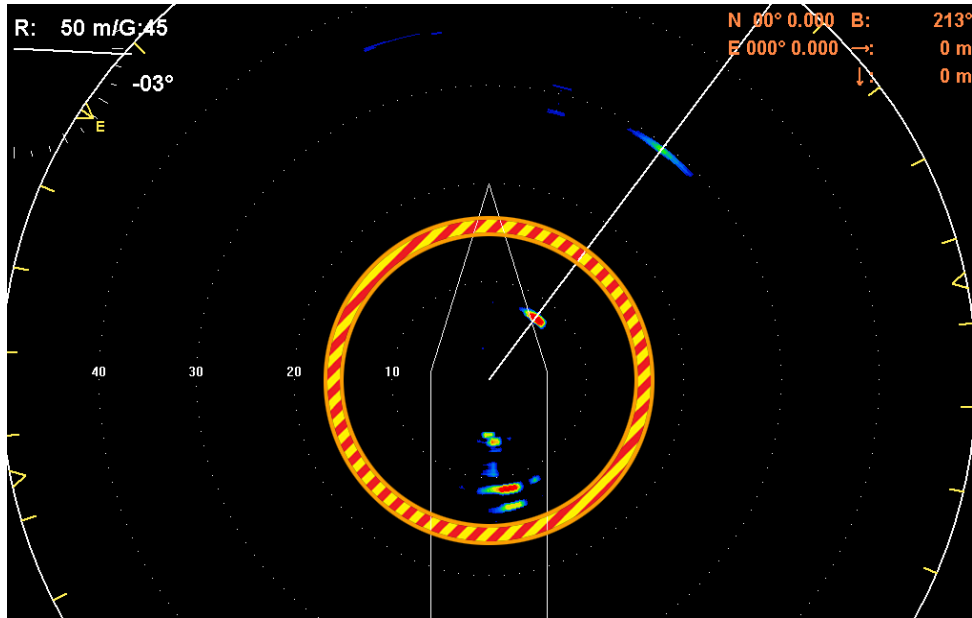


Figure 3.7: A circular area (yellow and orange stripes) with no presence of target was selected and background noises weighted to verify the homogeneity of reception among the beams.

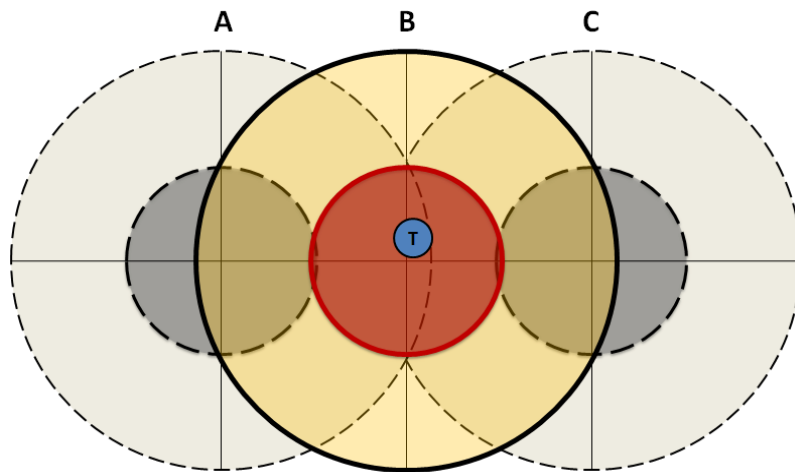


Figure 3.9 Sketch representing the overlapping of contiguous beams A, B, and C. It is clear that when the sphere is situated in the main acoustic axis of one beam, some echoes are logged by the peripheral areas of the adjacent beams.

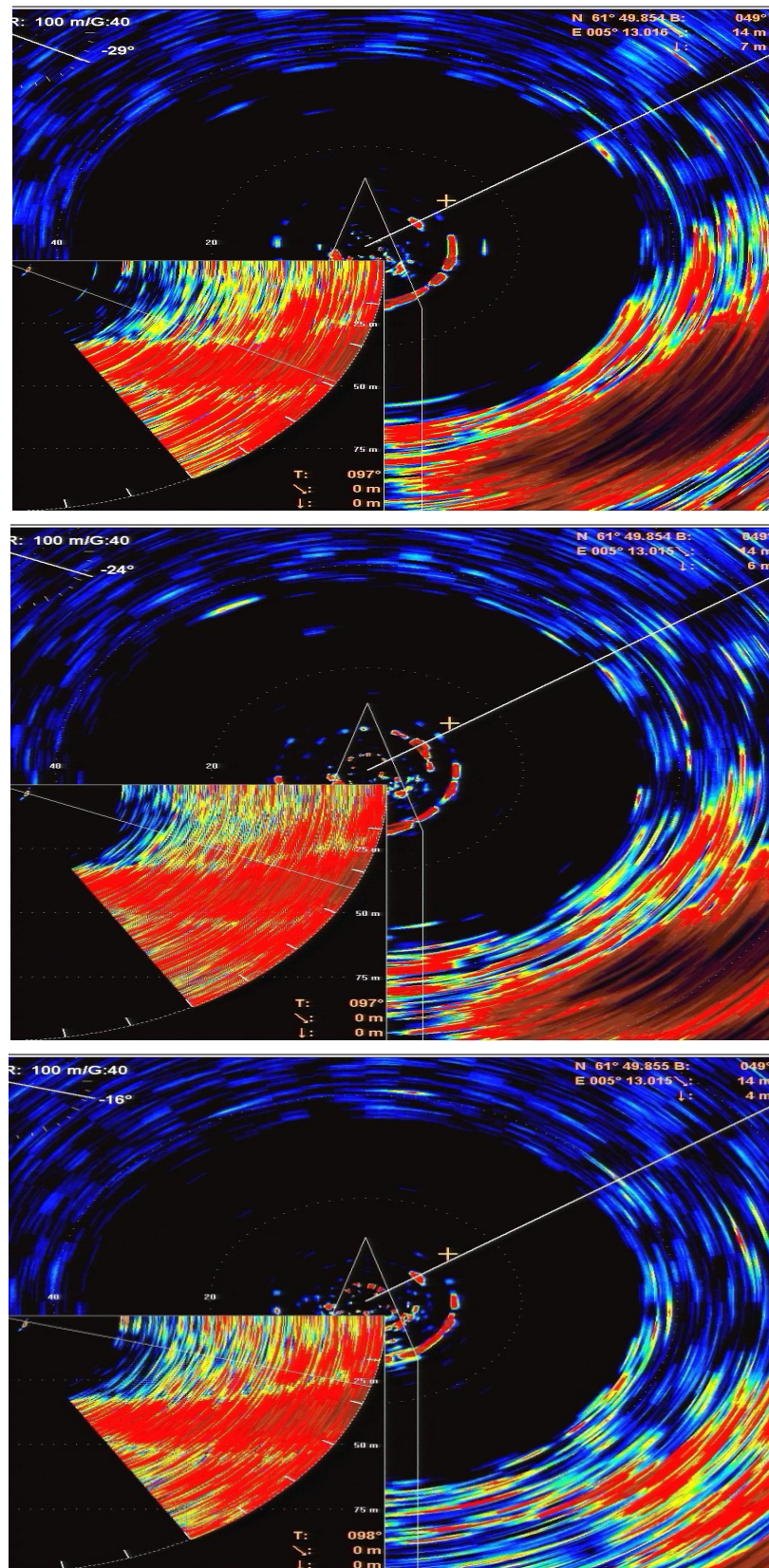


Figure 3.8 Sonar screen shots showing three distinct moments of the WC75 mm sphere scanning from -29° to -16°. Within this angle it was possible to shape and get a more detailed definition of the single beam for the Simrad SH80 omnidirectional sonar. It is possible to observe while the sphere is in the main axis of the beam the peripheral detections of the contiguous beams.

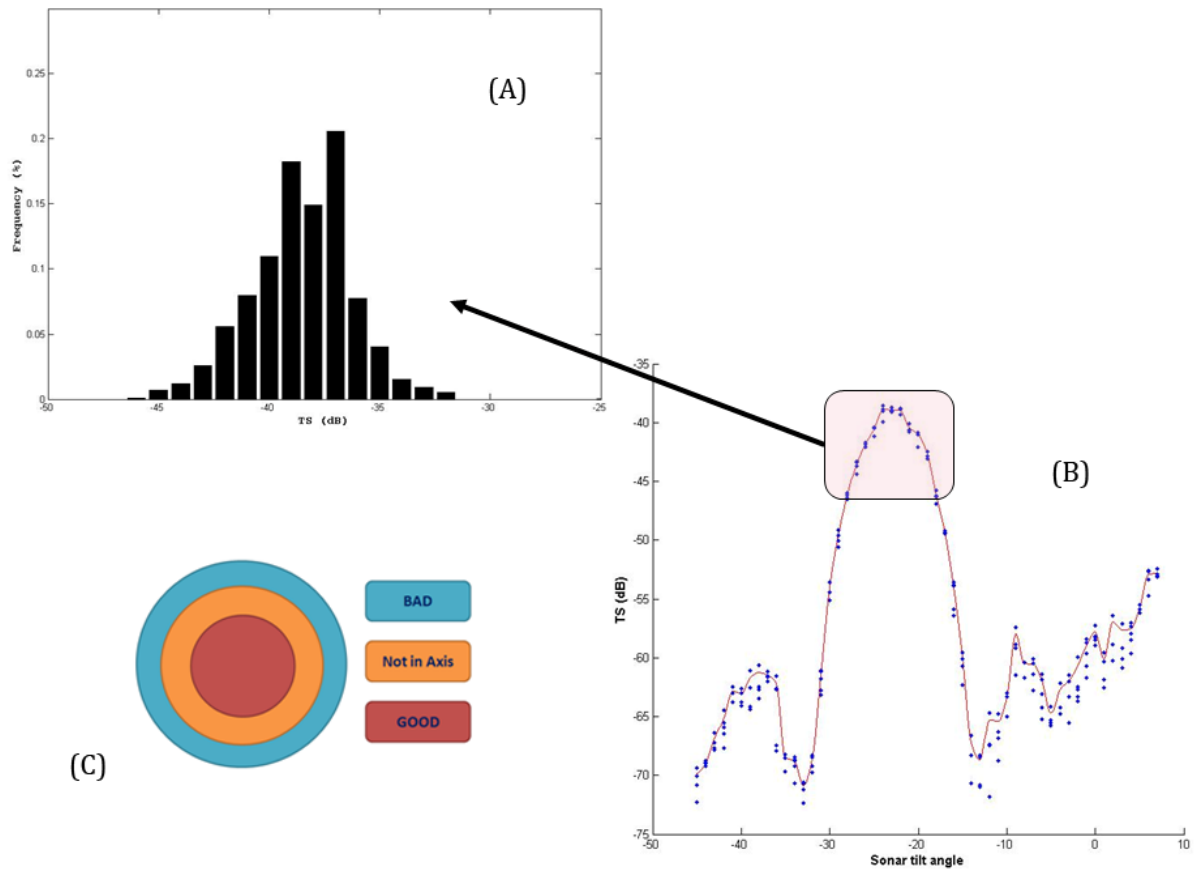


Figure 3.10 a) TS distribution of the sonar pings considered for calibration (n=3804) b) Electronic scan of the standard target used during the calibration experiment. Side lobe presence is clear, but well suppressed by the sonar manufacturer. The solid red line represents an interpolation of the resulting measures. c) Schematic representation of the categories defined after the electronic scan

3.6.4 Conclusions

A first attempt to calibrate the SH80 sonar was undertaken by analyzing eight single beams (from the total of 64). A detailed vertical scan of a individual beam gave good indications of the feasibility of the method, but it is time consuming (6 hour for less than one third of the total beams) to make measurements over the range of pulse length settings that have to be considered. The reliable output generated by the SH80 unit is easily analyzable, but the definition of the target's angular position inside the beam remains uncertain. This problem will be of limited importance for the application we are looking to develop, namely measuring TS of

large targets such as whales, but could be important if the aim were to detect and measure the biomass of fish schools or perform unsupervised (automated) whale detection. Nonetheless, the data collected show the potential for quantitative sonar studies. Dedicated effort on further development is highly recommended, aimed at developing an efficient and fast *in situ* calibration method for this sonar class, based upon the procedure described in this report. There are also very high expectations for the new omnidirectional Simrad SX sonar class, since quantitative data output requirements were considered from the onset of the instrument design.

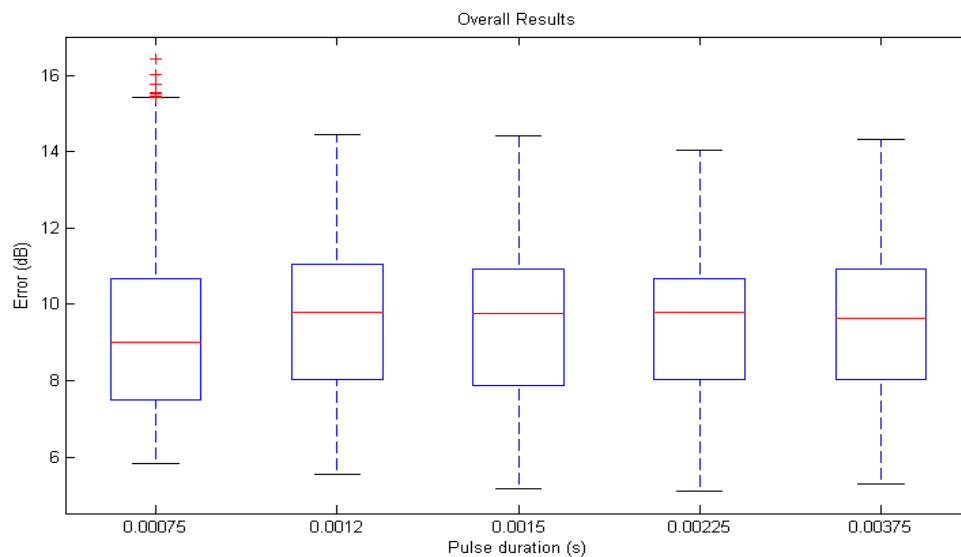


Figure 3.11 Box plot of the error coming from all measured pings for WC75 calibration sphere at all pulse duration used during our surveys.

Table 3.1 Generated correction values for the different pulse duration settings used during the experiment. Even if the values seem very high the variability can be considered regular. It has to be underlined that this sonar class has not yet been advocated for quantification purposes, even if provided with an expansion scientific module to store data.

<i>Pulse (ms)</i>	<i>Mean</i>	<i>Median</i>	<i>95% Confidence Interval</i>	
0.75	10.15	8.99	9.97	10.33
1.2	10.15	9.79	10.00	10.30
1.5	10.02	9.75	9.87	10.16
2.2	9.97	9.80	9.80	10.15
3.8	10.02	9.75	9.87	10.16

CHAPTER 4



METHODS FOR MEASURING CETACEAN TARGET STRENGTH

4. METHODS FOR MEASURING CETACEAN TARGET STRENGTH

Despite being considered ‘potentially’ strong acoustic targets at fishery sonars frequencies because of their lung size, few recent scientific studies on active acoustic detection of cetaceans have been conducted. The literature on the subject is limited. A detailed overview of past studies is presented in the following paragraphs, and will give the reader a key to understand the scientific contribution provided in the subsequent chapters of this thesis. This chapter reviews the present knowledge about cetacean target strength (TS), introducing the scenario that brought to life my PhD project, a short and comprehensive explanation of the design of the acoustic systems I have used, and a description of my contribution to improve the use of omnidirectional sonar for quantitative applications in cetacean research and conservation.

4.1 Overview of past studies

The first publication regarding cetacean TS was by Dunn (1969). Using calibrated sonobuoys he recorded sounds and echoes from an unseen target, and identified it from its sounds as a solitary sperm whale (*Physeter macrocephalus*). During the experiment, after the sonobuoy had been left recording background noise for some minutes an aircraft returned over the sonobuoy and dropped an explosive charge (1.8 lb of TNT). The explosion from this charge insonified the water column, and the resultant volume reverberation was measured. At a center frequency of 1 kHz the recorded TS from three different explosive charge drops were: -7.3, -8.5 and -7.9 dB//1dyn/cm². Dunn (1969) considered that the whale was probably orientated towards the hydrophones (the recorded click dB level was 73.5 dB//1dyn/cm²) and concluded that if the measured TS value arose from the bow aspect it should be expected that beam aspect TS values would be between 0 and 10 dB // 1dyn/cm².

A few years later Love (1973) made TS measurements of six individual humpback whales at short range (between 20 and 78 meters) from an oceanic tower using a horizontally-mounted echosounder. The measurements were made at 10 and 20 kHz utilizing standard transducers transmitting 10 millisecond pulses every second. The position and aspect determination of the targets were excellent because the whales could be observed from the tower for the entire time they were insonified. The resulting TS measurements at 20 kHz for a 14 m long humpback whale were + 7dB from the side aspect and -4 dB from the head aspect. One of the insonified whales was a juvenile and for that, the resulting TS at 20 kHz from the side aspect was + 2 dB.

One year later Levenson (1974) used a technique similar to that used by Dunn (1969) to investigate sperm whale TS. When a whale contact was made, three calibrated sonobuoys, with hydrophones

were deployed at 20 meters depth at different positions. Subsequently a series of explosive charge (31.5 g of tetryl) were used to insonify the water column, and echoes with a bandwidth between 50 Hz and 20 kHz were recorded. Additionally, visual and photographic evidence indicating sperm whales in the vicinity of the hydrophones were collected, and the approximate positions of the whales were calculated by triangulation. A total of five calculated whale positions showed mean target strength of -2.5 dB in the 250-500 Hz band and of 10.8 dB in the 8-16 kHz band. No information on the insonified aspect was collected. However, the TS values were similar to those collected by Dunn (1969) and are hence considered representative for this species of whale.

Au (1996) ran an experiment under controlled conditions measuring the TS of an Atlantic bottlenose dolphin (*Tursiops truncatus*) as (i) a function of acoustic frequency with the animal at broadside (Figure 4.1a), (ii) as a function of the dolphin's aspect angle (Figure 4.1b), and (iii) to determine the relative amount of reflection from different parts of the dolphin's body. Using a system with a frequency bandwidth between 23 and 80 kHz and three different signals (two of the signals were frequency modulated - FM - pulses, one for low frequencies and the other for high frequencies; the third signal was a broadband short transient-like signal with a peak frequency of 67 kHz) he observed that TS decreased as the frequency increased, and with maximum TS values coming from the dolphin broadside and minimum from the tail.

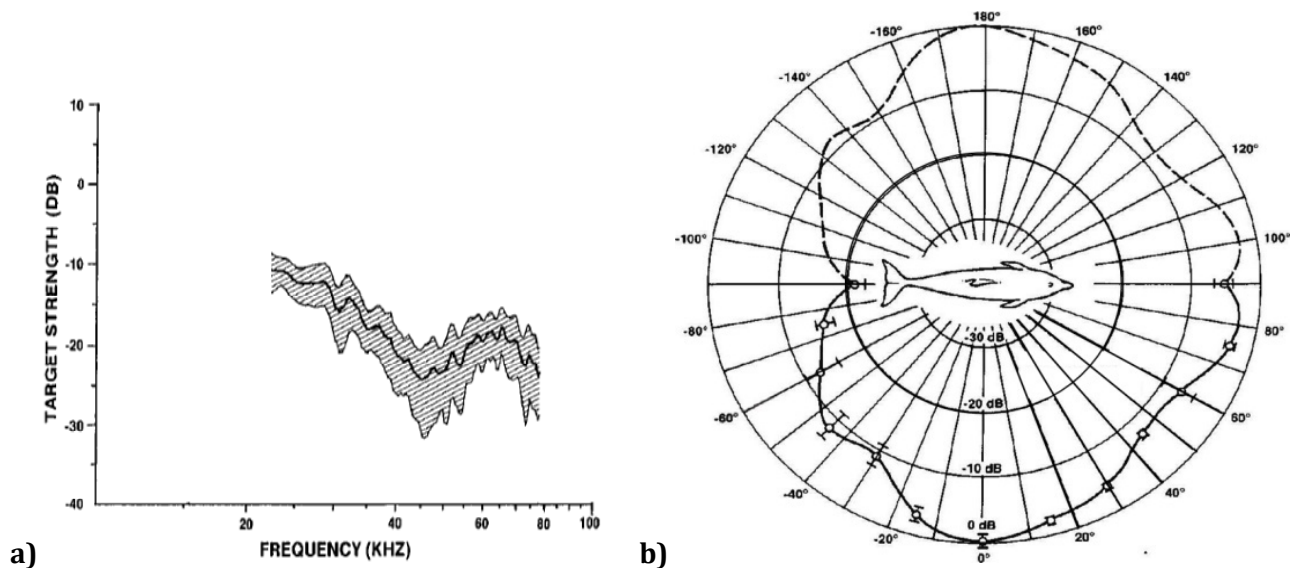


Figure 4.1: Acoustic reflectivity of *Tursiops truncatus* as presented by Au (1996). a) Multi-frequency response at broadside b) TS polar response of cetacean body.

The echo levels were 21 dB lower at tail aspect than at broadside aspect, while the difference from broadside to the head aspect was only 5 dB. Au (1996) also described using a high resolution acoustic system how the highest TS occurred in the area between the dorsal and pectoral fin, suggesting that

the lungs were the main reflective structure of a cetacean's body, underlining a clear analogy with the swimbladder in some fish species (Love 1971).

An interesting application of active acoustics to cetacean conservation was proposed by Miller et al. (1999), who tested a high frequency sonar (86 kHz) with the aim of developing a tool to prevent ship strikes, a major cause of death for large whales. Miller et al. (1999) were able to measure the TS of North Atlantic Right whales (*Eubalaena glacialis*) and Humpback whales (*Megaptera novaeangliae*). During two different sets of measurements at sea they used a system with a center frequency of 86 kHz pinging with a continuous wave (CW) pulse of 3 ms and a source level of 170 dB. His data showed how size and aspect angle play predictable roles in target strength determination. The maximum broadside target strength for the Northern Right whale was about -1 dB, suggesting that that North Atlantic Right whale TS may be 5 dB lower than that of the Humpback whale of similar size at 86 kHz. Miller (1999) suggested that the presence of a thicker blubber layer on the North Atlantic Right whale body could explain this difference, by introducing a blubber-related attenuation factor. He tested the reflective property of the blubber using a multisensor Core Logger, an instrument used by geologists to measure the electrical resistance of sediments and rocks, yielding some concrete but not exhaustive indication about his hypothesis.

The most recent report on cetacean TS came from Lucifredi and Stein (2007), who used a bottom-mounted transducer and recorded Gray whale (*Eschrichtius robustus*) TS with the aim of distinguishing, in post-processing analysis, the whale's backscatter responses from backscatters generated by environmental clutter (background noise). The sonar system they used had a frequency span between 21 and 25 kHz and operated at a source level of 214 dB/ μ Pa. The pulse duration was unspecified, while the ping rate was of 1 every 5 seconds. Lucifredi and Stein (2007) clearly described the potential application of active acoustics in future development of automated whale detection systems. Unfortunately the low ping rate and the fixed position of the system didn't allow the collection of a large data set. TS averages were made based on 4 to 6 pings, and ranged from -2.9 dB at the tail to 12.8 dB at broadside.

Au et al. (2007) measured, as a further contribution to this field of science, the TS of a trained dolphin at depth. The results of this experiment varied from about -26 dB to -40 dB (Au personal communication), and agreed with the *in situ* TS measurements of dusky dolphins recorded off the coast of Namibia, which are presented in Chapter 5 (Bernasconi et al. 2011).

Active acoustics have also been used for cetacean behavioral studies, but few studies have quantified the sonar output. The advent of digital sonar systems with software capable of target tracking and connectivity to 'friendly' software interfaces that can handle large amounts of data is a development

no older than 20 years. Papers such as those by Vabø and Nøttestad (1997), Nøttestad et al. (1999), Axelsen et al. (2000) and Nøttestad et al. (2002) can be considered the base of a new generation of active acoustic studies of behavior, and give first indications on how active acoustics could be used for applications other than standard fishery research. However, such studies were essentially descriptive since they relied just on the patterns observed on the sonar screen (i.e. not logged digitally or quantifiable acoustically). More quantitative acoustic data came later from Benoit-Bird et al. (2004) who used a fish finder to evaluate Dusky dolphin (*Lagenorhynchus obscurus*) relative abundance, linking relatively strong target detections presumed to be dolphins with the presence of deep scattering layers of its schooling prey. More recently Benoit Bird and Au (2009) used a multibeam sonar (an instrument similar to the omnidirectional unit used in this thesis work) to observe Spinner dolphins' (*Stenella longirostris*) hunting tactics in an attempt to understand the benefits of group foraging and the mechanisms of prey aggregation to assess the potential importance of group foraging in predator survival.

One last paper by Oliver and Kvitek (1984) has to be mentioned for its uniqueness: They used sidescan sonar to determine the bottom disturbance and its relative intensity generated by the presence of the Gray whale (*Eschrichtius robustus*). The method showed a possible and interesting application of active acoustics to Gray whale ecological studies. Even in the absence of a sighted animal, the use of such technology can give precise indications on the habitat use and on the passage of this peculiar whale species: Gray whales are unique among baleen whales as being the only species characterized by bottom feeding (Oliver et al. 1983; 1984). Sidescan sonar has then the clear potential of visualizing and allow to count the ridges left by that characteristic feeding behavior.

4.2 Coordinated ecosystem survey in the Norwegian Sea

The whale TS project that comprises a major portion of my thesis was conducted under the umbrella of the Coordinated Ecosystem Survey in the Norwegian Sea and surrounding waters. The major aim of that survey was to map the large-scale oceanic distribution, and quantify the abundance, aggregation patterns and feeding ecology, of Northeast Atlantic mackerel (*Scomber scombrus*), Norwegian spring-spawning herring (*Clupea harengus* L.) and Atlantic blue whiting (*Micromesistius poutassou*) in relation to the physical and biological environment during summer in the Norwegian Sea and surrounding waters. A strong ecological perspective has been put into these cruises, involving concurrent measurements at each station of the physical environment, plankton communities, pelagic fish species (mackerel, horse mackerel, herring, blue whiting, Atlantic salmon, snakefish, lump sucker etc), including systematic stomach sampling of mackerel, herring and blue whiting. This approach enables

us to study ecological questions across spatial and temporal scales, which is important to reveal new knowledge about the functioning and food web dynamics of the Norwegian Sea (Nøttestad et al. 2010).

The survey vessel fleet included two chartered commercial fishing vessels, M/V *Libas* and M/V *Eros*. These two vessels have adjustable drop keels and state of the art acoustic instrumentation, making them excellent for large-scale scientific surveys. Their instrument suites included: two omnidirectional sonars, the low frequency (20-30 kHz) Simrad SP90 (upgraded in the last year of the project with the new SX90) and the high frequency (110-122 kHz) Simrad SH80 with scientific output; a calibrated EK60 scientific echosounder with five frequencies (18-38-70-120-200 kHz), and an Acoustic Doppler Current Profiler (ADCP) operating at 75 kHz. In addition, hydrographic profiles (CTD cast) were collected using a SEABIRD carousel water sampler SBE 32, and a dedicated SAIV SD204 CTD unit was used to generate data required to simulate the variance in sonar performance expected along the survey track due to environmental variability (see paragraph 4.3.3). The vessels covered substantial areas (7395 nmi²) in the Norwegian Sea and surrounding waters between 62° - 75° N and 18°W - 22°E (Figure 4.2). Mackerel and herring schools and other looser shoals (dense mixed layers) were recorded mostly near the surface using the omnidirectional sonars in most areas within the Norwegian Sea. This typical 3D vertical distribution of fish schools may strongly influence the quantitative conclusions drawn from vertical echosounder (e.g. EK60) observations because of the effect of the so- called near-surface dead zone to which vertical sounders are essentially blind (Patel et al. 2009; Scalabrin et al. 2009; Totland et al. 2009). Most of the schools were quite small in size (school biomass typically ranged from about 100 kg to 20 tons.) with shallow distribution between 0-50 m. More than 30 000 individual schools were encountered along the cruise tracks. The Norwegian Sea habitat is characterized by long summer days at higher latitudes and by low temperatures; these conditions force fish and nutrients to stay close to the surface (Skjoldal 2004) and generate a requirement to survey the near-surface region of the water column by pointing the omnidirectional sonar horizontally: this both increases the horizontal coverage of the survey and reduces the uncertainty and potential bias brought by dead zone effects and vessel avoidance (Patel and Ona 2009). With these requirements, it was decided to start the development of a reliable quantitative method for the use of omnidirectional sonar (instruments normally not used for scientific estimations) for biomass studies: omnidirectional sonars are normally used only to locate schools, and to aid fishers to catch them, rather than for quantitative biomass estimation. In order to progress towards biomass estimation, numerous processing advances were required, including calibration and data collection methods, and the development of analysis tools not immediately on the market (e.g. LSSS and ECHOVIEW modules for omnidirectional sonar or dedicated MATLAB data processing applications); and this thesis tackles some of these issues.

A problem faced during the sonar sampling was the impact that temperature variations throughout the survey had on sound velocity, c . Temperatures in the upper part of the water column varied from 14 °C along the Norwegian coast down to 0.2 °C along the ice-edge in the Greenland Sea. Unpredictable changes and mixing of different water masses (physical fronts) along the ships' tracks, affected the performances of sonar systems pointing in the horizontal plane. The sonar settings were constantly updated to prevent the effect of ray bending, a phenomenon that influences sound wave propagation in the horizontal direction, and that can drastically reduce sonar performances (see paragraph 4.3.3).

Systematic visual observations of marine mammals were also performed for the entire duration of the surveys, and approximately 12 different species were sighted (Nøttestad et al. 2010).

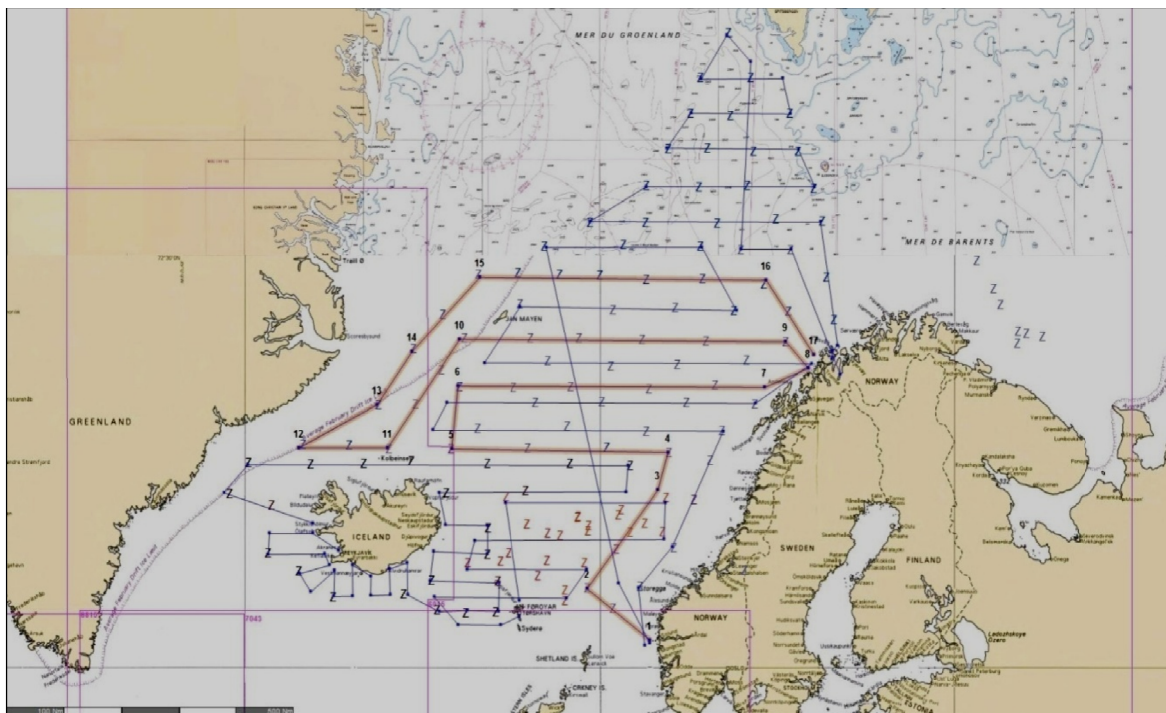


Figure 4.2: Typical area covered during the last four years of survey of the Norwegian Sea and surrounding waters. In the last years the collaboration was extended to Icelandic and Faroese vessels to increase the spatial coverage of the southern areas of this portion of Northeast Atlantic Ocean.

In this context, the study presented in my thesis was included as an important subgoal of the survey, to develop omnidirectional sonars as quantitative tools: starting the process of data quantification with large, prominent targets the acoustic backscatter from which could be easily distinguished from the environmental background noise and tracked visually at the surface was beneficial acoustically, as well as opening a new window for observations of whales. In association with selected whale sightings, the ship operations and standard survey design were interrupted and dedicated sonar/whale experiments as described in Chapters 5, 6, and 7 were opportunistically attempted.

4.3 Instruments

Many instruments are employed to gather data on different topics during the survey. In this paragraph I describe the tools that have been used to achieve the preliminary results obtained with this pilot project on cetacean body acoustic backscattering characteristics.

4.3.1 Scientific echosounders: Simrad EK500 and EK60

Scientific echo sounders are widely used for navigation, fish abundance estimation and other marine research (e.g. detailed bathymetry studies). Acoustic information obtained from scientific echo sounders, such as target strength and target position, can be valuable in describing individual targets of marine animals, whereas measurements of volume backscattering strength are suitable for describing a large number of targets distributed over a volume of water. The Simrad EK60 scientific echo sounder system provides high-quality target strength data, target position, and volume backscattering strength measurements over a large dynamic range (160 dB//1 μ Pa) for a wide range of frequencies (18–400 kHz), and is the natural evolution of the previous EK500 system (see Chapter 5). The basic EK60 system is comprised of one or more transducers and general purpose transceivers (GPT) - if more than one transceiver is used, an Ethernet switch is required to connect the GPTs to the computer - and a personal computer connected to a network.

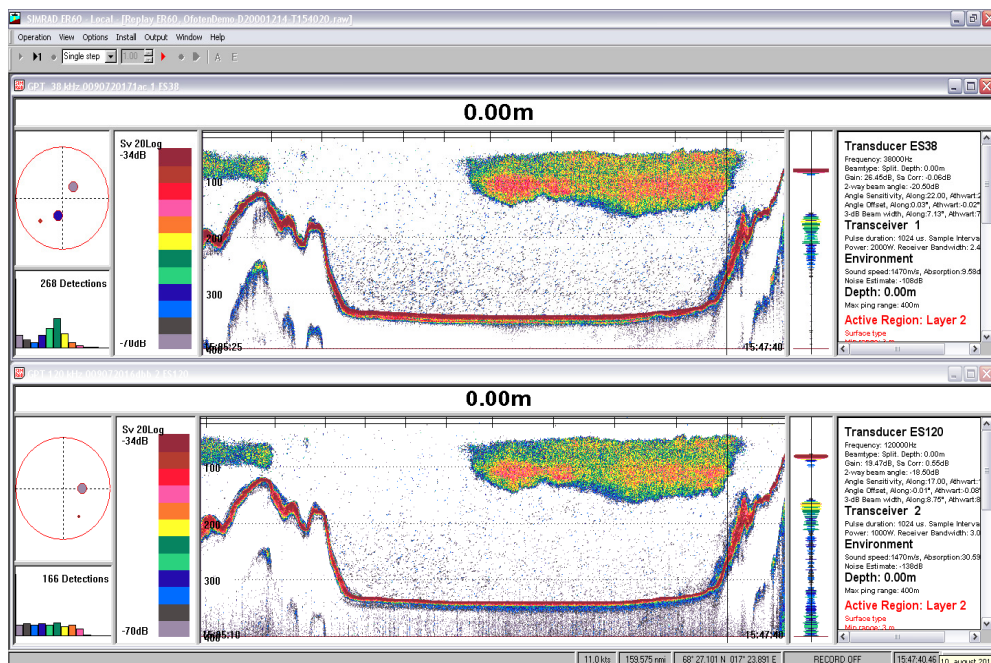


Figure 4.3: Echogram screen dump sample showing the Simrad ER60 software friendly interface running two echosounder frequencies. It is very easy for a windows user to learn the approach for the use of this software. The main window is divided in two sub-windows tiled horizontally as one for each frequency. From left to right it is possible to observe the following: a circle showing the position of the target in the beam, a histogram representing the frequency distribution of the detected targets, an adjustable colour scale legend, the echogram visualization, an oscilloscope visualization and the description of the echosounder settings.

A GPT unit is the heart of the system, containing the transmitter and receiver electronics. The receivers are designed for low noise, and they can handle input signals spanning a very large instantaneous dynamic amplitude range (160 dB//1 μ Pa). All targets are measured and displayed through the software interface called ER60 (Figure 4.3).

The system can be connected to other peripheral sensors and systems including navigation (GPS is usually the basic sensor used for scientific purposes), motion, trawl sensor inputs, datagram output and remote control. Raw data for further processing can be stored on the system's hard disk, or other recordable media. During replay, signals are input into the echo sounder software as if they were received directly from a transceiver.

4.3.2 Omnidirectional sonars: SIMRAD SH80 and SX90

The Simrad SH80 and SX90 fish finding sonars are long range frequency selectable omnidirectional sonars. They are both designed for medium and large sized fishing vessels, principally for purse seiners, but they are also suitable for pelagic trawlers. The sonars enable the operational frequency to be chosen, in 1 kHz steps between 110 to 122 kHz (SH80) and 20 to 30 kHz (SX90). The multi-element transducers enable the omnidirectional sonar beam to be tilted electronically down to -60 degrees. This enables the operator to track schools of fish, and to observe the whole water volume around the vessel. A stabilization system is included for electronic pitch and roll compensation. A friendly interface gives very good data visualization on a high resolution color display (Figure 4.4).

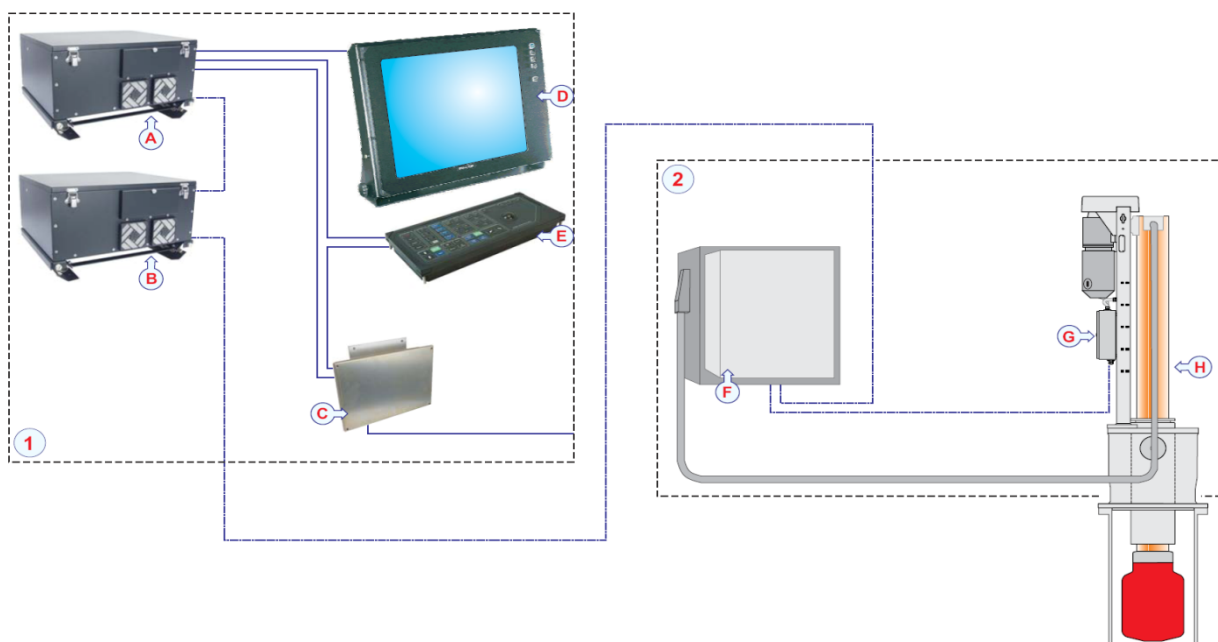


Figure 4.4. Schematic view of the SH/SX system and definition of its components. (1)WHEEL HOUSE (BRIDGE): A) Processor unit B) Beamformer unit C) Interface unit D) Colour display E) Operating panel (2) SONAR ROOM: F) Transceiver unit G) Motor control unit H) Hull unit.

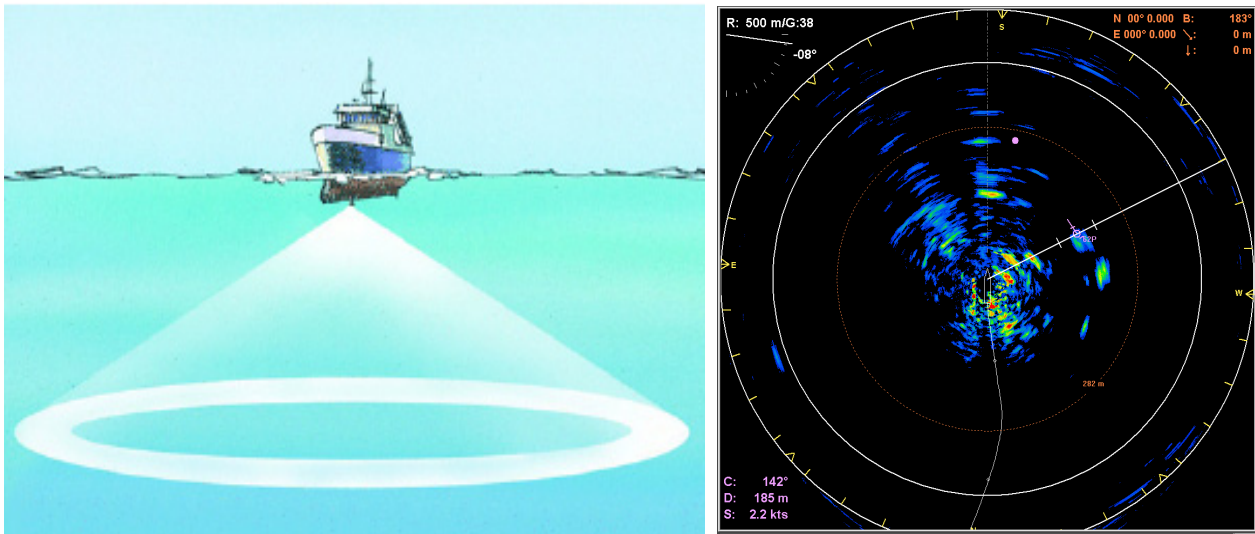


Figure 4.5: The horizontal beam configuration opens and closes as an umbrella changing the tilt angle setting with a radar like coverage of 360°.

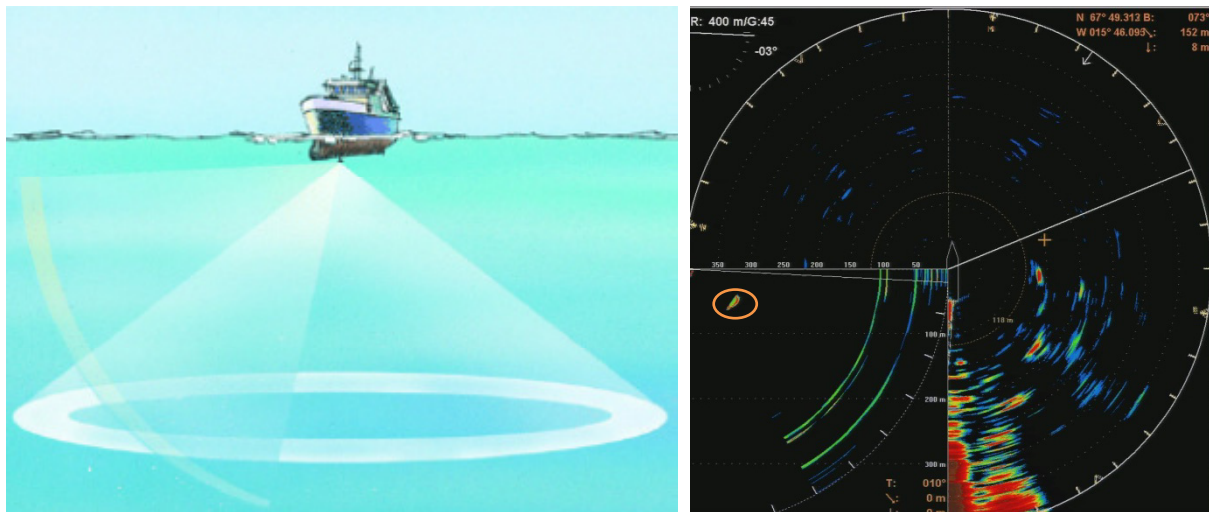


Figure 4.6: The vertical slice view allows scanning and observing in more detail areas of interest aiming the beam in the direction of the target. During the whale experiments it was possible to record the first phases of the dive of different species for few seconds.

The signal processing and beamforming is performed in a fast digital signal processing system using the full dynamic range of the signals. The Simrad omnidirectional sonar units are characterized by a unique configuration of the 240 transmitter and 480 receiver channels of the SH80 and 256 separate transmitter and receiver channels of the SX90, with transducer elements spread around a cylindrical transducer array. The transmission, reception and data processing are under computer control, and the powerful capabilities of the sonar are the results of sophisticated digital signal processing software that is not discussed in this thesis.

When the Omni beam is tilted, the total beam picture can be envisaged as a partially folded umbrella (Figure 4.5), with all beams in the 360 degree observation window around the vessel having the same tilt angle. In addition to seeing the target from above, it is also possible to see the target from the side, by using the vertical slice presentation. In this case the beam covers a continuous vertical sector from 0 to -60 degrees in one transmission. This vertical slice, which is presented by the white audio line in the horizontal picture, can be chosen from any bearing by the manual training control (Figure 4.6).

The combination of the Omni mode and the vertical slice provide an optimal visualization of the catch situation. In addition to the Omni picture, the vertical slice is especially useful for visualizing the vertical distribution of a school or aggregation of fish. In that way, it is not necessary to sail over the target to see the distribution with a vertical echo sounder, which may result in disturbance of the targeted fish school and subsequent avoidance behavior (Olsen 1971 and 1975; Mitson 1995).

4.3.3 CTD samples and the Lybin ray tracing model

During broad scale surveys the different physical conditions of the water encountered may strongly influence the performance of the acoustic instruments. When transducers are facing downwards these variations do not affect systematically the perception of the observed volume of the water column, but a strong influence can be felt when sonars are directed horizontally. The travelling acoustic wave can suddenly bend and be channeled by different water layers, possibly misleading the operator about what is really detected and its 3D position in the water column. What is visualized on the sonar screen as a school close to the surface (having just the tilt angle parameters setting as a reference), may in reality be a school with a position that is actually a hundred meters deeper (Figure 4.7).

Ray bending is the main problem to consider while navigating in different areas of the oceans; the effect this physical phenomenon has on sonar performance has to be evaluated in terms of detection range and probability for different areas and season of the year. Avoiding any over-interpretation was the primary objective during these first quantification tests of omnidirectional sonar data. Information about water masses was collected with a SAIV SD204 CTD unit and the data were used to run simulations through the LYBIN acoustic ray trace model (Hjelmervik and Sandsmark 2008). This model, owned by the Norwegian Defence Logistic Organization, is well established and frequently used to evaluate sonar performance under different environmental conditions.

The choice of the SAIV SD204 unit for this purpose was made considering the capability of the SAIV Minisoft SD200W. This software generates directly, through an easy interface, .xml files ready to be processed with the software Lybin 4.0, and was used to update the sonar settings during the survey after every sampling station.

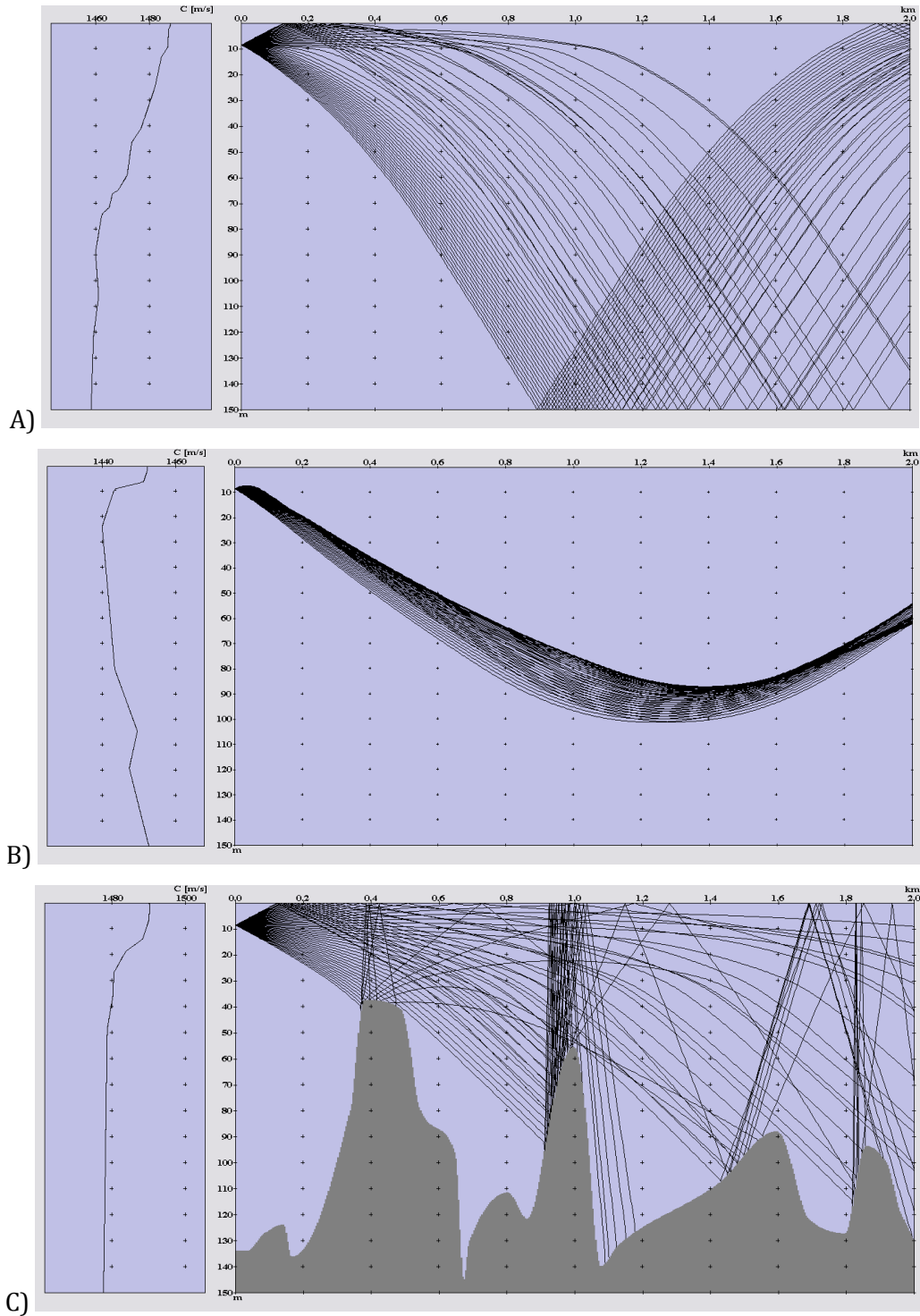


Figure 4.7: Ray trace simulations for three CTD stations for the Simrad SH80 unit operating at 110 kHz with a tilt angle setting of 0° and a pulse duration of 6 ms. A) A typical bending that can be encountered in pelagic habitats that reduces the horizontal detection range of the sonar. B) An extreme situation encountered with the sound drastically channeled by fresh water masses close to east Greenland. C) Close to shore the presence of shallow sea mounts can complicate the situations. Wave refraction and reflection can mislead the observer and generate bias which must be investigated in more detail (the represented bottom is a hypothetical illustration and not taken from real bathymetric data of a particular area).

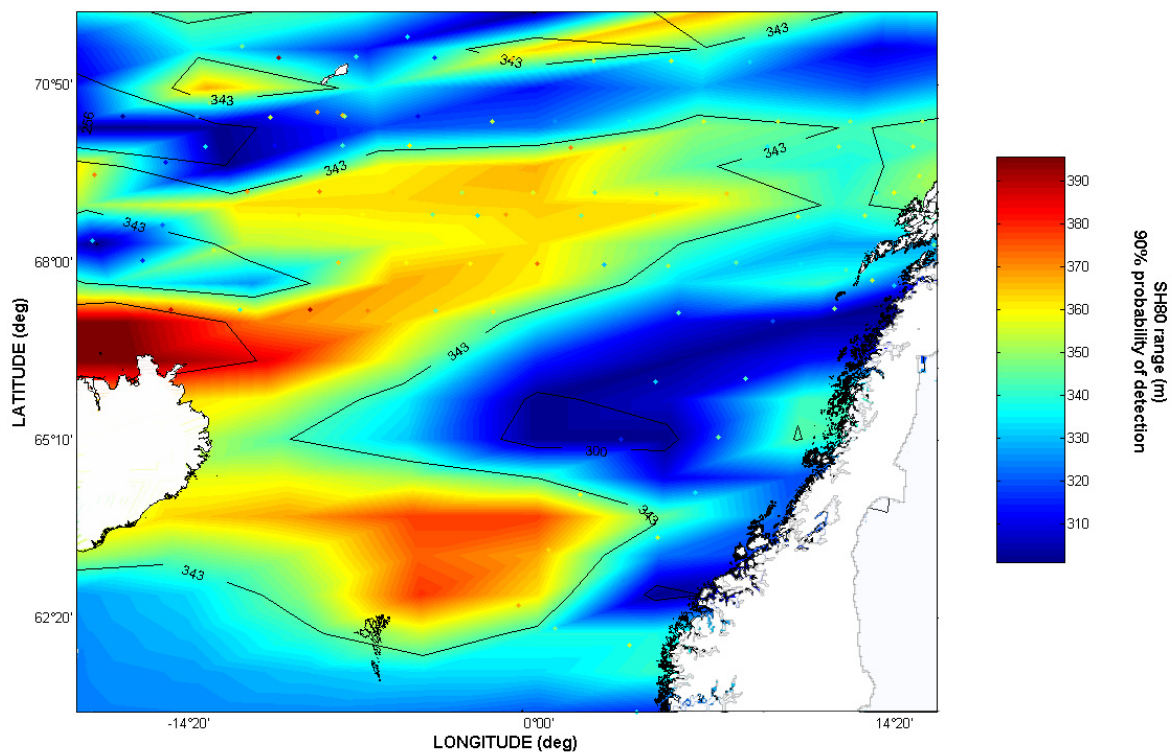


Figure 4.8: Simrad SH80 detection range performance. The map is the result of 104 CTD casts and 520 simulations performed using the Lybin detection model. The simulation represent data collected with the sonar tilt angle set at 0° and 6 ms pulse duration (Nøttestad et al. 2010).

The SAIV SD204 is a self-contained CTD unit (maximum operative depth 6000 m) that measures, calculates and records sea water conductivity, salinity, temperature, pressure and sound velocity *in situ*. Data recorded in the instrument are in physical units and can be copied to a PC and presented immediately after the measurements have been completed. This makes the performance of the SD204 comparable to much more voluminous and expensive cable based CTD-systems. From a preliminary qualitative analysis (Figure 4.8) using data collected in the last four years it is clear that it will be useful in the near future to adopt and standardize the use of the Lybin probability model if sonar data are to be used for biomass estimation of fish stocks and to fully capitalize the potential of omnidirectional sonar units for fish assessment and whale detections (Nøttestad et al. 2010).

4.4 Omnidirectional sonar signal processing: basic MATLAB code.

There are different ways to read the omnidirectional sonar raw data. For the purpose of this thesis I will explain an easy and immediate way to extract, calibrate and visualize them (see Appendix A). The first step after having stored the raw binary data to a hard drive is to convert them from binary to .csv files. Simrad provides with the SH/SX scientific output module an application called Sonar Data Converter (I used the version 9.0.4).

From every ping four .csv files were generated and named with a precise time stamp year-month.day-hh.mm.ss, and a code named **beam** or **hdr** (beam data and header). Two of the .csv files correspond to the omnidirectional data log while the other two come from the sonar vertical slice data log.

Due to the large amount of beam data (1hour of raw data at 110 kHz is approximately 1.36 GB), it was convenient to import and convert the data into a more manageable MATLAB format (1hour of data at 110 kHz is approximately 1.76 GB) defining structures to combine the setting files (hdr) with the beam signals (beam). The basic MATLAB code for processing our received sonar signals is presented here, applied to a single ping converted in .csv files.

Essentially, raw sonar data are comprised simply of a voltage and its corresponding arriving time. The raw data signal processing starts by giving the different variables specific names (e.g. Range, EL, TVG...). The converted name-beam.csv files are imported into MATLAB as a matrix (1:65 columns, 1:2800 lines) where the first column represents time. It is convenient in practice to split this matrix, generating a vector with the time data and a matrix with the beam data and combining them in the generated MATLAB file structure. The next step in the data processing route is then to convert the ping time stamp into range by:

$$\text{Range} = ((\text{time}(i,1) - \text{time}(1,1)) * c) / 2; \quad (4.1)$$

where time is in seconds and c (m/s) is the sound speed determined from data from dedicated CTD casts.

The SH80 scientific output is an A/D signal scaled to mV, but the stored beam signals are squared voltage values. The various signal forms coming from the beam former are scaled too, but all the advanced signal processing required to present the information to the Processor Unit takes place in the Beamformer unit (see paragraph 4.3.2 and figure 4.4 - system component 1B). If we take $10\log$ (beam values) we get dB//V that is proportional to dB// μPa (see paragraph 2.2.3). At this point the beam data need a first correction that considers the estimated ambient noise and determines the sonar receiving sensitivity (named dBIMCorrected in the dedicated MATLAB scripts described in this paragraph). This correction factor depends on the sonar carrying frequency. At 110 kHz it was calculated by Simrad as -204.8 dB// μPa . If the data matrix (1:64, 1:2800) is named as 'beam', the data can be process to obtain the received echo level (EL) as follow:

$$\text{EL} = 10\log_{10}(\text{beam}/1000000) - \text{dBIMCorrected}; \quad (4.2)$$

where the factor 1000000 is $1/(\text{mV} * \text{mV})$ that transforms the output data to dB//V and consequently to dB// μPa . We can now define the TVG (see paragraph 3.3) for single target detections:

$$\text{TVG} = (40) * \log_{10}(\text{Range}) + (2 * \alpha * (\text{Range})); \quad (4.3)$$

Where 40 is the applied TVG factor for TS measurements, alpha is the absorption coefficient, converted in dB/m, calculated using CTD data cast with the Francois and Garrison (1982) formula, and Range from equation (4.1) is in m.

At this point the sonar equation (2.31) can be applied to determine TS considering a dedicated *in situ* calibration experiment (as described in Paragraph 3.6) that gives us a correction value (C) to correct the sonar equation and obtain calibrated TS measurement by:

$$TS = EL - 210 + TVG + C; \quad (4.4)$$

Now we can reproduce the omnidirectional sonar view using the plot commands:

```
% OMNIDIRECTIONAL BEAMS VIEW
if SectorType==0 % the sector type is represented by this number in the hdr.cvs
TSt=(real(TS))';
[b s]=size(TSt);
n = s-1;
angStep=2*pi/b; % gives the omnidirectional view
theta=(0:(b))*angStep;
theta=theta+pi/2;
X = (lRange*cos(theta))';
Y = (lRange*sin(theta))';
TSt=[TSt;TSt(1,:)];

surface(X,Y,TSt,'EdgeColor','none'); whitebg('k'); set(gcf, 'color', 'k');

% VERTICAL BEAMS VIEW
elseif SectorType==2 % the sector type is represented by this number in the hdr.cvs
TSt=(real(TS))';
[b s]=size(TSt);
n = s-1;
angStep=-(1/3*pi)/b; % gives the vertical slice
theta=(0:(b))*angStep;
theta=theta;
X = (lRange*cos(theta))';
Y = (lRange*sin(theta))';
TSt=[TSt;TSt(1,:)];
```

This plot command recognizes and plots the different sector types (named previously SectorType in the MATLAB file structure), omnidirectional or vertical, using a MATLAB if-elseif statement. During the conversion of the data into MATLAB format, I recommend generating file structures to handle the large amount of data more easily and to link the sonar settings with the beam data (see Appendix A). With a simple plot command it is also possible to visualize the received EL over range of the received signal for a beam of interest.

$$\text{plot}(\text{Range}, TS(\text{beam number}, \text{Range of interest})); \quad (4.5)$$

Figure 4.9 shows a screen sample of an analysis tool I developed using MATLAB to monitor and extract calibration data. It combines the two different views (omnidirectional and EL by range), and employs a java application (that I am still developing) and a hidden MATLAB script (similar to the one presented here) to extract the processed data into .txt files.

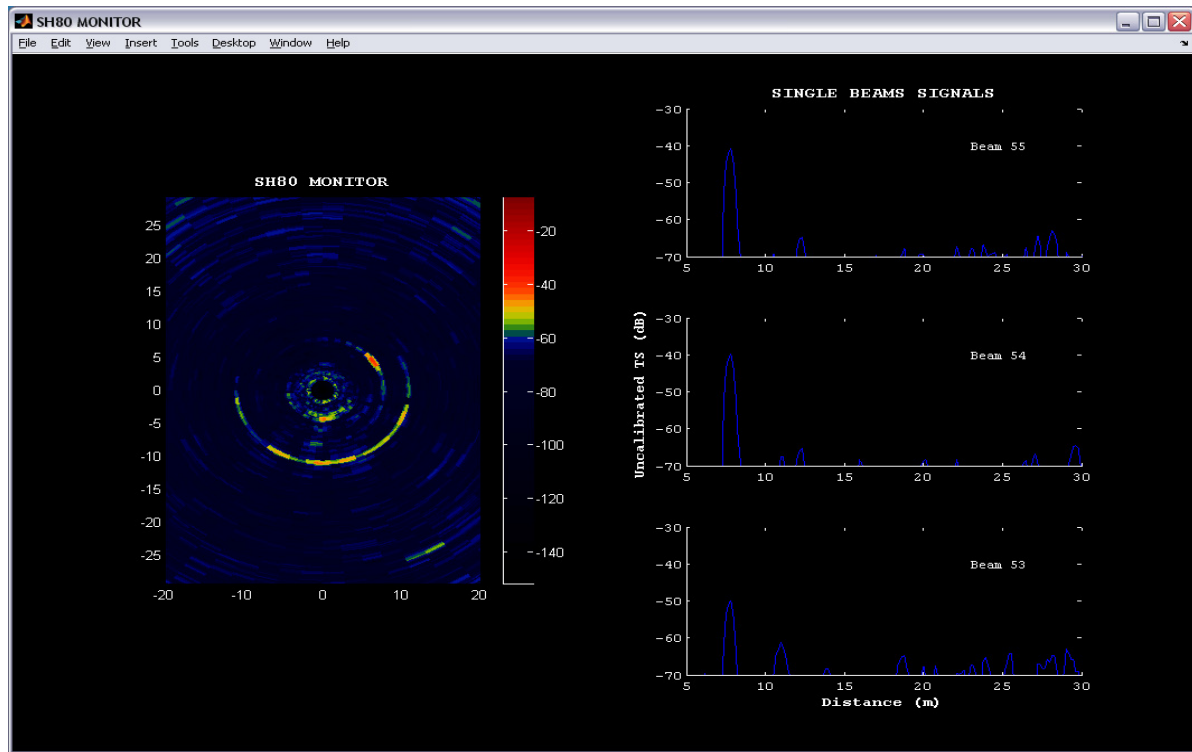
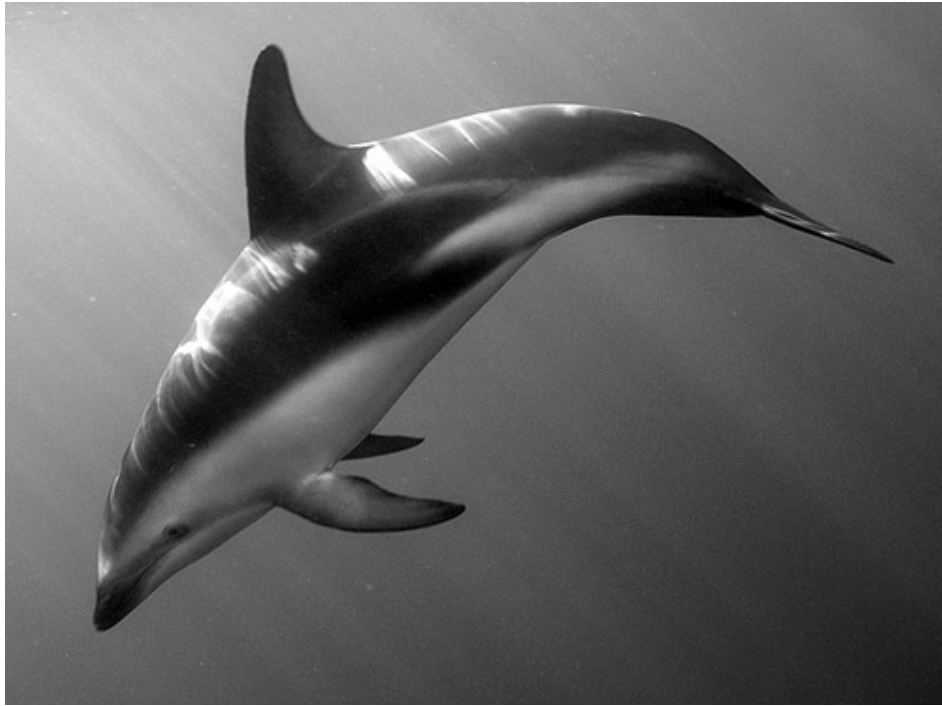


Figure 4.9: Sonar screen capture of a dedicated MATLAB application written by Matteo Bernasconi and Ruben Patel to monitor the post processing of the SH80 calibration data. On the left side of the window the raw data are visualized in the omnidirectional view, on the right side selected beams are observed in terms of power spectra.

CHAPTER 5



**ACOUSTIC OBSERVATIONS OF DUSKY DOLPHINS
(*Lagenorhynchus obscurus*) HUNTING CAPE HORSE
MACKEREL (*Trachurus capensis*) OFF NAMIBIA.**

5. ACOUSTIC OBSERVATIONS OF DUSKY DOLPHINS (*LAGENORHYNCUS OBSCURUS*) HUNTING CAPE HORSE MACKEREL (*TRACHURUS CAPENSIS*) OFF NAMIBIA.

ABSTRACT: Predator–prey interactions of mammals and their fish prey in marine ecosystems are rarely identified and recorded. I document for the first time the underwater behaviour of hunting dusky dolphins *Lagenorhynchus obscurus* and the responses of their prey, Cape horse mackerel *Trachurus capensis*, observed in open ocean waters off northern Namibia. Predator–prey interactions were monitored acoustically during a continuous period of 2 h with a split-beam scientific echo sounder, and the surface behaviour of the dolphins was observed from the ship’s deck. In total 54 predator–prey events were observed (mean, 0.45 events min⁻¹). The maximum burst speed during attack was 9.9 m s⁻¹, while the average attack speed was 3.4 m s⁻¹ (mean swimming speed: 1.4 m s⁻¹). Dolphin traces were predominantly located underneath the fish aggregation (63% of the time), as the dolphins attacked the schools from underneath (mean depth: 120 m; maximum depth: 156 m). The dolphin target strength at 38 kHz was, on average, –31.5 dB (95% CI: –33.4 to –30.2 dB). The attacks caused immediate reactions in the Cape horse mackerel aggregations: subschools were forced towards the surface where they were herded into dense aggregations by the dolphins. Observed predator response patterns included ‘Vacuole’ (n = 21), ‘Split’ (n = 19), ‘Bend’ (n = 10) and ‘Hourglass’ (n = 4). Packing densities changed significantly before (0.4 fish m⁻³), during (2.0 fish m⁻³) and after (0.3 fish m⁻³) the dolphin attacks, and when predators burst into the fish aggregations, intraschool packing densities of horse mackerel were significantly lower in front of the predators (0.33 ± 0.17 fish m⁻³) than behind (6.65 ± 1.76 fish m⁻³).

5.1 INTRODUCTION

The Benguela current system is one of the world’s four major western boundary upwelling regions (Fig. 5.1 A) and has historically been considered one of the most productive marine ecosystems in the world (Shannon 1985). In the south it borders the Agulhas Bank region in South Africa at about 35° S, while the northern border of the system is the Angola-Benguela frontal zone between 14° S and 17° S (Shannon & Nelson 1996). The Benguela Current Large Marine Ecosystem (BCLME) is one of the largest wind-driven coastal upwelling systems in the world (Shannon & O’Toole 2003). Cape horse mackerel *Trachurus capensis* is currently the most abundant commercial species within the northern BCLME, and as an important predator and prey it plays a key ecological role in the ecosystem (Boyer & Hampton 2001). Abundance estimation of horse mackerel is primarily done by identification of

acoustic targets and ground-truthing by pelagic trawling (Axelsen et al. 2004, Vaz Velho et al. 2006). Cape horse mackerel is known to exhibit considerable vertical migrations that have been adapted to the prevailing local conditions (e.g. Pearre 2003, Vaz Velho et al. 2010). In the southern BCLME, Cape horse mackerel generally form dense shoals in midwater or close to the bottom during the day, and they migrate to midwater at night and disperse before aggregating and descending again at dawn (Pillar & Barrange 1998). Although more variable, a similar pattern has been found for the northern BCLME, where Cape horse mackerel typically remain in midwater during the day and ascend to near the surface at night (Axelsen et al. 2004).

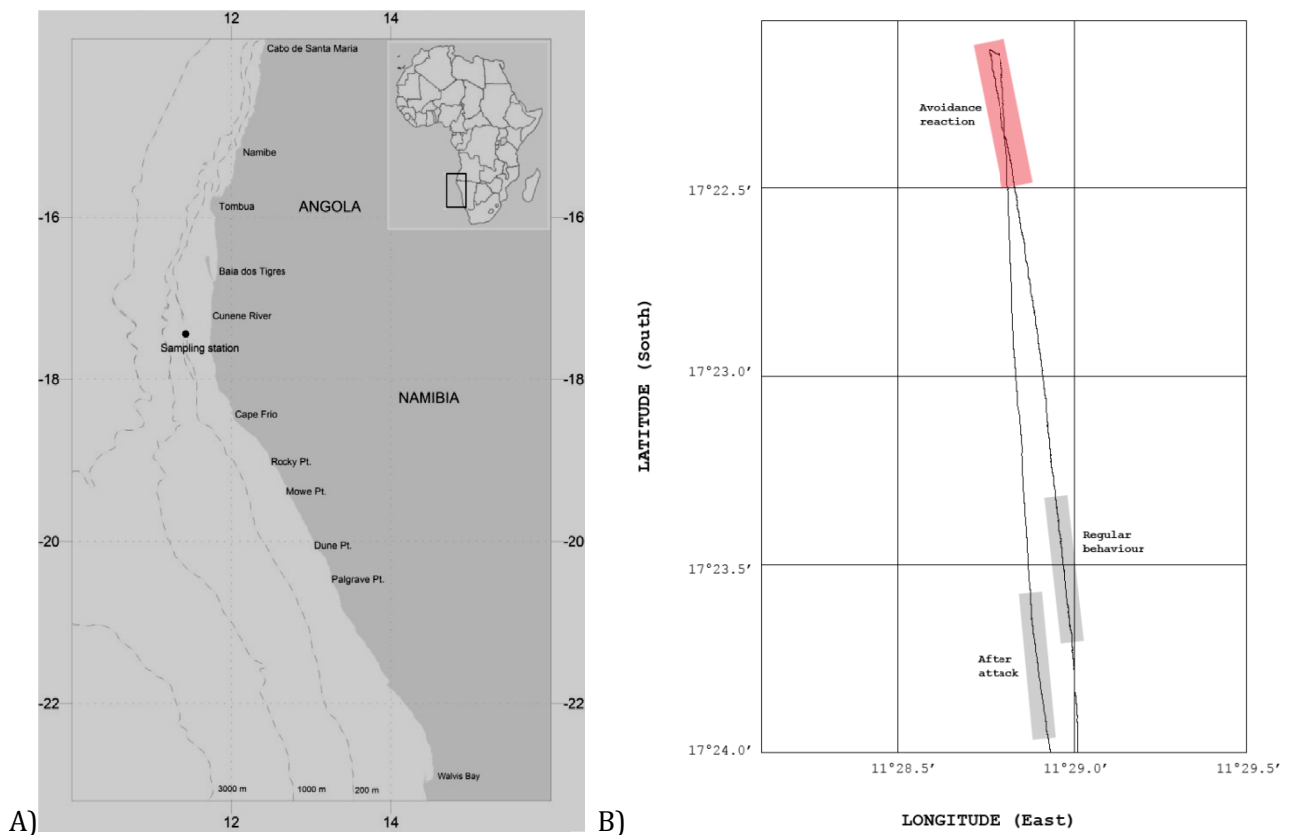


Figure 5.1: A) Study area (black dot) off the coast of northern Namibia in the Benguela Current Large Marine Ecosystem (BCLME), which is off southern Angola, Namibia and South Africa (west coast). Inset shows location of study area in Africa. B) Detail of the ship's track over the area of interest relating to the acoustic observations reported in this chapter.

Top predators such as dolphins often target schooling pelagic fish as their main prey, thereby affecting their behaviour, distribution and abundance (e.g. Perrin et al. 2002). Protection against predators at the individual level is one of the primary functions of schooling (Pitcher & Parrish 1993), and predator attacks may considerably affect internal school structure and density (Pitcher & Wyche 1983, Hall et al. 1986, Similä & Ugarte 1993, Vabø & Nøttestad 1997, Nøttestad & Axelsen 1999, Axelsen et al. 2000,

2001, Nøttestad et al. 2002a,b). Studying school-level prey responses to predator attacks is thus necessary to better understand the nature of prey–predator interactions (Pitcher & Wyche 1983, Kenney et al. 1997, Axelsen et al. 2001). Animal energetic fitness can be substantially affected by foraging decisions, because the amount of food that an animal can obtain has a major influence on its survival in the wild (Beyer 1995). Moreover, group foraging may increase survival probabilities, not necessarily by increasing the overall feeding rate, but rather by decreasing its variance (Thompson et al. 1974, Clark & Mangel 1984). When studying predator–prey interactions in nature, quantifying predator attack rates and the corresponding rates of school response events are essential to understand the behavior causing the observed school dynamics (Axelsen et al. 2001), and hydroacoustics have proven to be a powerful tool for these types of quantifications (Nøttestad & Axelsen 1999, Axelsen et al. 2001, Nøttestad et al. 2002a, Benoit-Bird et al. 2004). While some knowledge exists on the behaviour of Cape horse mackerel (e.g. Axelsen et al. 2004), the behavior of dusky dolphin *Lagenorhynchus obscurus* in this area of the world has only rarely been investigated (Van Waerebeek & Würsig 2009). Dusky dolphins are widespread in the Southern Hemisphere, but their distribution is probably discontinuous (Van Waerebeek & Würsig 2009). They are found along the coast of Southern Africa from Lobito in southern Angola to Cape Agulhas in Cape Province; however, little information is available on the relative abundance of *L. obscurus* within its distribution range (Jefferson et al. 2008). Dusky dolphins are usually found over the continental shelf and slope (Aguayo et al. 1998, Jefferson et al. 2008), and their distribution within the BCLME is primarily associated with the cold waters of the Benguela Current along the west coast of South Africa. Dusky dolphins are gregarious animals, with average observed group sizes varying from 6 to about 300 individuals, with regular, stable subgroups (Würsig & Würsig 1980). Dusky dolphin underwater behaviour was studied by Würsig (1982) and more recently by Benoit-Bird et al. (2004), who used a fish finder to evaluate the dolphin's relative abundance by linking relatively strong target detections presumed to be dolphins with the presence of deep scattering layers of its schooling prey. While interaction processes between dusky dolphins and their prey during predation events have been documented in other parts of the world (Vaughn et al. 2007, 2010), there are no previous reports from African waters. The main aims of the present study were to study *in situ* predator–prey interactions between dusky dolphins and Cape horse mackerel, and to quantify attack rates, diving speeds and depths of attacking dolphins along with corresponding school response events and changes in school structure and packing densities of the schooling prey. These were accomplished by the use of high-resolution, calibrated echosounder data, thus taking advantage of the large sampling volumes and high spatial and temporal resolutions offered by the hydroacoustic method. Parallel visual surface observations and targeted pelagic trawling served to verify the presence of the dolphins and the horse mackerel at the study site, as well as to obtain biological samples of the populations under study.

5.2 METHODS

The data presented were collected during a fisheries acoustic survey with the RV 'Dr. Fridtjof Nansen' in Namibia. Predator-prey interactions reported were observed in northern Namibia, near the border to Angola (17° 24' S, 11° 29' E), on 23 September 2002 between 10:00 and 12:00 h (UTC). The bottom depth in the area was about 160 to 180 m. Acoustic data were logged throughout the observation period with a 38 kHz calibrated scientific echosounder (Simrad EK500) (Foote 1987) while the vessel drifted passively (Fig. 5.1 B) over the aggregations at low speed (1 to 2 knots). The acoustic data were logged and analyzed with Echolog/ Echoview v. 3.40 software (Myriax Software®). The presence of the submerged dolphins observed acoustically in the water column was verified by visual observations of the dolphins when they were at the surface before and after diving. The visual observations were done at close range (10 to 50 m) from the ship's main deck, located about 10 m above sea level, and were recorded with a camcorder. Biological samples of Cape horse mackerel were obtained by means of targeted pelagic trawling with a pelagic sampling trawl (Åkrehamn, about 15 m vertical opening). Oceanographic data were sampled by means of a CTD probe (Seabird) submerged to near the bottom immediately before and after the acoustic observations were made. A weather station onboard the research vessel recorded data on wind stress, solar irradiance and wave conditions at the study site.

5.2.1 Dolphin behavior.

Candidate dolphin traces were first identified by manual scrutiny of the volume backscattering strength (s_v) echograms (Simmonds & MacLennan 2005). Dolphin traces were subsequently verified by means of single target tracking according to the following criteria: minimum number of detections per trace: 6; maximum number of missed detections per trace: 2; maximum distance between consecutive detections within each trace: 5 m; and maximum aspect angle from acoustic axis: 5°. For each acoustic dolphin trace, the horizontal and vertical position of the dolphin, the mean compensated target strength (TS, dB), the mean and maximum within trace swimming speed ($m s^{-1}$) and the mean and maximum swimming depths (m) were measured. Selected traces were plotted in 3 dimensions (3D) for visualization of the dolphin swimming pattern (Fig. 5.2). The risk of misinterpreting large fish for dolphins was further diminished by inspection of the trend in the variation of the TS detections, which were consistent with the dorso-ventral swimming pattern typical for cetaceans (Fig. 5.3) (Love 1973, Au 1996, Miller et al. 1999, Benoit-Bird et al. 2004, Au et al. 2007, Lucifredi & Stein 2007, Bernasconi et al. 2009). All computations on TS were carried out in the linear domain.

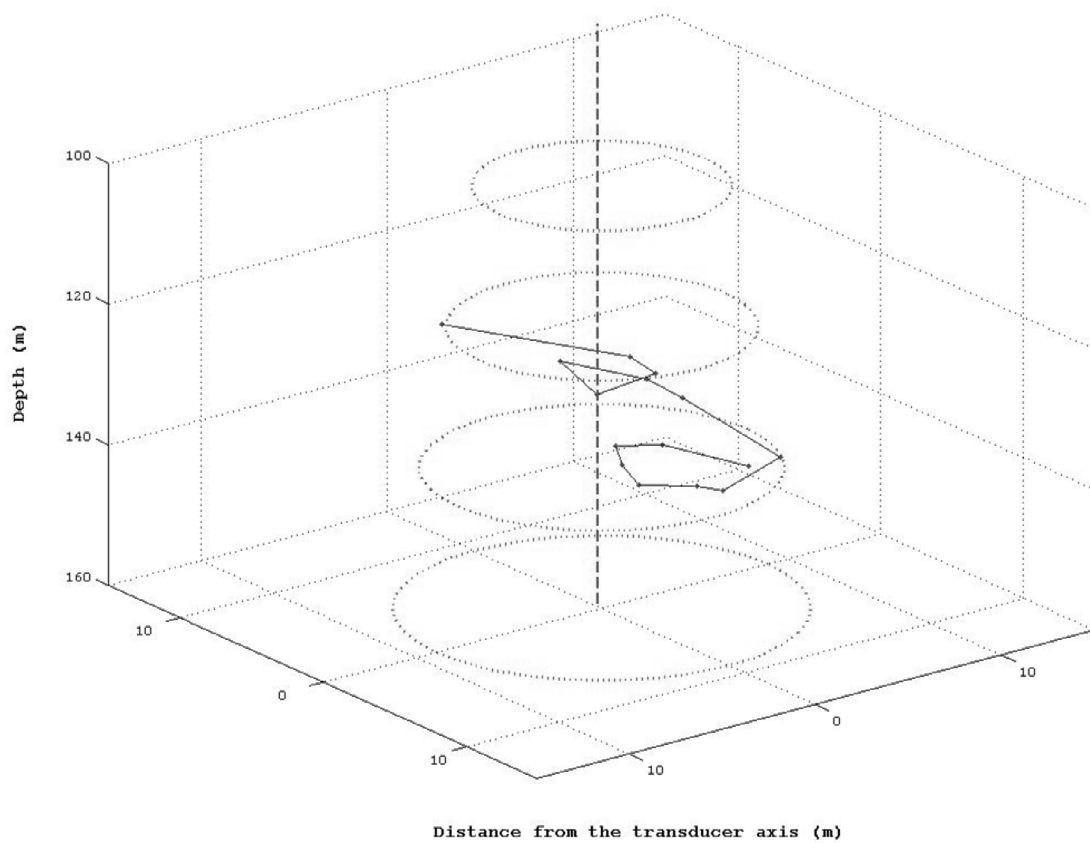


Figure 5.2: *Lagenorhynchus obscurus*. Three-dimensional plot showing the trace of an individual dusky dolphin (the filled points are single target detections; the fitted, solid line represents the projected movements) spanning from 132.6 to 136.1 m depth. The dotted circles indicate the -3 dB beam width by depth, corresponding to a 14.3 m diameter or 160 m² area at the beamfront at 160 m range. The observation was made immediately underneath the Cape horse mackerel layer

5.2.2 Predator response reactions.

The predator response reactions were readily identified by visual inspection of the echograms in terms of the presence of dolphin traces and associated response patterns in the fish layer. First, attack and non attack situations were defined and polygons drawn along the perimeter of the schools. All school response events were then recorded and classified as 'Split' (fragmentation of the school), 'Bend' (inflection of the school), and 'Vacuole' (an empty space created in the centre of the school) or 'Hourglass' (a constriction in the centre of the school) (Nøttestad & Axelsen 1999). Attack-response scenarios were standardized to observation periods corresponding to sailed distances of 0.5 nautical miles (n miles) and aggregated into the following subsections: before, during and after the dolphin attack. The observation periods were further divided into integrator bins of 0.1 n mile (185.2 m) horizontally by 25 m vertically. The volume densities were then integrated over the integrator bins

producing acoustic backscattering coefficient s_A ($\text{m}^2 \text{n mile}^{-2}$) (MacLennan et al. 2002). The fish volume fish densities (ρ_v , fish m^{-3}) were then calculated according to:

$$\rho_v = \frac{s_A}{\langle \sigma_{bs} \rangle (1852)^2 \Delta z} \quad (5.1)$$

where s_A is the acoustic backscattering coefficient in $\text{m}^2 \text{nmi}^{-2}$, Δz the corresponding depth interval over which the acoustic data were integrated, and the mean estimated acoustic backscattering cross-section of the fish, relating to the fish TS by:

$$\langle \sigma_{bs} \rangle = 4\pi \cdot 10^{(\overline{TS}/10)} \quad (5.2)$$

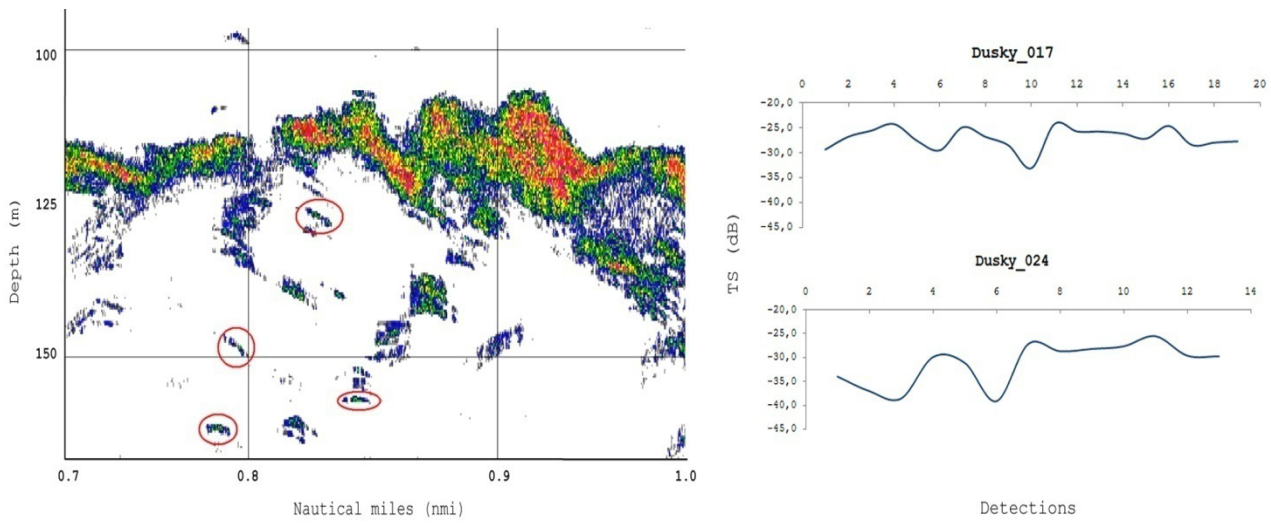


Figure 5.3: *Lagenorhynchus obscurus*. (a) Volume backscattering strength (s_v) (dB) echogram showing the Cape horse mackerel layer with dolphins (encircled) located underneath the school and (b) target strength (TS) (compensated) detections for 2 individual dusky dolphin target traces

Assuming that the mean TS of the Cape horse mackerel did not change during the attack scenarios, the mean TS was estimated according to Pena (2004):

$$\overline{TS} = 20 \cdot \log_{10}(L) - 66.0 \quad (5.3)$$

where L is the mean total length of the Cape horse mackerel as determined from the trawl samples (17.0 cm, thus corresponding to an average TS of -41.4 dB). To investigate the effect of the attacking predators on the local packing densities within the layer, the volume backscattering strength (s_v , dB) and the acoustic backscattering cross-section (s_A , $\text{m}^2 \text{n mile}^{-2}$) for small subsections of the school immediately in front of and immediately behind the predators entering into the fish layer were extracted, converted to fish densities according to Eq. (1) and then compared.

5.3 RESULTS

During the observation period the weather conditions were favorable, with partial cloud cover (mean sun radiation: 281.5 W m^{-2}), light southwesterly winds (mean wind speed: $5.8 \text{ knots} \Leftrightarrow 2.9 \text{ m s}^{-1}$) and a calm sea (wave height: 0.5 to 1.0 m). The temperature and salinity were stable throughout the water column, with approximately 16°C temperature at the surface, decreasing to about 15°C at 100 m depth, and salinity of 35.5 psu throughout the water column. Surface waters were well oxygenated (about 5.1 mg l^{-1} dissolved oxygen), dropping to about 3.06 mg l^{-1} at 75 m and about 1.02 mg l^{-1} below 100 m depth. The dolphins were most often located underneath the fish aggregation (63% of the time) rather than above the fish aggregations (37%) (whenever they were not located within the layer). The dolphins dove to a maximum recorded diving depth of 156 m (mean recorded depth, 120 m) in an area where seabed depth was 177 m . Mean attack speed was estimated at 3.4 m s^{-1} , while the maximum recorded attack speed (burst speed) was 9.9 m s^{-1} , which was recorded at 125 m depth as the tracked dolphin penetrated inside the school (21 single target detections were recorded within this trace).

Table 5.1: *Lagenorhynchus obscurus*. Swimming speeds and depths of the tracked dusky dolphins (35 traces, 385 detections)

Statistic	Detections per trace	Depth (m)	Swimming speed (m s^{-1})	
			Mean	Max.
Min.	6	42.2	0.6	1.6
Max.	21	156.0	2.3	9.9
Mean	11	120.3	1.4	3.4
SD	± 5.1	± 28.3	± 0.4	± 1.6
CV	45.1 %	23.5 %	32.5 %	46.4 %

The mean overall swimming speed was 1.4 m s^{-1} . Swimming speeds and depths are summarized in Table 5.1. The mean recorded TS for the dusky dolphins at 38 kHz was -31.5 dB (95% CI: -33.4 to -30.2 dB ; range: -39.9 to -22.7 dB) (Fig. 5.4). An example of a dolphin trace obtained underneath the horse mackerel layer is shown in 3D in Fig. 5.2, which illustrates the dolphin encircling behavior underneath the school. Examples of echograms before, during and after attack–response scenarios and histograms of fish density (fish/ m^3) by depth intervals are shown in Fig. 5.5, while the corresponding fish volume packing densities are shown in Fig. 5.6.

Initially, before the dolphin attacks, the horse mackerel were predominantly aggregated in a horizontally extended layer at 100 to 125 m depth with a vertical distribution of the main layer being approximately 20 m (0.7 fish m^{-3}). The mean s_A for the undisturbed situation was $2275 \text{ m}^2 \text{ n mile}^{-2}$ (Fig. 5.5a), corresponding to 0.4 fish m^{-3} . During the attacks the horse mackerel aggregation split into

2 far more distorted main fractions, with the larger of the components moving towards the upper pelagic (approximately 50 m vertical extension) and the other remaining at the same depth (30 to 40 m vertical extension). The shape of both school components immediately changed, becoming highly amorphous (Fig. 5.5b). The fish thus concentrated in the top layer of the water column (25 to 50 m: 2.6 fish m^{-3} ; 50 to 75 m: 1.4 fish m^{-3} ; 75 to 100 m: 0.8 fish m^{-3}), and the mean s_A increased to 12440 $\text{m}^2 \text{ n mile}^{-2}$, or 2.0 fish m^{-3} . After the attacks, the horse mackerel reorganized as a 'regular' (undisturbed) daytime school aggregation at 100 to 150 m depth (100 to 125 m: 0.5 fish m^{-3} ; 125 to 150 m: 0.1 fish m^{-3}), and the mean s_A decreased to 1883 $\text{m}^2 \text{ n mile}^{-2}$ (0.3 fish m^{-3}) for the post attack period (Fig. 5c). The mean packing densities before, during and after attacks were significantly different (ANOVA Type II Wald test: $p < 0.01$). Altogether 54 predator response events were observed throughout the observation period, corresponding to 0.45 events min^{-1} on average (Table 5.2).

Table 5.2: *Trachurus capensis*. Predator response events ($n = 54$, ~ 0.45 events min^{-1}) in attacked schools with corresponding depths and packing density ranges. See 'Method: Predator response reactions' for a description of each behavior

School response	No. of obs.	Depth (m)		Density (fish m^{-3})	
		Min.–Max.	Mean \pm SD	Min.–Max.	Mean \pm SD
Vacuole	21	24–131	51.2 \pm 36.1	2.67–3.70	3.19 \pm 0.48
Split	19	47–146	113.2 \pm 23.4	0.37–1.02	0.56 \pm 0.23
Bend	10	40–125	98.9 \pm 31.5	1.10–3.12	1.92 \pm 1.06
Hourglass	4	66–89	78.5 \pm 9.7	0.71–1.10	0.96 \pm 0.17

Table 5.3: *Trachurus capensis*. Acoustic volume densities and corresponding packing densities for random subsamples of unattacked and attacked schools

School state	n	Density (fish m^{-3})			s_V (dB)		
		Min.	Max.	Mean \pm SD	Min.	Max.	Mean (95% CI)
Unattacked	5	1.15	3.02	1.91 \pm 0.76	-51.77	-47.59	-49.57 (-51.46 to -48.26)
Attacked	5	5.90	12.50	8.77 \pm 2.71	-44.68	-41.43	-42.96 (-46.98 to -40.90)

The most common response pattern was Vacuole ($n = 21$), followed by Split ($n = 19$), Bend ($n = 10$) and Hourglass ($n = 4$). Attacked schools had, on average, 4.6 times higher packing densities than did unattacked schools (Table 5.3). An example of a Vacuole formation as a dolphin enters into the fish aggregations is shown in Fig. 5.7a. The avoidance of individual fish can be seen as locally reduced packing densities in front of (mean s_V : -57.2 dB, 95% CI: -58.6 to -56.1 dB; or 0.33 \pm 0.17 fish m^{-3}) and to the sides of the predator where the fish avoided the predator, and increased packing densities behind the predator (mean s_V : -44.1 dB, 95% CI: -44.8 to -43.6 dB; or 6.65 \pm 1.75 fish m^{-3}) (Fig. 5.7b), where they rejoined. The packing densities in front of and behind the predator were significantly different (Welch 2-sample t -test, $p < 0.01$).

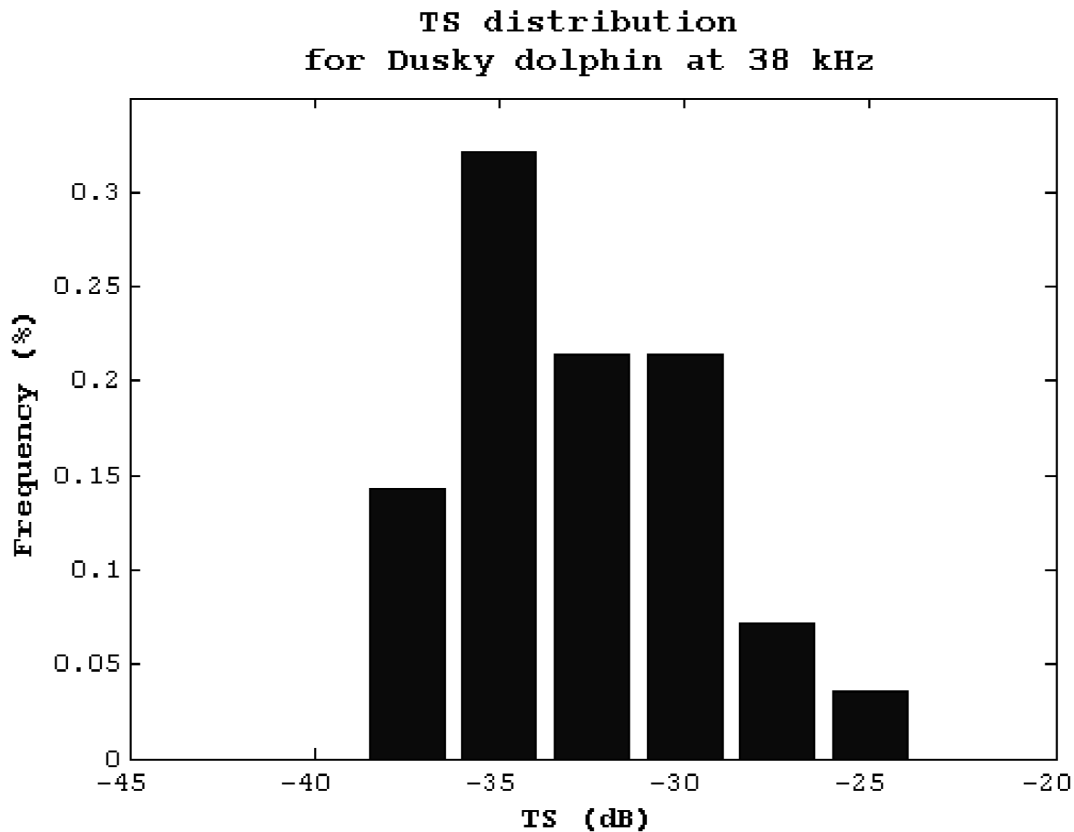


Figure 5.4: *Lagenorhynchus obscurus*. Frequency distribution of the recorded compensated target strength (TS) at 38 kHz for dusky dolphin (35 traces, 390 single detections). The mean overall TS was -31.5 dB (range: -39.9 to -22.7 dB; 95% CI: -33.4 to -30.2 dB)

5.4 DISCUSSION

I have for the first time documented dusky dolphins diving down to depths of 156 m (mean: 120 m depth). Previous studies have reported diving depths of up to 135 m (Benoit-Bird et al. 2004). In my study, groups of 10 to 20 hunting dolphins were found to have major effects on the swimming behavior, structure, density and depth of schooling Cape horse mackerel. The dolphins forced the horse mackerel towards the surface (25 to 50 m depth), thereby making the mackerel easier to prey upon (Nøttestad et al. 2002b).

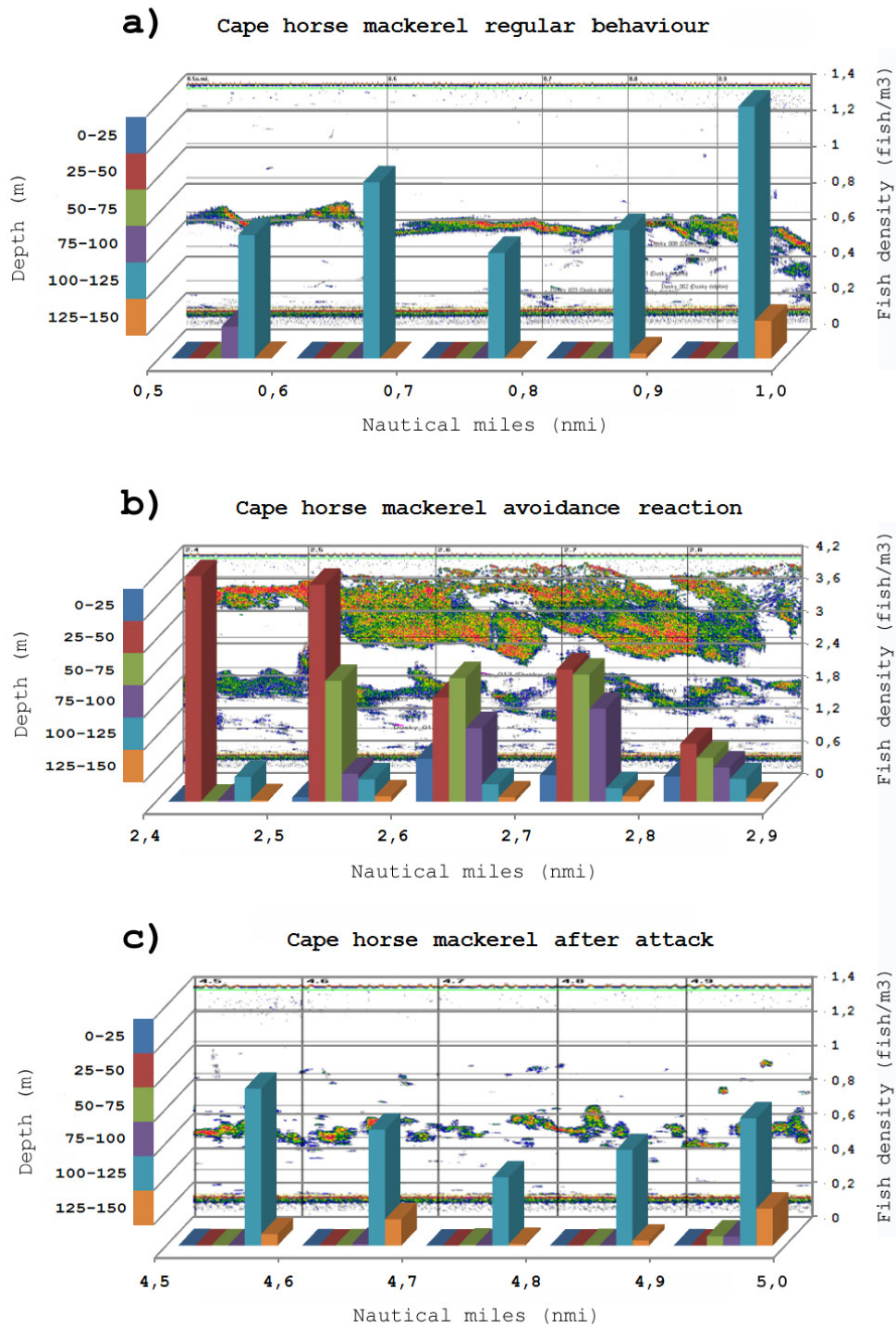


Figure 5.5: *Trachurus capensis*. Example of s_V (dB) echograms (back panel) showing Cape horse mackerel (a) before, (b) during and (c) after attacks by dusky dolphins. Histograms show fish density (fish/m³ in the right y-axis) by depth intervals (left y-axis).

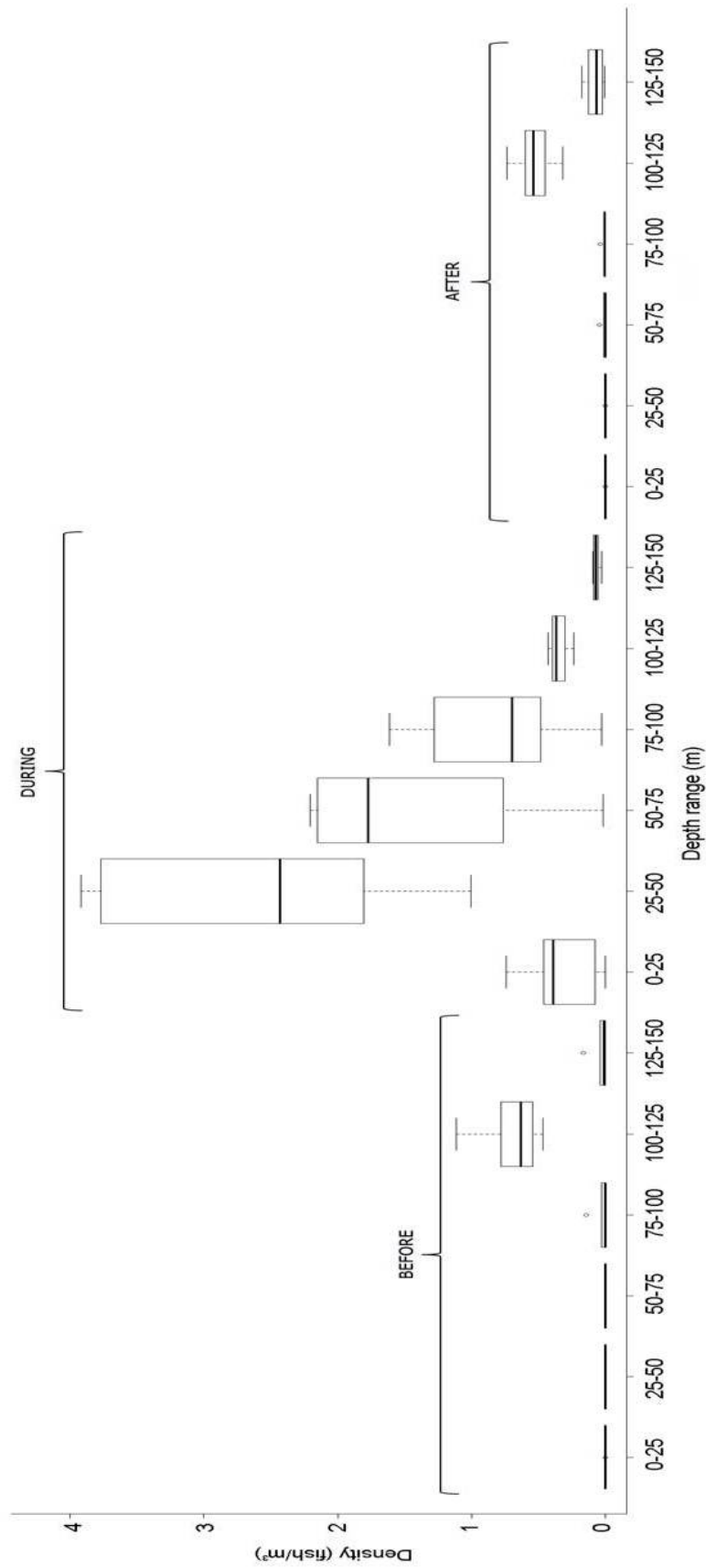


Figure 5.6: *Trachurus capensis*. Cape horse mackerel volume packing densities in fish m-3 by depth before, during and after attacks by dusky dolphins. Boxes represent the 25 % quartiles, lines the median value, whiskers minimum and maximum values while dots plot the outliers (values more than 2 times the upper quartiles).

This type of cooperative behavior, to dive underneath schools, force the prey into a tight ball near the surface and then launch direct, coordinated attacks into the densely packed schools, is consistent with recent studies on cetacean hunting techniques (Nøttestad & Axelsen 1999, Vaughn et al. 2010). My finding that the dolphins deliberately herded the horse mackerel towards the surface was supported by 3D traces of individual dolphins that showed the dolphins encircling underneath the horse mackerel aggregations (Fig. 5.3). Dusky dolphins are also known to lift their prey to the surface before feeding as has been shown in documentary films (National Geographic Society 1999). Killer whales *Orcinus orca* have been observed to dive down to a maximum of 180 m depth in order to lift aggregations of Atlantic herring *Clupea harengus* (Nøttestad & Similä 2001, Nøttestad et al. 2002b), and Nøttestad et al. (2002a) proposed a maximum diving depth of 200 m for fin whales *Balaenoptera physalus*. The present study is, however, the first to document that a much smaller odontocete, the dusky dolphin, may dive deeper than 150 m and lift their prey towards the surface, no doubt with considerable energetic efforts.

In our study, dusky dolphins were observed to attack their prey 54 times in 2 h, corresponding to an average observed attack rate of 0.45 events min⁻¹. This is considerably higher than attack rates reported for fin whales attacking Atlantic herring (0.12 events min⁻¹) (Nøttestad et al. 2002a) and also for killer whales attacking Atlantic herring (0.26 events min⁻¹) (Nøttestad & Axelsen 1999), while it was lower than attack rates found for diving puffins *Fratercula arctica* attacking juvenile Atlantic herring (1.48 events min⁻¹) (Axelsen et al. 2001). However, all those studies used multi-beam sonar with a much higher spatial resolution than the split-beam vertical echosounder used in the present study, and the actual event rate in the present study is likely to have been even higher. Large predators bursting into fish schools cause individual fish to try to escape from the predators (Pitcher & Wyche 1983, Axelsen et al. 2001), while the fish attempts to maintain a minimum approach distance of approximately 15 body lengths (Pitcher & Wyche 1983), which in turn will lead to predator response reactions at the school level as seen in Table 5.2. The horse mackerel aggregation under attack in the present study divided into 2 stable, vertically separated components (Axelsen et al. 2000). The dolphins then forced the fish from the deep towards the surface at high swimming speed, similar to that reported in other studies of dolphins attacking pelagic fish (Nøttestad & Similä 2001, Nøttestad et al. 2002b). In the present study, the dolphins spent 63% of the time swimming underneath the school and only 37% of the time swimming above the horse mackerel aggregations, supporting the observation that the dolphins deliberately forced their prey towards the surface and kept

them from returning to deeper waters (Similä & Ugarte 1993). The horse mackerel response observed in the present study was to aggregate in much denser and more synchronized aggregations (Nøttestad & Axelsen 1999, Axelsen et al. 2001).

The densities of the Cape horse mackerel we reported changed significantly in the periods before (0.4 fish m^{-3}), during (2.0 fish m^{-3}) and after (0.3 fish m^{-3}) the dolphin attacks, and unattacked schools had significantly lower densities compared with attacked schools, which conforms with the study by Nøttestad & Axelsen (1999) and model simulations (Vabø & Nøttestad 1997). The dolphins attacked at high speeds, with a maximum recorded burst speed of 9.9 m s^{-1} . The average attack speed was 3.4 m s^{-1} , whereas the overall average swimming speed was only 1.4 m s^{-1} . The attack swimming speeds and diving depths recorded here indicate that dolphins spend considerable energy on attacking their prey, suggesting that it was necessary for the dolphins to deliberately herd the horse mackerel towards the surface, pack them into 'tight balls' and keep them near the surface to feed on them (Würsig & Würsig 1980, Wells et al. 1999, Nøttestad et al. 2002b). This is supported by the higher densities recorded for attacked than for unattacked schools (Table 5.2), which conforms with the findings of Nøttestad et al. (2002a, b) for example. The relatively low oxygen levels ($<1 \text{ ml l}^{-1}$) found below 100 m depth may have restricted the horse mackerel from diving deeper while under attack at depth. However, Cape horse mackerel are reported to tolerate oxygen levels $<1 \text{ ml l}^{-1}$ (G. Bauleth-D'Almeida *unpubl.* data), and the presence of dolphins below the schools at depth, combined with their active encircling behavior, suggest that downward movements by the horse mackerel was not limited by oxygen levels here.

The large vertical Hourglass formation found for horse mackerel here is similar to those reported for Atlantic herring (Axelsen et al. 2001). This could be an adaptation in 'trapped' schooling fish that enables them an escape passage to more secure locations - in the case of the present study towards deeper, darker waters - that dolphins attempted to counteract by encircling underneath the schools (Nøttestad & Axelsen 1999, Nøttestad et al. 2002b, Vaughn et al. 2010). The dusky dolphins maintained a dense aggregation of fish in the upper 50 m of the water column for a prolonged period of time ($\sim 50 \text{ min}$). The Vacuole school responses, leading to empty spaces forming around the predators, were equivalent to responses in adult Atlantic herring to attacks from killer whales (Similä & Ugarte 1993, Nøttestad & Axelsen 1999) and in juvenile Atlantic herring to attacks from puffins (Axelsen et al. 2001) off northern Norway. In the present study, prey avoidance reactions caused significantly lower fish densities in front of the attacking predators ($0.33 \pm 0.17 \text{ fish m}^{-3}$) than behind them ($6.65 \pm 1.76 \text{ fish m}^{-3}$). Fish in

aggregations generally maintain a minimum approach distance to predators of about 15 body lengths (Pitcher & Wyche 1983) and high density regions shifting within schools, or density propagation (Axelsen et al. 2001), are thus a natural consequence of individual fish avoiding predators (Breder 1954, Hamilton 1971, Pitcher & Wyche 1983, Axelsen et al. 2001). The reduced densities in front of and the increased densities behind the predators as they burst into the school are indicative of fish moving away from the predator and rejoining behind them, i.e. the fountain effect (Hall et al. 1986).

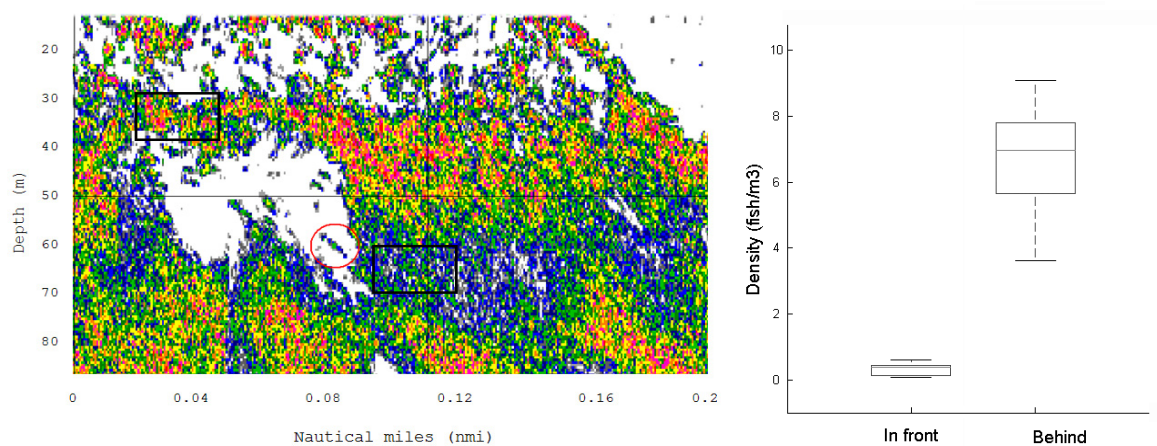


Figure 5.7: *Trachurus trachurus capensis*. (a) sv (dB) echogram subsection showing a typical ‘Vacuole’ formation caused by the intrusion of a dusky dolphin (encircled) into a Cape horse mackerel school and (b) plot of volume densities (fish m⁻³) recorded immediately in front of and behind (e.g. black squares in figure 5.7 a) the dolphin, illustrating the fountain effect (Hall et al. 1986)

Vacuole formation around attacking dolphins observed in large aggregations in the present study is supported by other studies (Vabø & Nøttestad 1997, Nøttestad & Axelsen 1999, Axelsen et al. 2001) despite the limited spatial resolution offered by the conventional single-beam (split-beam) we used. The evolution of swimming speed within the dusky dolphin traces observed in the present study suggests that rapid accelerations were followed by gliding behavior. This is consistent with studies of trained *Tursiops* (Williams et al. 1999), in which acceleration followed by gliding at depth was put forward as a strategy to conserve energy. The *in situ* TS measurements reported here (range: -22.7 to -39.9 dB) are consistent with Au et al. (2007), who measured the TS of a trained bottlenose dolphin *Tursiops truncatus* under controlled conditions to range from -40 to -26 dB. Cetacean TS should, however, be explored in more detail to establish length dependencies and interspecies variation. Multifrequency target triangulation (Pedersen et al. 2004) may be one approach to help to identify and isolate dolphin targets and,

thus, explain observed variability. The results reported in the present study demonstrate the power of acoustic target tracking as a tool for mapping underwater movements of marine mammals, and we believe that advanced acoustic methods combined with visual observations and underwater video recording have the potential to improve our understanding of marine mammal behavior considerably (Hedgepeth et al. 2000).

Acknowledgements. This work was supported by the Benguela Environment Fisheries Interaction Programme (BENEFIT), now the Benguela Current Commission (BCC) and partly funded by the Dr. Fridtjof Nansen Programme and Norwegian Agency for Development Cooperation (NORAD). The authors acknowledge the support of officers and crew of the RV 'Dr. Fridtjof Nansen' and fellow researchers and technicians at the National Marine Information and Research Centre (NatMIRC) in Swakopmund, the National Institute of Fisheries Research (INIP) in Luanda, the Institute of Marine Research (IMR) in Bergen and the Research Council of Norway. Many thanks for the revision of the manuscript at different stages go to Prof. E. Ona and Dr. L. Calise, Institute of Marine Research, Bergen, and Prof. A. S. Brierley and Dr. M. Cox, Pelagic Ecology Research Group, University of St Andrews. A special thank you is expressed to Dr. M. Wilson, Myriax Software, for the constant technical support and to Prof. R. Groppali and Prof. S. Frugis, Università degli Studi di Pavia, from M.B. for their constant support.

CHAPTER 6



FIN WHALE (*Balaenoptera physalus*) TARGET STRENGTH MEASUREMENTS

6. FIN WHALE (*Balaenoptera physalus*) TARGET STRENGTH MEASUREMENTS

ABSTRACT: Active acoustic techniques can be used to detect whales. The ability to detect whales from moving vessels could reduce conflicts between seismic survey operations and whales, and help prevent tankers, container ships or other vessels from striking whales. In order to identify acoustic targets as whales and so to trigger cessation of seismic shooting or an alteration of course, knowledge of whale target strength (TS) is required. Detections of fin whales (*Balaenoptera physalus*) were made in the Norwegian Sea with a calibrated omnidirectional fisheries sonar (operating frequency 110 to 122 kHz). Three fin whales of length 17.0 ± 1.0 m had an average TS for all insonified body aspects of -11.4 dB [95% CI -12.05 -10.8], with a total spread of nearly 14 dB. Individual fin whale TS varied by approximately 12 dB, probably due to variation in lung volume with breathing and to dynamic swimming kinematics. Our reported TS values are consistent with values for other large whales, and all data together pave the way for development of automated acoustic whale detection protocols that could aid whale conservation purposes.

6.1 INTRODUCTION

Many human activities at sea are potentially harmful to marine mammals (Harwood 2002; Weilgart and Whitehead 2004; Hildebrand 2005). Whales and dolphins have well developed auditory systems and may be particularly sensitive to sound produced during seismic surveys (Kastak et al. 2005; Finneran et al. 2005; Madsen et al. 2006; Miller et al. 2009). Shipping traffic can also disturb marine mammals (Laist et al. 2001; Jensen et al. 2004), and direct collisions by ships with whales have had major impacts on some whale populations (Kraus 1990; Knowlton et al. 2001). There is a growing requirement to prevent, or at least minimize, anthropogenic impacts on cetaceans: shipping routes have been altered to reduce conflict (CFR 2008), and in many regions (e.g. The MMPA 1972; EPBC Act 1999; JNCC guidelines 2009) seismic survey vessels are required to deploy marine mammal observers and to cease seismic shooting if whales are seen in the vicinity of the vessel. Visual surveys are however ineffective during hours of darkness, low visibility in foggy conditions, and the ability of observers to detect whales declines in rough seas: other techniques are thus required to detect whales reliably. Passive Acoustic Monitoring – detecting the presence of whales by listening for their vocal communications / foraging sounds - can work in some circumstances, but is limited by the directionality of vocalizations (Møhl 2000; Miller 2002) and the fact that animals do not vocalize all the time (Stafford et al. 2005; Wiggins et al. 2005).

Active acoustic techniques are used commonly to detect a range of organisms in the water column, and could potentially be used to detect whales. Some, although few, reports of whale TS do exist (Bernasconi et al. 2009; Lucifredi and Stein 2007; Miller et al. 1998; Love 1973; Dunn 1969). This chapter reports efforts to determine the feasibility of such detections using conventional fisheries sonar. My motivation is to progress towards the ultimate goal of development of an automated whale-detection apparatus that could be operated routinely from various vessels to prevent detrimental impacts on whales. Taking advantage of a survey opportunity in the Norwegian Sea, where whales are seen regularly, I sought first to demonstrate that whales could be detected with a standard calibrated fisheries sonar (Simrad SH80), and then to determine target strength (TS; the proportion of incident sound backscattered by a target) and its variability. Knowledge of TS will be required for target identification, and is of academic interest.

There is a growing body of data on whale TS. My own first marine mammal *in situ* TS measurements came from acoustic data collected off the coast of Namibia in 2002 (Bernasconi et al. 2011; see Chapter 5) with a Simrad EK500 at 38 kHz. A large group of dusky dolphins (*Lagenorhynchus obscurus*) was insonified from the R/V “Dr. Fridtjof Nansen” using a vertically orientated transducer. The *in situ* TS data collected off Namibia were in good agreement with experimental measurements made of a trained dolphin (Au et al. 2007) sent beneath a Simrad EK60 at 70, 120 and 200 kHz. These initial studies (Au et al. 2007; Bernasconi et al. 2007) had their limitations because the transducers used looked downward only, and insonified a very limited volume of water (7° beam). Subsequent studies have overcome this limitation by using omni-directional sonar that enabled the acoustic beams to be directed at the targets of interest (Nøttestad et al 2002; Bernasconi et al. 2009).

First indications that whales were strong acoustic targets came from sonobuoy data: strong backscatter at 1 kHz for an unknown target was attributed to a sperm whale because the detections coincided in time with recognizable recorded click-like sounds (Dunn 1969). Following this, Love (1973) made direct measurements of humpback whale (*Megaptera novaengliae*) TS at 10 and 20 kHz from an oceanographic tower. His data revealed particularly the variation in received energy with insonified whale aspect (8 dB from broadside and -4 dB from the head). This variation was elaborated upon by Au (1996) with an experiment that generated a polar plot of the acoustic reflectivity of a bottlenose dolphin (*Tursiops truncatus*). Au (1996) also showed how cetaceans’ blubber may have anechoic properties, and how it may adversely affect the use of high frequency sound for detection of cetaceans because of signal attenuation in the body. Miller (1999) tested higher frequency sonar (86 kHz) at sea with the aim of developing a tool to help prevent ships striking whales. He measured the TS of the right whale (*Eubalena glacialis*) and found it to vary, for a 15 m long animal at broadside, from -4 to -8 dB. He also made measurements of a humpback whale but found lower TS values than Love (1973). He explained the differences by the presence of a thicker blubber layer in the right

whale's body and by the higher frequency of the sonar system he used. More recently efforts to detect whales using active acoustic techniques have been reinvigorated: Lucifredi and Stein (2007) measured gray whale (*Eschrichtius robustus*) TS using a 21-25 kHz active sonar system mounted on a fixed array with a low sampling rate (1 ping every 5 seconds), and Bernasconi et al. (2009) used a high frequency sonar (110 kHz) from a moving vessel with high sampling rate (1 ping every second) to insonify different species of the *Balaenopteridae* family.

The data presented in this paper were collected from fin whale with a Simrad SH80 (110 kHz) omnidirectional fishery sonar in July and August 2008 in the Norwegian Sea. The objective of this study was to determine TS and explore observed TS variation in terms of physiology and behavior of the fin whale. The ultimate goal is to use omnidirectional fisheries sonars to detect cetaceans in coastal and offshore waters during seismic operations, to use such detections as informative and reliable triggers to stop potentially harmful seismic shooting in the presence of whales, and to prevent ships from colliding with whales.

6.2 METHODS

6.2.1 Data Collection

Active acoustic detections of whales were performed between the 26th of July and the 10th of August 2008 from the Norwegian vessel Eros M-60 HØ, a 72 m combined purse seiner and pelagic trawler adapted and equipped as a modern scientific research platform. Its instrument suite included two multibeam sonars with scientific output, and a calibrated five frequency echosounder. Observations of whales were included as an integrated sub goal of an ecosystem survey that covered substantial areas (7395 nmi²) of the Norwegian Sea between 62°30'-75.00°N and 18°W-22°E. This ecosystem is a well known marine mammal feeding and migration area (Nøttestad et al. 2004; see paragraph 4.2).

A. Acoustic data

Acoustic data were collected using a calibrated omnidirectional Simrad SH80 sonar operating at a discrete frequency of 110 kHz. The calibration experiment was performed after the survey at Lysefjorden with the ship anchored and ideal weather conditions (Beaufort 0) using a 75 mm tungsten carbide sphere (see paragraph 3.6). The sonar had a source level of 210 dB//1μPa, a ping repetition interval of 1 s, and a continuous wave (CW) pulse with duration varying from 0.8 to 3.8 ms depending on the sonar range setting (from 100 to 500 m). The transceiver unit performs the signal processing and the digital beamforming of 240 transmit and 480 receive channels. The unit is designed to be lowered from a hull hatch below the ship's hull. The deployment depth was 6.2 m in this case. The cylindrical transducer array enables the sonar beam to give complete 360 degrees (radar-like)

instantaneous horizontal coverage, and it can be tilted 60 degrees from the horizontal. The 360 degrees are divided in 64 beam sectors, each with beam opening angles of 8 degrees in the horizontal and vertical planes. The sonar can also transmit vertically to give a slice view of 60 degrees aperture that can be aimed manually in the direction of targets of interest (Figure 6.1).

B. Whale position data

Two dedicated marine mammal observers (MMOs) collected cetacean sighting data from a platform on the vessel 13 m above the sea surface. Data collected included positions of whales relative to the ship, their swimming direction, blow occurrence, and the estimated distance from the vessel, on a time frame synchronized to the acoustic logging. These observations were logged using the GPS radio linked software Hval 2.0 (developed by the Marine Mammal Research Unit of the Institute of Marine Research, Norway), which stores the exact time related to the observation position recorded via the GPS system connected to the sonar.

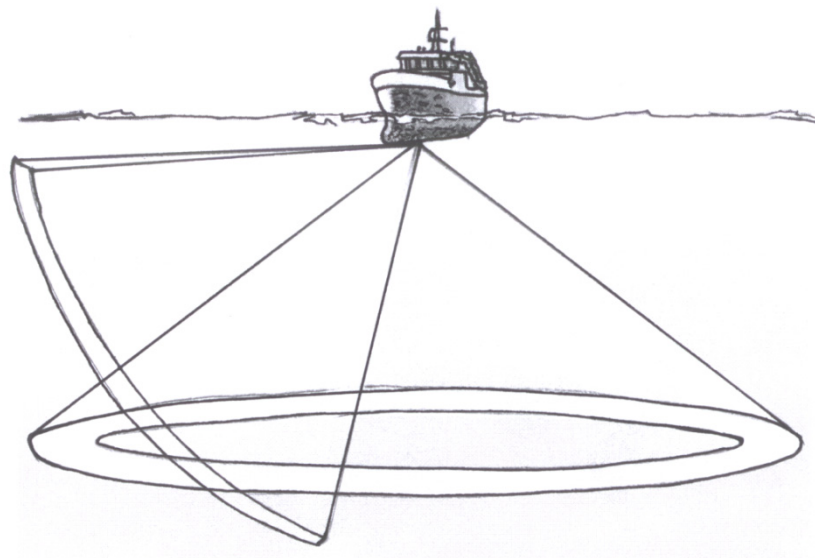


Figure 6.1: Graphical representation of the combined omni-vertical settings from the Simrad SH80 omni-directional sonar.

C. Vertical CTD cast

CTD casts were collected after each whale observation at the sighting location to determine appropriate sound speed profiles and to obtain data needed for post processing the sonar equation, for calculating the absorption coefficient α (Francois and Garrison 1982) for the sighting area, and to run detection probability and ray tracing simulations using the software Lybin 4.0 (Hjelmervik and Sandsmark 2008). Ray tracing simulations are particularly important in the definition of the blind zone close to the vessel, caused by the sonar tilt angle setting, which must be considered during data analysis to validate short range detections (Figure 6.2). Ray tracing simulations also enable the sonar

operators to be confident of what they are looking at on the sonar screen, and prevent over-interpretation and mistakes during post-processing.

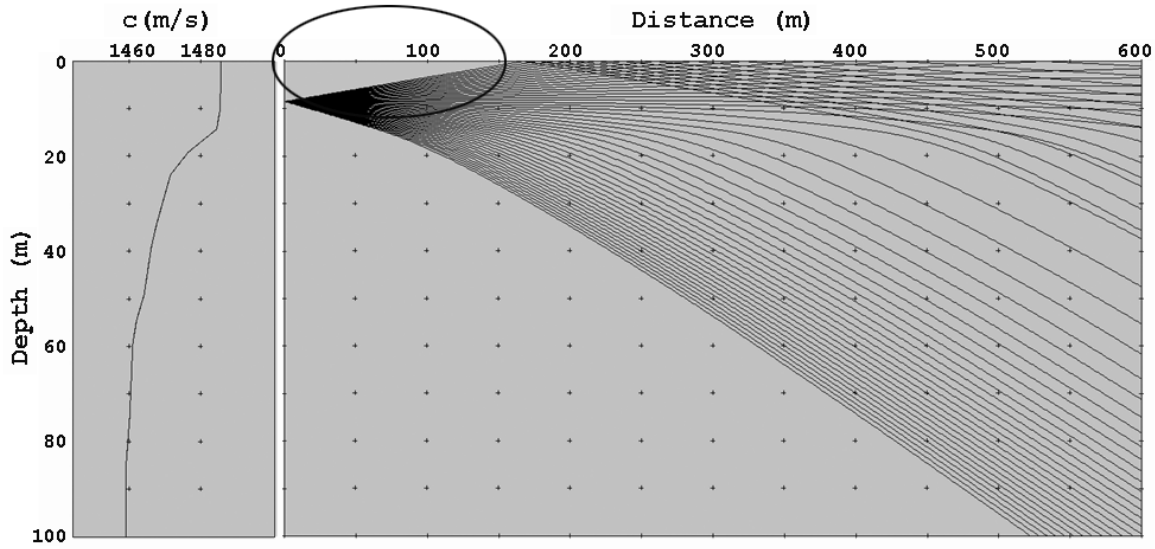


Figure 6.2: Sound speed profile and ray tracing simulation. Inside the circle is the blind zone of detection that depends on the sonar tilt angle setting. This aspect has to be considered by the sonar operator while measuring TS at short distances.

6.2.2 Data Analysis

To be sure of the presence of the whale in the main lobe of the beam of interest, only pings coinciding directly with the MMO observations of whales were considered for analysis. The selected pings were scrutinized one by one to determine TS and to discard any detections made by side lobes. The Simrad SH80 scientific output module gives binary raw data files for each ping. The data were processed using a dedicated MATLAB script (See paragraph 4.4). For quantitative TS estimates the data output were considered with reference to the sonar equation:

$$TS = EL - SL + TVG + GC \quad (6.1)$$

where EL is the received dB level; SL is the source level of the sonar; TVG is the time varied gain calculated for every sighting with reference to CTD data, and corresponding to $40\log_{10}(R) + 2\alpha R$ (where R is the range and α the absorption coefficient); GC is a gain correction value for each beam obtained with reference to echoes detected from a 75 mm tungsten carbide sphere in a dedicated calibration experiment (see paragraph 3.6), where the TS of the sphere is a known function of the sound speed (Foote 1990; Nishimori et al. 2009).

Variance about the point TS measurements ($n=120$) was computed in the linear domain and converted back to dB for statistical analysis. The lengths of the whales were estimated visually at ranges closer than 50 m from the vessel. The insonified aspect of the whales was calculated for each ping by triangulation using the relationship of the angles formed by the position of the whale in respect to the

ship and its swimming direction. The whale aspects presented to the transducer were then categorized into nine sections, with the head corresponding to 0 degree assigned as Category 1, to the tail corresponding to 180 degrees assigned as Category 9.

Possible TS variations were also related to the observed breathing events. As whales inhale their lung volume increases, and this may increase TS. To do so, influence of incidence angle over TS was first corrected by fitting a quadratic regression model before analyzing the residuals. Breathing events vs TS peaks were then investigated using a simple predictive model (Hastie et al. 2009; Nemes and Hartel 2010), the performance of which was evaluated using standard summaries for binary classification models, with the breathing events considered to be the positive class.

Further analysis considered how TS in fish with swim bladders depends upon the volume of air contained in the swim bladder (Foote, 1997; Ona, 1990; Love, 1978). Physoclist fish (e.g. *Theragra chalcogramma*) are able to adjust the volume of gas in the bladder by way of a gas gland or other mechanism, but physostomes (e.g. *Clupea harengus*) are not and their bladder volume, and hence TS, is thus highly depth dependent. The depth dependency can be modeled as a function of Boyle's law that formalizes the proportionality between pressure and volume ($P_1V_1 \propto P_2V_2$). It is known that whales and dolphins dive after inspiration (Wartzok 2008; Ridgway and Harrison 1979). This makes depth related lung compression a possible explanation of observed TS variation. The lungs of a cetacean are sealed once the animal dives, and to a first approximation may be modeled by Boyle's Law (Venegas et al. 1998). TS is a function of the acoustic backscattering cross-section σ_{bs} , to which it is linked by the formula:

$$TS = 10 \times \log_{10} (\sigma_{bs}) \quad (6.2)$$

(MacLennan et al., 2002). To explore the possibility that variations in my data could be due to a pressure effect, I applied a general model for a target swimming at depth (Ona, 2003), to the measured average TS at broadside using the formula:

$$\sigma_z = \sigma_0 \cdot \left(1 + \frac{z}{10}\right)^\gamma \quad (6.3)$$

where σ_z is the mean backscattering cross-section at depth z , equal to σ_0 at the sea surface ($z=0$), and γ corresponds to -0.67, the estimated contraction-rate parameter of a free spherical balloon, the volume of which decreases with depth in accordance with Boyle's law.

Finally some attention was given, with a preliminary qualitative analysis, to swimming behavioral patterns observable on the sonar screen every time a whale was in sight. This pattern could be related to the mechanical formation of the typical footprints that whales leave on the sea surface while

swimming (Levy et al. 2011) and are of great interest as a possible classifier in the development of an automated whale detector.

6.3 RESULTS AND DISCUSSION

6.3.1 TS measurements

The TS measurements originated from three different fin whale sightings. I logged data for a total of 80 min in the presence of fin whales. Due to the sometimes extended distances of the whales (> 300 m) from the ship and to the periodic bad weather conditions encountered (up to Beaufort 5), I had to discard lots of pings close to the maximum sonar operative range (≈ 400 m). I considered 120 measurements, which were not influenced by these factors, as valid for the analysis. Of these measurements, 73.3% come from directly calibrated sonar beams (see paragraph 3.6 and figure 6.3).

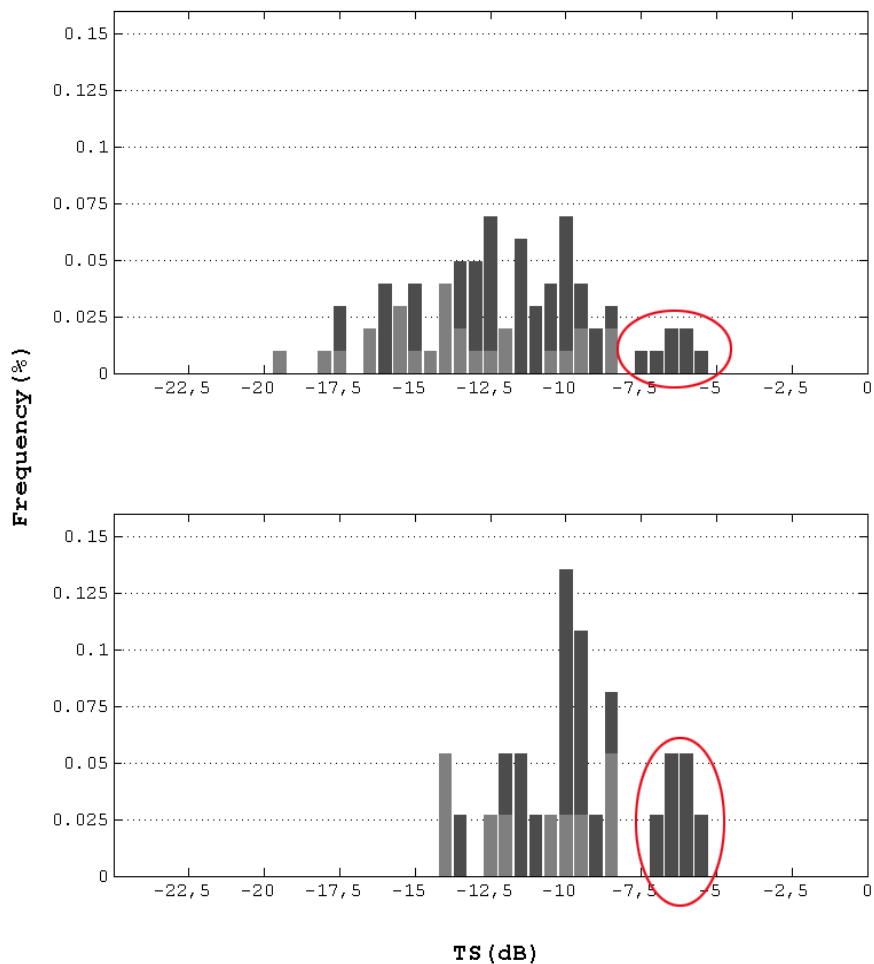


Figure 6.3: TS frequency distributions for the detected fin whales. A) Overall TS at all insonified aspects. B) TS at broadside angle. We assume measurements inside the red circles in each figure represent whales inhaling and filling their lungs completely with air at the surface. In dark grey the measurements coming from sonar beams directly calibrated, in light grey the ones coming from beams calibrated through weighted background noises (see paragraph 3.6).

The length distribution of the sighted fin whales was narrow (17.0 ± 1.0 m; with the error arising from the visual nature of the size estimation). Given the similarity in size of all three whales, I chose to treat all TS detections together, relating the measurement variations initially to the insonification angle only. Considering the average size and length span of the sighted fin whales, the bias should be negligible.

The resulting average TS at broadside angle (90°) for a fin whale of 17 m was -9.5 dB [95% CI -10.4 - 8.7], with a maximum recorded value of -5.6 dB and a minimum of -14.1 dB. TS values were thus variable, as expected. The average TS for all insonified body aspects was -11.4 dB [95% CI -12.05 - 10.8], with a total spread of the distribution of nearly 14 dB (Figure 6.3a). It was possible to obtain backscatter data from seven out of nine sectors of the whales' body aspects, and hence to generate a polar plot of fin whale body reflectivity (figure 6.4). The *in situ* observations did not reveal the expected marked butterfly effect (Urick 1983) as reported *ex situ* by Au in 1996, due to absence of detections in sector number 3, corresponding to approximately 45° from the head. However, although the data were insufficient to reveal a clear butterfly effect, the quadratic regression model showed that $TS=f(\text{angle})$ was consistent with it ($p < 0.0001$). The average TS values increased from the head aspect to broadside and decreased at the tail as expected for a cigar-shaped target. For such a large target, we should perhaps expect higher TS values.

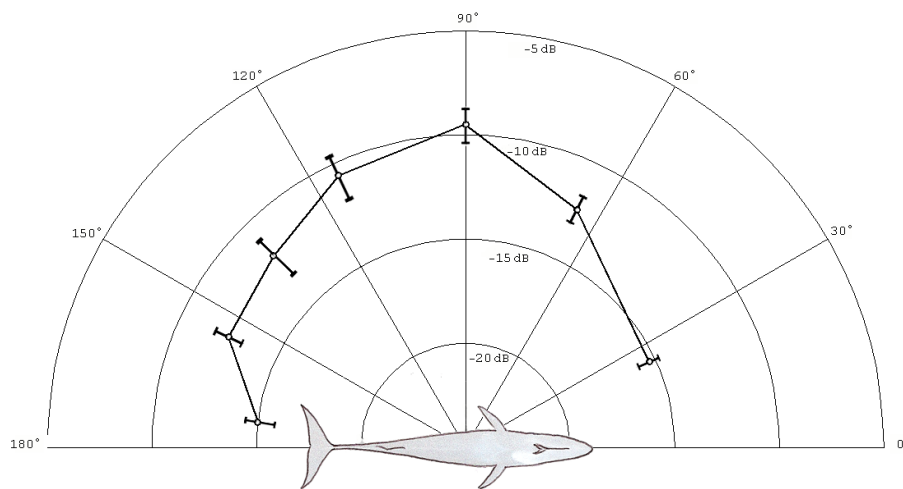


Figure 6.4: TS polar plot response for fin whale detected at 110 kHz. The bars represent the 95% CI of our measurements at different insonified aspects.

However, as underlined by Au (1996) for a dolphin, the absorption coefficient of cetacean skin and blubber may increase with frequency. This phenomenon might be more pronounced in large cetacean species, because the sound waves have to travel a greater distance into the body to reach the lungs (structures considered to be the major acoustic reflective component for cetaceans) before being

reflected, and travelling back through a thicker layer with a consequent larger absorption. Blubber layers of approximately 30 cm thick have been described for fin whales, in contrast to small odontocetes such as the harbor porpoise (*Phocoena phocoena*) that generally possess blubber of only 2.5-3 cm (Iverson 2002).

6.3.2 TS variation with breathing

The data presented here may show how breathing at the surface by whales could be an important source in term of TS variation that should be considered for active acoustic detection. The distribution of TS measurements at broadside (Figure 6.3b) showed a distinct high mode, that I consider represents detections when the lungs were full of air. While a whale is breathing at the surface it has the capacity to expel, for each breathing cycle, tidal air corresponding to 80% of the lung volume in less than two seconds (Sumich et al. 2008). Considering the Simrad SH80 sampling rate of 1 ping per sec, the observed periodicity of TS variation matches with what is known about breathing rate (Lafortuna et al. 2003) and with our behavioral observations (Bernasconi et al. 2011a). At the surface local temporal TS peaks alone may permit prediction of cetacean breathing events. The data comprise TS taken at 1 second intervals, insonification angle and visual observer recordings of cetacean breathing events. The local peaks of TS through time can be treated as a simple predictive model for the prediction of whale inhalation and validated against the MMOs observations. I evaluated the model's performance using summaries for binary classification, a standard procedure for assessing classifier's performance (Nemes and Hartel 2010), with the breathing events considered to be the positive class. The visual observer data here act as a genuine validation dataset, as that information was not used in the construction of the predictive model. We had 18 instances where a breathing/surfacing event was observed, giving potentially 18 trials of the model's ability to predict positives. It is assumed that all instances of breathing were identified and the time of recording is accurate ± 2 seconds. Under this assumption it is possible to determine the sensitivity of this model i.e. the probability of predicting a positive correlation given it is a positive. Of 18 breathing trials, 15 were correctly identified under the model giving a sensitivity of 0.83.

The data differed from a standard classification problem as the number of negative breathing events is not well defined. However for our purposes we have used a semi-arbitrary blocking of the data to 5 second intervals to match the approximate precision of the times in the visual observer data. Under this we have 88 trials in our validation dataset, 70 of which were negatives. A complete confusion matrix can be generated and is represented in Table 6.1.

As measured against the validation data, the model has a raw correct prediction rate of 66%, sensitivity (correct positive rate) of 83% and specificity (correct negative rate) of 61%. Overall the

model performance is modest, with a tendency to over-predict breathing events. It is however promising given its simplicity, based only on determining local peaks in TS, and inclusion of additional sonar derived predictors such as observable behavioral related patterns should improve TS predictions as done for fish by Handegard et al. (2009). Cetacean physiology is a major factor that influences instantaneously the observed acoustic variability of their body reflectivity at the surface. In fish, TS variation is strongly related to diel patterns (Ona 2003), whereas for cetaceans variation seems linked to the adaptations of mammals (air-breathers) inhabiting an aquatic environment (see figure 6.5a example). My data indicate the acoustic variation to be approximately 12 dB and we suggest this scale of variation should be considered in the development of acoustic-based cetacean detectors. Other factors connected to cetacean physiology and behavior related may influence the variability in TS at the surface.

Table 6.1: Confusion matrix for predicting breathing events from local peaks in TS.

	<i>Observed negative</i>	<i>Observed positive</i>
<i>Predictive negative</i>	43	3
<i>Predicted positive</i>	27	15

6.3.3 TS variation with swimming motion and depth

Assuming that the average offset of the surface swimming behavior of a large whale is around 15 m in depth (from DTAG data, Patrick Miller, personal communication), and that the volume of a 17 m fin whale's lungs is approximately 1800 liters at the surface (McMullen and McCarthy 1998), the TS variation estimated with the model for the broadside measurements would be around 4 dB. This variation expected under the model is not as great as the variability that I observed *in situ* (the observed variation span at broadside was 8.5 dB). Previous observations of dolphins swimming at depth showed a variation of 9 dB due to dorso-ventral swimming pattern (Bernasconi et al. 2007). These variations, related to the animal's tilt angle, are instantaneous and bring constant changes to the cross section it is presenting to the transducer when insonified from above. In this case fin whales were mostly insonified from the side. It is clear from the schematic representation of figure 6.5b how their swimming offset at the surface (0-15 m) will also involve an instrument related component in the variation of TS when the whale is swimming in a peripheral area of the acoustic beams. These observed variation factors could, if linked to the previously described and recognizable breathing patterns, be a series of signs to be used in real time to define detections of unknown targets and accept them as whale detections. In figure 6.5c data sequences of a swimming fin whale at the surface insonified at broadside are plotted considering the depth dependency model vs visual observations.

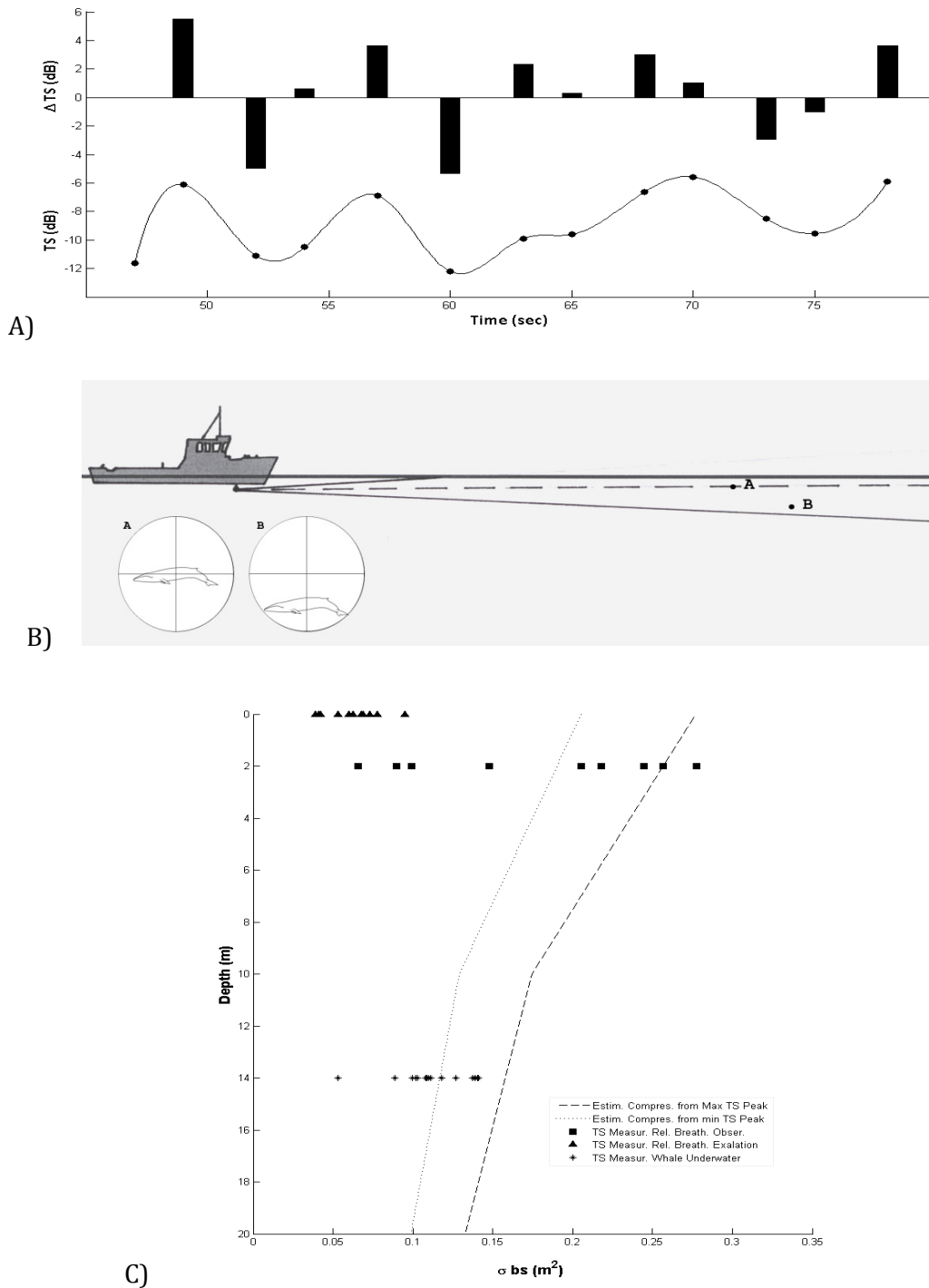


Figure 6.5: A) Instantaneous variation of fin whale TS at broadside for a 31 second sample. The bars represent the variation between samples. The line represents TS vs time; the black circles are samples linked to visual observations of the whale's breathing behavior. B) Respiration and swimming depth in the upper 15 m of the water column could be valid reasons to explain TS fluctuation. Whales' lung volume changes instantaneously at the surface by several hundreds of liters in a few seconds. Another source of variation could be instrument related. The position of the whale within the sonar beam (A, B) is continually affected by its swimming action. Detections from peripheral areas of the beam (B) generate lower TS values. C) General depth dependency model applied to a continuous backscattering cross-section (σ_{bs}) data set from broadside (approximately 5 min). The plot considered σ_{bs} in three categories defined by the observed behavior: full lungs (■), blow (exhalation) (▲) and whale swimming underwater (*). The dashed and dotted line represent the model range calculated using the maximum and minimum measured TS peaks, respectively. The measurements outside the model limit can be due to the instrumentation as underlined in figure 6B and by other factor linked to unknown compression mechanism of cetaceans' lungs.

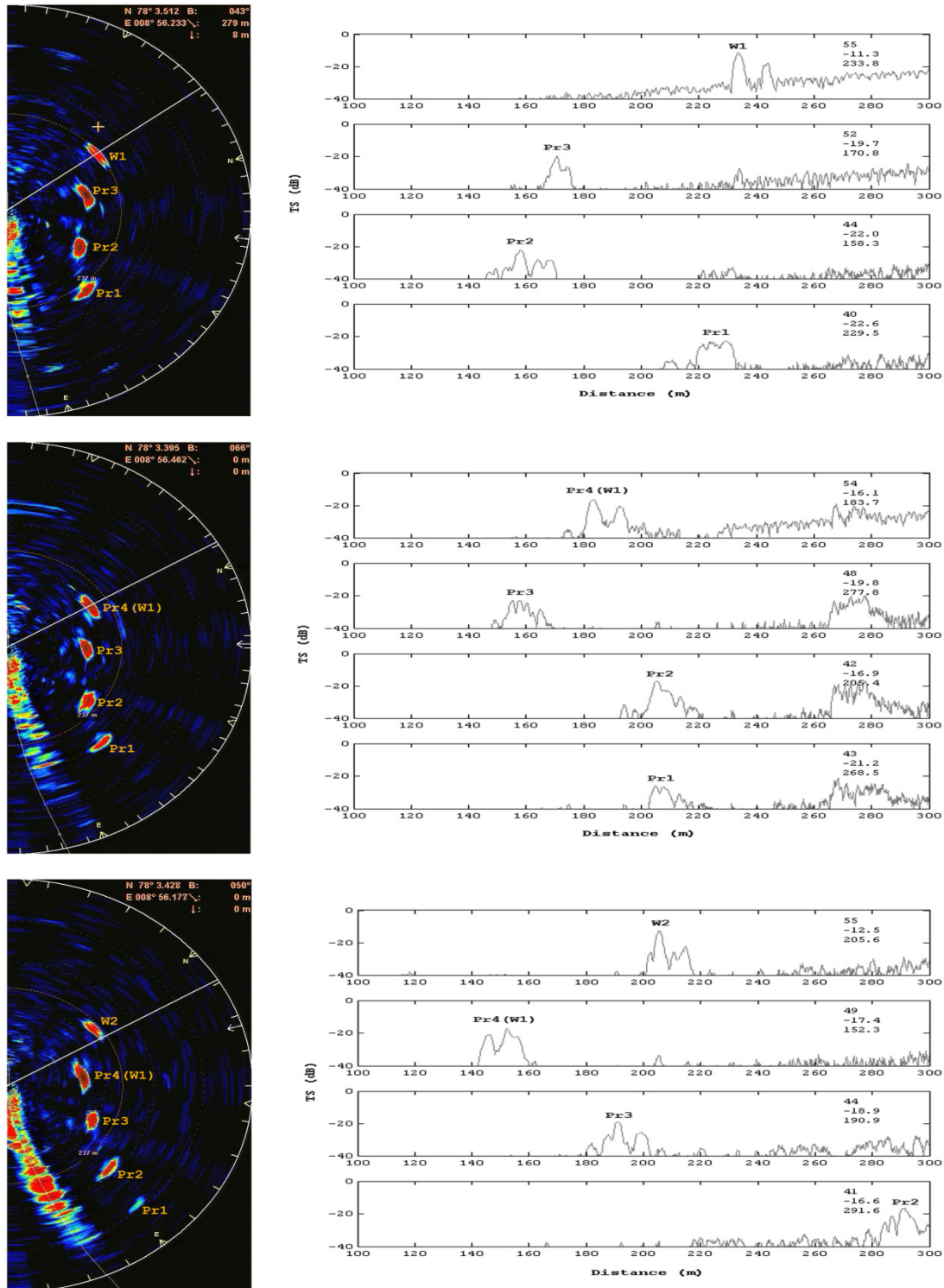


Figure 6.6: Example of whale swimming patterns detectable using our sonar. The picture represents three pings over a period of 40 seconds where the whales were visible but emerged to breathe just twice. The letter W represents the observed whale at the surface, Pr the print left behind that stays on the screen up to a minute. All the acoustic measurements described in this paper were validated by simultaneous visual observations. The three numbers in the top right of the graphics show in order: the beam involved in the detection (beams are counted anti clock wise from the ship bow), the measured peak TS value from the target of interest, and its range in meters.

6.3.4 Behavioral patterns observed in sonar screen video sequences and raw data

Fluke prints are a visible pattern that appears at the surface of the ocean when a whale is swimming at a shallow depth or beginning a dive. The print grows radially and may remain visible for as long as several minutes, depending on ocean and wind conditions. Two primary mechanisms have been proposed for the formation of fluke prints, a general “upwelling” of water off the fluke (Levy et al. 2011) and a surfactant-based explanation (Berta and Sumich 1999; Hogg et al. 2009). The prints are visible in the infrared images because the temperature of the water in the prints is less than that of the ocean surface temperature outside the prints. Churnside et al. (2009) modeled the difference in temperature between the nearby sea surface temperature and the temperature at the center of the prints. The measurable difference in surface temperatures inside and outside the fluke print support the theory that the prints are created as the motion of the flukes brings water to the surface of the ocean, but does not address the role of vorticity or surfactants in the formation of the prints.

Observations of fluke print (Levy et al. 2011) provided that fluke motion can create a pneumatic jet effect on the surface known as a pneumatic breakwater (Evans 1995; Taylor 1995). It has been demonstrated experimentally how fluke prints seen on the ocean surface are a direct consequence of a vortex ring shed from the fluke (Levy et al. 2011). Vorticity is created during the down stroke on the underside of the fluke and then shed on the upstroke toward the surface. As it drifts toward the surface, this vortex ring creates a powerful jet of fluid that creates the long-lasting and dramatic temperature gradients on the ocean surface found in fluke prints by bringing colder water from below the ring to the surface efficiently and in large quantities.

On the sonar screen fluke prints, caused by swimming under the water surface and by breathing behavior, are easily recognizable as marks that remain on the monitor for minutes. The energy plot confirms that the first trace of the series, corresponding to the actual sighted whale (visual confirmation), is always stronger in terms of acoustic energy (Figure 6.6). The surface prints left behind, decreased in intensity with time as the water dilutes and air bubbles generated by the whale tail stroke dissolve. The patterns observed on the sonar screen can be explained considering the basic concept of acoustic reflection described in paragraph 2.4 and resume by equation 2.25. Indeed acoustic reflection is given by the difference of density encountered in the path of a sound wave travelling. In this case the temperature difference creates a visible mark on the sonar screen with air bubbles generated by the whale tail strokes acting as an amplifier. It cannot be excluded that also physiological discharges due to respiration could take part in the change of density encounter at a fluke print boundary. Respiratory discharges are made of an emulsion of fine oil droplets from cells lining the air sinuses, mucus from the tracheal glands, and surfactants (a mix of lipoproteins) from the lungs. Their greasy nature should be responsible at least of a small part of the density change at the

surface and should be detectable using sonar as routinely done to detect leaks from oil pipes (Blondel 2009). Nonetheless, it is more reasonable to think that the large volume of colder water moved by the powerful tail strokes will have a major impact on the persistence of these characteristic marks on the sonar screen. Given that traditional detection methods are based on the principle of Constant False Alarm Rate that are well described in radar and sonar literature (Urlick 1983; Levanon 2004), I believe these behaviour related surface traces are important signs to study and understand, to be able to confirm future attempts of blind acoustic detections of whales while they are swimming at the surface (Nøttestad et al. 2010). Indeed these kinds of patterns can be used as a possible reliable classifier for targets detected in real time to initiate a target track and confirm the presence of a large cetacean swimming in proximity of the vessel. This is a similar approach to the one used to detect small surface watercraft for harbour security (Lo and Fergusson 2004).

6.4 CONCLUSIONS

Swimming kinematics, dives (depth), physiology and breathing behavior all appear to influence fin whale TS. These factors need to be considered in future progress towards automated active acoustic detection of whales and be linked to the instrument beam pattern sensitivity to predict precisely TS variation. The dorso-ventral swimming patterns of cetaceans have previously been described as a source of TS variation for dusky dolphin (see Chapter 5), and consequently underlined the effect of the sonar tilt angle setting when the target is detected at depth. At the surface much of the TS variation can be explained by known cetacean physiology and behavior. The lung volume variation due to respiration influences TS rapidly, but in a predictable manner. Automatic detection performance using acoustic systems usually consists of a relay process based on false alarm. The first results from this study suggest how a major attention to cetaceans' physiology and kinematics of movements are important factors to implement a reliable detection algorithm to develop an acoustic based whale detector using instruments available on the market.

Acknowledgments. I would like to thank the crew onboard M/V Eros, the Research Council of Norway, Dr. Marianne Holm for the sea time granted for calibration purposes, Dr. Frank Reier Knudsen and Ole Bernt Gammelsæter (Simrad, Kongsberg Maritime AS) for the constant supervision and technical support, Dr. Patrick Miller (Sea Mammal Research Unit, University of St Andrews) for sharing information about whale swimming behavior and Dr. Carl Donovan (Centre for Research into Ecological and Environmental Modelling, University of St Andrews) for the implementation of the statistical analysis. Special thanks to Mr. Terje Torkelsen (Marine Ecosystem Technologies AS) for his friendship and for his inspiring teaching about sonars.

CHAPTER 7



**THE EFFECTS OF FREQUENCY AND DEPTH ON TS OF
THE HUMPBACK WHALE (*MEGAPTERA
NOVAEANGLIAE*)**

7. THE EFFECTS OF FREQUENCY AND DEPTH ON TARGET STRENGTH OF HUMPBACK WHALE (*Megaptera novaeangliae*).

The air contained in body cavities, such as lungs, has a significant effect on the acoustic energy backscattered from a cetacean as also shown in chapter 6. In this chapter I describe a small set of data obtained while a humpback whale (*Megaptera novaeangliae*) dove and swam underneath a research vessel, providing a valuable record of its multi-frequency scattering characteristics from near surface to a depth of about 240 m. I analyzed the data here with reference to principles and ideas of sound scattering by cetaceans stated in previous chapters. This work is tightly linked to the ultimate goal of developing an automated whale detection system for mitigation purposes.

7.1 INTRODUCTION

To date, studies on cetacean TS (Bernasconi et al. 2009; Lucifredi and Stein 2007; Miller and Potter 1999; Levenson 1974; Love 1973; Dunn 1969) have explored variability neither as a function of sonar frequency nor as a function of depth. Au (1996) showed how the largest reflection comes from the region of the lungs from a bottlenose dolphin (*Tursiops truncatus*), but concluded that his results were applicable only for a dolphin close to the surface because as the animal swam deeper its lungs would be compressed and, according to Boyle's law, the volume would decrease (Moore et al. 2011; Ridgway and Howard 1979). As described for herring swimbladder (Ona 2003), the decrease in the lung volume will probably cause whale TS to change (see Chapter 6). Au (1996) described the multi-frequency response (between 23 and 80 kHz) of the backscatter energy coming from the dolphins' body, comparing his results with the one for fish of Love (1973). It was clear from Au's (1996) experiment that for cetaceans, lower frequencies gave better Signal to Noise ratio (SNR), opening a discussion about which frequencies better suits the application of active acoustics for cetacean detection (Fig. 7.1).

The long term goal of using sonar to detect marine mammals in the proximity of seismic vessels in order to mitigate the potential impact of seismic activities on whales, must consider the capability of detecting diving whales; It is indeed logical to think that deep diving species such as Sperm whales (*Physeter macrocephalus*) or Beaked whales (*Ziphiidae* family) will be detected underwater most of the time (Tyack et al. 2011 and 2006; Zimmer et al. 2008; Watwood et al. 2006). With this perspective, it is important to work with frequencies that provide high TS values, especially while dealing with targets at depth the TS of which will probably be smaller because of the lung compression hypothesized in Chapter 6 (Au 1996) and described by Ridgway for a bottlenose dolphin (1967) and recently reviewed

by Moore et al. (2011). It will also be important to link the information available from the literature about diving behavior of different species to start the identification process of the detected target - e.g. a sperm whale dives an average of perhaps 1000 m while a fin whale rarely reaches 300 m (Watwood et al. 2006; Croll et al. 2001; Panigada et al. 1999). For this pilot project, as described throughout my thesis, the task of measuring whale TS was not designed specifically to measure the variability of cetaceans TS as a function of diving depth. I designed the method to provide measurements of whale TS at the surface, and to describe the variation of TS as a function of behavior and body aspect. Nevertheless, I was able to collect a valuable data set when a humpback whale swam by chance underneath the ship's multi-frequency echosounder system. In this chapter I describe, and examine those data to bring to the attention of the reader some hypotheses that will need detailed investigation for the future development of an operative and reliable detector for subsurface swimming whales.

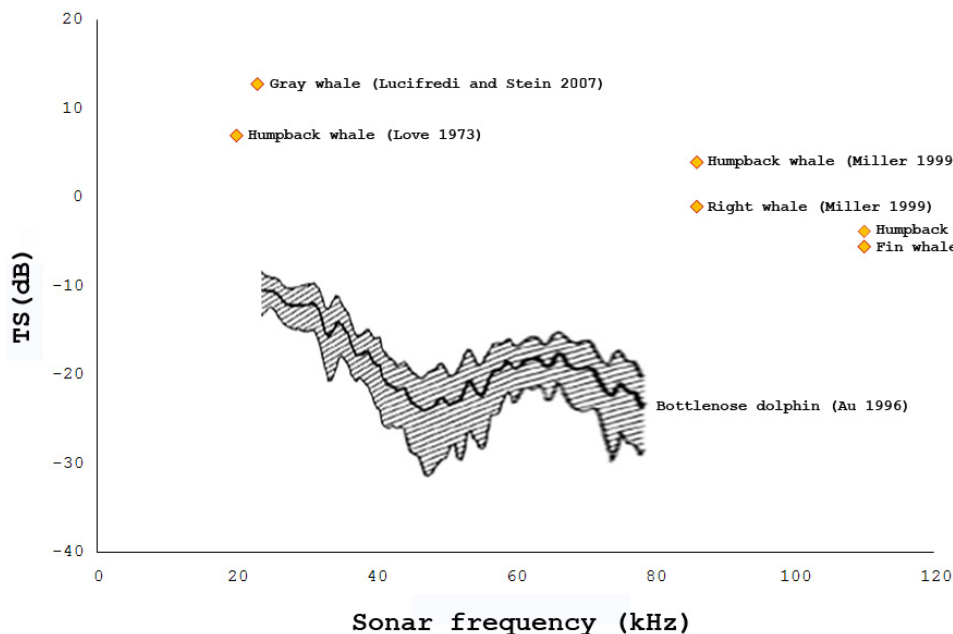


Figure 7.1: Overview of previous results of cetaceans TS studies presented as f (sonar frequency in kHz). Note how the historical records of cetaceans TS measurements also show how the use of lower frequencies result in higher received TS values.

7.2 METHODS

The TS measurements of a Humpback whale described here were made on 21st of July 2009 from the Norwegian vessel M/V “Libas”, a 94 m combined purse seiner and pelagic trawler adapted and equipped as a modern scientific research platform. Its instrument suite include two multibeam sonars with scientific output (Simrad SH80 and SX90), and a calibrated five frequency scientific echosounder (Simrad EK60).

The Simrad SH80 data protocol for measuring whale TS using omni-directional sonar is the same as described in paragraph 6.2.1 A and B. The method has been employed as standard procedure to collect acoustic data from whales swimming at the surface. In this case I used the omni-directional sonar data to describe the TS frequency distribution from broadside of the observed humpback whale at the surface. I also used these data as elements to compare with the data logged with the vertical orientated scientific echosounder. From the dataset presented here, I could test the basic compression model described in Chapter 6 based on real *in situ* measurements coming from a whale swimming at depth.

The objective of this chapter was to describe and evaluate detailed acoustic data (composed of 27 continuous pings for each frequency), which arose from the dive of a humpback whale underneath the ship. I used the established general principles of TS variability with depth (Ona 2003), to illustrate some considerations that will be necessary to be implemented in a sonar-based whale detector that can identify targets at depth. The EK60 transducers were co-aligned so that every measurement at each frequency came from the same range and target. The acoustic data were processed and extracted using the software Large Scale Survey System (LSSS) (Copyright © 2011 Christian Michelsen Research AS. All rights reserved). The software, through a user-friendly interface, enabled a quick view of the frequency response of the targets of interests, and allowed the TS measurements to be exported from the raw data in analyzable .csv files. Thus, I could see whether or not TS depth dependency was consistent with patterns shown in Chapter 6 for shallow dives when a whale dived between 180 and 240 m depth. After I defined the TS probability distribution function from the omni-directional sonar (110 kHz) data recorded at the surface, I compared the EK60 high frequencies (70 and 120 kHz) with the SH80 frequency (110 kHz). I corrected TS data recorded at depth to TS at surface using the basic compression model described in chapter 6 solving eq. (6.3) as:

$$\sigma_0 = \frac{\sigma_z}{\left(1 + \frac{z}{10}\right)^\gamma} \quad (7.1)$$

where σ_z is the recorded backscattering cross-section at depth (between 180 and 240 m), σ_0 the calculated backscattering at the sea surface ($z=0$), and γ corresponds to -0.67, the estimated contraction-rate parameter of a free spherical balloon, the volume of which varies with depth in accordance with Boyle's law. I tested the resulting distributions with the Wilcoxon Rank-Sum Test to verify the reliability of the model.

Afterwards, I analyzed the multi-frequency data obtained from the scientific echosounder to observe the whale frequency response from 18 to 200 kHz. I processed the data using a one way ANOVA to verify if differences among frequency were consistent *in situ* as described *ex situ* by Au (1996).

7.3 RESULTS AND DISCUSSION

7.3.1 Omni-directional sonar TS measurements

The average Humpback whale TS, measured using the Simrad SH80, while the animal was swimming at the surface (n=50; see Fig. 7.2 A and 7.3 A) was -10.4 dB [95% CI -9.5 -11.7] with a maximum recorded value of -4.2 dB. It was not possible as for the study regarding Fin whale TS (see Chapter 6) to define the polar response of TS describing variation between different insonified aspects of the animal. However, it is reasonable to assume that a similar backscattering response would be obtained due to their similarities in size and morphology. The measurements distribution based on these data contained a discrete mode of high TS values (between -4 and -6 dB) that can be linked, as shown in chapter 6, to the whale's respiration pattern (Fig. 7.2 A). I could also record a small data sample (n=10), coming from a whale swimming apparently parallel to the ship at a depth of 40 m (Fig. 7.3 A). The average TS at 40 m depth was -12.45 dB [95% CI -10.53 -15.97].

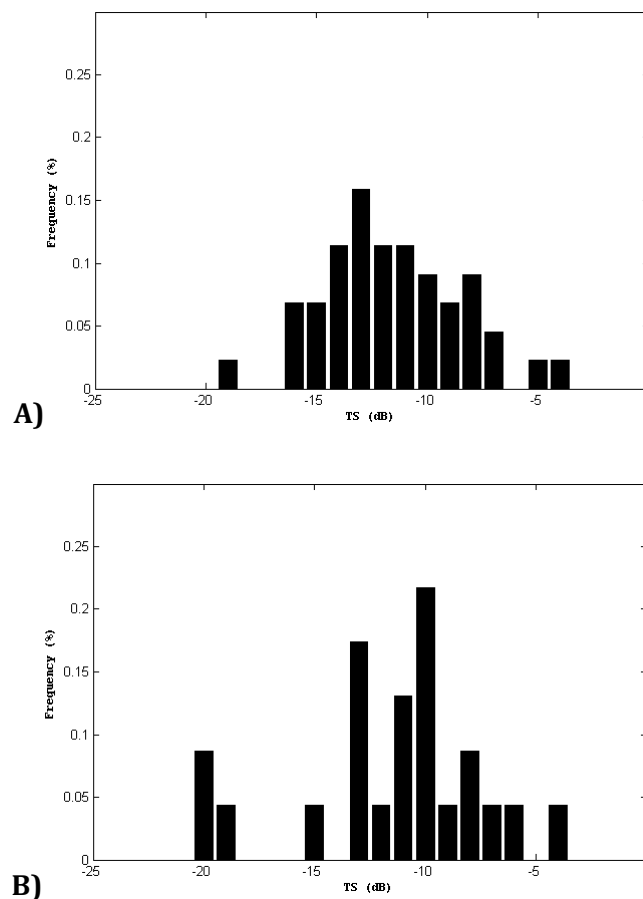


Figure 7.2: TS frequency distribution of TS measurements for an individual Humpback whale. A) SH80 measurements at the surface; also in this case it was possible to observe a small number of received signals linked to the whales' respiration patterns. B) EK60 log of Humpback whale at depth was post-processed through the general compression model described by Groska and Ona (2003). It is clear from this first qualitative analysis that the model, developed for herring swim bladder, can be adapted to cetacean lung structure.

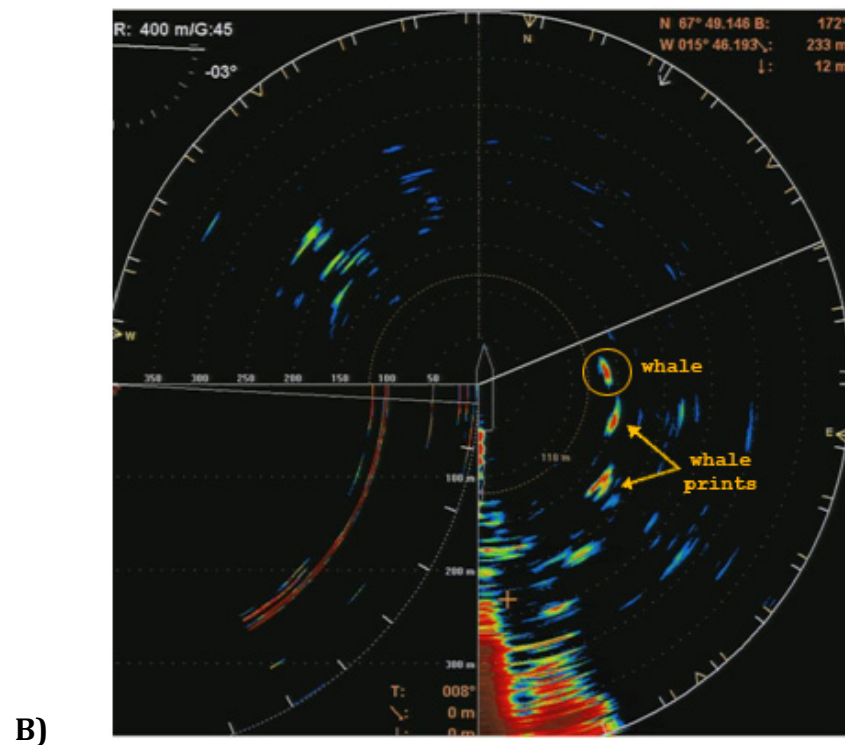
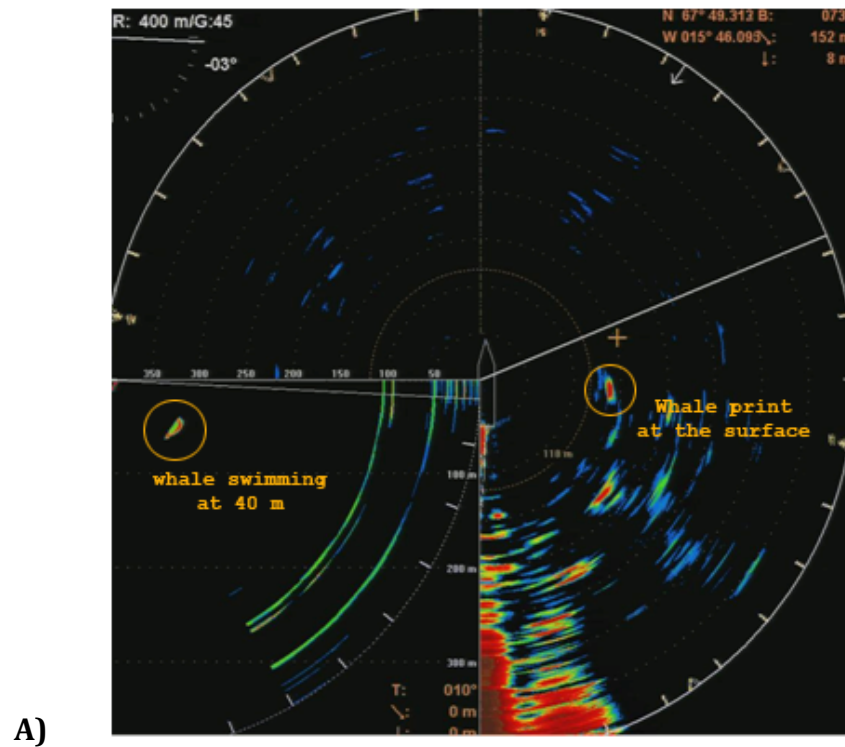


Figure 7.3: Sonar screen capture showing both omni-directional and vertical views of two distinct moments of the humpback whale tracking. The white line in the omni-directional view represents where the vertical slice is pointing. A) In the orange circle (vertical slice view) the whale can be observed while swimming at 40m depth. It is also possible to observe (omni-directional view) the print left on the surface before the shallow dive. B) Characteristic prints left behind by the whale. The persistence of print observation every time a whale was swimming at the surface should be investigated further as it could possibly be a strong classifier in future attempts to develop a sonar-based whale detector (see paragraph 6.3.4).

7.3.2 TS variation with depth

In Chapter 6 I explained how the air contained in the lungs could affect the backscattered energy reflected from a cetacean's body. In particular, I found a relation that linked breathing events with instantaneous variation of TS. It was not possible however to gain a clear cut record of TS at depth to test this effect while fin whales were diving. However, that was possible for the humpback whale which had an average measured TS at depth (between 190 and 240 m) that gave a deviation from the average TS at the surface quantifiable at 12 dB (n=54) (see paragraph 7.3.3). To verify the hypothesis, I post-processed the calibrated echosounder data set using eq. 7.1 applying it in reverse compared to the basic compression model (Gorska and Ona 2003) presented in Chapter 6. My results showed that the hypothesized effect of depth on TS is real and measurable. Indeed the data, tested with the Wilcoxon Rank-Sum, give no evidence against the null hypothesis of identical distribution of the echosounder data processed through the model and the sonar data collected at the surface with $p=0.488$.

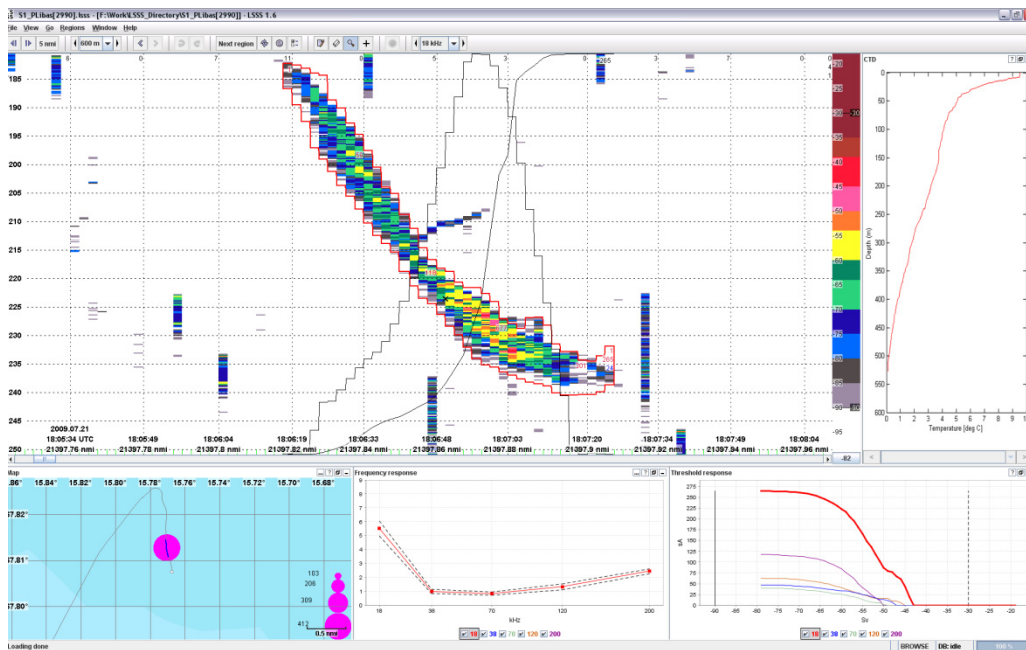


Figure 7.4: Multi-frequency echosounder screen capture, from the post-processing software LSSS, of a humpback whale passage underneath the ship's drop keel. In the main window the echogram and the dB reading scale is shown. The small windows at the bottom represent: map including the ship track (the pink circle represent the SH80 coverage while the tick blue line represent the one for EK60), frequency response of the selected area of the echograms and TS distribution of the same area.

I believe cetacean TS depth dependency is a fundamental parameter that must be considered for further implementation of a sonar-based whale detector. Although I applied a general contraction rate γ , the model fit the data roughly but consistently. The model appeared to be of valid use not only when the animals breathe at the surface, but also when swimming at depth (Fig 7.2 B). These observations need more exhaustive examination to define precise parameters to discriminate cetacean targets at depth, but I believe that the results presented in this chapter are a concrete starting point to generate

new hypotheses to be tested in dedicated experiments. It is important to note that the TS measurements presented in this thesis could be, not consistently, influenced by a certain degree of error due to a calibration procedure that is not yet as robust as standard protocols applied to scientific echosounder (Foote et al. 1995). However, this error would not influence the relative acoustic measurements that confirm quantitatively the depth dependency of cetacean TS of 12 dB comparing measurements from the same whale coming from deep waters and measurements taken at the surface.

7.3.3 Cetacean TS frequency response

When the whale dived beneath the ship, it was not only possible to observe the effect of compression on the measured humpback whale TS. Indeed the ship's calibrated scientific echosounder gave me a valuable multi-frequency data set (See Figure 7.4). The data clearly revealed which frequencies should be adopted for further attempts to detect whales using sonar. The average TS at depth was -18.1 dB (σ_{bs} 0.0155) at 18 kHz, -19.9 dB (σ_{bs} 0.0102) at 38 kHz, -22.3 dB (σ_{bs} 0.0059) at 70 kHz, -22.4 dB (σ_{bs} 0.0057) at 120 kHz and -22.6 dB (σ_{bs} 0.0054) at 200 kHz. From past studies (Lucifredi and Stein 2007; Miller and Potter 1998; Love 1973; Dunn 1969), it can be seen that lower frequencies provide higher TS values, and that the use of frequencies lower than 30 kHz gave signals easier to discriminate (Au 1996) from the background noise. This particular aspect could be fundamental in the attempt to classify strong sonar target as whales. Large TS values at the surface will decrease constantly and in a predictable manner for the same target under the effect of pressure when the animal commences a dive and the cross section of its lungs starts decreasing with the increasing depth (Moore et al 2011). It will then be convenient to use a frequency which provides strong signal responses.

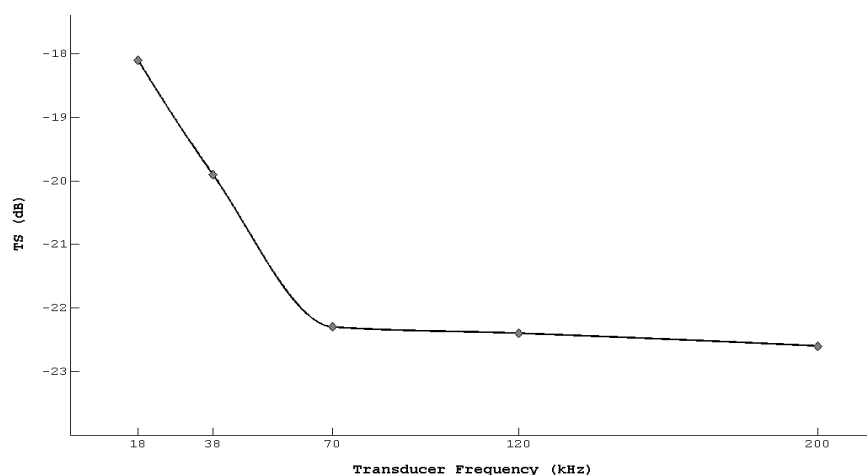


Figure 7.5: Frequency response for a humpback whale logged while the animal was diving between 180 and 220 m underneath the ship's drop keel. It seems very clear how lower frequency provide higher TS value that are easily identifiable from any background noise or from targets of other nature.

I tested the data coming from the EK60, while the whale was diving, to verify differences between frequencies with a one-way ANOVA. The result was $p < 0.0004$, $n=81$, which agreed with my hypothesis that increasing the frequency affects the intensity of the received signal. Higher frequency results in decreased received acoustic whale intensity and signature. This is quite clear from inspecting the results plotted in Figure 7.5 and agrees with the experimental data presented by Au (1996).

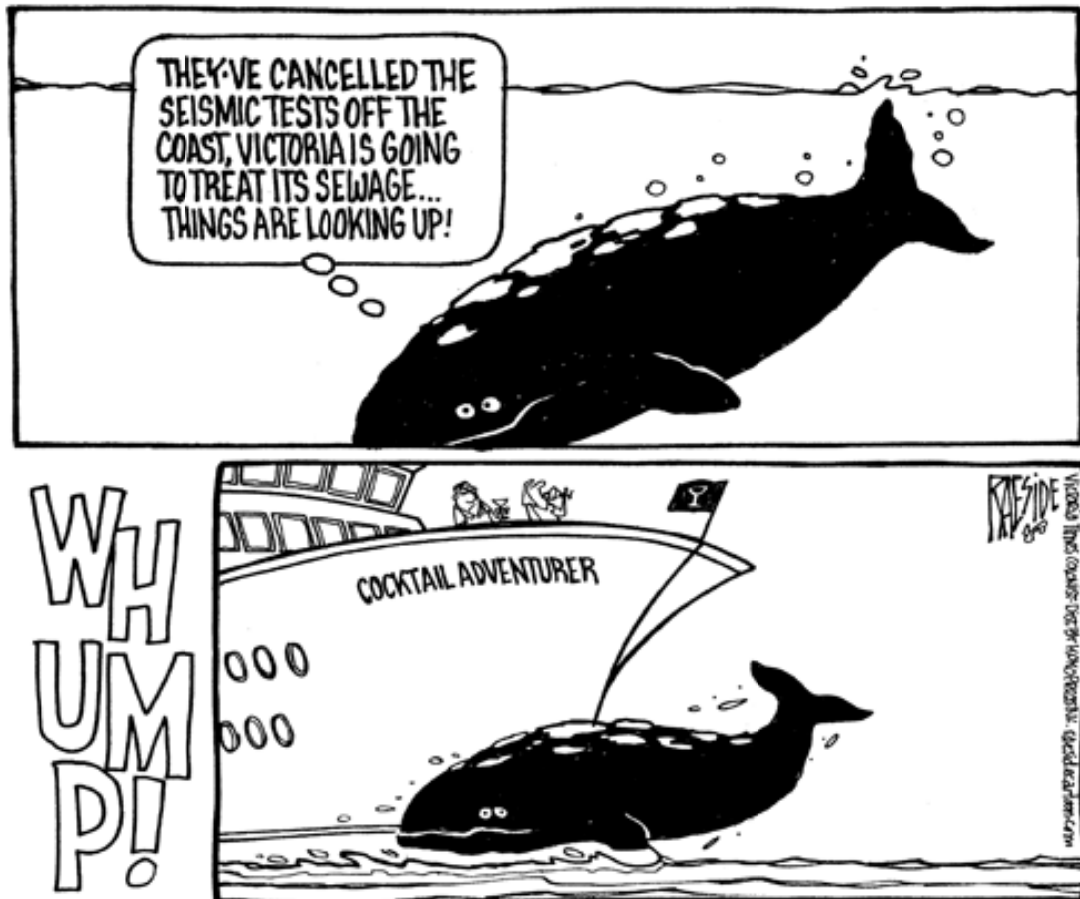
In my project, the decision to employ a high frequency sonar to test the feasibility of quantifying TS data from cetaceans was determined primarily by the ethical reason of being well above the hearing threshold of my target species (namely baleen whales); there is no proof that fish-finding sonars disturb cetaceans. The Simrad SH80 was not the optimal instrument but it's hardware was efficient to test quantitatively the potential of this technology for whale detections. My behavioral observations from Bernasconi et al. 2011a, allowed me to be confident and I thereby started to test the use of lower operating frequencies (20 kHz) in the latter part of an ongoing project. The detection range of the Simrad SH80 is indeed very short (< 400 m) if we consider the exclusion zone required during seismic surveys (at least 500 m in most cases). Using such high frequency would also have other limitations, i.e. a ship moving fast (more than 10 knots) will allow very little time to react from the time of detecting the whale and the possible decision to take a mitigation measurement (e.g. shutting down seismic operation) or changing the course. For this reason, the future of this field of study will be focused on gathering long-range detections (≈ 3000 m), continuing with the quantification of the acoustic signals and deepening the knowledge of the results arising from this thesis. It will be necessary to consider the possibility that some odontocetes could be disturbed by the use of lower frequencies. Odontocetes do not seem to be affected by sonar commonly used in fishery surveys (Nøttestad et al. 2010; Bernasconi et al. 2011b). This particular aspect should nevertheless be investigated in more depth through experiments similar to those conducted by Miller et al. (2009).

7.4 CONCLUSIONS

Humpback whale TS was measured using a calibrated scientific echosounder while the animal was diving underneath the ship at between 190 and 240 m depth. This preliminary *in situ* description of a cetacean's frequency response underlined how higher TS values result when frequencies lower than 38 kHz are used. The data presented here support the use of lower frequencies for cetacean detections and in particular the use of the new Simrad SX90 (operating frequencies span 20-30 kHz), a unit recently available on the market. The data set collected through a combined use of omni-directional sonar (measurements at the surface) and scientific echosounder (measurements at depth) enabled me to test the basic compression model I proposed in Chapter 6 using data collected *in situ*. This model has the potential to be implemented as a fundamental parameter to develop a concrete sonar-based

whale detector prototype. The observed TS variation of cetaceans is indeed tightly linked to their physiology and to Boyles' law. The data presented in paragraph 7.3.2 confirmed the hypothesis showing how low backscattering signals are received when a target, of average length 14 m, was detected in deep waters. New classifiers to discriminate possible diving whale targets with other targets have to be identified. I believe these are major challenges that research on active sonar applied to cetaceans has to identify and quantify as best as possible for reliable target identification. Finally, I strongly recommend a behavioral approach to the analysis of cetacean backscattering signals, to advance and implement the use of active acoustic techniques for relevant conservation issues linked to the well-being of cetaceans.

CHAPTER 8



GENERAL DISCUSSION

8. GENERAL DISCUSSION

Ship traffic and seismic explorations are well established and fundamental activities for the life styles of our modern society. But more restrictions and well defined rules may have to be applied to such activities given that they clearly bring a certain degree of disturbance and damage to the world's natural resources. The results presented in this thesis focus more on the technicalities that need to be developed and further tested for the use of active acoustics in cetacean conservation and less on the conservation issue itself. There is limited evidence for the impact of seismic activities on marine mammals, either on hearing (Lucke et al. 2009) or behavior (Miller et al. 2009). Although sightings of marine mammals close to vessels might be interpreted as zero or minimal impact on their populations (Harris *et al.* 2001), some researchers have associated cetacean stranding with seismic surveys (*e.g.* Malakoff 2002; Engel *et al.* 2004) and others have documented alterations in behavior due to noise from air-guns (*e.g.* Richardson et al. 1995; Goold 1996). If we exclude the work of Madsen *et al.* (2002), many other studies reported negative effects of loud anthropogenic noises on cetaceans (*e.g.* Evans *et al.* 1993; Mate et al. 1994; Goold 1996; McCauley *et al.* 2000; Malakoff 2002; Gordon *et al.* 2004). Goold and Coates (2006) showed how the airgun acoustical output covers, at substantial energy levels, the entire frequency span known to be used by cetaceans. This study is in agreement with the findings of Madsen et al. (2006), that reported substantive energy between 0.3 and 3 kHz received by sperm whales (*Physeter macrocephalus*) exposed to airgun pulses. Seismic airguns produce low frequency impulsive sounds at intervals of 10–15 s, with broadband source levels of 220–255 dB re 1 μ Pa at 1m. The dominant frequencies of airgun pulses lie within the 0–120 kHz range, reaching frequencies well beyond the interest of seismic exploration (Goold and Fish 1998). The dominant frequencies overlap with those used by baleen whales (10 Hz–1 kHz), with the high frequency component also overlapping with the frequency range used by many odontocetes in the range 10–150 kHz (Richardson et al. 1995).

Many countries have adopted regulations which emphasize mitigation of exposure to intense anthropogenic sound sources (Southall et al. 2008). The UK JNCC guidelines, although varying considerably in the details, are the base which is used by most national agencies to define their own regulations (see Weir and Dolman, 2007). Such guidelines have become a widely accepted approach to resolve the problem of the various effects of noise pollution during seismic surveys. However, this reliance on the JNCC guidelines could arguably be considered premature (Parson et al. 2009; Leite-Parente and Araújo 2011).

Currently, marine mammal observers (MMOs) are the most common method used to fulfill regulatory obligations proposed by different guidelines. In many countries MMOs do not need any experience or

expertise to be hired and their number onboard seismic vessels does not allow the scheduling of rotation for constant monitoring. The probability of detecting marine mammals at sea is often relatively low (e.g. Barlow 1999), this is especially true when operations persist in times of reduced visibility such as in fog and at night. Passive acoustic monitoring can additionally provide some detection capability in such conditions (e.g. Barlow and Taylor 2005), but this relies on animals actually vocalizing, which they certainly do not do all of the time (Gordon and Tyack, 2002). Fin whales ceased all vocalization during seismic surveys and did not resume vocalizing for hours or days afterward (Clark and Gagnon, 2006). Sperm whales have also decreased vocalizations or become completely silent in response to seismic surveys (IWC, 2007), as well as in the presence of pinger sounds (Watkins and Schevill, 1975), mid-frequency military sonar signals (Watkins et al., 1985), and low-frequency anthropogenic sounds (Bowles et al., 1994). Neither visual sightings nor passive detection fully resolve the problem of reliable detection of animals at risk in proximity of seismic activities. There is a strong need for a standard reliable protocol and a tool capable of detecting whales in proximity of seismic surveys with a higher probability of detection also during more adverse observational conditions.

The work presented in my thesis was developed to find some scientific answers, raise new relevant questions and to develop a basis for employing active sonar in the best interests of the whales involved in potentially harmful conflicts with humans.

My first intention was to use active acoustics to study cetacean behavior and predator-prey interactions as done previously with success by Nøttestad and Axelsen (1999), Nøttestad et al. (2002a) and Benoit-Bird et al. (2004). I had furthermore the advantage of a better digital output coming from a scientific echosounder. I could observe hydro-acoustically more or less continuously a predator-prey interaction event occurring between Dusky dolphins and Cape horse mackerel and analyzing quantitatively the acoustic data adapting the proper fishery acoustic method. To do so I used a vertically orientated scientific echosounder. Despite its high resolution, the system insonified only a limited volume of the water column. This did not allow me to observe all the events, but it did give me an insight into the overall situation with a clear indication of the potential to use active acoustics as a behavioral study tool. I could measure single events in part of the dolphin group and the mackerel school.

The new Simrad MS70, a 3D Multibeam sonar, will be the optimal tool to adopt in future efforts to study prey predator interactions. This new multibeam sonar with its 500 beams could insonify, with a single ping, an entire school of mackerel (Balabanian et al. 2007) and is capable to be calibrated with a robust standard methods (Ona et al. 2009). One interesting outcome from my first experience with

cetacean TS data was the observation of variation trends in the received backscattered energy that could represent a typical acoustic signature for marine mammals. Fish TS have been studied extensively for many different species (Fässler et al. 2009; Knudsen et al. 2004; McQuinn and Winger 2003; Foote 1997; Love 1978 and 1971). Individual TS variation in fish is linked/attached to schooling behavior in abundant pelagic fish species. During their diel vertical migration the fish tilt angle changes in a predictable and constant manner (Axenrot et al. 2004; McQuinn and Winger 2003; Huse and Ona 1996). Indeed, the backscattering cross section of pelagic fish, when they are insonified from above, varies solely with changing depths through swimming upwards or downwards in the water column (Huse and Ona 1996). More detailed observations showed also how single fish behavior can be describe and used to link TS variation at a finer scale that relates it to speed (Handegard et al. 2009; Knudsen et al. 2004; Pedersen 2001).

If we analyze consecutive pings for a chosen target, and not only the distribution of the values over a longer period, we can observe how the variance between one TS measurement and another is about an average of $TS = -0.23$ dB for a fish. Cetacean TS variation can be linked, as stated in paragraph 5.2.1, with the mammalian dorso-ventral posture. In this case, when a dolphin or a whale is swimming the variation will inherently be bigger, instantaneous and a function of their particular swimming behavior and size. Some preliminary analysis showed that for a dolphin the variation was around 0.1 dB, while for a large whale it was around 0.6 dB. The larger dimension of baleen whales lungs, structures considered to be the main reflective part of the cetacean body (Au 1996), could explain the difference but other very small differences may arise if we try to analyze them in more detail and relate them to species-specific swimming behaviors. Dolphins probably need a higher tail stroke frequency to swim, while large whales may use fewer but more powerful strokes over a similar time period, with more pronounced changes in the body tilt angle, and consequently of the acoustic backscattering cross section, shown to the sonar transducer but less constant if compared to dolphins.

I soon realized that active acoustics could be used for a more delicate conservation issues: the mitigation of seismic exploration over whales. I moved on to identify the proper active acoustic tool that suited the application of cetaceans' detection. First requirement considered was the possibility of pointing quickly the sonar in the direction of interest (something impossible when using the acoustic instrumentation described in paragraph 4.3.1 and adopted to collect some of the data presented in my thesis - see paragraph 5.2 and 7.3.3). For marine mammal detection, I have chosen an instrument capable of being operated from a moving ship, with multi-frequency options, 360 degree radar-like coverage with the possibility of scanning dedicated sectors around the ship, and an easy hardware interface capable of operational software implementation (see paragraph 4.3.2 for details on the

system). The long term goal is to develop a reliable quantitative acoustic tool with known probability of detecting cetaceans and other marine life with good coverage of the entire volume of the water column near the ship, and furthermore capable of detecting a target both close to the surface, in the so called blind zone (Patel et al. 2009; Scalabrin et al. 2009; Totland et al. 2009), and at depth.

I started to develop an *in situ* calibration method for omnidirectional sonar (ICES 2010) with the aim of detecting single targets. The method will have to be implemented into a robust standard procedure to be adopted also for other monitoring activities (e.g. abundance estimation of fish; Nishimori et al. 2009). The preliminary results seem to be very promising and showed great potential for further application of omnidirectional sonar in quantitative studies of marine life (Brehmer et al. 2006; Nishimori et al. 2009; Bernasconi et al. 2009; Løkkeborg et al. 2010).

We need to overcome the inherent doubt (still entrenched among marine mammal specialists) that using low frequency is generally bad for cetaceans. A clear distinction between different sonar systems is a prerequisite which need more attention from the biologist community (Jepson et al 2003; Cox et al. 2006). Naval sonar, the number one public enemy of environmental activists, use low frequencies between 3 and 10kHz and long pulse duration (>1 sec). This set of characteristics can be detrimental for cetaceans and may be a direct cause of death (Miller et al. 2000; Parson et al. 2000; Frantzis 1998). On the other hand civilian ships and fishing vessels use sonars too. By contrast these sonars tend to use shorter pulses (between 1 and 12 milliseconds) and higher frequencies (from 18 to 400 kHz). This may explain why they do not appear to cause beaching of marine mammals and were considered by ad hoc study groups not a direct threat for cetaceans (O'Brien 2004). While navy sonar could be reconfigured to avoid harming whales and dolphins, fisheries sonar could be used, in my opinion, with confidence as an aid in mitigation. My observations (Bernasconi et al. 2011a) showed how none of the whales, which interacted with our research vessels, had neither any immediate nor measurable (strong) avoidance reactions, in spite of the fact that the acoustic suite onboard the vessels were always operating and included transducers generating a maximum source level of 210 dB// μ Pa with a frequencies spanning between 18 and 200 kHz.

From the first sea trial it was clear that high frequency sonars have great limitations if operated horizontally because they offer only a very short detection range (< 400 m) not suitable to fulfill current rules adopted for mitigation. The recognition that temporary or permanent hearing impairment in marine mammals is greatly increased within a few hundred meters of the sound source (Richardson et al. 1995) informed the definition of exclusion or safety zones around the sound source to reduce the chance of causing physical damage to cetaceans. Generally, exclusion zones are defined as the radius where received sound levels are believed to have the potential for at least temporary

hearing impairment (HESS 1999). The safety radius common to the UK, USA and Canadian guidelines and regulations is 500 m, which is deemed to be the distance at which cetaceans may be reliably observed (JNCC 2009). My use of high frequency (110 kHz) was dictated by having in mind that possible disturbance, involving damage to our targets, could be generated. Fishery sonars may have some effect on whales and I recommend to test this through dedicated experiments but, in my experience, natural behavior could be observed without any noticeable interference using such technologies, as shown also in other studies (Nøttestad and Axelsen 1999; Nøttestad and Similä 2001; Nøttestad et al. 2002a and 2002b; Benoit-Bird 2004 and 2009; Bernasconi et al. 2011b).

Subsequently, later in the project, I started to test lower frequencies (20-30 kHz) using a new sonar unit (Simrad SX90) that in the meantime became available on the market; it was clear from the beginning that we found an appropriate instrument to use for whale detections (this work is actually an ongoing project). Considering I have never observed strong avoidance reactions to the vessel presence I believe we should try to use the best resolution, in terms of frequency, to reach the final goal of detecting cetaceans using sonar. This new sonar unit has split beam capabilities in the vertical axis, a characteristic which will help to define exactly the position in space of our target using the contiguous beam signal in the horizontal plane to resolve the uncertainty described in paragraphs 3.6 and 6.3.3 regarding the impossibility of defining the position of our target in the receiving beam.

In chapter 6, I underlined how the data collected at 110 kHz gave lower TS when compared with the data available in the literature (See figure 7.1; Dunn 1969; Love 1973; Miller and Potter 1999; Lucifredi and Stein 2007) and in chapter 7 I reinforced the concept, showing the multi-frequency response of a diving humpback whale detected using a calibrated Simrad EK60 (see paragraph 4.3.1 and 7.3.3), where clearly lower frequencies provided stronger echoes. Compared with the positive dB values reported in other studies (Dunn 1969; Love 1973; Lucifredi and Stein 2007), at a center frequency of 110 kHz fin whale had a resulting average TS for all insonified body aspects of -11.4 dB [95% CI -12.05 -10.8] with a maximum recorded TS of -5.6 dB for a total spread of nearly 14 dB. The average humpback whale TS (n=50) was -10.4 dB [95% CI -9.5 -11.7] with a maximum recorded TS of -4.2 dB and a consistent spread of about 12 dB.

An important aspect to consider while considering the outcome of the TS measurements presented in my work is the understanding of the distribution of the obtained values, which confirm *in situ* the butterfly effect showed by Au (1996). This side aspect dependency (see paragraph 2.4.2) of the energy backscattered is very important in fish (Huse and Ona 1996; Pedersen 2001; Handegard et al. 2009) but when I checked my TS measurements of cetaceans at a fine time scale (ping by ping) I could observe an instantaneous variation trend. To understand why the measured values were fluctuating

this much from one ping to another, because respiration in cetaceans happens at the surface, I could identify and link observable patterns with the typical physiology and morphology of marine mammals. Different behavioral displays can be identified acoustically, and could be used to link in real time sonar data to the presence of whales in proximity of a vessel (Chapter 6).

First among all these displays is the one related to the physiology of air breathing animals. When a whale is swimming at the surface, the variation due to breathing acts influences TS conspicuously. Using a simple prediction model against visual confirmation I could link those breathing acts with actual backscattering energy peaks. The model had a raw correct prediction rate of 66%, sensitivity (correct positive rate) of 83% and specificity (correct negative rate) of 61%. Nonetheless, these model results were encouraging given its simplicity. The identification and inclusion of additional sonar-derived predictors such as observable behavioral related patterns should improve in the near future to make omnidirectional sonar employable for our ultimate goal. With this approach, the observations made by the operator could be the trigger point to start the processing of different evidence of presence or absence of cetaceans in the vicinity of an operational seismic vessel through a quantitative rather than a qualitative method. This result could not be reported previously by others because none of the experiments used a high frequency ping rate (e.g. Lucifredi and Stein used 1 ping every 5 second) or visual observers to confirm that energy peaks were related to the actual whale breathing at the surface (Miller et al. 1999).

I have also been able to confirm the effect of depth on cetacean TS hypothesized by Au (1996) and introduced here in Chapter 6. The TS depth dependency model (Gorska and Ona 2003; Fässler et al. 2009) that I tested works and should be developed properly to detect cetaceans swimming at depth. Deep divers could get possible bends problems in case they attempt fast surfacing if scared by approaching vessels generating very high noise levels (Moore and Early 2003; Jepson et al. 2003). For humpback whales the compression effect generated a TS variation of $\cong 12$ dB when the animal was swimming at 200 m depth underneath the research vessel. Considering that the model worked properly, it is now important to implement it by integrating the above mentioned side aspect dependency presented in 2D in chapter 6 for whales swimming between 0 and 15 m with the sonar pointing horizontally. Once the animal left the surface for a dive, it will be insonified from different angles by the sonar (e.g. not only 90° downwards as usually done with vertical orientated echosounder - see chapter 5 and 7) with subsequent changes in its backscattering cross-section with side aspect effect that will have to be considered in 3D.

A series of important results of my work was the preliminary identification of behavioral patterns observable on the sonar screen and quantifiable using acoustic data. When I was measuring whales TS

at the surface, I could observe qualitatively in real time clearly identifiable patterns on the sonar screen (see paragraph 6.3.4). The observations were confirmed visually and the acoustic data linked with the typical whale ‘footprints’ left on the water surface when these large marine mammals dive (Figure 6.5). Those observations were not representative of sparse single events; they were indeed observed and recognized every time a whale was in sight. I am undertaking a deeper analysis of this phenomenon as I consider it a promising classifier to detect whales swimming at the surface. The physical nature of the footprints, due to the movement of cold water mass from under the surface (Levy et al. 2011) can be well explained by the basic acoustic theory presented in paragraph 2.4.

The starting point of dedicated research efforts, once a whale detector prototype will be available, has to be the choice of target species. Large whales (longer than 7 m) are probably easily detectable by an automated sonar prototype. Most of these whale species are listed as vulnerable or endangered on the IUCN Red List of Threatened Species (IUCN 2010). Guidelines on which species should be protected more and which one less exist, but I believe it is a good start to avoid disturbances and conflicts with the largest and more endangered species (considering their longer life cycles and longer weaning periods). It will be important to integrate the new sonar approach with the actual employed detection techniques (Visual and Pam), while at the same time generate new knowledge about the acoustic characteristics of smaller mammal species (Au 1996; Benoit-Bird and Au 2009; Bernasconi et al. 2011b). Smaller cetacean species are more difficult to detect, but are mostly affected by the same conservation issues as large whales. Despite the knowledge that seismic exploration produces high frequency sound (Goold and Fish 1998), which may affect small cetaceans, with hearing in this range, some guidelines fail to include adequate mitigation measures.

Onboard measures to monitor animals around the airguns are clearly not enough to protect individuals. The detection capability of the employed mitigation methods has theoretical limits both concerning visual and passive listening (Gordon and Tyack 2002; Parsons et al. 2009; Leite-Parente and Araújo 2011). Scheduling surveys around seasonal distributions of species of concern, limiting periods of exposure (by limiting the duration of the survey), and routing airguns to ensure that marine mammals are not driven ashore may be as important as monitoring safety zones in preventing possible injury and death (Bain and Williams, 2006). When seismic exploration concessions are granted, decisions have to be based on knowledge of distribution and habitat use of the species present in the areas of interest. The actual guidelines suggest that surveyors examine existing literature to determine if marine mammals are likely to be present in a region while designing seismic activity but roughly half of the cetacean species, including many of which are known to be sensitive to sound (e.g. beaked whales; Cox et al., 2006), are listed by IUCN as ‘data deficient’. No guidance is

provided about what to do where relevant data do not exist or are inadequate. No recommendations to gather data in a standardized and scientifically valid way are made (Parsons et al. 2009).

The shutting down of airguns is a mitigation measure that should be used on all seismic survey vessels, but there is no obligation under most guidelines to shut down production once an animal or a group of animals approaches the source. Failing to shut down the source when animals have approached within a predetermined distance of the source could be considered intentional disturbance (Parsons et al. 2009). I believe that the presence on board of MMOs hired by the oil companies does not allow any real and concrete application of the mitigation principles prescribed by law. Management agencies generally assume that the oil and gas industry and others using seismic airguns will adhere to seismic guidelines. Such voluntary systems frequently have poor compliance (Rachlinski 1998; Rivera and de Leon 2004; Wiley et al. 2008). A minimum of one trained governmental observer should accompany all seismic surveys in sensitive areas, and periodically in other locations, to oversee and monitor activities. MMO reports should be sent straight to government agency to prevent tampering and removal of data. The presence of Governmental Environmental Officers onboard together with the right technology could lead to a production shut down when it is only absolutely needed due to presence of marine mammals.

At present, considering the laws on the subject of noise pollution generated worldwide by seismic exploration and ship traffic, there are still issues about mitigation procedures (Parsons et al. 2009; Leite-Parente and Araújo 2011). Why do we not develop the whale detector prospected in this thesis? The idea of developing a sonar based cetacean detector has been proposed before, but extended efforts have so far been avoided (Miller and Potter 1999; Knudsen et al. 2007) and money has been invested in developing solutions that cannot be effective because their design did not consider tackling the problem generated by a 24/7 production activity such as seismic exploration (Parsons et al. 2009; Leite-Parente and Araújo 2011). Is it logical to allow seismic shooting but to be conservative in the use of a 20 kHz sonar for mitigation to avoid further noise in the environment? An effective and dedicated whale detection tool could be developed quickly, from existing sonar technologies.

The design of dedicated studies is the way to move forward in the application of sonar technology for cetaceans' conservation purposes to implement the deficiency over mentioned. There is still much information about cetaceans' body reflectivity to gather before reaching the level that the use of active acoustic has in fishery science. It is important at this stage that *ex situ* experiments are undertaken to better develop the basic compression model presented in this thesis. Experiments like the one of Fässler et al. (2009) could be attempted considering small cetaceans to verify the change in backscattering cross section of actual cetaceans' pulmonary structures under pressure. Repeating,

with a more extensive effort, the test performed by Miller and Potter (1999) regarding the acoustic absorption of cetaceans skin and blubber is another prerequisite and this could also be done for bones and other possible important reflective structures, such as a dolphin's melon.

In conjunction with these *ex situ* experiments it will be important to collect data *in situ*. Collecting as much information as possible on different cetacean species TS is important, but at this stage of the research is more important to define classifiers like the one presented in Chapter 6. It is, in my view, premature to talk about species identification, but this is not to exclude in the future the discrimination of targets at species level as done in fishery science (Simmonds and MacLennan 1995). As soon as cetacean body reflectivity will be better understood, an interesting experiment to repeat with modern technologies is that of Watkins et al. (1993). A combined use of tagging and omnidirectional sonar could provide a 3D representation of the reflectivity of a detected target at depth allowing the definition of a detection algorithm for diving cetaceans and the correction of the basic compression model adopted in my work.

I believe the enrollment of active acoustics technologies to detect cetaceans during seismic surveys will provide a more consistent approach into mitigation of such activities on cetaceans. Furthermore, the use of active acoustics could easily be expanded to highly needed behavioral and ecological studies of marine mammals. Multibeam sonars used in fisheries and marine science have some unique advantages compared to other sampling methods; cover large volumes of water, can be operated 24 h a day during variable conditions, have high spatial and temporal resolution and represent no detectable harm to the marine mammals being studied.

REFERENCES:

- Aguayo A, Bernal R, Olavarria C, Vallejos V and Hucker R (1998) Cetacean observations carried out between Valparaiso and Easter Island, Chile, in the winters of 1993, 1994 and 1995. *Rev Biol Mar Oceanogr* 33:101–123
- Anon (1993) SIMRAD BI500 Scientific Post Processing System (The Bergen Integrator). Operator manual. P2237E/P pp?
- Anon (1999) SonarData Echoview (User Guide Echoview V1.51), SonarData Pty Ltd, pp. 46
- Au WWL (1993) The sonar of dolphins. Springer-Verlag, New York, NY pp?
- Au WWL (1996) Acoustic reflectivity of a dolphin. *J Acoust Soc Am* 99:3844–3848
- Au WWL, Popper AN and Fay RR editors (2000). *Hearing by Whales and Dolphins*. Springer Handbook of Auditory Research. Springer-Verlag, New York pp?
- Au WWL, Houser DS and Dankiewicz LA (2007) Acoustic backscatter from a diving dolphin. *J Acoust Soc Am* 121(5):3106
- Axelsen BE, Nøttestad L, Fernö A, Johannessen A, Misund OA (2000) 'Await' in the pelagic: dynamic trade-off between reproduction and survival within a herring school splitting vertically during spawning. *Mar Ecol Prog Ser* 205:259–269
- Axelsen BE, Anker-Nilssen T, Fossum P, Kvamme C And Nøttestad L (2001) Pretty patterns but a simple strategy: predator-prey interactions between juvenile herring and Atlantic puffins observed with multibeam sonar. *Can J Zool* 79:1586–1596
- Axelsen BE, Krakstad JO, Bauleth-D'Almeida G (2004) Aggregation dynamics and behaviour of the Cape horse Mackerel (*Trachurus trachurus capensis*) in the Northern Benguela—implication for acoustic abundance estimation. In: Sumaila UR, Boyer D, Skogen MD, Steinshamn SI (eds) *Namibia's fisheries*. Eburon Academic Publishers, Delft, p 135–164
- Axenrot T, Didrikas T, Danielsson C and Hansson S (2004) Diel Patterns in pelagic fish behavior and distribution from a stationary, bottom-mounted, and upward-facing transducer. *ICES J Mar Sci* 61:1100–1104
- Bain DE and Williams RW (2006) Long range effects of airgun noise on marine mammals: responses as a function of received sound level and distance. In: Paper Presented to the Scientific Committee at the 58th Meeting of the International Whaling Commission, 26 May–6 June 2006, St. Kitts, SC58/E35.
- Balabanian JP, Viola I, Ona E, Patel R and Gröller E (2007) Sonar Explorer: A New Tool for Visualization of Fish Schools from 3D Sonar Data. *Eurographics/IEEE-VGTC Symposium on Visualization*. Norrköping, Sweden.
- Balls R (1948) Herring fishing with the Echometer. *ICES J Mar Sci* 15:193–206
- Balcomb KC III and Claridge DE (2003) A mass stranding of cetaceans caused by naval sonar in the Bahamas. *Bahamas J Sci* 2:2–12
- Bannister JL (1994) Continued increase in humpback whales off Western Australia. Report of the International Whaling Commission 44:309–310.
- Barlow J (1999) Trackline detection probability for long-diving whales. Pages 209–221 in G. W. Garner et al., eds. *Marine mammal survey and assessment methods*. Balkema Press, Netherlands
- Barlow J and Taylor BL (2005) Estimates of sperm whale abundance in the northeastern temperate Pacific from a combined acoustic and visual survey. *Mar Mam Sci* 21: 429–445
- Beale CM and Monaghan P (2004) Behavioral responses to human disturbance. A matter of choice. *Animal Behavior* 68: 1065–1069
- Beale CM (2007) The behavioral ecology of disturbance responses. *Int J Comp Psych* 20: 111–120
- Bearzi G, Politi E and Notarbartolo di Sciarra G (1999) Diurnal behavior of free-ranging bottlenose dolphins in the Kvarneri (northern Adriatic Sea). *Mar Mam Sci* 15: 1065–1097

- Benoit-Bird KJ, Würsig B, McFadden CJ (2004) Dusky dolphin (*Lagenorhynchus obscurus*) foraging in two different habitats: Active Acoustic detection of dolphins and their prey. *Mar Mam Sci* 20(2):215-231
- Benoit-Bird KJ and Au WWL. (2009) Cooperative prey hearing by the pelagic dolphin, *Stenella longirostris*. *J. Acoust. Soc. Am.* 125(1):125-137
- Best PB (1993) Increase rates in several depleted stocks of baleen whales. *ICES Journal of Marine Science* 50:169-186.
- Beyer JE (1995) Functional heterogeneity: using the interrupted Poisson process (IPP) model unit in addressing how food aggregation may affect fish ration. *ICES CM* 1995/ Q: 10, Copenhagen, p 14
- Blackwell SB, McDonald TL, Kim KH, Aerts LAM, Richardson WJ, Greene Jr CR and Streever B (2012) Directionality of bowhead whale calls measured with multiple sensors. *Mar Mam Sci* 28(1):200-212
- Blondel P. (2009). The handbook of sidescan sonar. Jointly published by Springer Science and Praxis Publishing UK pp?
- Bernasconi M, Nøttestad L, Krakstad JO and Axelsen BE (2007) In situ target strength measurements of a small cetacean: Tracking individual dusky dolphins (*Lagenorhynchus obscurus*) in deep water. On CD-ROM 17th SMM Biennial Conference Cape Town, South Africa, December 2007
- Bernasconi M, Patel R, Nøttestad L, Knudsen FR and Brierley AS (2009) Use of active sonar for cetacean conservation and behavioral-ecology studies: a paradox? *Proceedings of the Institute of Acoustics* Vol. 31(1):112-118 Loughborough, UK
- Bernasconi M, Patel R and Nøttestad L (2011a) Behavioral observations of baleen whales in proximity of a modern fishing vessel. *In* Effects of Noise on Aquatic Life. Popper AN and Hawkins A eds Springer Science+Business Media, LLC, New York. pp: 335-338.
- Bernasconi M, Nøttestad L, Axelsen BE and Krakstad JO (2011b) Acoustic observations of dusky dolphins *Lagenorhynchus obscurus* hunting Cape horse mackerel *Trachurus capensis* off Namibia. *Mar Ecol Prog Ser* 429: 209-218
- Berta A and Sumich JL (1999) Respiration, Diving, and Breath-Hold Physiology in Marine Mammals *Evolutionary Biology* edited by Academic Press San Diego (California), pp. 223-254 (234-235)
- Blue JE (1984) Physical calibration. *Rapp P.-v. Reun Cons Int Explor. Mer* 184:19-24
- Boyer DC and Hampton I (2001) An overview of the living marine resources of Namibia. *S Afr J Mar Sci* 23:5–35
- Bowles AE, Smultea M, Würsig B, DeMaster DP and Palka D (1994) The relative abundance and behavior of marine mammals exposed to transmissions from the Heard Island Feasibility Test. *J Acoust Soc Am* 96: 2469-2484
- Branch TA, Matsuoka K and Miyashita T (2004) Evidence for increases in Antarctic blue whales based on Bayesian modelling. *Mar Mam Sci* 20:726–754.
- Breder CM Jr (1954) Equations descriptive of fish schools and other animal aggregations. *Ecology* 35:361–370
- Brehmer P, Lafont T, Georgakarakos S, Josse E, Gerlotto F and Collet C (2006) Omnidirectional multibeam sonar monitoring: applications in fisheries science. *Fish and Fisheries* 7:165-179
- Brownell Jr. RL, Blokhin SA, Burdin AM, Berzin AA, Le Duc RG, Pitman RL and Minakuchi H (1997) Observations on Okhotsk-Korean gray whales on their feeding grounds off Sakhalin Island. *Report of the International Whaling Commission* 47:161-162.
- Carretta JV, Barlow J, Forney KA, Muto MM and Baker J (2001) U.S. Pacific marine mammal stock assessments: 2001. NOAA Technical Memorandum, NOAA-TM-NMFS-SWFSC-317. Pp?
- Churnside J, Ostrovsky L and Veenstra T (2009) Thermal footprints of whales. *Oceanography* 22(1): 206-209.
- CFR (2008) 50 CFR pt. 224. Endangered Fish and Wildlife; Final rule to implement speed restrictions to reduce the threat of ship collisions with North Atlantic Right Whales. *U.S. Federal Register* Vol. 73, No. 198. October 10, 2008/ Rules and Regulations
- Chapman DMF and Ellis DD (1998) The elusive decibel: thoughts on sonar and marine mammals. *Can Acoust* 26(2): 29-31.

- Chen C and Millero FJ (1977) Speed of sound in seawater at high pressure. *J Acoust Soc Am* 84:697-702
- Clark CW and Mangel M (1984) Foraging and flocking strategies: information in an uncertain environment. *Am Nat* 123:626-641
- Clark CW and Gagnon G.C (2006) Considering the temporal and spatial scales of noise exposures from seismic surveys on baleen whales. In: Paper Presented to the Scientific Committee at the 58th Meeting of the International Whaling Commission, 26 May-6 June 2006, St. Kitts, SC58/E9.
- Clapham PJ, Young SB and Brownell Jr. RL (1999) Baleen whales: conservation issues and the status of the most endangered populations. *Mam Rev* 29:35-60.
- Cochrane NA, Li Y and Melvin GD (2003) Quantification of a multibeam sonar for fisheries assessment applications. *J Acoust Soc Am* 114:745-758
- Colladon J D and Sturm J K F (1827) Speed of Sound in Liquids. *Ann. Chim. Phys. Series 2, Part IV*: pp. 236-257.
- Compton R, Goodwin L, Handy R and Abbott V (2008) A critical examination of worldwide guidelines for minimising the disturbance to marine mammals during seismic surveys. *Mar Pol'y* 32:255-262
- Cox TM, Read AJ, Solow A and Tregenza N (2001) Will Harbour porpoises (*Phocoena phocoena*) habituate to pingers? *J Cet Res Man* 3:81-86.
- Cox TM, Read AJ, Swanner D, Urian K and Waples D (2004) Behavioral responses of bottlenose dolphins, *Tursiops truncatus*, to gillnets and acoustic alarms. *Biol Cons* 115:203-212.
- Cox TM, Ragen TJ, Raed AJ, Vos E, Baird RW, Balcomb K, Barlow J, Caldwell J, Cranford T, Crum L, D'Amico A, Spain GD, Fernández A, Finneran J, Gentry R, Gerth W, Gulland F, Hildebrand J, Houser D, Hullar T, Jepson PD, Ketten D, MacLeod CD, Miller P, Moore S, Mountain DC, Palka D, Ponganis P, Rommel S, Rowles T, Taylor B, Tyack PL, Wartzok D, Gisiner R, Mead J and Benner L (2006) Understanding the impacts of anthropogenic sound on beaked whales. *J Cet Res Man* 7(3):177-187
- Craig RE and Forbes ST (1969) A sonar for fish counting. *Fisk Dir Skr Ser Havunders* 15:210-219
- Croll DA, Acevedo-Gutiérrez A, Tershy BR and Urbán-Ramírez J (2001) The diving behavior of blue and fin whales: is dive duration shorter than expected based on oxygen stores? *Comp Biochem Physiol Part A* 129:797-809
- Crum LA and Mao Y (1996) Acoustically enhanced bubble growth at low frequencies and its implications for human diver and marine mammal safety. *J Acoust Soc Am* 99:2898-907
- Del Grosso VA (1974) New equation for the speed of sound in natural waters (with comparison with other equations). *J Acoust Soc Am* 56:1084-1091
- Demer DA (1994) Accuracy and precision of echo integration surveys of Antarctic krill. PhD thesis. Scripps Institution of Oceanography, University of California, San Diego. 144 pp
- Department of Trade and Industry (2002) Strategic Environmental Assessment of Parts of the Central and Southern North Sea SEA 3. <http://www.offshoresea.org.uk/consultations/SEA_3/SEA3_Assessment_Document_Rev1_W.pdf>.
- DeRuiter SL, Tyack P, Lin YT, Newhall AE, Lynch JF, Miller PJO (2006) Modeling acoustic propagation of airgun array pulses recorded on tagged sperm whales (*Physeter macrocephalus*). *J Acoust Soc Am* 120, 4100-4114
- Dragonette LR, Vogt RH, Flax L and Neubauer WG (1974) Acoustic reflection from elastic spheres and rigid spheres and spheroids. II Transient analysis. *J Acoust Soc Am* 55:1130-1137
- Dunn JL (1969) Airborne measurements of the Acoustic Characteristics of a Sperm Whale. *J Acoust Soc Am* 46:1052-1054
- Economist (1998) Quiet, please. Whales navigating. *The Economist* 7th of March 1998 pp. 85
- Edwards JJ and Armstrong F (1983) Measurements of the target strength of live herring and mackerel. *FAO Fish Rep* 300:69-77
- Edwards JJ and Armstrong F (1984) Target strength experiments on caged fish. *Scot Fish Bull* 48:12-20

- Engel MH, Marcondes MCC, Martins CCA, Luna FO, Lima RP and Campos A (2004) Are seismic surveys responsible for cetacean strandings? An unusual mortality of adult Humpback whales on the Abrolhos Bank, northeastern coast of Brazil. 7p., Paper SC/56/E28 presented to Scientific Committee of the 56th International Whaling Commission, Sorento, Italy.
- EPBC Act (2008). Environment Protection and Biodiversity Conservation Act Policy Statement 2.1- Interaction between offshore seismic exploration and whales. Compiled by the Department of the Environment, water, heritage and arts. Canberra, Australia. p. 353
- Evans JT (1995) Pneumatic and similar breakwaters. Proc R Soc London A231:457-466
- Evans PGH, Lewis EJ and Fisher P (1993) A study of the possible effects of seismic testing upon cetaceans in the Irish Sea. 36p., Report from Sea Watch Foundation to Marathon Oil, Oxford, UK.
- Fässler SMM., Fernandes PG, Semple SIK. and Brierley AS (2009) Depth-dependent swimbladder compression in herring *Clupea harengus* observed using magnetic resonance imaging. J Fish Biol 74:296-303
- Finneran JJ, Carder DA, Schlundt CE and Ridgway SH (2005) Temporary threshold shift in bottlenose dolphins (*Tursiops truncatus*) exposed to mid frequency tones J Acoust Soc Am 118:2696-2705
- Foote KG (1990) Spheres for calibrating an eleven-frequency calibrating system. ICES J Mar Sci 46:284-286
- Foote KG (1997) Target strength of fish in Encyclopedia of Acoustics, edited by MJ Crocker. John Wiley & Sons Inc., New York, pp. 493-500
- Foote KG (1982) Optimizing copper spheres for precision calibration of hydroacoustic equipment. J Acoust Soc Am 71:742-747
- Foote KG and MacLennan DN (1984) Comparison of copper and tungsten carbide calibration spheres. J Acoust Soc Am 75:612-616
- Foote KG, Knudsen HP, Vestnes G, MacLennan DN and Simmonds EJ (1987) Calibration of acoustic instruments for fish density estimation: a practical guide. ICES Coop Res Rep 144, 57 pp
- Foote KG (1987) Fish target strengths for use in echo integrator surveys. J Acoust Soc Am 82:981-987
- Foote KG, Knudsen HP, Korneliussen RJ, Nordbø PE, and Røang K (1991) Postprocessing system for echo sounder data. J Acoust Soc Am 90(1):37-47.
- Foote KG, Chu D, Hammar TR, Baldwin KC, Mayer LA, Hufnagle Jr LC and Jech JM (2005) Protocols for calibrating multibeam sonar. J Acoust Soc Am 117: 2013-2027
- Foote KG (2007) Acoustic robustness of two standard spheres for calibrating broadband multibeam sonar. Oceans 2007 IEEE Conference Proceedings, pp. 1-4
- Francois RE and Garrison GR (1982) Sound absorption based on ocean measurements: Part II: Boric acid contribution and equation for total absorption, J Acoust Soc Am 72 (6):1879-1890
- Frankel AS and Clark CW (2002) ATOC and other factors affecting the distribution and abundance of Humpback whales (*Megaptera novaeangliae*) off the north shore of Kauai. Mar Mam Sci 18: 644-662
- Frantz A (1998) Does acoustic testing strand whales? Nature 329: 29
- Gambell R (1999) The International Whaling Commission and the contemporary whaling debate. Pp.179-198 in: Conservation and Management of Marine Mammals (eds. Twiss Jr. JR and Reeves RR). Smithsonian Institution Press, Washington, DC.
- Gerlotto F, Soria M and Fréon P (1999) From two dimension to three: the use of multibeam sonar for a new approach in fisheries acoustics. Can J Fisher Aquat Sci 56:6-12
- Goold JC (1996) Acoustic assessment of populations of common dolphin *Delphinus delphis* in conjunction with seismic surveying. J Mar Bio Ass UK 76(3): 811-820
- Goold JC and Fish PJ (1998) Broadband spectra of seismic survey air-gun emissions, with reference to dolphin auditory thresholds. J Acoust Soc Am 103(4): 2177-2184

- Goold JC and Coates RFW (2006) Near Source, high frequency air-gun signatures. In: Paper Presented to the Scientific Committee at the 58th Meeting of the International Whaling Commission, 26 May–6 June 2006, St. Kitts, SC58/E30.
- Gordon J and Moscrop A (1996) Underwater noise pollution and its significance for whales and dolphins. Pp.281-319 in: *The Conservation of Whales and Dolphins: Science and Practice* (eds. Simmonds MP and Hutchinson JD). Wiley, Chichester, UK.
- Gordon J and Tyack PL (2002) Acoustic techniques for studying cetaceans. In: Evans PGH and Raga JA (Eds.) *Marine Mammals: Biology and Conservation*. Kluwer Academic, New York, pp. 293-324.
- Gordon J, Gillespie D, Potter J, Frantzis A, Simmonds AP, Swift R and Thompson D (2004) A review of the effects of seismic surveys on marine mammals. *Mar Tech Soc J* 37(4): 16-34
- Gorska N and Ona E (2003) Modelling the acoustic effect of swimbladder compression in herring. *ICES J Mar Sci* 60(3): 548-554
- Hafsteinsson MT and Misund OA (1995) Recording the migration behavior of fish schools by multibeam sonar during conventional acoustic surveys. *ICES J Mar Sci* 52: 915-924
- Hall SJ, Wardle CS, MacLennan DN (1986) Predator evasion in a fish school: test of a model for the fountain effect. *Mar Biol* 91:143–148
- Hamilton WD (1971) Geometry of the selfish herd. *J Theor Biol* 31:295–311
- Handegard NO, Pedersen G and Brix O (2009) Estimating tail-beat frequency using split-beam echosounders. *ICES J Mar Sci* 66: 1252-1258
- Harris RE, Miller GW and Richardson WJ (2001) Seal responses to airgun sounds during summer seismic surveys in the Alaskan Beaufort sea. *Mar Mam Sci* 17(4):795-812
- Harwood J (2002) Mitigating the effects of acoustic disturbance in the oceans. *Aquatic Conserv: Mar Freshw Ecosyst* 12: 485-488
- Hastie T, Tibshirani R and Friedman J (2009) *The elements of statistical learning: data mining, interference and prediction* (2nd Edition). Springer Series in Statistics. 746 p
- Hedgepeth JB, Fuhrman D, Cronkite GMW, Xie Y, Mulligan TJ (2000) A tracking transducer for following fish movement in shallow water and at close range. *Aquat Liv Resour* 13:305–311
- Hickling R (1962) Analysis of echoes from a solid elastic sphere in water. *J Acoust Soc Am* 34:1582-1592
- High-Energy Seismic Survey Team (1999) High energy seismic survey review process and interim operational guidelines for marine surveys offshore Southern California. Report for the California State Lands Commission and the United States Minerals Management Service Pacific Outer Continental Shelf Region.
- Hildebrand J (2004) Impacts of anthropogenic sound on cetaceans. IWC Doc. SC/56/E13
- Hildebrand JA (2005) "Impacts of Anthropogenic Sound" in Reynolds et al. (eds), *Marine Mammal Research: Conservation beyond Crisis*. The Johns Hopkins University Press, Baltimore. Maryland. Pages 101-124
- Hjelmervik KT and Sandsmark GH (2008) In ocean evaluation of low frequency active sonar systems. *Proceedings of Acoustic'08 Paris*, pp. 2389-2843
- Hodgson WC (1950) Echosounding and the pelagic fisheries. *Fishery Investigations, Series 2* 17(4) 25 pp
- Hodgson WC and Fridriksson A (1955) Report on echosounding and Asdic for fishing purposes. *Rapp P.-v. Reun Cons Int Explor Mer* 139:1-45
- Hogg CJ, Rogers TL, Shorter A, Barton K, Miller PJO and Nowacek D (2009) Determination of steroid hormones in whale blow: it is possible. *Mar Mamm Sci* 25(3):605-618
- Hooker SK, Baird RW and Fahlman A (2009) Could beaked whales get the bends? Effect of diving behavior and physiology on modeled gas exchange for three species: *Ziphius cavirostris*, *Mesoplodon densirostris* and *Hyperoodon ampullatus*. *Resp Physiol Neurobiol* 167:235-246

- Huse I and Ona E (1996) Tilt angle distribution and swimming speed of overwintering Norwegian spring spawning herring. *ICES J Mar Sci* 53: 863-873
- IBAMA (2007) Marine Biota Monitoring Guide. IBAMA, Brazil, October 2007.
- ICES (2010) Report of the Working Group on Fisheries Acoustic Science and Technology (WGFAST), 27-30 April 2010, San Diego, USA. ICES CM 2010/SSGESST:12 54 pp
- IUCN (2010) IUCN Red List of threatened species. Version 2010.4 <www.iucnredlist.org> Downloaded on 10th of May 2011.
- IWC (1992) Report of the scientific committee. Report of the International Whaling Commission 42: 51-270.
- IWC (2001) Report of the workshop on the comprehensive assessment of right whales: a worldwide comparison. *Journal of Cetacean Research and Management (Special Issue)* 2, 1-60.
- IWC (2007) Report of the standing working group on environmental concerns. *Journal of Cetacean Research and Management* 9 (Suppl.): 227-296.
- Iverson SJ (2002) Blubber. *In* Encyclopedia of Marine Mammals. Edited by Perrin W. F., Wursig B. and Thewissen J. G. M. Academic Press, San Diego, California, USA, pp. 107-112
- IWC (2011) Status of whale populations <<http://iwcoffice.org/>> Downloaded the 20th of May 2011.
- Jefferson TA, Webber MA, Pitman RL (2008) Marine mammals of the world: a comprehensive guide to their identification. Academic Press/Elsevier, London
- Jensen AS and Silber GK (2004) Large whale ship strike database. Tech. Memo. NMFS-OPR-25, US. Dep. Commerce, National Oceanographic and Atmospheric Administration, National Marine Fisheries Service, Silver Spring, MD, USA. January 2004
- Jepson PD, Arbelo M, Deaville R, Patterson IAP, Castro P, Baker JR, Degollada E, Ross HM, Herráez P, Pocknell AM, Rodríguez F, Howie FE, Espinosa A, Reid RJ, Jaber JR, Martin V, Cunningham AA and Fernández A (2003) Gas bubble lesions in stranded cetaceans. Was sonar responsible for a spate of whale deaths after an Atlantic military exercise? *Nature* 425: 575-576
- Jepson PD, Deaville R, Patterson AP, Pocknell AM, Ross HM, Baker JR, Howie FE, Reid RJ, Colloff A and Cunningham AA (2005) Acute and chronic gas bubble lesions in cetaceans stranded in the United Kingdom. *Vet Pat* 42:291-305
- JNCC (2009) ANNEX A - JNCC guidelines for minimizing the risk of disturbance and injury to marine mammals from seismic surveys. Compiled by the Joint Nature Conservation Committee Marine Advice, Aberdeen United Kingdom, 9 pp
- Johannesson KA and Losse GF (1977) Methodology of acoustic estimations of fish abundance in some UNDP/FAO resource survey projects. *Rapp P.-v. Reun Cons Int Explor Mer* 170:269-318
- Jones ML and Swartz SL (2002) Gray whale *Eschrichtius robustus*. Pp.524-536 in: Encyclopedia of Marine Mammals (eds. Perrin WF, Würsig B and Thewissen JGM). Academic Press, San Diego, California
- Johnston DW and Woodley TH (1998) A survey of acoustic harassment device (AHD) use in the Bay of Fundy, NB, Canada. *Aqua Mam* 24:51-61
- Kastak D, Southall BL, Schusterman RJ and Kastak CR (2005) Underwater temporary threshold shift in pinnipeds: effects of noise level and duration. *J Acoust Soc Am* 118: 3154-3163
- Katona SK and Kraus SD (1999) Efforts to conserve the North Atlantic right whale. Pp.311-331 in: Conservation and Management of Marine Mammals (eds. J.R. Twiss, Jr. and R.R. Reeves). Smithsonian Institution Press, Washington, DC.
- Kenney RD, Scott GP, Thompson TJ, Winn HE (1997) Estimates of prey consumption and trophic impacts of cetaceans in the USA northeast continental shelf ecosystem. *J Northwest Atl Fish Sci* 22:155-171

- Knudsen FR, Fosseidengen JE, Oppedal F, Karlsen Ø and Ona E (2004) Hydroacoustic monitoring of fish in sea cages: target strength (TS) measurements on Atlantic salmon (*Salmo salar*). *Fish Res* 69: 205-209
- Knudsen FR, Gammelsæter OB, Kvadsheim PH and Nøttestad L (2007) Evaluation of fisheries sonar's for whale detection in relation to seismic survey operations. JIP report <<http://www.soundandmarinelife.org/Site/Products/SimradProgressReport.pdf>> Downloaded on the 27th of July 2008.
- Knudsen, HP (2009) Long-term evaluation of scientific-echosounder performance. *ICES J Mar Sc* 66: 1335–1340
- Knowlton, AR and SD Kraus. (2001) Mortality and serious injury of northern right whales (*Eubalaena glacialis*) in the western North Atlantic Ocean. *J Cet Res Manag* 2:193-208
- Korneliussen R (1993) Advances in Bergen Echo Integrator, ICES C.M.1993/B:28 (mimeo)
- Korneliussen RJ, Ona E, Eliassen I, Heggelund Y, Patel R, Godø OR, Giertsen C, et al. (2006) The Large Scale Survey System – LSSS. Proceedings of the 29th Scandinavian Symposium on Physical Acoustics; 29 January–1 February 2006; Ustaoset, Norway
- Kraus, SD (1990) Rates and potential causes of mortality in North Atlantic right whales (*Eubalaena glacialis*). *Mar Mamm Sci* 6(4):278-291
- Lafortuna CL, Jahoda M, Azzellino A, Saibene F and Colombini A (2003). Locomotory behavior and respiratory pattern of the Mediterranean fin whale (*Balaenoptera physalus*). *Eur j Appl Physiol* 90: 387-395
- Laist DW, Knowlton AR, Mead JC, Collet AS and Podesta M (2001) Collision between ships and whales. *Mar Mamm Sci* 17(1):35-75
- Leite-Parente C and Araujo ME (2011) Effectiveness of Monitoring Marine Mammals during Marine Seismic Surveys off Northeast Brazil. *Journal of Integrated Coastal Zone Management* 11(4): 409-419
- Levy R, Uminsky D, Park A and Calambokidis J (2011) A theory for the hydrodynamic origin of whale flukeprints. *Int J Non-Linear Mech* 46:616-626.
- Lichte H (1919) On the influence of horizontal temperature layers in sea water on the range of underwater sound signals. *Physik. Z.* 17:385. Translated by A. F. Wittenborn, Tracor Inc., Rockville, Md
- Lo KW and Ferguson BG (2004) "Automatic Detection and Tracking of a Small Surface Watercraft in Shallow Water using a High-Frequency Active Sonar," *IEEE Trans. on Aerospace and Electronic Systems*, Vol. 40, No. 4, pp. 1377-1388, October 2004
- Love RH (1971) Dorsal aspect target strength of individual fish. *J Acoust Soc Am* 49: 816-823
- Love RH (1973) Target strengths of humpback whales *Megaptera novaeangliae*. *J Acoust Soc Am* 54:1312–1315
- Love RH (1978) Resonant acoustic scattering by swimbladder-bearing fish. *J Acoust Soc Am* 64:571-580
- Lucifredi I and Stein P J (2007) Gray whale target strength measurements and the analysis of the backscattered response. *J Acoust Soc Am* 121:1383–1391
- Lucke K, Siebert U, Lepper PA and Blanchet MA (2009) Temporary shift in masked hearing thresholds in a harbor porpoise (*Phocoena phocoena*) after exposure to seismic airgun stimuli. *J Acoust Soc Am* 125(6): 4060-4070
- Løkkeborg S, Ona E, Vold A, Pena H, Salthaug A, Totland B, Øvredal JT, Dalen J and Handegard NO (2010) Effects of seismic survey on fish distribution and catch rates of gillnets and longlines in Vesterålen in summer 2009. *Fisken og Havet* nr. 2/2010
- Mackenzie KV (1981) Nine term equation for speed of sound in the oceans. *J Acoust Soc Am* 70:807-812
- MacLennan DN (1981) The theory of solid spheres as sonar calibration targets. *Scott Fish Res Rep* No 22, 17 pp
- MacLennan DN (1982) Target strength measurements on metal spheres. *Scot Fish Res Rep* No 25, 20 pp
- MacLennan DN and Armstrong F (1984) Tungsten carbide calibration spheres. *Proc Inst Acoust* 6:68-75

- MacLennan DN and Dunn J (1984) Estimation of sound velocities from resonance measurements on tungsten carbide calibration spheres. *J Sound Vib* 97:321-331
- MacLennan DN and Svelling I (1989) Simple calibration technique for the split beam echosounder. *FiskDir Skr Ser Havunders* 18:365-79
- MacLennan DN, Fernandes PG and Dalen J (2002) A consistent approach to definitions and symbols in fisheries acoustics. *ICES J Mar Sci* 59:365-369
- Madsen PT, Møhl B, Nielsen BK and Wahlberg M (2002) Male sperm whale behaviour during exposures to distant seismic survey pulses. *Aqu Mam* 28(3): 231-240
- Madsen PT, Johnson M, Miller PJO., Aguilar Soto N, Lynch J and Tyack PL (2006). Quantitative measures of air-gun pulses recorded on sperm whales (*Physeter macrocephalus*) using acoustic tag during controlled exposure experiments. *J Acoust Soc Am* 120:2366-2379
- Malakoff D (2002) Suit ties whale death to research cruise. *Science* 298(5594): 722-723
- Mayer L, Ly Y and Melvin G (2002) 3D visualization for pelagic fisheries research and assessment. *ICES J Mar Sci* 59: 216-225
- Mate BR, Stafford KM and Ljungblad DK (1994) A change in sperm whale (*Physeter macrocephalus*) distribution correlated to seismic surveys in the Gulf of Mexico. *J Acoust Soc Am* 96(5):3268-3269
- McCauley RD, Fewtrell J, Duncan AJ, Jenner C, Jenner MN, Penrose JD, Prince RIT, Adhitya A, Murdoch J and McCabe K (2000) Marine seismic surveys: a study of environmental implications. *APPEA J* 40: 692-708
- McMullen F and McCarthy E (1998). Acoustic Analysis of SWAC 4 Phase II. NATO unclassified document. SACLANTCEN Bioacoustics Panel. June 15-16, La Spezia (Italy)
- McQuinn IH and Winger PD (2003) Tilt angle and target strength: target tracking of Atlantic cod (*Gadus morhua*) during trawling. *ICES J. Mar. Sci.* 60: 575-583
- Mead JG and Mitchell ED (1984) Atlantic gray whales. Pp.33-53 in: *The Gray Whale Eschrichtius robustus* (eds. M.L. Jones, S.L. Swartz, and S. Leatherwood). Academic Press, Orlando, FL
- Medwin H and Clay CS (1998) *Fundamentals of acoustical oceanography*. Academic Press, San Diego, California
- Miller JH, Potter DC, Weber T and Felix J (1999) The target strength of the northern right whale (*Eubalaena glacialis*). *J Acoust Soc Am* 105: 992
- Miller PJO, Biassoni N, Samuels A and Tyack PL (2000) Whale song lengthened in response to sonar. *Nature* 405:903
- Miller PJO (2002) Mixed-directionality of killer whale stereotyped calls: a direction of movement cue? *Behav Ecol Sociobiol* 52: 262-270
- Miller PJO, Johnson MP, Madsen PT, Biassoni N, Quero M and Tyack PL (2009) Using at-sea experiments to study the effects of airguns on the foraging behavior of sperm whales in the Gulf of Mexico. *Deep-Sea Res I* 56:1168-1181
- Misund OA, Aglen A and Frønæs E (1995) Mapping the shape, size, and density of fish schools by echo intergarion and a high resolution sonar. *ICES J Mar Sci* 52:11-20
- Mitson RB (1995) Underwater noise of research vessels: review and recommendations. *ICES Coop Res Rep* 209. 61 pp.
- MMPA (1972) Marine Mammal Protection Act of 1972. Compiled by the Marine Mammal Commission and updated (2004, 2007) by the NOAA's National Marine Fisheries Service. United States of America. 114 pp
- Moore MJ and Early GA (2004) Cumulative sperm whale bone damages and the bends. *Nature* 306: 2215
- Moore M, Hammar T, Arruda J, Cramer S, Dennison S, Montie EW, Fahlman A (2011) Hyperbaric computed tomographic measurement of lung compression in seals and dolphins. *J Exp Biol* 214: 2390-2397

- Morton AB and Symonds HK (2002) Displacement of *Orcinus orca* (L.) by high amplitude sound in British Columbia, Canada. *ICES J Mar Sci* 59: 71-80.
- Munk W, Worcester P and Wunsch C (1995) *Ocean Acoustic Tomography*. Cambridge University Press, New York, 447 pp
- Møhl B, Wahlberg M, Madsen PT, Miller LA and Surlykke A (2000) Sperm whale clicks: Directionality and source level revisited. *J Acoust Soc Am* 107:638-648
- Møhl B, Wahlberg M, Madsen PT, Miller LA and Surlykke A (2000) Sperm whale clicks: Directionality and source level revisited. *J Acoust Soc Am* 107: 638-648.
- National Geographic Society (1999) *Dolphins: 'the wild side'*. Warner Home Video, Burbank, CA
- Nemes S and Hartel T (2010) Summary measures for binary classification systems in animal ecology. *North-West J Zool* 6 (2): 323-330
- Nishimori Y, Iida K, Furusawa M, Tang Y., Tokuyama K, Nagai S and Nishiyama Y (2009) The development and evaluation of a three-dimensional, echo-integration method for estimating fish-school abundance. *ICES J Mar Sci* 66:1037-1042
- NOAA (2010) Marine mammal stock assessment reports (SARs). < <http://www.nmfs.noaa.gov/pr/sars/>> Downloaded on the 10th of May 2011.
- Nøttestad L and Axelsen BE (1999) Herring schooling manoeuvres in response to killer whale attacks. *Can J Zool* 77:1540-1546
- Nøttestad L and Similä T (2001) Killer whales attacking schooling fish: Why force herring from deep water to the surface? *Mar Mamm Sci* 17:343-352
- Nøttestad L, Fernö A, Mackinson S, Pitcher T and Misund OA (2002a) How whales influence herring school dynamics in a cold-front area of the Norwegian Sea. *ICES J Mar Sci* 59:393-400
- Nøttestad L, Fernö A and Axelsen BE (2002b) Digging in the deep: killer whales' advance hunting tactic. *Polar Biol* 25:939-941
- Nøttestad L and Olsen E (2004) Whales and seals: Top predators in the ecosystem. In: *The Norwegian Sea Ecosystem*. Ed. H. R. Skjoldal. p. 395-434
- Nøttestad L, Brehmer P, Josse E, Doksæter E, Pavan G, Sancho G, Lebourges-Dhaussy A, Georgakarakos S, Aumeeruddy R and Dalen J (2007) Do whales really care about conventional fisheries acoustic? International conference on the Effect of Noise on Aquatic Life. Nyborg, Denmark.
- Nøttestad L, Patel R, Anthonypillai V, Tangen Ø, Henriksen I, Wennevik V, Ellersten B, Erices J, Langøy H, Bernasconi M, Petterson L, Golyak I, Holm M, Gill H, Pena H, Alvarez J, Skjold B, Hansen K, Kristiansen J, Johannessen M, Bente Martinussen M, Løkka G, Mulligan B and Holst JC (2009) Cruise report from the coordinated ecosystem survey and SALSEA salmon project with M/V "Libas" and M/V "Eros" in the Norwegian Sea, 15 July - 6 August 2009. Institute of Marine Research's survey number 2009818 (Libas) and 2009820 (Eros). Bergen, Norway, pp. 12-23
- Nøttestad L, Pena H, Totland A, Gastauer S, Tangen Ø, Anthonypillai V, Petterson L, Patel R and Bernasconi M (2010) Cruise report at the Institute of Marine Research, Norway. Nr.7-2010. ISSN 1503-6294
- Nowacek D, Johnson MP and Tyack PL (2004) North Atlantic right whales (*Eubalaena glacialis*) ignore ships but respond to alerting stimuli. *Proceedings of the Royal Society of London. Series B, Biological Sciences* 271: 227-231
- Nowacek D, Thorne LH, Johnston DW and Tyack PL (2007) Response of cetaceans to anthropogenic noise. *Mammal Rev* 37(2): 81-115
- O'Brien PE (2004) Report on the SCAR ad hoc Group on Marine Acoustic Technology and the Environment Workshop, September 2001. *Polarforschung* 72(2/3): 69
- O'Shea TJ (1999) Environmental contaminants and marine mammals. Pp.485-563 in: *Biology of Marine Mammals* (eds. Reynolds JE and Rommel SA). Smithsonian Institution Press, Washington, DC

- Oliver JS, Slattery PN, Silberstein MA and O'Connors EF (1983) A comparison of gray whale, *Eschrichtius robustus*, feeding in the Bering Sea and Baja California. *Fish Bull* 81: 513-522
- Oliver JS, Slattery PN, Silberstein MA and O'Connors EF (1984) Gray whale feeding on dense ampeliscid amphipod communities near Bamfield, British Columbia. *Can J Zool* 62(1): 41-49
- Olsen E, Budgell WP, Head E, Kleivane L, Nøttestad L, Prieto R et al. (2009) First satellite-tracked long-distance movement of a sei whale (*Balaenoptera borealis*) in the North Atlantic. *Aquat Mamm* 35(3): 313-318
- Olsen K (1971) Influence of vessel noise on the behaviour of herring. In *Modern Fishing Gear of the World*, pp. 291-293. Ed. by H. Kristjonsson. Fishing News Books, London.
- Olsen K (1979) Observed avoidance behaviour in herring in relation to passage of an echosurvey vessel. ICES Document CM 1979/B:18. 21 pp.
- Ona E (1990) Physiological factors causing natural variations in acoustic target strength of fish. *J Mar Biol Ass U.K.* 70: 107-127
- Ona E and Svellingen I (1998) Improved calibration of split-beam echosounders. ICES FAST WG document, La Coruna (Spain), April 1998
- Ona E (2003). An expanded target-strength relationship for herring. *ICES J Mar Sci* 60:493-499
- Ona E, Mazauric V and Noboe Andersen L (2009) Calibration methods for two scientific multibeam system. *ICES J Mar Sci* 66: 1326-1334
- Panigada S, Zanardelli M, Canese S and Jahoda M (1999) How deep can baleen whales dive? *Mar Ecol Prog Ser* 187:309-311
- Parson ECM, Birks I, Evans PGH, Gordon JCD, Shrimpton JH and Pooley S (2000) The possible impacts of military activity on cetaceans in West Scotland. *Europ Res Cet* 14: 185-190
- Parsons ECM and Dolman SJ (2004) Noise as a problem for cetaceans. In Simmonds M, Dolman S, Weilgart L, editors. *Oceans of noise*, A WDCS science report, p. 53-62
- Parsons ECM, Dolman SJ, Jasny M, Rose NA, Simmonds MP and Wright AJ (2009) A critique of the UK's JNCC seismic survey guidelines for minimising acoustic disturbance to marine mammals: Best practise? *Mar Pol Bul* 58(5): 643-651
- Patel R and Ona E (2009) Measuring herring densities with one real and several phantom research vessels. *ICES J Mar Sci* 66:1264-1269
- Patel R, Pedersen G and Ona E (2009) Inferring the acoustic dead-zone volume by splitbeam echo sounder with narrow-beam transducer on a noninertial platform. *J Acoust Soc Am* 125:698-705
- Pearre S Jr (2003) Eat and run? The hunger/satiation hypothesis in vertical migration: history, evidence and consequences. *Biol Rev Camb Philos Soc* 78:1-79
- Pedersen G (2001) Hydroacoustic measurements of swimming speed of North Sea saithe in the field. *J Fish Biol* 58:1073-1085
- Pedersen G., Korneliussen R. J. and Ona E. (2004) The relative frequency response, as derived from individually separated targets on cod, saithe and Norway pout. ICES CM 2004/ R:16, Copenhagen pp?
- Peña HE (2004) In situ target strength measurements of Chilean jack mackerel (*Trachurus symmetricus murphyi*, Nicholas) using a commercial vessel with split-beam echo sounder. MPhil thesis, University of Bergen pp?
- Perrin WF, Würsig B and Thewissen JCM (2002) *Encyclopedia of Marine Mammals*. Academic Press, San Diego CA, 1414 p
- Pierson MO, Wagner JP, Langford V, Birnie P and Tasker ML (1998) Protection from, and mitigation of, the potential effects of seismic exploration on marine mammals. In Tasker ML, Weir C., editors. In: *Proceedings of the seismic and marine mammals workshop*, London 23-25 June.
- Pillar SC and Barrange M (1998) Feeding habits, daily ration and vertical migration of Cape horse mackerel south of South Africa. *S Afr J Mar Sci* 19:263-274

- Pitcher TJ and Parrish JK (1993) Functions of shoaling behavior in teleosts. *In* Pitcher TJ (ed) The behaviour of teleost fishes, 2nd edn. Chapman & Hall, London, p 364–439
- Pitcher TJ and Wyche CJ (1983) Predator avoidance behaviour of sand-eel schools seldom split. In: Noakes DLG, Linquist BG, Helfman GS, Wards JA (eds) Predators and prey in fishes. Dr. W. Junk, The Hague, p 193–204
- Potter JR (1994) ATOC: sound policy or enviro-vandalism? Aspects of a modern media-fueled policy issue. *J Environ Dev* 3(2): 47-62
- Rachlinski JJ (1998) Protecting endangered species without regulating private land owners: the case of endangered plants. *Cornell J L & Pub Pol'y* 8: 1-36
- Reeves RR, Clapham PJ, Brownell Jr. RL and Silber GK (1998) Recovery plan for the blue whale (*Balaenoptera musculus*). Office of Protected Resources, National Marine Fisheries Service, National Oceanic and Atmospheric Administration, Silver Spring, MD.
- Reid DG (2000) Report on echo trace classification. ICES Coop. Res. Rep. 238
- Reijnders PJH, Aguilar A and Donovan GP (1999) Chemical pollutants and cetaceans. *J Cet Res Man* (Special Issue) 1, Cambridge, UK.
- Rendell LE and Gordon JCD (1999) Vocal responses of long-finned pilot whales (*Globicephala melas*) to military sonar in the Ligurian Sea. *Mar Mam Sci* 15: 198-204
- Richardson WJ, Greene CR Jr, Malme CI and Thomson DH editors (1995) Marine Mammals and Noise. Academic Press, USA
- Ridgway SH, Scrone BL and Kanwisher J (1969) Respiration and Deep Diving in the Bottlenose Porpoise. *Science* 166:1651-1654
- Ridgway SH and Harrison RJ (1986) *In* Research on Dolphins. Ed. by MM Bryden and RJ Harrison Oxford University Press p.35-58
- Rivera J and de Leon P (2004) Is greener whiter? Voluntary environmental performance of western ski areas. *Pol'y Stud J* 32: 417-437
- Runnström S (1937) A review of Norwegian herring investigations in recent years. *J Cons Int Explor Mer* 42:123-143
- Scalabrin C, Marfia C and Boucher J (2009) How much fish is hidden in the surface and bottom acoustic blind zones? – ICES *J Mar Sci* 66:1355–1363
- Scantrol(2010)<http://sites.web.123.no/ScantrolAS/marineresearchproductguide.cfm?pArticleId=8945&pArticleCollectionId=447>
- Schevill WE, Watkins WA and Backus RH (1964) The 20-cycle signals and *Balaenoptera* (fin whales). In: Marine Bio-acoustics (ed. W. N. Tavolga), pp 147-152. Pergamon Press, New York
- Skjoldal HR (2004) The Norwegian Ecosystem. Hein Rune Skjoldal Editor. Tapir Academic Press Trondheim pp?
- Shannon LV (1985) The Benguela ecosystem. 1. Evolution of the Benguela, physical features and processes. In: M. Barnes M (ed) Oceanography and marine biology. An annual review, Vol 23. University Press, Aberdeen, p 105–182
- Shannon LV and Nelson G (1996) The Benguela: large scale features and processes and system variability. In: Wefer G, Berger WH, Siedler G, Webb DJ (eds) The South Atlantic: present and past circulation. Springer-Verlag, Berlin p 163–210
- Shannon LV and O'Toole MJ (2003) Sustainability of the Benguela: ex Africa simper aliquid novi. In: Hempel G, Sherman K (eds) Large marine ecosystems of the world trends in exploitation, protection and research. Elsevier, Amsterdam, p 227–253
- Shapiro AD, Tyack PL and Solow AR (2006) Analysis of sperm whale orientation response to controlled exposure of sonar. Abstract, 20th annual conference of the European Cetacean Society, Gdynia, Poland.
- Sigurjónsson J and Gunnlaugsson T (1990) Recent trends in abundance of blue (*Balaenoptera musculus*) and humpback whales (*Megaptera novaeangliae*) off west and southwest Iceland, with a note on occurrence of other cetacean species. Report of the International Whaling Commission 40: 537-551.
- Similä T (1997) Sonar observations of killer whales (*Orcinus orca*) feeding on herring schools. *Aquat Mamm* 23: 119-126

- Similä T and Ugarte F (1993) Surface and underwater observations of cooperatively feeding killer whales in northern Norway. *Can J Zool* 71:1494–1499
- Simmonds EJ (1984) A comparison between measured and theoretical equivalent beam angles for seven similar transducers. *J Sound Vib.* 97:117-128
- Simmonds EJ, Petrie IB, Armstrong F and Copland PJ (1984) High precision calibration of a vertical sounder system for use in fish stock estimation. *Proc Inst Acoust* 6:129-138
- Simmonds EJ (1990) Very accurate calibration of vertical echosounders, a five-year assessment of performance and accuracy. *Rapp P.-v. Reun Cons Int Explor Mer* 189: 183-191
- Simmonds EJ and MacLennan DN (2005) *Fisheries Acoustics: theory and practice* (second edition) Blackwell Science Ltd, Oxford UK
- Simmonds M and Lopez-Jurado LF (1991) Whales and the military. *Nature* 337: 448
- Smith TD, Allen J, Clapham PJ, Hammond PS, Katona S, Larsen F, Lien J, Mattila D, Palsbøll PJ, Sigurjónsson J, Stevick PT and Øien N (1999) An ocean-basin-wide mark-recapture study of the North Atlantic humpback whale (*Megaptera novaeangliae*) *Mar Mam Sci* 15: 1-32.
- Southall B, Bowles AE, Ellison WT, Finneran JJ, Gentry RL, Greene Jr CR, Kastak D, Ketten DR, Miller JH, Nachtigall PE, Richardson WJ, Thomas JA and Tyack PL (2008) Structure of the noise exposure criteria. *Aquatic Mammals* 33 (4): 427-436
- Stafford KM, Moore SE and CG Fox. (2005). Diel variation in blue whale calls recorded in the eastern tropical Pacific. *Anim Behav* 69: 951–958
- Stone CJ (2003) The Effects of Seismic Activities on Marine Mammals in UK Waters 1998–2000. JNCC Report 323, Joint Nature Conservation Committee, Peterborough.
- Stone CJ and Tasker ML (2006) The effects of seismic airguns on cetaceans in UK waters. *J Cet Res Manag* 8: 255-263
- Sumich JL, Dudley G and Morrissey JF (2008) *Laboratory and Field Investigations in Marine Life* (9th Edition): Chapter 6. Jones & Bartlett Publishers, 2008
- Sund O (1935) Echo sounding in fishery research. *Nature* 135: 953
- Taylor GI (1995) The action of a surface current used as a breakwater. *Proc R Soc London A* 231:466-478
- Thompson WB, Vertinsky I and Krebs JR (1974) The survival value of flocking in birds: a simulation model. *J Anim Ecol* 43:785–820
- Totland A, Johansen GO, Godø OR, Ona E and Torkelsen T (2009) Quantifying and reducing the surface blind zone and the seabed dead zone using new technology. – *ICES Journal of Marine Science*, 66: 1370-1376
- Tucker DG and Gazey BK (1966) *Applied Underwater Acoustics*. Pergamon Press, London
- Tyack PL, Johnson MP, Aguilar de Soto N, Sturlese A and Madsen PT (2006b) Extreme diving behavior of beaked whale species known to strand in conjunction with use of military sonars. *J Exp Biol* 209:4238-4253
- Tyack PL, Zimmer WM, Moretti D, Southall BL, Claridge DE, Durban JW, Clark CW, D'Amico A, DiMarzio N, Jarvis S, McCarthy E, Morrissey R, Ward J and Boyd IL (2011) Beaked whales respond to simulated and actual navy sonar. *PLoS One*. 14 6(3):e17009
- UN.org (2009) Ocean and Law of the Sea. < <http://www.un.org/Depts/los/index.htm> > Downloaded the 10th of January 2010 from www.un.org
- Urick RJ (1983) *Principles of underwater Sound* (Third Edition). Peninsula Publishing. Los Altos CA, USA
- Vabø R and Nøttestad L (1997) An individual based model of fish school reactions: predicting antipredator behaviour as observed in nature. *Fish Oceanogr* 6:155–171
- Van Waerebeek K and Würsig B (2009) Dusky dolphin (*Lagenorhynchus obscurus*). In: Perrin WF, Würsig BG, Thewissen JGM (eds) *Encyclopedia of marine mammals*, 2nd edn. Academic Press, San Diego, CA, p 335–338

- Vaughn RL, Shelton DE, Timm LL, Watson LA, Würsig B (2007) Dusky dolphin (*Lagenorhynchus obscurus*) feeding tactics and multi-species associations. *NZ J Mar Freshw Res* 41:391–400
- Vaughn RL, Würsig B and Packard J (2010) Dolphin prey herding: prey ball mobility relative to dolphin group and prey ball sizes, multispecies associates, and feeding duration. *Mar Mamm Sci* 26:213–225
- Vaz Velho F, Axelsen BE, Barros P and Bauleth-D’Almeida G (2006) Identification of acoustic targets off Angola using General Discriminant Analysis. *Afr J Mar Sci* 28:525–533
- Vaz Velho F, Barros P and Axelsen BE (2010) Day–night differences in Cunene horse mackerel (*Trachurus trecae*) acoustic relative densities off Angola. *ICES J Mar Sci* 67: 1004-1009
- Venegas JG, Scott Harris R and Simon B (1998) A comprehensive equation for the pulmonary pressure-volume curve. *J Appl Physiol* 84:389-395
- Wakefield ED (2001) The vocal behaviour and distribution of the short-beaked common dolphin *Delphinus delphis* L. (1785) in the Celtic Sea and adjacent waters, with particular reference to the effects of seismic surveying. MSc Thesis. School of Ocean Sciences, University of Wales, Bangor, UK.
- Watkins WA and Schevill WE (1975) Sperm whales (*Physeter catodon*) react to pingers. *Deep Sea Res* 22: 123-129.
- Watkins WA, Moore KE and Tyack PL (1985) Investigations of sperm whale acoustic behaviors in the southeast Caribbean. *Cetology* 49: 1-15.
- Watkins WA, Daher MA, Fristrup KM, Howald TJ and Notarbartolo di Sciara G (1993) Sperm whale tagged with transponders and tracked underwater by sonar. *J Acoust Soc Am* 94(1): 55-67
- Watwood SL, Miller PJ, Johnson M, Madsen PT and Tyack PL (2006) Deep-diving foraging behaviour of sperm whales (*Physeter macrocephalus*). *J Anim Ecol* 75(3):814-25
- Wartzok D, Popper A, Gordon J and Merrill J (2003) Factors affecting the responses of marine mammals to acoustic disturbance. *Mar Tech Soc J* 37(4): 6–15
- Wartzok D (2008) “Breathing” in *Encyclopedia of Marine Mammals* (2nd edition, Academic Press), pp 152-156
- Weaver W (1964) Max Mason 1877-1961. Biographical Memoir, National Academy of Science, Washington D. C.
- Weilgart L and Whitehead H (2004) The threat of underwater noise on whales: management in light of scientific limitation. *Polarforschung* 72: 99-101
- Weir CR and Dolman SJ (2007) Comparative review of the regional marine mammal mitigation guidelines implemented during industrial seismic surveys, and guidance towards a worldwide standard. *J Int Wildl Law Policy* 10: 1–27
- Weller DW, Burdin AM, Würsig B, Taylor BL and Brownell Jr. RL (2002) The western gray whale: a review of past exploitation, current status and potential threats. *J Cet Res Man* 4:7-12
- Wells RS, Boness DJG, Rathbun B (1999) Behavior. In: Reynolds JE III, Rommel SA (eds) *Biology of marine mammals*. Smithsonian Institution Press, Washington DC, p 324–422
- Welsby VG and Hudson JE (1972) Standard small targets for calibrating underwater sonars. *J Sound Vib* 20:399-406
- Wier CR (2008) Short-Finned pilot whales (*Globicephala macrorhynchus*) respond to an airgun ramp-up procedure off Gabon. *Aquatic Mammals* 34: 349–354
- Wiggins SM, Oleson EM, McDonald MA and Hildebrand JA (2005) Blue whale (*Balaenoptera musculus*) diel call patterns offshore of Southern California. *Aquat Mamm* 31: 161–168
- Wiley DN, Moller JC, Pace RM and Carlson C (2008) Effectiveness of voluntary conservation agreements: case study of endangered whales and commercial whale watching. *Cons Bio* 22: 451-457

- Williams TM, Haun JE, Friedl WA (1999) The diving physiology of bottlenose dolphins (*Tursiops truncatus*) I. Balancing the demands of exercise for energy conservation at depth. *J Exp Biol* 202:2739–2748
- Wood AB, Smith FD and McGeachy JA (1935) A magnetostriction echo-depth recorder. *J Inst Elect Eng* 76:550-567
- Wright, AJ, Aguilar Soto N, Baldwin AL, Bateson M, Beale C, Clark C, Deak T, Edwards EF, Fernández A, Godinho A, Hatch L, Kakuschke A, Lusseau D, Martineau D, Romero LM, Weilgart L, Wintle B, Notarbartolo di Sciara G, Martin V (2007a) Anthropogenic noise as a stressor in animals: a multidisciplinary perspective. *Int J Comp Psych* 20: 250–273
- Wright JW, Aguilar-Soto N, Baldwin AL, Bateson M, Beale CM, Clark C, Deak T, Edwards EF, Fernandez A, Godinho A, Hatch LT, Kakuschke A, Lusseau D, Martineau D, Romero LM, Weilgart LS, Wintle BA, Notarbartolo di Sciara G and Martin V (2007b) Do marine mammals experience stress related to anthropogenic noise? *Int J Comp Psy* 20: 274-316.
- Würsig B (1982) Radio tracking dusky porpoises in the South Atlantic. In: *Mammals in the seas, Vol 4: small cetaceans, seals, sirenians and otters*. FAO Adv Comm Experts Mar Resour Res, Rome, p 145–160
- Würsig B and Würsig M (1980) Behaviour and ecology of the Dusky dolphin, *Lagenorhynchus obscurus*, in the South Atlantic. *Fish Bull* 77:871–890
- Würsig B, Reeves RR and Ortega-Ortiz JG (2001) Global climate change and marine mammals. Pp. 589-608 in: *Marine Mammals: Biology and Conservation* (eds. P.G.H. Evans and J.A.Raga). Kluwer Academic/Plenum Publishers, New York
- Würsig B and Richardson WJ (2002) Effects of noise. Pp.794-802 in: *Encyclopedia of Marine Mammals* (eds. Perrin WF, Würsig B and Thewissen JCM). Academic Press, San Diego, California
- Zeh JE, Clark CW, George JC, Withrow D, Carroll GM and Koski WR (1993) Current population size and dynamics. Pp.409-489 in: *The Bowhead Whale* (eds. Burns JJ, Montague JJ and Cowles CJ). Society for Marine Mammalogy, Special Publication No. 2, Allen Press, Lawrence, Kansas
- Zimmer WM, Harwood J, Tyack PL, Johnson MP and Madsen PT (2008) Passive acoustic detection of deep-diving beaked whales. *J Acoust Soc Am* 124(5): 2823-2832

LIST OF SYMBOLS:

c	Sound speed in water
f	Frequency (cycles for second)
λ	Wavelength, distance between successive peaks of a sound wave
T	Period, time between two peaks in a sound wave
τ	Pulse duration
n	Number of samples
I	Intensity of a sound wave (power transmitted per unit area)
p	Pressure
ρ	Water density
R	Resistor value (ohm)
P	Power
U	Voltage
Z	Acoustic impedance of a medium, equal to the density times the sound speed
P_1	Reference power of 1 Watt
P_2	All measured powers
U_1	Reference voltage of 1 Volt
U_2	All measured voltages
I_1	Reference intensity of e.g. dB//1 η Pa
I_2	All processed intensities ref to a pressure (e.g. in water 1 η Pa)
r	radius of a sphere (check better about r_2 and r_1) MAYBE just write range!
r_1	Reference radius (range) set at a distance of 1 meter
α	Acoustic absorption coefficient in dB per unit distance
TL	Transmission loss
TL_s	Geometrical spreading
A	Fraction of acoustic intensity absorbed by the water and converted to heat
TL_a	Absorption loss
β	Beamwidth
L	length

ψ	Equivalent beam angle of a transducer in steradians
b	The beam pattern; function of direction describing the amplitude sensitivity
θ, φ	Angular coordinates of the scattering direction relative to the incident wave
t	Time
t_e	Time between the transmitter pulse and the echo being recieved
R	Range or distance
Z_w	Acoustic impedance of the water
Z_r	Acoustic impedance of the reflector
r_b	Reflection coefficient; proportion of incident energy reflected at a boundary
σ_{bs}	Backscattering cross-section
I_i	Intensity of the incident wave
I_{bs}	Intensity of the backscattered wave
TS	Target strength
S_v	Volume backscattering coefficient (linear measure)
S_v	Volume backscattering strength (log measure, in dB//1m ⁻¹)
V_0	Sample volume
s_A	Nautical area scattering coefficient (NASC)
s_a	Area scattering coefficient (units m ² /m ²)
EL	Received echo level
SL	Source level
TVG	Time-varied-gain
a	Radius of a sphere, or the side of a square (refer to transducers dimensions)
R_b	Range at the boundary between the near and far fields
R_{opt}	Optimum distance between the transducer and the standard target
d	Linear size of the transducer face
f_0	Frequency of the sonar
$A(t)$	Actual TVG function of the sonar (t , time after the start of the transmitted pulse)
$a_o(t)$	Exact Time-varied-gain (TVG) function at long range
ω	Angular frequency (radians per second)
β	Acoustic absorption coefficient in nepers (1 Np=8.686 dB)
ρ_v	Fish density (fish/m ³)

$\langle \sigma_{bs} \rangle$	Mean backscattering cross-section per fish
C	Echo-integrator calibration gain factor
σ_0	Backscattering cross-section at 0 meter depth
σ_z	Backscattering cross-section at z meters depth
γ	Estimated contraction-rate parameter of a free spherical balloon

APPENDIX A

This appendix summarizes how, in practice, omnidirectional sonar raw data were processed and how received signals from semi-submerged large targets (in our case a whale) moving/swimming at the water surface or in shallow waters (no deeper than 15 m) can be quantified.

```
% SIMRAD SH80 DATA PROCESSING - FROM CALIBRATION TO TS MEASUREMENTS
% written by Matteo Bernasconi (Bergen, 06-07-2010)
% the codes presented here are a first attempt to quantify the scientific output of a Simrad
% SH80 omnidirectional fishery sonar. The following scripts represent the practical way used
% between 2007 and 2010 to process the sonar data presented in the PhD thesis title: The use of
% active sonar to study cetaceans. If you want to use these Matlab codes for your research,
% please contact the author (matteo@imr.no) for permission. No acknowledges are required through
% your published science or reports but possible collaborations to develop the codes and make
% sonar data processing faster would be appreciated. I am actually developing the basic codes
% presented here to implement the possibility of a real time reading of the data for calibration
% purposes through a GUI interface. When you are reading this I maybe just have what you need
% for your research...
Have a fair sea

MATTEO BERNASCONI
ECOSYSTEM PROCESSES
Institute of Marine Research,
Bergen (NORWAY)
```

Before processing the Simrad SH80 raw data (.dat file) and start the analysis, it is very important to organize the data chronologically and, if necessary, to divide them into representative portions of different experiments. E.g. it is convenient to record video sequences of different activities as a reference and organize data clusters for subsequent analysis. Once the data are ready, their binary format can be converted into .csv files using the software Sonar Data Converter (provided by the sonar manufacturer). The first code presented here (Conversion I) gives the command to start the data conversion process defining the data directory source, the data destination directory and the prefix name to add to the timestamp name of a single ping raw data. The ensuing code (Conversion II) is a Matlab function that classifies all the sonar settings, time and signals recorded corresponding to a single ping. The result of this first data processing is the transformation of the raw data in manageable .m files ready to be processed through the sonar equation (paragraph 2.5). The 2 step conversion flow from binary to m. files can be summarized as follow:

$$175218 - 644.dat > \begin{matrix} 175218 - 644 - beam.csv \\ 175218 - 644 - hdr.csv \end{matrix} > Bm54 - 175218644.m$$

This is an important part of the data conversion because it merges two .csv files into a single .m file ready to be analyzed.

CONVERSION I

```
% LOAD SH80 SONAR DATA
% Written by Matteo Bernasconi and Ruben Patel. Bergen, February 2008.

clear all
close all
thdrFname=dir('C:\Sonardata\Calibration\SH80\Beam54\*hdr.*');
tbeamFname=dir('C:\Sonardata\Calibration\SH80\Beam54\*beam.*');
destDir='C:\Survey2009\Cal_SH80\';
i=1;
```



```

sonarData.ZoomDesimation=data(i);i=i+1;
sonarData.Stabilize=data(i);i=i+1;
sonarData.Normalization=data(i);i=i+1;
sonarData.SpeedAlongShip=data(i);i=i+1;
sonarData.SpeedAthwartShip=data(i);i=i+1;
sonarData.SignalProcessing=data(i);i=i+1;
sonarData.TxCentreFrequency=data(i);i=i+1;
sonarData.Bandwith=data(i);i=i+1;
sonarData.PgaGain=data(i);i=i+1;
sonarData.VcaGain=data(i);i=i+1;
sonarData.NoOfTxBeams=data(i);i=i+1;
sonarData.NoOfStavesInTxBeam=data(i);i=i+1;
sonarData.NoOfRxBeams=data(i);i=i+1;
sonarData.NoOfStavesInRxBeam=data(i);i=i+1;
sonarData.TestSignal=data(i);i=i+1;
sonarData.TxElements=data(i);i=i+1;
sonarData.Spare0=data(i);i=i+1;
sonarData.Spare1=data(i);i=i+1;
sonarData.Spare2=data(i);i=i+1;
sonarData.Spare3=data(i);i=i+1;
sonarData.OwnShipLatPos=data(i);i=i+1;
sonarData.OwnShipLonPos=data(i);i=i+1;
sonarData.OwnShipSpeedAlong=data(i);i=i+1;
sonarData.OwnShipSpeedAthwart=data(i);i=i+1;
fclose(fid);

M=dlmread(bfname, ';', 1, 0);
sonarData.ping.time=M(:,1);
sonarData.ping.data=M(:,2:end);

```

```
I=sonarData;
```

While measuring whale TS can be complicated due to the unpredictable swimming behavior of the animal, a good way to understand how the omnidirectional sonar data process works is through the use of a standard target. To do so, here I explain the passages I went through in most of the calibration tests I had (see paragraph 3.6). It is good practice to record sonar screen videos for the entire duration of the experiments and note down when the standard target is moved from one beam to another or when other tests are performed (Figures 3.8 and 3.10b). For each beam (see paragraph 3.6) data sets were organized in folders with post processing purposes aimed at defining Calibration gain factors and performing the TS experiments described in Chapters 6 and 7.

To obtain the gain correction and proceed using the sonar in the field, 3 different steps are requested:

- I. Check if the target is positioned clearly on axis. This is done by checking, for a finite number of pings (≈ 10) chosen randomly in the data set, the plots of three contiguous beams (see figure A.1) and verifying if clearly the central one gave a conspicuous signal peak when compared with the signal received from the other two beams.
- II. Extract a data matrix of the beam selected through the previous check defining: the received echo level (EL) and the exact range of the target for subsequent statistical analysis. This matrix contains for each ping the following information: sonar center frequency, uncalibrated TS, received Echo Level, transmission power, pulse duration, sonar tilt angle, ping time and target range.
- III. Process the data obtained describing the basic statistics need to obtain the calibration gain factor.

STEP I

```

% BEAM CHECK
% written by Matteo Bernasconi (Bergen, 12/11/2008) updated (Bergen, 24/11/2009)

```

```

% this script plot single pings and is aimed to give the operator the knowledge of which of
three contiguous beam has the standard target on axis or if the target is in between

close all
clear all

mdir=input('Data directory:', 's'); % E.g. C:\Survey2009\Cal_SH80\Beam55\
Ping=input('Ping:', 's'); % E.g. B55_215920_984
load([mdir Ping]);

if I.SectorType~=0
    continue
end

warning off
i = [1:length(I.ping.time)];
lRange = ((I.ping.time(i,1)-I.ping.time(1,1))*1505.4)/2;
MBRange= repmat(lRange,1,64); clear Range;
findex=((I.TxCentreFrequency-110000)/1000)+1;
dB1Correction= [-204.8 -204.8 -204.8 -204.8 -204.8 -204.9 -205.2 -205.5 -205.8 -206.1 -206.4];
SIMRAD=dB1Correction(findex);
dB1=10*log10(I.ping.data/1000000)-SIMRAD; clear Bbeam;
TVG=(40)*log10(MBRange)+(2*0.0353*(MBRange));
TSunc=dB1-210+TVG; clear TVG;

[h l]=size(MBRange); clear l
RangeScale=linspace(MBRange(1:1),MBRange(h:h),10);
RangeScale=(RangeScale)';
MatScale=linspace(0,h,10); clear h
MatScale=(MatScale)';
format bank

% Range_legend=[RangeScale MatScale]

R1=35; R2=135;
% every ship has its own calibration range: 35 and 135 is the acoustic sampling range
corresponding respectively to 5 and 20 meters)

B1=input('Beam:');
B2=B1-1;
B3=B1+1;

Bnum1=[B1]; Bnum1=num2str(Bnum1); s1=['Beam ' Bnum1];
Bnum2=[B2]; Bnum2=num2str(Bnum2); s2=['Beam ' Bnum2];
Bnum3=[B3]; Bnum3=num2str(Bnum3); s3=['Beam ' Bnum3];

% a plot (Figure A.1) is generated to verify qualitatively and quantitatively the on/off axis
position of the standard target
scrsz = get(0, 'ScreenSize');
figure('Position',[50 50 400 650]); whitebg('w')

H=subplot(3,1,1); plot(MBRange(R1:R2,1:1),TSunc(R1:R2,B2:B2), 'b')
set(H, 'FontName', 'Courier New', 'FontSize', 10)
axis([5 18 -80 -30])
title('CALIBRATION CHECK', 'FontName', 'Courier New', 'FontSize', 14, 'FontWeight', 'Bold')
text(11, -40, s2)

H=subplot(3,1,2); plot(MBRange(R1:R2,1:1),TSunc(R1:R2,B1:B1), 'b') % axis ([Xmin Xmax Ymin
Ymax]);
set(H, 'FontName', 'Courier New', 'FontSize', 10)
axis([5 18 -80 -30])
ylabel('TS (dB)', 'FontWeight', 'Bold')
text(11, -40, s1)

H=subplot(3,1,3); plot(MBRange(R1:R2,1:1),TSunc(R1:R2,B3:B3), 'b')
axis([5 18 -80 -30])
set(H, 'FontName', 'Courier New', 'FontSize', 10)
xlabel('Distance (m)', 'FontWeight', 'Bold')
text(11, -40, s3)

% EXTRACTION OF TS PEAK VALUE
TSPeak=max(max(TSunc(R1:R2,B2:B3)))

```

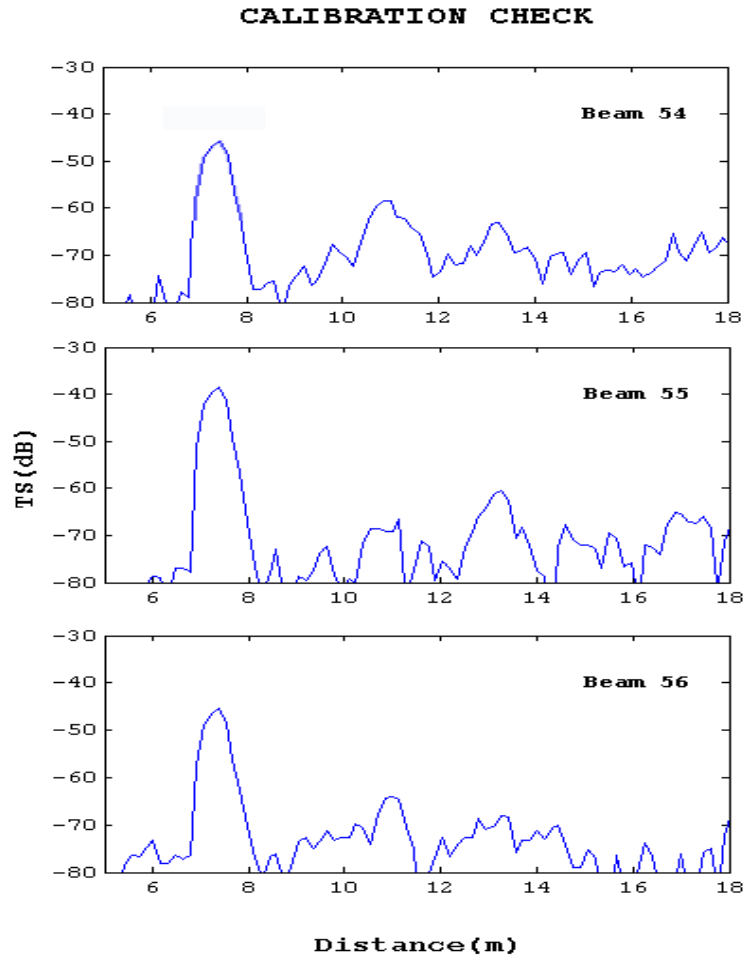


Figure A.1: Result of an on/off axis check used during the pre-scrutinization of the data from a calibration experiment like the one described in paragraph 3.6

STEP II

```
% EXTRACT CALIBRATION MATRIX
% written by Matteo Bernasconi (onboard Eros August 2008)
clear all
close all % dont do this if u want to visualize the signal during the data extraction

mdir=input('Data directory:','s'); % e.g. C:\Survey2009\Cal_SH80\Beam55\
mdirbis=[mdir '*mat.*'];
Fname=input('Name the processed data file:','s'); %I named the .txt file that will be save
after data processing e.g. B55_data
Fname=num2str(Fname); Fname=[Fname '.txt']; Fname=[Fname '.mat'];
fid=fopen(Fname,'a+');
j=1;
files = dir([mdir '*mat*']);
B=input('Beam to calibrate:');
D=dir(mdirbis);
[h l]=size(D); clear l; clear D;

for f=1:h
disp(files(f).name)
load([mdir files(f).name]);

    if I.SectorType~=0
        continue;
    end
%% SIGNAL PROCESSING THROUGH SONAR EQUATION
i =[1:length(I.ping.time)];
lRange =((I.ping.time(i,1)-I.ping.time(1,1))*1501)/2;
MRange= repmat(lRange,1,64);clear lRange;
```

```

findex=((I.TxCentreFrequency-110000)/1000)+1;
dBLCorrection= [-204.8 -204.8 -204.8 -204.8 -204.8 -204.9 -205.2 -205.5 -205.8 -206.1 -206.4];
SIMRAD=dBLCorrection(findex);
warning off
dB1=10*log10(I.ping.data/1000000)-SIMRAD;clear Bbeam;
TVG=40*log10(MBRange)+(2*0.0357*(MBRange)); % m * dB/km = m * dB/(1000 *m)
TSunc=dB1-210+TVG;clear TVG;
warning on

Calib= dB1(40:100,B:B); % The calibration range is fix (it changes depending on the ship and
the sonar transducer position); the beam (B), which signal will be extract, has been
previously defined.
UnCalibTS=TSunc(40:100,B:B);
MBRange=MBRange(40:100,B:B);

CalibrationPEAK=max(max(Calib)); %find calibration dB1 peak in the matrix
UnCalibratedPEAK=max(max(UnCalibTS)); %find calibration TS peak in the matrix

X=find(Calib==CalibrationPEAK)
Range=MBRange(X,:);
Range=Range(1:1); % avoid data processing block due to pings failure

plot(MBRange,UnCalibTS);
whitebg('w')
axis([6 14 -90 -30])
pause(0.08)

format short g; Calibration(j,:)= [I.TxCentreFrequency UnCalibratedPEAK CalibrationPEAK
I.TxPower I.PulseLength I.Tilt I.ping.time(1:1) Range];
j=j+1;

% I print on file the calibration data results processed through the sonar equation for
subsequent statistical analysis
fprintf(fid,'%3.3e %-3.3f %-3.3f %1.4f %1.4f %-1.5f %-3.15f %-3.3f \r\n',I.TxCentreFrequency,
UnCalibratedPEAK, CalibrationPEAK, I.TxPower, I.PulseLength, I.Tilt, I.ping.time(1:1), Range);
end
fclose(fid)
save(Fnamem)

```

STEP III

```

% GAIN COMPENSATION
% written by Matteo Bernasconi 12/06/2009 (St Andrews, UK)
% this script performs a basic statistic analysis of the data extracted in step II. The re-
sults consist of two files (.m and.txt) which output is: Pulse Duration, Average distance of
the target, Average EL of the target and 95% Confidence interval of the measurements.

clear all
close all

mdir=input('Data directory:','s'); % specify the directory where is the file to analyze
Beam=input('Beam:','s'); % data file to analyze e.g. 'B55EL' (generated in step II)
load([mdir Beam]);

fid=fopen('CALIBRATION_CORRECTIONS.txt','a+');
[A AA]=size (Calibration);
Cal=Calibration(1:A,:);

% At this point we define the pulse duration (corresponding to a range setting on the sonar)
we calibrated during the experiment and ask to the script to analyze statistically just the
ones of interest. In this case we are calibrating 2 pulse durations: 2.2 ms and 3.8 ms

R300=0.00225; %Range 300 m
R500=0.00375; %Range 500 m

R1=100;
I100=find(Cal(:,5)==R100);
p100=Cal(I100,:);
sigma100=(10.^(p100/10)); % da qui lavoro in lineare
M100= mean (sigma100(:,3));
M100log=10*log10(M100); % qui trasformo la media in dB
SD100=std(sigma100(:,3));
[n n1]=size(I100); clear n1;

```

```

CIm= M100-(1.96*(SD100/sqrt(n)));
CIM= M100+(1.96*(SD100/sqrt(n)));
Mx100=10*log10(CIM); %in questa linea e nella seguente trasformo in dB il mio 95% Confidence
Interval
Mn100=10*log10(CIm);
Dist100=mean (sigma100(:,8)); % qui la media della distanza di standard target

R4=300;
I300=find(Cal(:,5)==R300);
p300=Cal(I300,:);
sigma300=(10.^(p300/10)); % EL is converted into the linear domain for statistical analysis
M300= mean (sigma300(:,3));
M300log=10*log10(M300); % I convert my average in the proper dB unit
SD300=std(sigma300(:,3));
[n n1]=size(I300); clear n1;
CIm= M300-(1.96*(SD300/sqrt(n))); % I calculate in the linear domain the 95% CI
CIM=M300+(1.96*(SD300/sqrt(n)));
Mx300=10*log10(CIM); % This and the next line convert the 95% CI in dB
Mn300=10*log10(CIm);
Dist300=mean (sigma300(:,8)); % here I have the average range of the standard target

R5=500;
I500=find(Cal(:,5)==R500);
p500=Cal(I500,:);
sigma500=(10.^(p500/10));
M500= mean (sigma500(:,3));
M500log=10*log10(M500);
SD500=std(sigma500(:,3));
[n n1]=size(I500); clear n1;
CIm= M500-(1.96*(SD500/sqrt(n)));
CIM=M500+(1.96*(SD500/sqrt(n)));
Mx500=10*log10(CIM);
Mn500=10*log10(CIm);
Dist500=mean (sigma500(:,8));

% I have finally my result save in a .txt and a .m files
format bank
Range_Mean_Confidence=[R4 Dist300 M300log Mn300 Mx300;R5 Dist500 M500log Mn500 Mx500]

RMC=Range_Mean_Confidence';
fprintf(fid,'%3.0f %-2.1f %-2.1f %-2.1f %-2.1f \r\n',RMC(:,4),RMC(:,5));
fclose(fid);

```

The last example provided in this Appendix refers back to paragraph 4.4. The script allows the visualization and measurement of the TS of a target sighted visually and recognizable on the screen. Here I provide and summarise how the ping by ping analysis, presented in Chapter 6 and 7, was performed. This code is an ongoing project and it is still under development. The next step needed, through a GUI, is to make the ping by ping analysis faster and the data managing easier reducing the time consuming effort needed to analyze the data (e.g. a single ping can take up to 5 minutes to be processed correctly).

TS MEASUREMENTS OF TARGET DETECTED *IN SITU*

```

% WHALE TS MEASUREMENTS
% written by Matteo Bernasconi (St Andrews, 28/1/2009)
% with this script is possible to measure the TS of a target identified visually at the sur-
face by an observer considering a single gain compensation (I am actually working on a more
efficient GUI version of this TS measuring tool). The final result obtainable through this
script is the TS of a selected target and the plots of: sonar screen and signal peaks from
defined sonar beams.
It is possible to implement the script to measure at the same time different pulse duration.
If more info about this are needed please contact matteo@imr.no
close all
clear all

mdir=['F:\Whale_sightings_2008\Sgt_023_FNHval\']; % Data has to be organize in folders before
start measuring TS
Ping=input('Ping:','s'); % Enter the ping file name
load([mdir Ping]);

```



```

if I.SectorType~=0 %we are interested just in the omnidirectional data defined by the sonar
as sector type 0
    continue
end

warning off
i = [1:length(I.ping.time)];
lRange = ((I.ping.time(i,1)-I.ping.time(1,1))*1476.56)/2; % sound speed (here 1476.56 m/s)
based on CTD data taken after every sighting
MBRange= repmat(lRange,1,64); clear Range;
findex=((I.TxCentreFrequency-110000)/1000)+1;
dB1Correction= [-204.8 -204.8 -204.8 -204.8 -204.9 -205.2 -205.5 -205.8 -206.1 -206.4];
SIMRAD=dB1Correction(findex);
dB1=10*log10(I.ping.data/1000000)-SIMRAD; clear Bbeam;
TVG=(40)*log10(MBRange)+(2*0.03242*(MBRange)); %calculate the correct alpha with CTD data
TSunc=dB1-210+TVG; clear TVG;
Cor=9.6; % gain correction obtained during the calibration experiment
TS=TSunc+Cor;

% the following command load a color map similar to the original used by Simrad and displayed
on the sonar screen
load('E:\Work\PhD_MBp4Whales_Nov2009\DATA\SonarRAWDATA_Analysis\MATLAB_Whales Detec-
tions\MBp4_Directory\SH80-Scripts\Colormaps\SH80_TEO')

figure ('Position',[900 40 500 500]);

% OMNIDIRECTIONAL BEAM
if I.SectorType==0
TSt=(real(TS))';
[b s]=size(TSt);
n = s-1;
angStep=2*pi/b;
theta=(0:(b))*angStep;
theta=theta+pi/2;
X = (lRange*cos(theta))';
Y = (lRange*sin(theta))';
TSt=[TSt;TSt(1,:)];

% This command plot the gridlines representing fixed range in the sonar view here are present-
ed the pulse duration used in paragraph 3.6 of this thesis
theta=deg2rad(0:365);
hold on
surface(X,Y,TSt,'EdgeColor','none')
whitebg('k')
set(gcf, 'color', 'k');

if I.PulseLength==0.00075
    for i=1:2
        rx1=(50*i*cos(theta));
        ry1=(50*i*sin(theta));
        plot(rx1,ry1,'w:')
    end
elseif I.PulseLength==0.0012
    for i=1:3
        rx1=(50*i*cos(theta));
        ry1=(50*i*sin(theta));
        plot(rx1,ry1,'w:')
    end
elseif I.PulseLength==0.0015
    for i=1:2
        rx1=(100*i*cos(theta));
        ry1=(100*i*sin(theta));
        plot(rx1,ry1,'w:')
    end
elseif I.PulseLength==0.0023
    for i=1:3
        rx1=(100*i*cos(theta));
        ry1=(100*i*sin(theta));
        plot(rx1,ry1,'w:')
    end
elseif I.PulseLength==0.00375
    for i=1:5
        rx1=(100*i*cos(theta));
        ry1=(100*i*sin(theta));
        plot(rx1,ry1,'w:')
    end

```

```

    end
end

axis ('equal')
colormap(SH80_TEO)
colorbar

%% PING INTERROGATION %%

%TS THRESHOLD and PEAKS PLOT
TSts=TS;
Tshold=input('Threshold:');
TSts(TSts<Tshold)=Tshold;
% TSts(TSts<-30)=-30;

[h l]=size(MBRange); clear l %cercare di scrivere questo passaggio in modo da inserire nella
ping interrogation la distanza in metri
RangeScale=linspace(MBRange(1:1),MBRange(h:h),10);
RangeScale=(RangeScale)';
MatScale=linspace(0,h,10); clear h
MatScale=(MatScale)';
format bank
Range_legend=[RangeScale MatScale]

% Once the target is identified visually, the next step is to verify which is the beam with
the TS peak that is the one involved directly in the detection
R1=input('Range:');
R2=input('Range:');
B1=input('Beam:');
B2=B1-1;
B3=B1+1;

Bs=[B1 B2 B3];
Bs=(Bs)';
Bs=num2str(Bs);

%% Plot Peaks
Bnum=input('Graphics title:','s'); % give a title to the graphic. This can be done automatic
too just as Bnum='title'
scrsz = get(0,'ScreenSize');
figure('Position',[50 50 800 600])
whitebg('w')

H=subplot(3,1,1); plot (MBRange(R1:R2,1:1),TSts(R1:R2,B3:B3))
set(H,'FontName','Courier New','FontSize',10)
axis([100 400 -45 0])
text(400-15,-10, Bs(3,:))
title (Bnum(1,:), 'FontName','Courier New','FontSize',18,'FontWeight','Bold'); % do il titolo
alla sequenza di grafici

H=subplot(3,1,2); plot (MBRange(R1:R2,1:1),TSts(R1:R2,B1:B1))
set(H,'FontName','Courier New','FontSize',10)
axis([100 400 -45 0])
text(400-15,-10,Bs(1,:))
ylabel('TS (dB)','FontName','Courier New','FontSize',11,'FontWeight','Bold')

H=subplot(3,1,3); plot (MBRange(R1:R2,1:1),TSts(R1:R2,B2:B2))
set(H,'FontName','Courier New','FontSize',10)
axis([100 400 -45 0])
text(400-15,-10,Bs(2,:))
xlabel('Distance (m)','FontName','Courier New','FontSize',11,'FontWeight','Bold');

%% EXTRACTION OF TS PEAK VALUE (I finally obtain the TS measure of the sighted target)
format bank
if I.SectorType==0
    TSPeak=max(max(TSts(R1:R2,B1:B3)))
elseif I.SectorType==2
    TSPeak=max(max(TS(280:length(TS),1:10)))
end

```

